Non-Traditional Platinum Compounds for Improved Cellular Accumulation and Tumor Targeting

by

Katherine Summer Lovejoy
B.A., Chemistry; B.A., Integrated Science
Northwestern University, 2003

SUBMITTED TO THE DEPARTMENT OF CHEMISTRY IN PARTIAL FULFILLMENT OF THE REQUIREMENTS FOR THE DEGREE OF

DOCTOR OF PHILOSOPHY IN INORGANIC CHEMISTRY
AT THE
MASSACHUSETTS INSTITUTE OF TECHNOLOGY

September 2009

Signature of Author: _____
Department of Chemistry
June 30, 2009

Certified by: _____
Stephen J. Lippard
Arthur Amos Noyes Professor of Chemistry
Thesis Supervisor

Accepted by: _____
Robert W. Field
Haslam and Dewey Professor of Chemistry
Chairman, Departmental Committee on Graduate Studies

This doctoral thesis has been examined by a committee of the Department of Chemistry as follows:

Alice Y. Ting
Pfizer-Laubach Career Development Associate Professor of Chemistry
Committee Chair

Stephen J. Lippard
Arthur Amos Noyes Professor of Chemistry
Thesis Supervisor

Richard R. Schrock
Frederick G. Keyes Professor of Chemistry
Committee

Non-Traditional Platinum Compounds for Improved Cellular Accumulation and Tumor Targeting and Determination of Resulting Cellular Response

by
Katherine Summer Lovejoy

Submitted to the Department of Chemistry on June 30, 2009, in partial fulfillment of the requirements for the degree of Doctor of Philosophy in Inorganic Chemistry

Abstract

Chapter 1. Introduction to Non-Traditional Platinum Compounds for Improved Uptake, Oral Bioavailability, and Tumor Targeting

The path to more potent platinum anticancer drugs with fewer side effects lies in the exploration of non-traditional platinum compounds, which do not necessarily contain the canonical ligand set of two labile leaving groups and two am(m)ine ligands. Cationic, platinum(IV), and multinuclear complexes are considered. Advances in tumor targeting using platinum complexes are also discussed.

Chapter 2. Structure-Activity Relationship for the Uptake of Platinum(II) Compounds by Human Organic Cation Transporters

Although the platinum-based anticancer drugs cisplatin, carboplatin, and oxaliplatin form similar adducts on DNA, only oxaliplatin is active in colorectal cancer. Human organic cation transporters hOCT1 and hOCT2 markedly increase oxaliplatin, but not cisplatin or carboplatin, accumulation and potency in cells. These transporters are also present in human colorectal cancers and are likely to play an important role in the efficacy of oxaliplatin.

Chapter 3. Synthesis of Pt(II) and Pt(IV) Compounds for Uptake by the Organic Cation Transporters: Extension of Structure-Activity Relationships

A structure-activity relationship for the cellular accumulation of platinum compounds due to the organic cation transporters was developed and extended to design cationic compounds as particularly potent colorectal cancer drugs.

Chapter 4. Pyriplatin, *cis*-[Pt(NH_3)$_2$(pyridine)Cl]Cl, a Monofunctional, Cationic Platinum(II) Antitumor Agent

A cationic, monofunctional platinum(II) complex, *cis*-[Pt(NH_3)$_2$(py)Cl]Cl or pyriplatin, was synthesized and found to be an excellent substrate for the human organic cation

transporters 1 and 2. Pyriplatin displays what appears to be a unique mechanism of action in cancer cells. The repair of DNA damage induced by pyriplatin and the inhibition of RNA polymerase II by pyriplatin-DNA adducts are implicated in the mechanism.

Chapter 5. Characterization of the Role of HMGB1 in Cellular Response to Cisplatin

Cisplatin-DNA adducts are recognized by the nuclear protein and cytokine HMGB1. The contribution of HMGB1 to the potency of cisplatin is explored in the presence of androgens, retinoic acid, or under reducing conditions. HMGB1 binds more tightly to cisplatin-DNA adducts in the presence of 10 mM DTT.

Chapter 6. Pre-Clinical Evaluation of Pyriplatin

Pyriplatin was evaluated in human cancer cell lines for the purpose of gathering information for future Phase I trials. Pyriplatin has a unique cytotoxicity profile that is distinct from that of either the "platinum dach" class of compounds or cisplatin. The distinct profile suggests a significantly different mechanism of action than either oxaliplatin or cisplatin. Pyriplatin is about 10-fold less potent than either oxaliplatin or cisplatin. Although the compound shows synergy in combination with taxol or cisplatin in vitro, the drug is unlikely to be developed clinically due to its low potency.

Chapter 7. Pre-Clinical Evaluation of Mitaplatin

Mitaplatin, *c,c,t*-$[Pt(NH_3)_2Cl_2(O_2CCHCl_2)_2]$, was evaluated as a drug for potential Phase I clinical trials. The cytotoxicity profile, cell cycle inhibition results, and potential predictive factors (correlation of mRNA levels vs. IC_{50} values) suggest that mitaplatin acts very similarly to cisplatin. The results are supported by a correlation factor of 0.719 between the two compounds, found using the NCI's COMPARE algorithm. Although it is a promising dual functional platform for the delivery of both cisplatin and dichloroacetic acid, the results obtained closely resemble those for cisplatin and advantages of the dichloroacetic acid delivery are not apparent in data collected in this work.

Appendix A. Examination of the Platination of Plasmid DNA in Carbonate Buffer

Appendix B. Cellular Properties of a Cell-Permeable Zn^{2+}-Sensitive MRI Contrast Agent and the Effect of Zinc Chelators on Cisplatin Cytotoxicity

Thesis Supervisor: Stephen J. Lippard

Title: Arthur Amos Noyes Professor of Chemistry

To Mom and Dad

Acknowledgements

I joined the lab of my advisor Steve Lippard, because he knows in great detail and cares intensely about the project of each student. His commitment to education of each student as an individual and his demand for perfection made him my ideal choice then and today, as he continues to improve me and my work almost five years later. The technical advantages of working in a lab where I can learn and perform virtually any needed protocol have been crucial to this work as well. I thank Steve for his support and for providing an excellent environment and an outstanding group.

Thank you to Prof. Alice Ting, my thesis chair, for critical assessments of the progress and direction of my thesis over the years. Thank you to Prof. Schrock for serving on my thesis committee.

I am extremely privileged to have learned from and worked in two of the best labs in the world. Thank you to the RayLab at Beaujon Hospital for making the work in Chapters 6 and 7 possible and for teaching me as much about clinical oncology as I could absorb. Eric Raymond, Sandrine Faivre, Maria Serova, and, most importantly, Steve Cvitkovic are an outstanding team and have been wonderful to work with. Additionally, I was allowed to work with a master of DNA repair, Aziz Sancar at UNC-Chapel Hill, during my second year. He and Joyce Reardon trusted and taught me so I could perform the work for part of Chapter 4 in their lab. Aziz and Joyce also gave me critical advice and a reality check on the direction of my thesis and critical help prior to the publication of chapter 4. I am very thankful for their support and strive to meet their high standards in all biochemical work.

Thank you to frequent co-author Ryan Todd, to Dong Xu for the tissue culture advice, stories, and coffee, to Datong Song for his mentorship and technical advice and to Evan Guggenheim for having a cheery "good morning!" for me every day and reminded us all to laugh. Guangyu Zhu, Wee Han Ang and Paresh Agarwal have also been instrumental co-workers in the subgroup. Katie Barnes showed me all the ways of the lab during my first year and gave me the four-leaf clover that sometimes cures the various illnesses of our AA spectrometer, for which I am very grateful. I welcome Justin Wilson (and Nora Graf) to the lab and bequeath the clover to him. Thank you to Semi Park for being a second brain to solve HMGB1-related puzzles and I wish you the best in your work. Thanks to Tanya Wyss for assistance with material presented in Chapter 3. Thanks to Rodney Feazell for discussions, support in the tissue culture lab and advice on all topics. Thanks to Matthias Ober, my deskmate of a year, for discussions lasting late into the night and for keeping me motivated with your tireless presence. All lab protocols from your amazing mind and technical hands work the first time, every time.

Thanks to Shanta Dhar for solving my crystal structures, including pyriplatin and for originating all the work on mitaplatin that made Chapter 7 possible. I have asked for much advice, reassurance, and help from you in my last years in lab and you have given selflessly every time.

Thank you, Carmen Barnes, for allowing me access to the electronic materials at Harvard Med's library, many of which were unavailable in any form at MIT. Thanks to Yongwon Jung for providing protein used in Chapter 5.

Beyond the subgroup, it was a pleasure to enter the lab with Brian, Erik, and Simone. We have grown and learned a lot since then and I am honored to have been your classmate in lab.

Thanks to microscope folks Brian Wong, Elisa Tomat, Lindsey McQuade, and Xiao-an Zhang. It has not been easy to learn our new instrument. Best wishes especially, for Xiao-an as you begin your Canadian adventure. It has been a pleasure to work with and learn from you.

Thanks to Rich Girardi for exuding a sense of supreme control and rationality in all situations. Thanks to Leslie Murray for his friendship and mentorship, to Erwin Reisner for platinum discussions, to Christy Tinberg for being from NU and for fun inside and outside working hours, and to Woon Ju Song, Viviana Izzo, Laurence Beauvais, and Mi Hee Lim for good times. Thanks go to Liz Nolan for always *knowing* and I wish you good luck in your new adventure.

Thank you to ONCOETHIX/OTD for funding in my fifth year and thank you to the NSF-GRFP for funding in my first three years. Thank you to Susan Brighton for help sorting out many technical difficulties. Thank you to Northwestern Profs. Craig Bina, Fred Lewis, and Sonbinh Nguyen for believing in me.

Thanks to Simone for befriending me from the start, for many dinners cooked, nights out, coffee breaks, and laughs and miseries shared. Your friendship is indispensable. We are almost done! Thanks to Erik for your kindness, genius, and spirit of adventure. Whether at CalTech, MIT, or in the western wilderness, your stories amaze, inspire: you have always put it all on the line and made it out unscathed and I am sure this is also the case for grad school. I've turned to you again and again in deep despair or in need of understanding and I thank you.

Thanks Cass, most recently, for getting Obama elected, hauling me home for Christmas 2008 when my world was in crisis, teaching me French, and other things. Thanks to Mom and Dad for making everything possible for me. Things have always worked out perfectly and it is because you have constantly worked to make it so. Thanks to Rolf, who has suffered with me and given selflessly to make everything work out in lab. I love you all deeply. This work is only possible because of you.

Table of Contents

List of Tables

List of Charts

List of Schemes

List of Figures

Goals and Organization of the Thesis

The purpose of this thesis is to venture into a new area of research for the lab, the investigation of cellular accumulation of platinum drugs and design of compounds that will preferentially accumulate in cancer cells. Chapter one reviews some considerations for producing cationic compounds, which are not traditionally used in cancer treatment due to the difficulty of passing the lipophilic cell membrane. In chapter two, a structure-activity relationship is developed for the design of platinum compounds as substrates for the organic cation transporters. In chapter 3, the synthesis and biochemical testing of compounds designed along this structure-activity relationship is described, and extensive biochemical testing of one of the new compounds, pyriplatin is presented in chapter 4. Chapter 6 and 7 describe preclinical testing of pyriplatin and mitaplatin and study of these compounds in a 10-cell line panel.

The desire to produce platinum compounds that affect only cancer cells has also led to investigations in an area of research that has also been the subject of past and ongoing work in the Lippard lab. Cisplatin is a drug that is highly effective in testicular cancer, but less effective in other cancer types. In chapter 5, we have identified intracellular redox potential as a factor that could play a role in the variation in potency of cisplatin across cell types. The nuclear protein and cytokine, HMGB1, can form a disulfide bond under oxidizing cellular conditions, which reduces its affinity for DNA.

Chapter 1

Introduction to Non-Traditional Platinum Compounds for Improved Uptake, Oral Bioavailability and Tumor Targeting

I. Status of clinically useful platinum compounds

The first and most effective platinum-based drug is cisplatin, which is currently sold in the United States as Platinol. Initially approved by the FDA in December 1978, it is currently approved for use in bladder, non-small cell lung cancer, squamous cell carcinoma of the head and neck, and advanced ovarian, cervical and testicular cancer. Cisplatin is curative in nearly all cases of testicular cancer. In the three years prior to generic entry in 1999, net annual sales of cisplatin ranged from $100 to $250 million for Bristol-Myers Squibb.[1] Carboplatin (Chart 1.1), marketed as Paraplatin by Bristol-Myers Squibb, was the second FDA-approved platinum-based drug and is approved for use in advanced ovarian cancer and non-small cell lung cancer.[2] Sales of carboplatin were $769 million in 2003 and, like cisplatin, it is currently not patent protected.

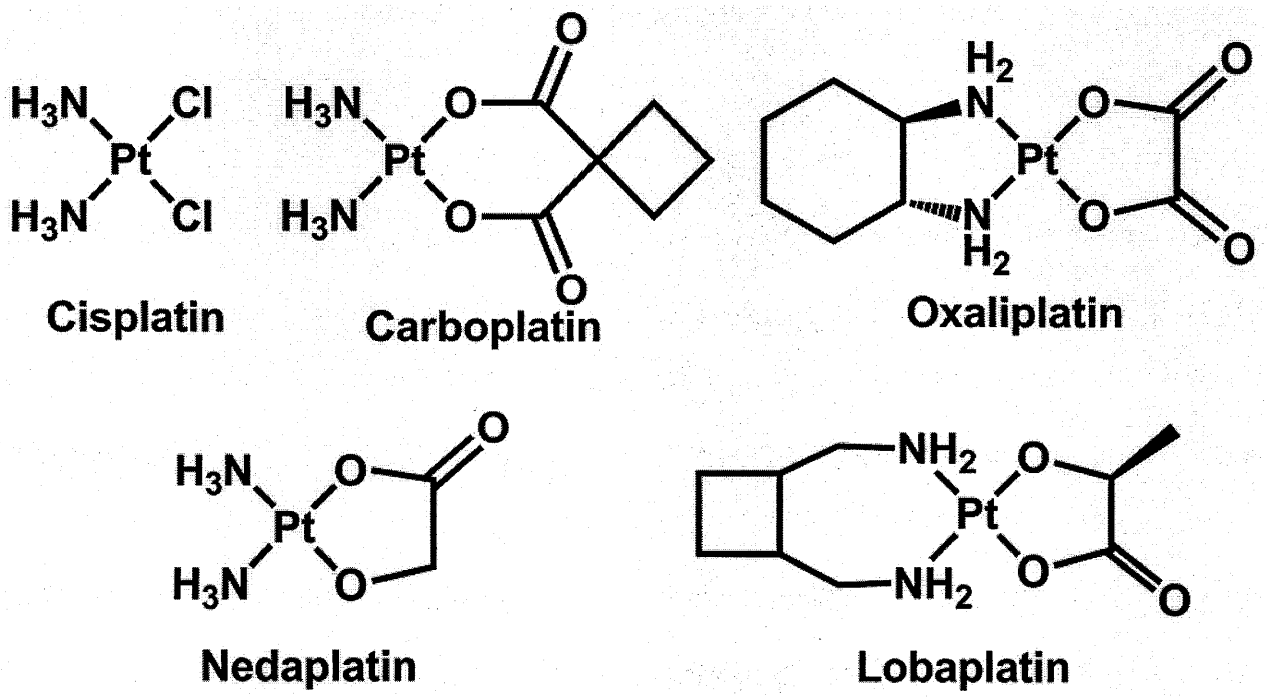

Chart 1.1. Platinum compounds in clinical use.

One drug similar to both cisplatin and carboplatin, nedaplatin, is marketed in Japan. Oxaliplatin, marketed as Eloxatin by Sanofi-Aventis, generated over $1.4 billion in sales

in 2004. When combined with 5-fluorouracil, oxaliplatin is approved by the FDA for treatment of stage III colon cancer and advanced colorectal cancer. Lobaplatin, which has a structure similar to that of oxaliplatin, is marketed in China as a diastereomeric mixture.

II. Mechanisms of action

The activity of platinum(II) anticancer compounds lies in the reaction of the platinum center with nuclear DNA. Aquation yields cationic, highly electrophilic species that react with various nucleophiles in the cell, including amino acid sulfhydryl groups and nitrogen donor atoms on nucleic acids.[3] Reactions with sulfhydryl groups are implicated in platinum resistance.[4] Reactions with DNA, the most nucleophilic site of which is in the major groove at the N7 position of guanine bases, are the crucial anticancer interactions and induce major distortions in the DNA.[5]

The predominant lesion formed by both cisplatin and carboplatin is the 1,2-d(GpG) intrastrand adduct.[6,7] This adduct, which has been structurally characterized on dodecamer DNA by x-ray crystallography, locally unwinds the double helix by 25° and both widens and flattens the minor groove.[8] The GG lesion formed by oxaliplatin on dodecamer DNA is very similar to that of cisplatin: both have similar helix bend angles of about 30° and a hybrid A/B-DNA conformation.[9]

The distortion of DNA induced by platinum lesions disrupts vital cellular processes, such as replication and transcription, and elicits a cellular defense response. The cell is capable of several responses to platinum-induced DNA damage. Four types of pathways that assist the cell in managing DNA damage have been identified.[10] DNA

can be repaired by one of several repair mechanisms, which restores the DNA to its undamaged state. Secondly, the cell cycle can be arrested by activation of a DNA damage checkpoint, a process that allows the cell time to repair the damage. Additionally, changes in the transcription of genes in response to DNA damage can aid cell survival. Finally, cells that have sustained significant damage undergo apoptosis, or programmed cell death.

Damage that involves covalent modifications of DNA are processed by DNA repair and recombination pathways. These pathways can be divided into five categories: direct repair, base excision repair, nucleotide excision repair, double-stranded break repair, and repair of interstrand cross-links.[10]

Cell cycle arrest is triggered upon detection of DNA damage by damage sensors. Among other proposed damage sensor proteins, RNA polymerase II (RNAP II) has been identified as especially important.[11,12] The particular suitability of RNAP II as a damage sensor is that it is not only highly specific, with the ternary RNAP II-RNA-DNA complex found at sites of UV-induced thymine dimers having a half-life of ~20 h,[13] but also constantly transcribes the genome, except during cell division. The close interaction of RNAP II with a large portion of the genome suggests that the protein can act as an inspector of the genome, which allows for a rapid detection of and response to DNA damage.

The downstream events that evolve following identification of DNA damage and lead to cell cycle arrest are dependent on the damage type. Cisplatin damage results in a delay of the cell cycle in S phase, eventually progressing to a block in G2 phase.[14,15] While the cell cycle is paused, changes in gene transcription that allow the cell to

respond to DNA damage occur. Many genes that are involved in DNA repair are not transcribed at a high level until DNA damage is detected. Upon detection of damage, the transcription of genes associated with repair is increased and the capability of the cell to repair damage is enhanced.[16] These changes include increased transcription of genes associated with repair. Finally, if the cell fails to respond sufficiently, it succumbs to the damage and apoptosis is triggered. Designing drugs that cause damage to DNA but do not induce cancer cells to mount a checkpoint response or begin DNA repair is crucial to the improvement of anticancer therapy.[10]

III. Nucleotide Excision Repair

Nucleotide excision repair (hereafter "excision repair") is the repair pathway by which the major product of cisplatin-induced DNA damage, the intrastrand d(GpG) lesion,[6,7] is repaired.[17] DNA lesions formed by cisplatin are repaired by excision repair, and cells in which this pathway is disrupted, such as in patients with xeroderma pigmentosum,[18] are particularly sensitive to cisplatin damage.

The process of nucleotide excision repair begins with cellular recognition of damage and formation of an open complex.[19] An excision complex is then formed, which involves the proteins RPA, XPA, XPG, and XPF/ERCC1, and a DNA fragment of 24 to 32 nucleotides (length dependent on species) is excised.[19] The structural details of the protein-protein interaction between XPA to the ERCC1 subunit of the XPF/ERCC1 complex show that only a small portion of XPA is involved in the interaction.[20]

Excision repair of 1,2- and 1,3-intrastrand cisplatin cross-links in human tumors results in oligomeric excision products of 27 to 29 nucleotides.[17] Conversely, interstrand cisplatin-DNA cross-links produce no excision products.[21]

Much investigation has been based on the fact that the high mobility group box 1 protein (HMGB1) binds 1,2-intrastrand cross-links and blocks the nucleotide excision repair of these adducts under *in vivo* conditions.[17,21] HMGB1 is a highly abundant protein that can be found associated with chromatin or in the cytosol acting as a cytokine (see section X, below). When associated with nuclear DNA, the protein protects intrastrand 1,2-d(GpG) and 1,2-d(ApG) cisplatin-DNA lesions from repair, but not the 1,3-d(GpTpG) adduct.[21] The interaction of a testicular cell-specific high mobility group protein with platinated DNA has also been of particular interest because of the high efficacy of cisplatin in testicular cancer. Work on mouse testicular teratocarcinoma extracts revealed deficient repair of 1,2-intrastrand cross-links, which was hypothesized to be due to shielding of the adducts by tsHMG.[22]

Other proteins that interact with cisplatin-damaged DNA include the TATA-binding protein, which also protects 1,2-intrastrand cross-links from repair in *in vitro* assays.[23] The tumor suppressor protein p53 also recognizes DNA with the cisplatin 1,2-d(GpG) cross link, but not the 1,3-d(GpTpG), interstrand, or monofunctional adducts.[24] Poly(ADP-ribose) polymerase 1 (PARP-1), a protein that responds to DNA damage by modifying other key proteins with poly(ADP-ribose), also has affinity to 1,2-d(GpG) adducts.[25,26] Additionally, the nucleosome has also been shown to inhibit nucleotide excision repair of the major d(GpG) intrastrand cross-links by about 30%.[27]

IV. Transcription Inhibition

After platinum compounds cross the cell membrane and form adducts with DNA, the ultimate consequences of the DNA lesions are mediated by the proteins that first arrive at the damaged site.[28] In many cases, the damage is initially recognized and then repaired by proteins involved in the nucleotide excision repair pathway.[17] Other proteins that may quickly appear at the adduct side include those capable of facilitating DNA repair, interfering with DNA repair, or otherwise affecting the processing of damaged DNA.[28] Cellular processing of the adduct and the eventual fate of cancer cells depends on the proteins that associate quickly with the newly damaged site.

One group of proteins that encounter cisplatin-DNA adducts soon after lesion formation are the transcriptional factors. Unlike DNA polymerases, which briefly pause at and then bypass cisplatin cross-links, presumably without major down-stream effects,[29-31] RNA polymerases are greatly affected by the presence of cisplatin adducts. Transcription by the phage T7 RNA polymerase is strongly inhibited by both cisplatin 1,2-intrastrand cross-links and oxaliplatin 1,3-intrastrand cross-links.[32] The progress of human RNA polymerase II (Pol II) along the DNA strand is almost completely blocked by platinum DNA adducts.[33] Furthermore, Pol II does not resume transcription after stalling,[33] and the stalled polymerase becomes ubiquitylated, triggering various signal cascades in the cell.[33,34] In particular, the arrest and ubiquitylation of Pol II is believed to be involved in initiation of a repair pathway called transcription-coupled repair, which is a subpathway of nucleotide excision repair.[34] Investigations of proteins involved in transcription will lead to a greater understanding of the mechanisms by which cells cope with and become resistant to platinum-DNA adducts.

V. Traditional structure-activity relationships

All five compounds in clinical use (Chart 1.1), conform to the structure-activity relationship developed coincidently with the discovery of cisplatin.[35] These compounds are all neutral, platinum(II) species with two am(m)ine ligands or one bidentate chelating diamine, and two ligands that can be replaced by aquation reactions, eventually leading to the formation of a bifunctional adduct on DNA.

As we learn more about cellular interactions with platinum compounds, the canonical structure activity relationships that guide the design of new platinums must constantly be revisited. Exciting areas of development in the platinum anticancer community include insights on ways to improve uptake, oral bioavailability, and tumor targeting of platinum compounds.

VI. Non-traditional compounds in clinical trials

The three year interval between initial testing of cisplatin in mouse tumor models by the National Cancer Institute in 1968 to clinical trials with terminal cancer patients, which began in 1971, is unusually short by today's standards. Discomfort over the use of heavy metals in medicine and the novelty of the class of compounds were overcome in favor of rapid introduction of the promising new treatment.[36] The platinum compounds currently in clinical trials that violate the canonical structure-activity relationship have also overcome significant barriers on their way to the clinic, and the lag between benchtop and clinical use has been considerably longer than that of cisplatin.

Compounds that have entered clinical trials include platinum(IV) compounds such as satraplatin, or *c,c,t*-[$Pt(NH_3)_2$(cyclohexylamine)$Cl(COOCH_3)_2$] (also known as JM216), the first orally administered platinum compound to undergo active clinical investigation, multinuclear compounds of the form $[\{PtCl_m(NH_3)_{3-m}\}_2(H_2N\text{-}R\text{-}NH_2)]^{2(2-m)+}$ (m = 0-3) and R is a linear or substituted aliphatic linker), and picoplatin, *cis*-[$Pt(NH_3)$(2-picoline)Cl_2] (also known as AMD473) (Chart 1.2).

The first patient received satraplatin, the first oral dose of platinum anticancer treatment, in 1993. A phase II trial in patients with hormone-refractory prostate cancer showed a median overall survival of 14.9 months for the patients receiving satraplatin and prednisone and a survival of 11.9 months for patients receiving prednisone alone and a phase III trial in patients with similar cancer profiles also showed that patients on the combination therapy had an improved prognosis for disease progression.[37]

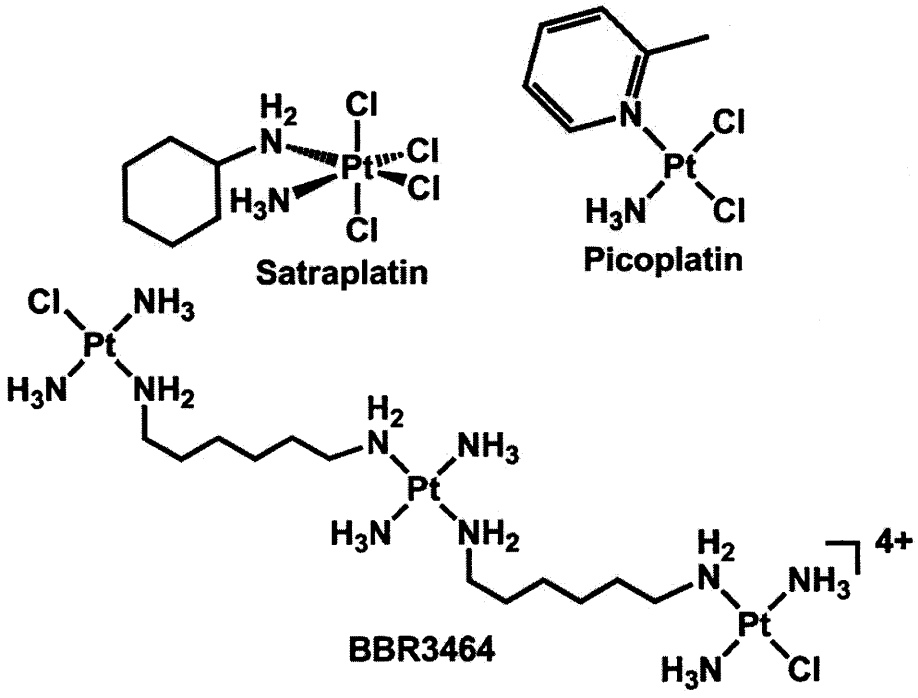

Chart 1.2. New and non-traditional compounds in clinical trials.

Satraplatin was considered by the FDA in 2007 as a treatment for hormone-resistant prostate cancer and, despite having entered into a "special protocol assessment" with the FDA, was not approved. According to *Forbes* magazine, the confidential panel convened on satraplatin concluded that the FDA had agreed to most of the trial, but not to one key measure of pain, which was the basis for rejection,[38] although other sources disagree on the reasons for rejection. Satraplatin's development is under the control of Spectrum Pharmaceuticals in the United States, where it is currently under investigation for the treatment of non-small-cell lung cancer and GPC Biotech in Europe, where it is in phase II trials in patients with hormone-refractory prostate cancer.

The dose-limiting side-effect to satraplatin is myelosuppression, specifically, a reduction in the production of white blood cells and platelets. Biotransformation of satraplatin in the body produces several products, but the major product is the result of biological reduction to platinum(II), *cis*-[$PtCl_2(NH_3)$(cyclohexylamine)] (JM118).[39] The DNA adducts formed by this reduced and activated form of satraplatin are similar to those formed by cisplatin[40] and are repaired by the nucleotide excision repair pathway.[41] A comparison of excision repair for cisplatin, oxaliplatin, and JM118, the reduced form of oxaliplatin, revealed only modest differences for the rate of *in vitro* repair. The percent excision after 60 minutes was about 2.0% for 1,2-d(GpG) adducts of JM118, about 1.5% for cisplatin and about 1.0% for oxaliplatin GG adducts.

Picoplatin, a drug in development under the control of Poniard Pharmaceuticals, was designed with additional steric bulk around the platinum center to reduce inactivation by cellular thiols, such as glutathione.[39] In fact, the binding of cisplatin to

DNA is significantly more inhibited relative to the binding of picoplatin to DNA in the presence of 5 mM glutathione, and cells that are resistant to cisplatin, such as A2780cis, are not cross-resistant to picoplatin.[42] Picoplatin also exhibits synergistic behavior when administered as a combination therapy with paclitaxel, as does cisplatin. Phase II clinical trials of picoplatin demonstrated a survival benefit for patients with small cell lung cancer who were treated with picoplatin after relapsing within six months of initial therapy with other drugs. The phase III trial of picoplatin, SPEAR (Study of Picoplatin Efficacy After Relapse) is underway in Europe and India and is also focused on patients with small cell lung cancer. A phase I trial in colorectal cancer (combination therapy with 5-fluorouracil) and a phase II trial in prostate cancer (combination therapy with docetaxel and prednisone) are also underway.

VII. Cationic non-traditional compounds.

Cationic Compound in Clinical Trials, BBR3464

The trinuclear compound BBR3464, or [{*trans*-$PtCl(NH_3)_2$}$_2${μ-*trans*-$Pt(NH_3)_2(H_2N(CH_2)_6NH_2)_2$}]$^{4+}$, is composed of two *trans*-{$PtCl(NH_3)_2$}$^+$ units linked by the bridging tetra-amine *trans*-{$Pt(NH_3)_2${$H_2N(CH_2)_6NH_2$}$_2$}$^{2+}$ (Chart 1.2) and is undergoing phase II clinical trials. The platinum atoms at either end of this compound react in a monofunctional manner with non-adjacent DNA bases to form a variety of adducts and it is not clear which adduct, if any, predominates *in vivo*.[43] The charge on the internal platinum atom is important to the anticancer activity of the complex and is linked to increased cellular accumulation postulated to be due to polyamine transporters.[44] The dose-limiting suppression of blood cell production in the bone marrow and

gastrointestinal side effects, which reduce the maximum-tolerated dose below that of cisplatin, limit the potency of the drug and may prevent it from entering phase III trials. Trials in patients with advanced gastric or gastroesophageal adenocarcinomas resulted in 5 of 7 patients receiving 1.1 mg/m^2 every four weeks experiencing side effects requiring a reduction in dose. Of 17 patients on a reduced dose of 0.9 mm/m^2, only 1 showed a significant response.[45]

Cationic Drug Candidates

Cationic platinum compounds are not commonly thought of as active species due to their inability to diffuse through the neutral, hydrophobic lipid bilayer. Having identified platinum compounds as potential substrates for cation transporters in cell membranes, investigations into the cationic platinums have been reignited.

Once inside the cell, the cationic nature of these compounds lends them immediate affinity for the negative charge of DNA, similar to the interaction of the aquated, cationic form of cisplatin with DNA. As a practical advantage, cationic platinum compounds are significantly more soluble in water than their neutral relatives, which aids in drug formulation. Also, unlike some organic drugs, they are unlikely to partition into or stick to the hydrophobic plastics used in common clinical and cell culture practice.

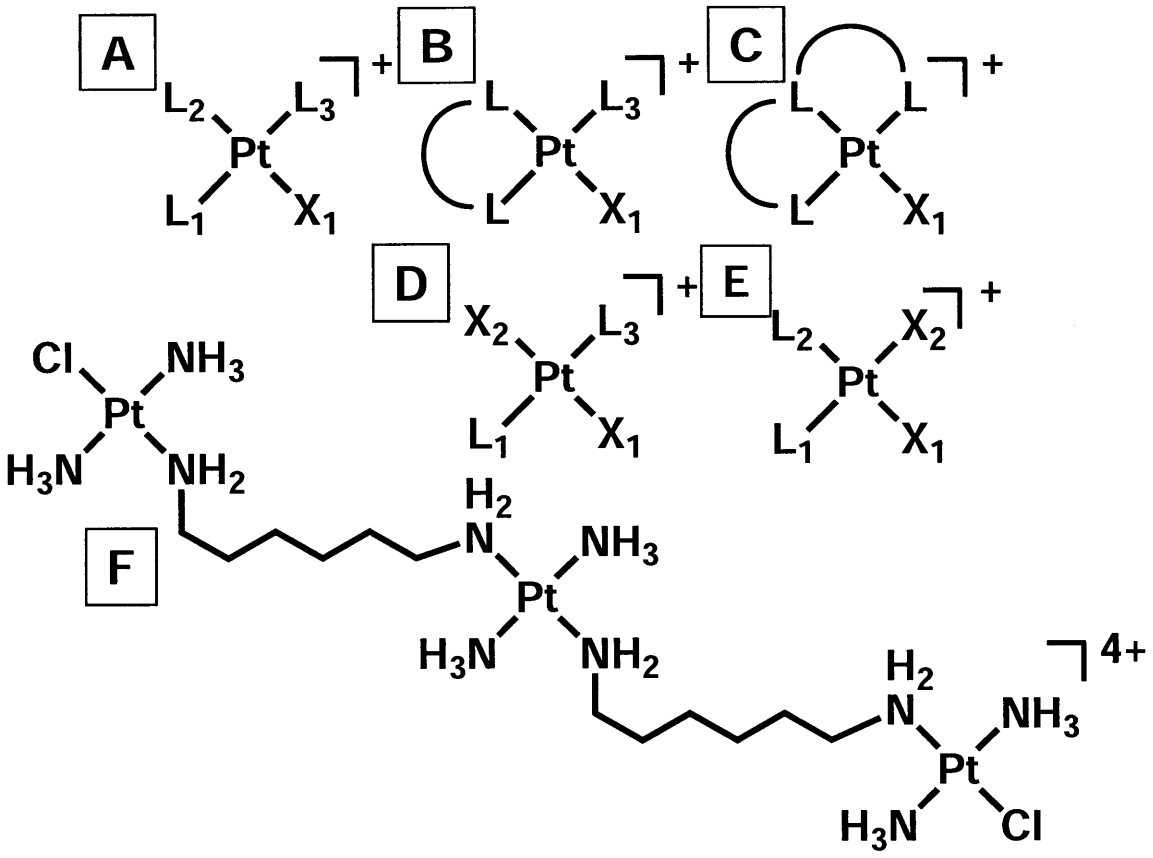

Chart 1.3. Structural frameworks for cationic platinum(II) complexes with antitumor activity.

Strategies for the design of active cationic complexes fall into several categories. An early successful Pt(II) framework that produced a number of active complexes involved complexes with three non-labile nitrogen donor ligands and one chloride leaving group (Chart 1.3, A).[46] A variation on this structure involves linking two such monofunctional complexes to form binuclear, bifunctional,[47] or trinuclear, bifunctional (Chart 1.3, F)[48] complexes. Instead of three nitrogen donor ligands, ligand sets such as a bidentate (Chart 1.3, B) or tridentate (Chart 1.3, C) nitrogen donor ligand plus a halogen, thiourea,[49,50] or sulfoxide also yield cationic complexes. Another framework involves replacement of one ammine on cisplatin or *trans*-$[Pt(NH_3)_2Cl_2]$ with a positively charged non-labile nitrogen donor ligand, such as piperazine (Chart 1.3, D and E).[51] The replacement on cisplatin tends to result in a compound with reduced cytotoxicity

compared with cisplatin, whereas the corresponding replacement on *trans*-$[Pt(NH_3)_2Cl_2]$ tends to enhance cytotoxicity.

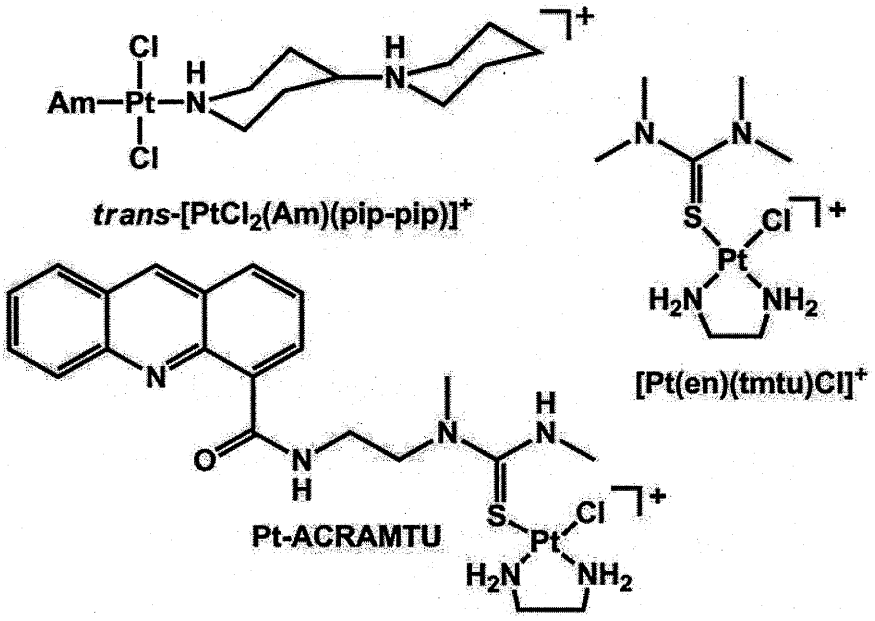

Chart 1.4. Three cationic platinum(II) anticancer drug candidates.

Monofunctional platinum-acridine complexes bind to N3 of adenine in the minor groove due to an intercalator-mediated minor groove association at adenine-containing base pair steps.[52] The IC_{50} for the most cytotoxic member of this series (Pt-ACRAMTU, Chart 1.4) was 16.0 μM in the human leukemia cell line HL-60 and was 2.4 μM in the human lung carcinoma cell line NCI-H460.[53]

Another cationic series of compounds showing significant cytotoxicity have the general formula *trans*-$[PtCl_2(Am)(pip\text{-}pip)]\cdot HCl$ (pip-pip = 4-piperidinopiperidine) (Chart 1.4).[54] Of the seven compounds of this series and cisplatin, the compound with Am = NH_3 was the most cytotoxic in the cisplatin-resistant ovarian cancer cell lines A2780cisR, CH1cisR, and 41McisR. In the murine carcinoma line C-26, cellular accumulation of *trans*-$[PtCl_2(NH_3)(pip\text{-}pip)]\cdot HCl$ was 10- to 25-fold greater than cisplatin,

Table 1.1. Structural parameters for some cationic complexes designed as antitumor drugs.

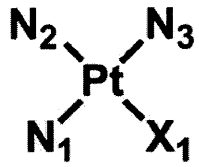

Compound	L_1	L_2	L_3	X_1	Pt-L_1	Pt-L_2	Pt-L_3	Pt-X_1	N_2-Pt-N_1	N_2-Pt-N_3	N_1-Pt-X_1
cis-[Pt(NH_3)$_2$(*N3*-cytosine)Cl]Cl [46]	NH_3	NH_3	cytosine	Cl	2.045(7)	2.059(7)	2.033(7)	2.309(2)	90.1(3)°	90.1(3)°	91.5(2)°
cis-[Pt(NH_3)$_2$(*N1*-pyridine)Cl]Cl [55]	NH_3	NH_3	pyridine	Cl	2.054(13)	2.028(13)	2.002(13)	2.312(4)	89.9(6)°	89.2(5)°	89.7(4)°
[PtI(Me_2phen)(AmPIC)]I [56]	2,9-dimethyl-1,10-phenanthroline		6-amino-2-picoline	I	2.044(6)	2.079(6)	2.036(6)	2.592(1)	80.9(2)°	96.7(2)°	98.8(2)°
[Pt_3(HPTAB)Cl_3](ClO_4)$_3$ [57] (trinuclear compound w/ 3 monofunctional Pt centers)	2,2′-bis(pyridylmethyl)amine			Cl	1.986(8)	2.027(8)	2.001(8)	2.283(2)	81.8(3)°	85.1(3)°	96.6(2)°
[PtCl(en)($C_{19}H_{23}N_4$)](NO_3)$_2$ [53]	en		*N*-[2-(acridin-9-ylamino)ethyl]-*N*-methylpropion amidine	Cl	2.013(7)	2.025(7)	2.023(3)	2.313(2)	83.3(3)°	90.9(2)°	90.5(2)°
[PtCl(en)(PICAC-*N*)] [58] (neutral form, only closed form is cationic)	en		6-(methylpyridin-2-yl)acetate	Cl	2.033(3)	2.047(3)	2.048(3)	2.3093(9)	83.78(13)°	93.82(12)°	91.96(10)°
[Pt(bampy)Cl]$^+$ [59]	*C*-(6-aminomethylpyridin-2-yl)methylamine			Cl	2.033(6)	1.936(5)	2.040(6)	2.308(2)	83.2(2)°	81.4(2)°	97.4(2)°
[PtCl(dach)(tmtu)]NO_3 [49]	dach		1,1,3,3-tetramethylthio urea	Cl	2.080(6)	2.042(6)	2.281(2)	2.298(2)	83.2(2)°	92.3(2)°	92.7(2)°

although the level of platinum bound to DNA was roughly the same. The charged complexes also bind DNA up to 10-fold more quickly than neutral complexes such as cisplatin and *trans*-$[Pt(NH_3)_2Cl_2]$.[60]

A summary of structural parameters for eight known cationic, monofunctional platinum(II) complexes is shown in Table 1.1. The weakening of the Pt-X_1 bond can be seen in the variance of bond length, but this value does not relate to the cytotoxicity of the complexes. The ^{195}Pt NMR chemical shift for these complexes does not scale with cytotoxicity either.

VIII. Influx transporters and platinum compounds

The mechanisms by which platinum anticancer compounds accumulate in cells have been of interest since the early work on cisplatin, where it was already suspected that cisplatin enters the cell by passive diffusion through the cell membrane.[36] Although the small, neutral cisplatin may not need to take advantage of an active transport system, new drug candidates that are either sterically bulky, charged, or both, have been shown to interact with influx and efflux transporters.

Human genes that encode transporters make up 3.0% of all open reading frames and code for a predicted 841 transporter proteins.[61] Solute transporters are divided into four major classes, according to the transporter classification system.[62] Channels move water, ions, or hydrophilic small molecules down a gradient. Primary active transporters utilize ATP hydrolysis to drive the transport process. Transport in secondary transporters is driven by an ion or solute electrochemical gradient. Finally, group transporters are characterized by their requirement for modification of the substrate,

such as by phosphorylation, during transport.[61] In humans, the percentages of channels, primary transporters, secondary transporters, and phosphotransferases are 43.3, 14.9, 38.9, and 0, respectively.[61]

As a group, secondary transporters accept a wide variety of substrates, including sugars, lipophilic molecules, cations and anions, and nucleosides. Organic cation transporters (OCTs) are members of the solute carrier family of secondary transporters (SLC22A) with a broad range of substrate specificity. Of greatest interest for drug metabolism, they are found, among other organs, in the intestine, liver, and kidney[63-65] and facilitate the movement of endogenous and xenobiotic substrates across cell membranes. The presence of these transporters in the intestine facilitates drug uptake from the gastrointestinal tract, while presence in the liver and kidney affects excretion of drugs and can give rise to renal and nephrotoxicity. Examples of drugs that are organic cations can be found among antihistamines, β-adrenergic antagonists, calcium channel blockers, and skeletal muscle relaxants.[66] Examples of endogenous substrates of the organic cation transporters include guanidine, a small molecule formed during protein metabolism, and thiamine, which is needed for the metabolism of carbohydrates and lipids.[67]

The presence of OCTs in the intestine allows for both desirable and undesirable biomedical effects. Organic cations that would otherwise not be orally bioavailable are removed from the intestine by organic cation transporters and passed into the bloodstream. Certain foods may interfere with the uptake of organic cations, as has been shown for caffeine and the uptake of the OCT substrate MPP^+ (1-methyl-4-phenylpyridinium).[68] Changes in the pH of the contents of the small intestine may also

affect the uptake of some drugs. Additionally, mutations of the transporters may lead to variability in drug accumulation among patients.[69] Studies of the colorectal adenocarcinoma cell line Caco-2 under conditions that simulate the *in vivo* environment and allow differentiation between apical and basolateral membranes have clarified the location of OCTs under polarized conditions.[65] The transporter hOCT1 is localized to the basolateral membrane and plays a role in uptake and efflux at the interstitium (Figure 1.1). Uptake of cations occurs under a normal membrane potential of -60 mV. Alternately, efflux of a particular cation can occur if the intracellular concentration becomes much higher than the extracellular concentration.

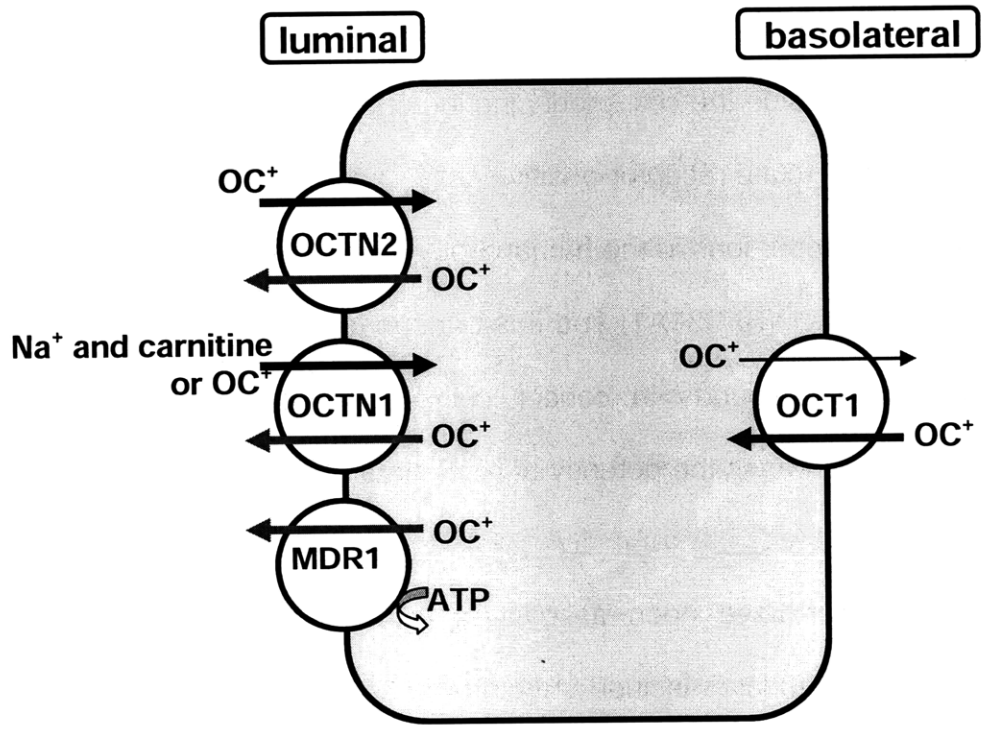

Figure 1.1. Transporters of organic cations in enterocytes of the human small intestine. Figure is based on a figure in Koepsell, *et. al.*, 2007.[69] OCT1 transports cations in either direction depending on the electrochemical potential. In the presence of a normal membrane potential (-60 mV), cation uptake (thick arrows) is preferred. Efflux can occur if the intracellular concentration of the cation is 10 times higher inside the cell than outside the cell.

IX. Other connections between transport and platinum sensitivity

Besides organic cation transporters, other transporters that have proven influential in the efficacy of platinum anticancer drug candidates. Folate receptor-α, which is overexpressed on the cell membrane of a variety of human tumors, has been targeted using platinum-folate constructs. An early example carboplatin was modified with a folic acid-PEG construct to produce a complex that efficiently entered folate receptor-positive cells, but seemed to then be sequestered in a way that prevented reaction of the platinum with nuclear DNA.[70] In a more successful example, a platinum (IV) complex modified with folic acid derivative at one axial position and a single-walled carbon nanotube at the second axial position.[71] The Pt(IV) construct undergoes reductive release of cisplatin inside the cell, producing increased platinum-DNA adducts in and selective destruction of folate receptor-positive cells.

The homeostasis of copper ions in the human body is mediated for the most part by the copper transporter CTR1 (SLC31A1) and this transporter has been linked to the accumulation of platinum compounds in cancer cells.[72] The presence of copper increases the uptake, but decreases the potency of cisplatin and increases both uptake and potency of BBR3464.[73]

Other transporters that have been associated with the efficacy of platinum anticancer drugs and drug candidates include steroid receptors. Targeting cancer cells using platinum complexes tethered to estrogen derivatives has met with success in pre-clinical experiments.[74-76] The combination of estrogen and platinum complexes is of interest because estrogen potentiates the upregulation of HMGB1,[77] a protein that binds with high affinity to platinum-DNA adducts.

X. Influence of HMGB1 on cellular processes

The high-mobility group box-1 protein is an abundant, highly conserved protein that is a critical component of a wide variety of cellular processes. It binds to cisplatin-modified DNA with a specificity between 10- and 100-fold over unmodified DNA with a K_d values from 0.3-370 nM.[78] At a concentration of 8 μM, HMGB1 inhibits the overall repair of cisplatin-DNA adducts by over 70% (where [DNA substrate] = 20 pM).[17] This finding suggested that tumors with high levels of HGMB1 may have increased susceptibility to cisplatin due to decreased excision repair of cisplatin adducts. In support of this hypothesis, the cytotoxicity of cisplatin is potentiated by pretreatment of breast and cervical cancer tumor cells with estrogen and progesterone,[77] a protocol that increases the level of HMGB1 in the nucleus.[79,80]

Paradoxically, increased expression of HMGB1 is also linked to enhanced resistance seen in cisplatin-resistant cells. Activity in the HMGB1 promoter region was 3- to 10-fold higher in cisplatin-resistant KB-CP20 cells than in the parent KB cell line.[81] These data and other connections between HMGB1 and the evolution of cancer have led to an alternate hypothesis: the possibility that cisplatin-modified DNA sequesters HMGB1 from its role in the progression of cancer and that cisplatin acts as an anti-HMGB1 agent in a way that is key to its activity as an anticancer drug.[82]

The reason for the two hypotheses is the dual nature of HMGB1: it acts both as a transcription factor in the nucleus, but also as a cytokine in the cytosol.

HMGB1 in the Nucleus

In resting, healthy cells, HMGB1 is found in the nucleus and acts as a transcription factor and as a chromatin remodeler. Two nuclear localization signal sequences (amino acids 28-44 and 180-185) are present in the amino acid sequence of human HMGB1.[83] In its role as a transcription factor, HMGB1 is involved in the regulation of gene transcription of a limited number of genes. Steroid receptors, for example, including the progesterone and estrogen receptors, are activated upon steroid binding and bind to DNA at sites that contain hormone response elements of target genes, thereby stimulating transcription of those genes. HMGB1 establishes a protein-protein interaction with these steroid receptors and, upon binding DNA, induces a structural distortion of the DNA that stabilizes the steroid receptor-DNA interaction. HMGB1 therefore enhances the interaction of the steroid receptor and its hormone response element, which leads to increased transcription of the associated genes.[80]

HMGB1 also interacts in a non-gene-specific way with chromatin. The basic unit of chromatin is the nucleosome, which is composed of DNA and an octamer of histones, consisting of two copies of each of four histone proteins. Each nucleosome in eukaryotic cells also contains one of a fifth type of histone, H1, which is transiently associated with chromatin. H1 modulates chromatin function depending on the length of time it is associated with the nucleosome and its competition with nuclear proteins that also bind to nucleosomal DNA.[84,85] HMGB1 competes with histone H1 and weakens its interaction with chromatin. The replacement of H1 with HMGB1 creates the possibility for transcription regulatory factors to access chromatin.[85]

HMGB1 as a Cytokine

In addition to activity in the nucleus, HMGB1 can also be released into the cytosol and into the extracellular environment by both active and passive mechanisms. Movement into the nucleus occurs in cells dying a deregulated, necrotic death and not in cells that succumb to apoptosis. Migration into the cytosol may be mediated by post-translational modification of either Cys106[86] or several of the 43 lysine residues.[83] Phosphorylation has also been investigated as a signal for migration between the cytosol and nucleus, and other post-translational modifications of HMGB1, including ADP ribosylation, glycosylation, and methylation, may also be involved.[87,88]

Following localization into the cytosol, HMGB1 switches roles to facilitate immune response to cell death and microbial invasion. Necrotic cells have leaky cell membranes, which allows cytosol-localized HMGB1 to escape into the extracellular milieu. HMGB1 then causes an inflammatory response, which brings macrophages to the necrotic site to clean up the aftermath of necrotic cell death and prevent infection and causes neighboring tissue to initiate repair.[89] Immune cells such as monocytes and macrophages, can actively release HMGB1 via secretory vesicles, in effect mimicking necrotic cell death and bringing about a similar immune response. The signaling capabilities of HMGB1 require partner target receptors, which include the receptor for advanced glycation end products (RAGE), Toll-like Receptor 2 and 4 (TLR2 and TLR4), syndecan, phosphacan/protein-Tyr phosphatase γ/β, and plasminogen.[82] Much of the work linking HMGB1 to cancer has focused on the interactin of HMGB1 and RAGE. RAGE is a member of the immunoglobulin superfamily, which is composed of proteins that act as cytokine or antigen receptors, or are involved in the binding, or adhesion of

cells. Most members of the Ig superfamily play a role in the immune system.[89] RAGE is expressed by monocytes and macrophages, dendritic cells, endothelial cells, and vascular smooth muscle cells. Levels of RAGE are low in normal tissues, but the level increases in areas where HMGB1 accumulates.[90] Increased expression of either HMGB1 or RAGE has been identified in breast, colon, melanoma, metastatic prostate, and metastatic pancreatic cancer cells. One exception has been found in lung tissue, in which RAGE and HMGB1 are down-regulated.[82]

The relevance of the inflammation-inducing, cytokine properties of HMGB1 to cancer is based on the realization that tumor cells, which undergo messy, necrotic cell death, use HMGB1 to promote the growth of the surrounding non-necrotic, viable portions of the tumor. The RAGE-HMGB1 interaction has also been linked to proteins involved in the cytoskeletal remodeling process required for cell movement.[91] Importantly, inhibition of the interaction of RAGE and HMGB1 decreases the growth and metastasis of tumors in mice.[92]

HMGB4

Besides HMGB1, other members of the HMG family exist and differ mostly in which organs they are expressed. A new member of the family, HMGB4 (NCBI Reference Sequence: NP_660206.2), has recently been characterized.[93] It is expressed in the testis and in sperm cells, which is of interest because of the particular efficacy of cisplatin in testicular cancer. The sequence alignment (Chart 1.5) indicates that the disulfide bond formed in HMGB1 between Cys23 and Cys45 cannot be formed in HMGB4 due to the absence of a cysteine at position 23.

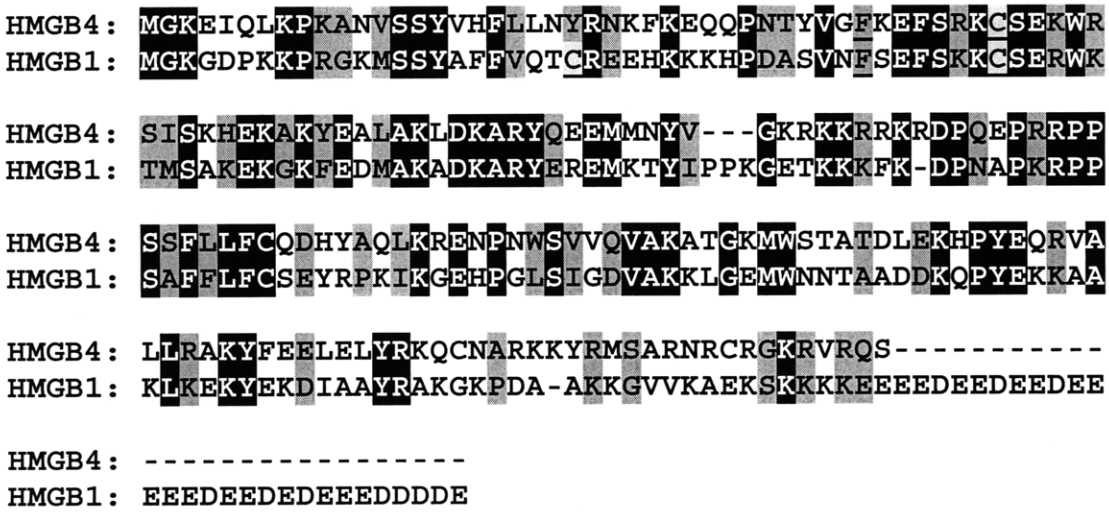

Chart 1.5. Sequence alignment of human HMGB4 and human HMGB1. Identical residues are highlighted in black, similar residues are highlighted in grey, and the Phe38, Cys23, and Cys45 residues are underlined.

Additionally, the acid C-terminal residues found in HMGB1, which reduce the affinity of HMGB1 for DNA[94] are not found in HMGB4. The binding affinity of HMGB4 for cisplatin-modified DNA is unknown and, given the lack of disulfide bond formation and inhibitory acidic tail in HMGB4, the interaction may be of great relevance for the repair of cisplatin-modified DNA in testicular cancer.

References

(1) "Generic Drug Entry Prior to Patent Expiration: An FTC Study," Federal Trade Commission, July 2002.
(2) National Cancer Institute.
(3) B. Lippert (2000). Multiplicity of metal ion binding patterns to nucleobases. *Coord. Chem. Rev.*, **200-202**, 487-516.
(4) M. Kartalou and J. M. Essigmann (2001). Mechanisms of resistance to cisplatin. *Mutat. Res.*, **478**, 23-43.
(5) E. R. Jamieson and S. J. Lippard (1999). Structure, Recognition, and Processing of Cisplatin-DNA Adducts. *Chem. Rev.*, **99**, 2467-2498.
(6) A. M. J. Fichtinger-Schepman, R. A. Baan, A. Luiten-Schuite, M. Van Dijk and P. H. M. Lohman (1985). Immunochemical quantitation of adducts induced in DNA by cis-diamminedichloroplatinum(II) and analysis of adduct-related DNA-unwinding. *Chem. Biol. Interact.*, **55**, 275-288.

(7) A. M. Fichtinger-Schepman, A. T. van Oosterom, P. H. Lohman and F. Berends (1987). cis-Diamminedichloroplatinum(II)-induced DNA adducts in peripheral leukocytes from seven cancer patients: quantitative immunochemical detection of the adduct induction and removal after a single dose of cis-diamminedichloroplatinum(II). *Cancer Res.*, **47**, 3000-3004.
(8) P. M. Takahara, C. A. Frederick and S. J. Lippard (1996). Crystal Structure of the Anticancer Drug Cisplatin Bound to Duplex DNA. *J. Am. Chem. Soc.*, **118**, 12309-12321.
(9) B. Spingler, D. A. Whittington and S. J. Lippard (2001). 2.4 Ã... Crystal Structure of an Oxaliplatin 1,2-d(GpG) Intrastrand Cross-Link in a DNA Dodecamer Duplex. *Inorg. Chem.*, **40**, 5596-5602.
(10) A. Sancar, L. A. Lindsey-Boltz, K. Ünsal-Kacmaz and S. Linn (2004). Molecular mechanisms of mammalian DNA repair and the DNA damage checkpoints. *Annu. Rev. Biochem.*, **73**, 39-85.
(11) B.-B. S. Zhou and S. J. Elledge (2000). The DNA damage response: putting checkpoints in perspective. *Nature*, **408**, 433-439.
(12) L. A. Lindsey-Boltz and A. Sancar (2007). RNA polymerase: The most specific damage recognition protein in cellular responses to DNA damage? *Proc. Natl. Acad. Sci. U. S. A.*, **104**, 13213-13214.
(13) C. P. Selby, R. Drapkin, D. Reinberg and A. Sancar (1997). RNA polymerase II stalled at a thymine dimer: footprint and effect on excision repair. *Nucleic Acids Res.*, **25**, 787-793.
(14) C. M. Sorenson and A. Eastman (1988). Mechanism of cis-diamminedichloroplatinum(II)-induced cytotoxicity: role of G2 arrest and DNA double-strand breaks. *Cancer Res.*, **48**, 4484-4488.
(15) C. M. Sorenson and A. Eastman (1988). Influence of cis-diamminedichloroplatinum(II) on DNA synthesis and cell cycle progression in excision repair proficient and deficient Chinese hamster ovary cells. *Cancer Res.*, **48**, 6703-6707.
(16) S. A. Jelinsky and L. D. Samson (1999). Global response of Saccharomyces cerevisiae to an alkylating agent. *Proc. Natl. Acad. Sci. U. S. A.*, **96**, 1486-1491.
(17) J.-C. Huang, D. B. Zamble, J. T. Reardon, S. J. Lippard and A. Sancar (1994). HMG-domain proteins specifically inhibit the repair of the major DNA adduct of the anticancer drug cisplatin by human excision nuclease. *Proc. Natl. Acad. Sci. U. S. A.*, **91**, 10394-10398.
(18) M. F. Pera, F. Friedlos, J. Mills and J. J. Roberts (1987). Inherent sensitivity of cultured human embryonal carcinoma cells to adducts of cis-diamminedichloroplatinum(II) on DNA. *Cancer Res.*, **47**, 6810-6813.
(19) J. Q. Svejstrup (2002). Mechanisms of transcription-coupled DNA repair. *Nature Reviews Molecular Cell Biology*, **3**, 21-29.
(20) O. V. Tsodikov, D. Ivanov, B. Orelli, L. Staresincic, I. Shoshani, R. Oberman, O. D. Schaerer, G. Wagner and T. Ellenberger (2007). Structural basis for the recruitment of ERCC1-XPF to nucleotide excision repair complexes by XPA. *EMBO J.*, **26**, 4768-4776.
(21) D. B. Zamble, D. Mu, J. T. Reardon, A. Sancar and S. J. Lippard (1996). Repair of Cisplatin-DNA Adducts by the Mammalian Excision Nuclease. *Biochemistry*, **35**, 10004-10013.

(22) D. B. Zamble, Y. Mikata, C. H. Eng, K. E. Sandman and S. J. Lippard (2002). Testis-specific HMG-domain protein alters the responses of cells to cisplatin. *J. Inorg. Biochem.*, **91**, 451-462.
(23) Y. Jung, Y. Mikata and S. J. Lippard (2001). Kinetic studies of the TATA-binding protein interaction with cisplatin-modified DNA. *J. Biol. Chem.*, **276**, 43589-43596.
(24) J. Kasparkova, S. Pospisilova and V. Brabec (2001). Different recognition of DNA modified by antitumor cisplatin and its clinically ineffective trans isomer by tumor suppressor protein p53. *J. Biol. Chem.*, **276**, 16064-16069.
(25) C. X. Zhang, P. V. Chang and S. J. Lippard (2004). Identification of Nuclear Proteins that Interact with Platinum-Modified DNA by Photoaffinity Labeling. *J. Am. Chem. Soc.*, **126**, 6536-6537.
(26) E. R. Guggenheim, D. Xu, C. X. Zhang, P. V. Chang and S. J. Lippard (2009). Photoaffinity isolation and identification of proteins in cancer cell extracts that bind to platinum-modified DNA. *ChemBioChem*, **10**, 141-157.
(27) D. Wang, R. Hara, G. Singh, A. Sancar and S. J. Lippard (2003). Nucleotide Excision Repair from Site-Specifically Platinum-Modified Nucleosomes. *Biochemistry*, **42**, 6747-6753.
(28) S. D. Cline and P. C. Hanawalt (2003). Who's on first in the cellular response to DNA damage? *Nature Reviews Molecular Cell Biology*, **4**, 361-373.
(29) W. J. Heiger-Bernays, J. M. Essigmann and S. J. Lippard (1990). Effect of the antitumor drug cis-diamminedichloroplatinum(II) and related platinum complexes on eukaryotic DNA replication. *Biochemistry*, **29**, 8461-8466.
(30) K. M. Comess, J. N. Burstyn, J. M. Essigmann and S. J. Lippard (1992). Replication inhibition and translesion synthesis on templates containing site- specifically placed cis-diamminedichloroplatinum(II) DNA adducts. *Biochemistry*, **31**, 3975-3990.
(31) A. L. Pinto and S. J. Lippard (1985). Sequence-dependent termination of in vitro DNA synthesis by cis- and trans-diamminedichloroplatinum(II). *Proc. Natl. Acad. Sci. U. S. A.*, **82**, 4616-4619.
(32) Y. Jung and S. J. Lippard (2003). Multiple States of Stalled T7 RNA Polymerase at DNA Lesions Generated by Platinum Anticancer Agents. *J. Biol. Chem.*, **278**, 52084-52092.
(33) Y. Jung and S. J. Lippard (2006). RNA Polymerase II Blockage by Cisplatin-damaged DNA: stability and polyubiquitylation of stalled polymerase. *J. Biol. Chem.*, **281**, 1361-1370.
(34) K.-B. Lee, D. Wang, S. J. Lippard and P. A. Sharp (2002). Transcription-coupled and DNA damage-dependent ubiquitination of RNA polymerase II in vitro. *Proc. Natl. Acad. Sci. U. S. A.*, **99**, 4239-4244.
(35) M. J. Cleare and J. D. Hoeschele (1973). Studies on the Antitumor Activity of Group VIII Transition Metal Complexes. Part I. Platinum(II) Complexes. *Bioinorg. Chem.*, **2**, 187-210.
(36) B. Rosenberg (1980). Clinical aspects of platinum anticancer drugs. *Met. Ions Biol. Syst.*, **11**, 127-196.
(37) C. N. Sternberg, P. Whelan, J. Hetherington, B. Paluchowska, P. H. T. J. Slee, K. Vekemans, P. Van Erps, C. Theodore, O. Koriakine, T. Oliver, D. Lebwohl, M. Debois, A. Zurlo and L. Collette (2005). Phase III Trial of Satraplatin, an Oral Platinum plus

Prednisone vs. Prednisone alone in Patients with Hormone-Refractory Prostate Cancer. *Oncology*, **68**, 2-9.
(38) M. Herper In *Forbes*; Online Edition. Available at: http://www.forbes.com/2008/08/06/pharmaceuticals-fda-biz-healthcare-cx_mh_0807fda.html ed., 2008.
(39) L. Kelland (2007). The resurgence of platinum-based cancer chemotherapy. *Nat. Rev. Cancer*, **7**, 573-584.
(40) A. P. Silverman, W. Bu, S. M. Cohen and S. J. Lippard (2002). 2.4-.ANG. Crystal Structure of the Asymmetric Platinum Complex {Pt(ammine)(cyclohexylamine)}2+ Bound to a Dodecamer DNA Duplex. *J. Biol. Chem.*, **277**, 49743-49749.
(41) J. T. Reardon, A. Vaisman, S. G. Chaney and A. Sancar (1999). Efficient nucleotide excision repair of cisplatin, oxaliplatin, and bis-acetoammine-dichloro-cyclohexylamine-platinum(IV) (JM216) platinum intrastrand DNA diadducts. *Cancer Res.*, **59**, 3968-3971.
(42) J. Holford, S. Y. Sharp, B. A. Murrer, M. Abrams and L. R. Kelland (1998). In vitro circumvention of cisplatin resistance by the novel sterically hindered platinum complex AMD473. *Br. J. Cancer*, **77**, 366-373.
(43) N. Farrell In *Metal Ions in Biological Systems.*; Sigel, H., Ed.; Marcel Dekker Inc., New York: New York, 2004; Vol. 42, pp 251-296.
(44) J. D. Roberts, J. Peroutka, G. Beggiolin, C. Manzotti, L. Piazzoni and N. Farrell (1999). Comparison of cytotoxicity and cellular accumulation of polynuclear platinum complexes in L1210 murine leukemia cell lines. *J. Inorg. Biochem.*, **77**, 47-50.
(45) D. I. Jodrell, T. R. J. Evans, W. Steward, D. Cameron, J. Prendiville, C. Aschele, C. Noberasco, M. Lind, J. Carmichael, N. Dobbs, G. Camboni, B. Gatti and F. De Braud (2004). Phase II studies of BBR3464, a novel tri-nuclear platinum complex, in patients with gastric or gastro-oesophageal adenocarcinoma. *Eur. J. Cancer*, **40**, 1872-1877.
(46) L. S. Hollis, A. R. Amundsen and E. W. Stern (1989). Chemical and biological properties of a new series of cis-diammineplatinum(II) antitumor agents containing three nitrogen donors: cis-[Pt(NH3)2(N-donor) Cl]+. *J. Med. Chem.*, **32**, 128-136.
(47) T. Kapp, A. Dullin and R. Gust (2006). Mono- and Polynuclear [Alkylamine]platinum(II) Complexes of [1,2-Bis(4-fluorophenyl)ethylenediamine]platinum(II): Synthesis and Investigations on Cytotoxicity, Cellular Distribution, and DNA and Protein Binding. *J. Med. Chem.*, **49**, 1182-1190.
(48) N. Farrell, Y. Qu, U. Bierbach, M. Valsecchi and E. Menta (1999). Structure-activity relationships within di- and trinuclear platinum phase-I clinical anticancer agents. *Cisplatin*, 479-496.
(49) U. Bierbach, T. W. Hambley and N. Farrell (1998). Modification of Platinum(II) Antitumor Complexes with Sulfur Ligands. 1. Synthesis, Structure, and Spectroscopic Properties of Cationic Complexes of the Types [PtCl(diamine)(L)]NO3 and [{PtCl(diamine)}2(L-L)](NO3)2 (L = Monofunctional Thiourea Derivative; L-L = Bifunctional Thiourea Derivative). *Inorg. Chem.*, **37**, 708-716.
(50) U. Bierbach, J. D. Roberts and N. Farrell (1998). Modification of Platinum(II) Antitumor Complexes with Sulfur Ligands. 2. Reactivity and Nucleotide Binding Properties of Cationic Complexes of the Types [PtCl(diamine)(L)]NO3 and [{PtCl(diamine)}2(L-L)](NO3)2 (L = Monofunctional Thiourea Derivative; L-L =

Bifunctional Thiourea Derivative) in Relation to Their Cytotoxicity. *Inorg. Chem.*, **37**, 717-723.
(51) Y. Najajreh, J. M. Perez, C. Navarro-Ranninger and D. Gibson (2002). Novel Soluble Cationic trans-Diaminedichloroplatinum(II) Complexes that Are Active against Cisplatin Resistant Ovarian Cancer Cell Lines. *J. Med. Chem.*, **45**, 5189-5195.
(52) Z. Ma, G. Saluta, G. L. Kucera and U. Bierbach (2008). Effect of linkage geometry on biological activity in thiourea- and guanidine-substituted acridines and platinum-acridines. *Bioorg. Med. Chem. Lett.*, **18**, 3799-3801.
(53) Z. Ma, J. R. Choudhury, M. W. Wright, C. S. Day, G. Saluta, G. L. Kucera and U. Bierbach (2008). A Non-Cross-Linking Platinum-Acridine Agent with Potent Activity in Non-Small-Cell Lung Cancer. *J. Med. Chem.*, **51**, 7574-7580.
(54) Y. Najajreh, E. Khazanov, S. Jawbry, Y. Ardeli-Tzaraf, J. M. Perez, J. Kasparkova, V. Brabec, Y. Barenholz and D. Gibson (2006). Cationic Nonsymmetric Transplatinum Complexes with Piperidinopiperidine Ligands. Preparation, Characterization, in Vitro Cytotoxicity, in Vivo Toxicity, and Anticancer Efficacy Studies. *J. Med. Chem.*, **49**, 4665-4673.
(55) K. S. Lovejoy, R. C. Todd, S. Zhang, M. S. McCormick, J. A. D'Aquino, J. T. Reardon, A. Sancar, K. M. Giacomini and S. J. Lippard (2008). cis-diammine(pyridine)chloroplatinum(II), a monofunctional platinum(II) antitumor agent: uptake, structure, function, and prospects. *Proc. Natl. Acad. Sci. U. S. A.*, **105**, 8902-8907.
(56) N. Margiotta, G. Natile, F. Capitelli, P. Fanizzi Francesco, A. Boccarelli, P. De Rinaldis, D. Giordano and M. Coluccia (2006). Sterically hindered complexes of platinum(II) with planar heterocyclic nitrogen donors. A novel complex with 1-methyl-cytosine has a spectrum of activity different from cisplatin and is able of overcoming acquired cisplatin resistance. *J. Inorg. Biochem.*, **100**, 1849-1857.
(57) Y. Zhao, W. He, P. Shi, J. Zhu, L. Qiu, L. Lin and Z. Guo (2006). A positively charged trinuclear 3N-chelated monofunctional platinum complex with high DNA affinity and potent cytotoxicity. *J. Chem. Soc., Dalton Trans.*, 2617-2619.
(58) Y. Ma, C. S. Day and U. Bierbach (2005). Synthesis, structure, and reactivity of monofunctional platinum(II) and palladium(II) complexes containing the sterically hindered ligand 6-(methylpyridin-2-yl)acetate. *J. Inorg. Biochem.*, **99**, 2013-2023.
(59) S. W. Annie Bligh, A. Bashall, C. Garrud, M. McPartlin, N. Wardle, K. White, S. Padhye, V. Barve and G. Kundu (2003). Reaction of (C-(6-aminomethyl-pyridin-2-yl)methylamine)chloroplatinum(II) with nucleosides and its biological activity. *J. Chem. Soc., Dalton Trans.*, 184-188.
(60) Y. Najajreh, Y. Ardeli-Tzaraf, J. Kasparkova, P. Heringova, D. Prilutski, L. Balter, S. Jawbry, E. Khazanov, J. M. Perez, Y. Barenholz, V. Brabec and D. Gibson (2006). Interactions of Platinum Complexes Containing Cationic, Bicyclic, Nonplanar Piperidinopiperidine Ligands with Biological Nucleophiles. *J. Med. Chem.*, **49**, 4674-4683.
(61) Q. Ren and I. T. Paulsen (2005). Comparative analyses of fundamental differences in membrane transport capabilities in prokaryotes and eukaryotes. *PLoS Comput. Biol.*, **1**, 190-201.
(62) W. Busch and M. H. Saier, Jr. (2002). The Transporter Classification (TC) system, 2002. *Crit. Rev. Biochem. Mol. Biol.*, **37**, 287-337. Database at http://www.tcdb.org.

(63) M. J. Dresser, M. K. Leabman and K. M. Giacomini (2001). Transporters involved in the elimination of drugs in the kidney: organic anion transporters and organic cation transporters. *J. Pharm. Sci.*, **90**, 397-421.
(64) N. Kitada, K. Takara, T. Minegaki, C. Itoh, M. Tsujimoto, T. Sakaeda and T. Yokoyama (2008). Factors affecting sensitivity to antitumor platinum derivatives of human colorectal tumor cell lines. *Cancer Chemother. Pharmacol.*, **62**, 577-584.
(65) J. Müller, K. S. Lips, L. Metzner, R. H. H. Neubert, H. Koepsell and M. Brandsch (2005). Drug specificity and intestinal membrane localization of human organic cation transporters (OCT). *Biochem. Pharmacol.*, **70**, 1851-1860.
(66) L. Zhang, C. M. Brett and K. M. Giacomini (1998). Role of Organic Cation Transporters in Drug Absorption and Elimination. *Annu. Rev. Pharmacol. Toxicol.*, **38**, 431-460.
(67) J. E. van Montfoort, B. Hagenbuch, G. M. M. Groothuis, H. Koepsell, P. J. Meier and D. K. F. Meijer (2003). Drug uptake systems in liver and kidney. *Curr. Drug Metab.*, **4**, 185-211.
(68) R. Monteiro, C. Calhau, F. Martel, A. Faria, N. Mateus and I. Azevedo (2005). Modulation of MPP+ uptake by TEA and some of its components in Caco-2 cells. *Naunyn-Schmiedeberg's Arch. Pharmacol.*, **372**, 147-152.
(69) H. Koepsell, K. Lips and C. Volk (2007). Polyspecific organic cation transporters: structure, function, physiological roles, and biopharmaceutical implications. *Pharm. Res.*, **24**, 1227-1251.
(70) O. Aronov, A. T. Horowitz, A. Gabizon and D. Gibson (2003). Folate-Targeted PEG as a Potential Carrier for Carboplatin Analogs. Synthesis and in Vitro Studies. *Bioconjug. Chem.*, **14**, 563-574.
(71) S. Dhar, Z. Liu, J. Thomale, H. Dai and S. J. Lippard (2008). Targeted Single-Wall Carbon Nanotube-Mediated Pt(IV) Prodrug Delivery Using Folate as a Homing Device. *J. Am. Chem. Soc.*, **130**, 11467-11476.
(72) R. Safaei (2006). Role of copper transporters in the uptake and efflux of platinum containing drugs. *Cancer Lett.*, **234**, 34-39.
(73) P. Kabolizadeh, J. Ryan and N. Farrell (2007). Differences in the cellular response and signaling pathways of cisplatin and BBR3464 ([[trans-PtCl(NH3)(2)]2mu-(trans-Pt(NH3)(2)(H2N(CH2)(6)-NH2)2)]4+) influenced by copper homeostasis. *Biochem. Pharmacol.*, **73**, 1270-1279.
(74) J. Altman, T. Castrillo, W. Beck, G. Bernhardt and H. Schoenenberger (1991). Metal complexes with biologically important ligands. 62. Platinum(II) complexes of 3-(2-aminoethoxy)estrone and -estradiol. *Inorg. Chem.*, **30**, 4085-4088.
(75) O. Gandolfi, H. C. Apfelbaum, Y. Migron and J. Blum (1989). Syntheses of cis-dichlorodiammineplatinum analogs having steroidal hormones bound to the metal atom via malonato bridges. *Inorg. Chim. Acta*, **161**, 113-123.
(76) A. Jackson, J. Davis, R. J. Pither, A. Rodger and M. J. Hannon (2001). Estrogen-derived steroidal metal complexes: agents for cellular delivery of metal centers to estrogen receptor-positive cells. *Inorg. Chem.*, **40**, 3964-3973.
(77) Q. He, C. H. Liang and S. J. Lippard (2000). Steroid hormones induce HMG1 overexpression and sensitize breast cancer cells to cisplatin and carboplatin. *Proc. Natl. Acad. Sci. U. S. A.*, **97**, 5768-5772.

(78) Y. Jung and S. J. Lippard (2007). Direct Cellular Responses to Platinum-Induced DNA Damage. *Chem. Rev.*, **107**, 1387-1407.
(79) K. Y. Chau, H. Y. P. Lam and K. L. D. Lee (1998). Estrogen treatment induces elevated expression of HMG1 in MCF-7 cells. *Exp. Cell. Res.*, **241**, 269-272.
(80) V. Boonyaratanakornkit, V. Melvin, P. Prendergast, M. Altmann, L. Ronfani, M. E. Bianchi, L. Taraseviciene, S. K. Nordeen, E. A. Allegretto and D. P. Edwards (1998). High-Mobility Group Chromatin Proteins 1 and 2 Functionally Interact with Steroid Hormone Receptors to Enhance Their DNA Binding in Vitro and Transcriptional Activity in Mammalian Cells. *Mol. Cell. Biol.*, **18**, 4471-4487.
(81) G. Nagatani, M. Nomoto, H. Takano, T. Ise, K. Kato, T. Imamura, H. Izumi, K. Makishima and K. Kohno (2001). Transcriptional activation of the human HMG1 gene in cisplatin-resistant human cancer cells. *Cancer Res.*, **61**, 1592-1597.
(82) J. E. Ellerman, C. K. Brown, M. de Vera, H. J. Zeh, T. Billiar, A. Rubartelli and M. T. Lotze (2007). Masquerader: High Mobility Group Box-1 and Cancer. *Clin. Cancer Res.*, **13**, 2836-2848.
(83) T. Bonaldi, F. Talamo, P. Scaffidi, D. Ferrera, A. Porto, A. Bachi, A. Rubartelli, A. Agresti and M. E. Bianchi (2003). Monocytic cells hyperacetylate chromatin protein HMGB1 to redirect it towards secretion. *EMBO J.*, **22**, 5551-5560.
(84) M. Bustin, F. Catez and J.-H. Lim (2005). The dynamics of histone H1 function in chromatin. *Mol. Cell*, **17**, 617-620.
(85) F. Catez, H. Yang, K. J. Tracey, R. Reeves, T. Misteli and M. Bustin (2004). Network of dynamic interactions between histone H1 and high-mobility-group proteins in chromatin. *Mol. Cell. Biol.*, **24**, 4321-4328.
(86) G. Hoppe, K. E. Talcott, S. K. Bhattacharya, J. W. Crabb and J. E. Sears (2006). Molecular basis for the redox control of nuclear transport of the structural chromatin protein Hmgb1. *Exp. Cell Res.*, **312**, 3526-3538.
(87) L. Ulloa and D. Messmer (2006). High-mobility group box 1 (HMGB1) protein: Friend and foe. *Cytokine Growth Factor Rev.*, **17**, 189-201.
(88) Q. Zhang and Y. Wang (2008). High mobility group proteins and their post-translational modifications. *Biochim. Biophys. Acta Protein Proteonomics*, **1784**, 1159-1166.
(89) I. E. Dumitriu, P. Baruah, A. A. Manfredi, M. E. Bianchi and P. Rovere-Querini (2005). HMGB1: guiding immunity from within. *Trends Immunol.*, **26**, 381-387.
(90) A. M. Schmidt, S. D. Yan, S. F. Yan and D. M. Stern (2001). The multiligand receptor RAGE as a progression factor amplifying immune and inflammatory responses. *J. Clin. Invest.*, **108**, 949-955.
(91) H. J. Huttunen, C. Fages and H. Rauvala (1999). Receptor for advanced glycation end products (RAGE)-mediated neurite outgrowth and activation of NF-kB require the cytoplasmic domain of the receptor but different downstream signaling pathways. *J. Biol. Chem.*, **274**, 19919-19924.
(92) A. Taguchi, D. C. Blood, G. Del Toro, A. Canet, D. C. Lee, W. Qu, N. Tanji, Y. Lu, E. Lalla, C. Ful, M. A. Hofmann, T. Kislinger, M. Ingram, A. Lu, H. Tanaka, O. Hori, S. Ogawa, D. M. Sternm and A. M. Schmidt (2000). Blockade of RAGE-amphoterin signalling suppresses tumour growth and metastases. *Nature*, **405**, 354-360.
(93) R. Catena, E. Escoffier, C. Caron, S. Khochbin, I. Martianov and I. Davidson (2009). HMGB4, a novel member of the HMGB family, is preferentially expressed in the

mouse testis and localizes to the basal pole of elongating spermatids. *Biol. Reprod.*, **80**, 358-366.
(94) K.-B. Lee and J. O. Thomas (2000). The Effect of the Acidic Tail on the DNA-binding Properties of the HMG1,2 Class of Proteins: Insights from Tail Switching and Tail Removal. *J. Mol. Biol.*, **304**, 135-149.

Chapter 2

Structure-Activity Relationship for the Uptake of Platinum(II) Compounds by Human Organic Cation Transporters

This chapter consists of material from a published work (*Cancer Research* **2006**, 66 (17), 8847-8857).[1]

Introduction

Platinum-based drugs are among the most active anticancer agents and cisplatin represents one of the three most widely used cancer chemotherapeutics.[2] Although cisplatin is effective against a number of solid tumors, especially testicular and ovarian cancer, its clinical use is limited because of its toxic effects as well as the intrinsic and acquired resistance of some tumors to this drug.[3] To overcome these limitations, platinum analogs with lower toxicity and greater activity in cisplatin-resistant tumors have been developed and tested, resulting in the approval of carboplatin and oxaliplatin in the United States (see Figure 2.1). Carboplatin has the advantage of being less

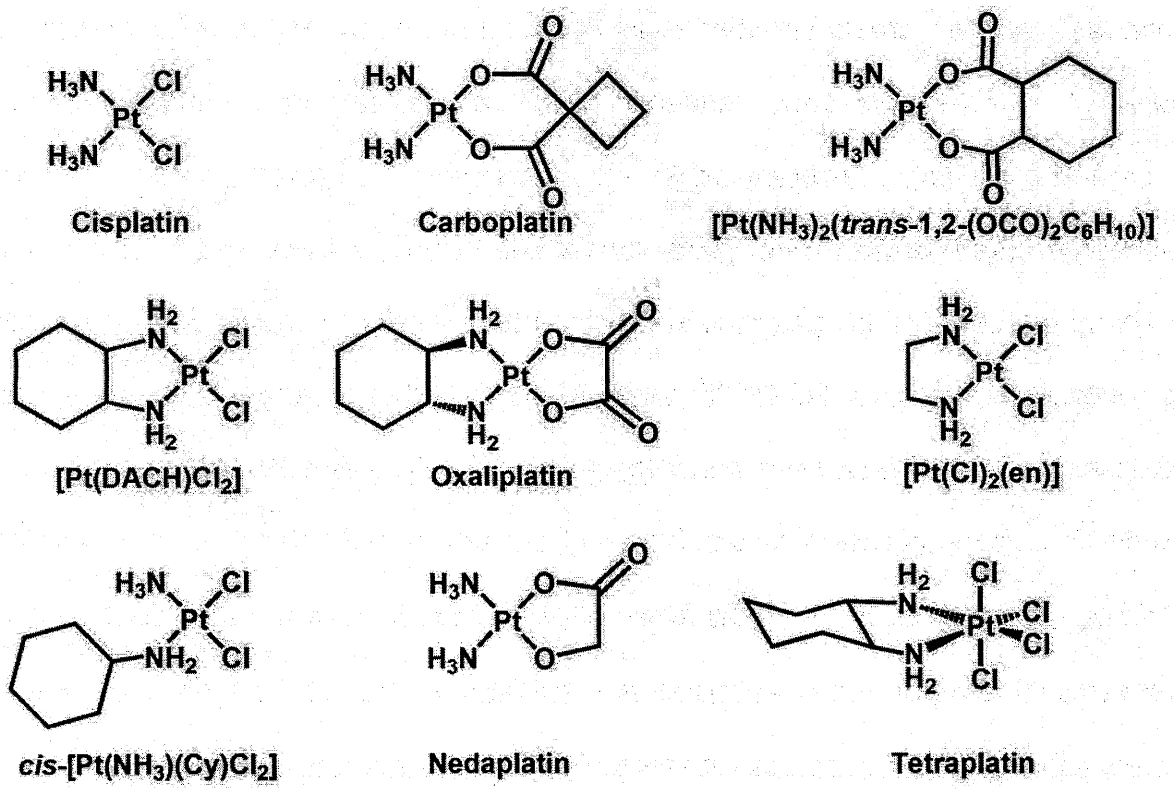

Figure 2.1. Chemical structures of platinum compounds.

nephrotoxic, but its cross-resistance with cisplatin limits its application in otherwise cisplatin-treatable diseases.[3] Oxaliplatin, however, exhibits a different anticancer spectrum from that of cisplatin.[4,5] It has been approved as the first or second line therapy in combination with 5-fluorouracil/leucovorin for advanced colorectal cancer, for which cisplatin and carboplatin are essentially inactive.[6] In spite of their distinct antitumor specificities, cisplatin and oxaliplatin, as well as other platinum compounds, share similar mechanisms of action. In particular, their cytotoxicity arises primarily from covalent binding to DNA after aquation to form mono- and diaqua complexes.[7,8] This chemistry initiates a series of biochemical cascades, eventually leading to cell death.[7,9]

Because cisplatin and oxaliplatin target similar DNA sites for binding and form similar types of DNA adducts,[10-12] mainly 1,2- and 1,3-intrastrand cross-links involving purine nucleotides, the mechanisms responsible for their distinct tumor specificities may involve events other than their interaction with and binding to DNA. Studies aiming to identify such mechanisms have focused largely on the cellular processing of cisplatin- and oxaliplatin-DNA adducts.[13,14] However, differences in the mechanism(s) controlling the cellular uptake and efflux of these platinum compounds, although rarely investigated, could also be important, since reduced intracellular accumulation is the most common observation in cisplatin-resistant cells.[15,16]

Recent studies suggest a direct involvement of the human copper influx transporter, Ctr1, in the cellular uptake of cisplatin, carboplatin and oxaliplatin to a varying extent.[17] Studies in tumor cell lines suggest, however, that Ctr1 may

not affect the formation and corresponding cytotoxicity of cisplatin-DNA adducts.[18] The human copper efflux transporters, ATP7B and ATP7A, also recognize these platinum compounds[19,20] and their elevated expression has been associated with cisplatin resistance.[21-24] The importance of these interactions in modulating the differential activity and tumor specificity of the platinum compounds is currently unknown.

The organic cation transporters (OCTs), OCT1 (solute carrier 22A1, SLC22A1), OCT2 (SLC22A2), and OCT3 (SLC22A3) are in the class of plasma membrane transporters belonging to the solute carrier (SLC) 22A family. The OCTs mediate intracellular uptake of a broad range of structurally diverse organic cations with molecular weights generally lower than 400 Da.[25] Substrates of OCTs include endogenous compounds, such as choline, creatinine and monoamine neurotransmitters, and a variety of xenobiotics such as tetraethylammonium (TEA, a prototypic organic cation), 1-methy-4-phenylpyridinium (MPP^+, a neurotoxin) and clinically used drugs such as metformin, cimetidine and amantadine.[25] In humans, OCT1 is primarily expressed in the liver[26,27] and less so in the intestine,[28] whereas OCT2 is predominantly expressed in the kidney.[27] OCT3 is expressed in many tissues including placenta, heart, liver and skeletal muscle.[29,30] The expression of the OCTs has also been detected in a number of human cancer cell lines.[31] The interaction of cisplatin with human OCTs has been investigated and the results are discordant.[32,33] Previous studies suggest that cisplatin is not a substrate of human OCT1 or OCT2,[32] whereas more recent work indicates that the drug

interacts with human OCT2 but not OCT1.[33] It is not known whether oxaliplatin or carboplatin interacts with these transporters, however, or whether such interactions contribute to their cytotoxicities and differential tumor specificities.

The goals of the present study were to characterize the interaction of cisplatin, carboplatin and oxaliplatin with human OCT1, OCT2 and OCT3; to determine whether the OCTs play a role in the cytotoxicity of these and related platinum compounds; to determine whether interactions with OCTs contribute to the differential antitumor specificity of oxaliplatin versus cisplatin; and to understand in a broader context the underlying chemical principles that determine these differences. Our data indicate that OCT1 and OCT2 play a critical role in mediating the uptake and consequent cytotoxicity of oxaliplatin, but not cisplatin or carboplatin. Structure-activity relationship studies suggest that the 1,2-diaminocyclohexane (DACH) moiety of oxaliplatin is an important pharmacophore for its interaction with the OCTs and that an organic component on the non-leaving portion of the platinum complexes is essential. Finally, our experiments suggest that interactions with OCT1 and OCT2 are likely to be important contributors to the sensitivity of colorectal cancer to oxaliplatin.

Results

OCT Expression and Function in Stably Transfected Cell Lines

The expression and function of human OCTs in the stably transfected cells was confirmed by RT-PCR and by examining the uptake of the model OCT substrates (TEA for OCT1 and OCT2, MPP^+ for OCT3). The expression of the

mRNA transcripts of OCT1, OCT2 and OCT3 and uptake of model compounds were clearly much higher in OCT-transfected cells (MDCK-hOCT1, HEK-hOCT2 or HEK-hOCT3) in comparison to empty vector-transfected control counterparts (MOCK cells) (Figures 2.7 and 2.8). OCT inhibitors (disopyramide (120 μM) for OCT1, cimetidine (1.5 mM) for OCT2 and OCT3) substantially decreased the uptake of the model compounds in the OCT-transfected cells ($p < 0.001$) (Figure 2.8).

Effect of OCTs on the Cytotoxicity of Cisplatin, Carboplatin and Oxaliplatin

The IC_{50} values of oxaliplatin, determined in MTT assays, in MDCK-MOCK cells after different time periods (7, 24 and 72 hr) of drug exposure were all significantly higher than those in MDCK-hOCT1 cells. Resistance factors (RF), defined as the ratio of the IC_{50} value in MOCK cells to that in the corresponding OCT-transfected cells, ranged from 5.73 to 8.48 ($p < 0.01$ or $p < 0.001$; Table 2.1A and Figure 2.2A). In contrast, the IC_{50} values of both cisplatin and carboplatin were similar in the OCT1-transfected and in the MDCK-MOCK cells with RF values close to unity ($p > 0.05$) (Table 2.1A). Co-incubation with a known OCT1 inhibitor, disopyramide (150 μM), substantially increased the IC_{50} value of oxaliplatin in MDCK-hOCT1 (control vs. disopyramide-treated: 3.79 ± 1.57 μM vs. 22.8 ± 10.5 μM) by 6.01-fold ($p < 0.05$) with little effect in MDCK-MOCK (control vs. disopyramide-treated: 30.4 ± 9.28 vs. 32.2 ± 13.0 μM, $p > 0.05$) tested in parallel (Figure 2.2D). Disopyramide itself did not manifest any cytotoxicity up to a concentration of 400 μM under the same test conditions (data not shown).

A. Cytotoxicity, expressed as IC_{50}, of the platinum drugs in MDCK-MOCK and MDCK-hOCT1 cells.

Platinum Drugs	Drug Exposure Time (hour)	MDCK-MOCK (μM)	MDCK-hOCT1 (μM)	RF
cisplatin	7	19.6 ± 7.56	15.4 ± 2.84	1.27
carboplatin	7	258 ± 86.3	227 ± 85.8	1.13
oxaliplatin	7	33.0 ± 9.12	3.89 ± 1.30	8.48***
oxaliplatin	24	14.3 ± 5.55	1.79 ± 0.58	7.95**
oxaliplatin	72	9.64 ± 1.85	1.68 ± 0.27	5.73***

B. Cytotoxicity, expressed as IC_{50}, of the platinum drugs in HEK-MOCK and HEK-hOCT2 cells.

Platinum Drugs	Drug Exposure Time (hour)	HEK-MOCK (μM)	HEK-hOCT2 (μM)	RF
cisplatin	7	2.95 ± 0.23	1.32 ± 0.18	2.23***
carboplatin	7	110 ± 46.3	61.6 ± 46.3	1.78
oxaliplatin	7	2.99 ± 1.51	0.039 ± 0.025	76.7**
oxaliplatin	24	1.50 ± 0.69	0.02 ± 0.001	73.8*
oxaliplatin	72	0.93 ± 0.056	0.019 ± 0.004	48.4***

C. Cytotoxicity, expressed as IC_{50}, of the platinum drugs in HEK-MOCK and HEK-hOCT3 cells.

Platinum Drugs	Drug Exposure Time (hour)	HEK-MOCK (μM)	HEK-hOCT3 (μM)	RF
cisplatin	7	2.83 ± 0.90	2.44 ± 0.71	1.16
carboplatin	7	84.8 ± 9.71	48.1 ± 23.4	1.76
oxaliplatin	7	1.47 ± 0.28	2.22 ± 0.41	0.66
oxaliplatin	24	0.47 ± 0.05	0.62 ± 0.19	0.75
oxaliplatin	72	0.47 ± 0.12	0.69 ± 0.19	0.68

*: $p < 0.05$; **: $p < 0.01$ and ***: $p < 0.001$

Table 2.1. The IC_{50} values (μM) of cisplatin, carboplatin and oxaliplatin in (A) human OCT1- (B) OCT2- and (C) OCT3-transfected cell lines were determined in parallel with those in the corresponding MOCK cells using MTT assay as described in the Experimental Procedures. Briefly, the cells were seeded in 96-well plates at a density of 5,000 cells/well for the transfected MDCK cells or 12,000 cells/well for the transfected HEK 293 cells. The platinum drugs were added on the following day. After the specified time periods of drug exposure, the drug-containing medium was replaced with fresh, drug-free medium, and the incubation was continued for a total of 72 hours (starting from the time when the drug was added). After incubation, the cell growth was determined by an MTT assay. Data are expressed as mean ± SD from 3 to 6 independent experiments with each performed in quadruplicate. The resistance factor (RF) was defined as the ratio of the mean IC_{50} value in the MOCK cells to that in the OCT-transfected cells.

These results indicate that OCT1 enhances the cytotoxicity of oxaliplatin, but not that of cisplatin or carboplatin. A similar pattern of observations was obtained in human OCT2-transfected cells, but the increase in oxaliplatin cytotoxicity was

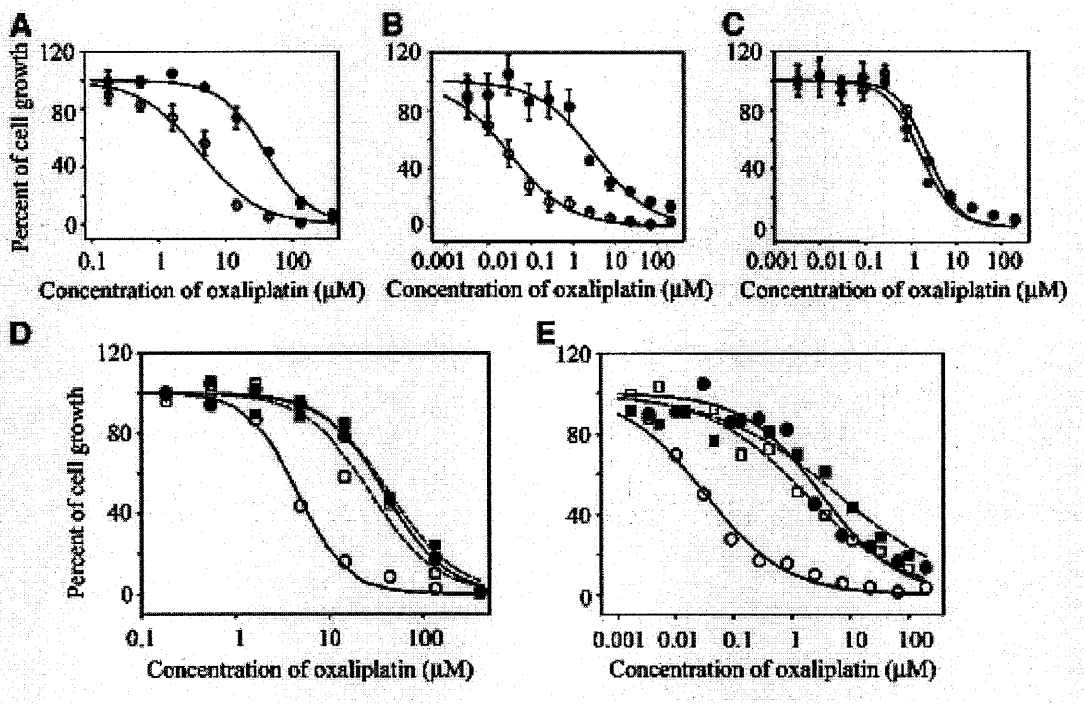

Figure 2.2. The cytotoxicity of oxaliplatin in (A) OCT1-, (B) OCT2- and (C) OCT3-transfected cells (○) and in the corresponding MOCK cells (●) was determined as described in the Experimental Procedures. Cells were seeded in 96-well plates at a density of 5,000 cells/well for the transfected MDCK cells and 12,000 cells/well for the transfected HEK 293 cells and exposed to the test compounds for 7 hours on the following day. After a total of 72 hours, cell growth was determined by an MTT assay. In addition, the cytotoxicity of oxaliplatin in (D) OCT1- and (E) OCT2-transfected cells (open symbols) and in the corresponding empty vector-transfected cells (MOCK cells) (solid symbols) in the presence (squares) or absence (circles) of an OCT inhibitor (disopyramide for OCT1, and cimetidine for OCT2) was also simultaneously determined in a similar fashion. When the OCT inhibitors were used, disopyramide (150 μM) or cimetidine (1.5 mM) was added to the incubation medium immediately before the addition of oxaliplatin. The lines represent the predicted data obtained by fitting the observed data using WinNonlin as described in the Experimental Procedures. Presented are the data from a typical experiment. Three to six independent experiments were performed and similar results were obtained. For clarity, the standard deviation bars in panel D and E were eliminated.

much more pronounced (Figure 2.2B). The IC_{50} values of oxaliplatin after different time periods (7, 24 and 72 hr) of exposure were all markedly greater in

HEK-MOCK cells than in HEK-OCT2 cells with RF values ranging from 48.4 to 76.7 ($p < 0.05$ to $p < 0.001$) (Table 2.1B and Figure 2.2B). However, the IC_{50} values of cisplatin and carboplatin were only slightly greater in HEK-MOCK cells than in HEK-OCT2 cells with RF values around 2 after 7-hour drug exposure (Table 2.1B). Co-incubation with an OCT inhibitor, cimetidine (1.5 mM), dramatically increased the oxaliplatin IC_{50} (control vs. cimetidine-treated: 0.039 ± 0.025 μM vs. 2.81 ± 1.63 μM) by 72-fold ($p < 0.05$) in HEK-hOCT2 cells, with only a 3.18-fold increase in HEK-MOCK cells (control vs. cimetidine-treated: 2.99 ± 1.51 vs. 9.50 ± 2.95 μM, $p < 0.05$) (Figure 2.2E). Cimetidine itself did not exhibit cytotoxicity up to a concentration of 5 mM under the same test conditions (data not shown). These results indicate that OCT2 markedly enhances the cytotoxicity of oxaliplatin with only slight effects on the cytotoxicities of cisplatin and carboplatin. In contrast to OCT1 and OCT2, overexpression of human OCT3 did not affect the cytotoxicity of any of the platinum drugs (Table 2.1C and Figure 2.2C).

Platinum Accumulation Rates in Cells After Exposure to Cisplatin, Carboplatin and Oxaliplatin

The cellular platinum accumulation rate after two hours of exposure to oxaliplatin (3 μM) was 2.90-fold higher ($p < 0.001$) in MDCK-hOCT1 cells (8.53 ± 0.52 pmol / (mg protein-hr)) than that in MDCK-MOCK cells (2.94 ± 0.11 pmol / (mg protein-hr)) (Figure 2.3A). Co-incubation with disopyramide (150 μM) resulted in a two-fold decrease in the rate of platinum accumulation in MDCK-hOCT1 cells (control vs. disopyramide-treated;

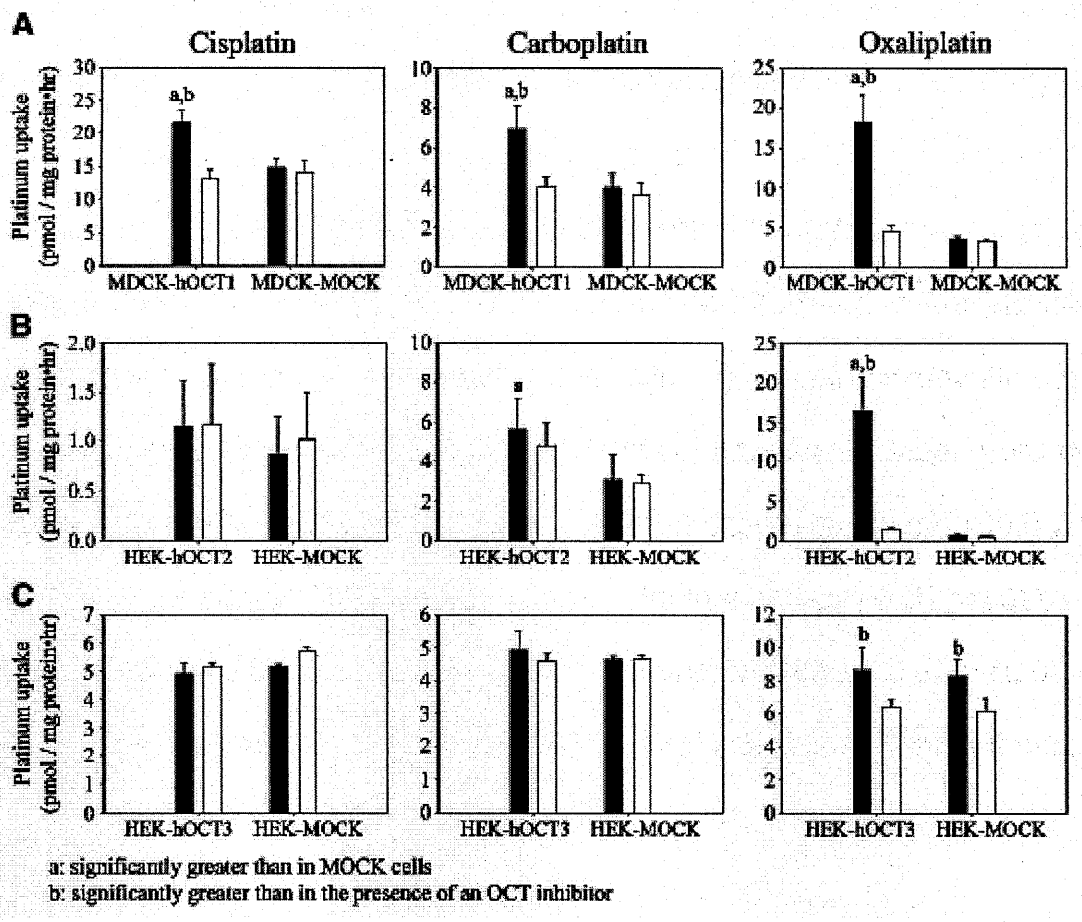

Figure 2.3. Cellular accumulation of platinum after 2-hour exposure to cisplatin, carboplatin and oxaliplatin. The cellular accumulation rates of platinum in (A) OCT1-, (B) OCT2- and (C) OCT3-transfected cells and in the corresponding MOCK cells after incubation with cisplatin, carboplatin and oxaliplatin in the presence (open bars) and absence (solid bars) of an OCT inhibitor (disopyramide for OCT1, cimetidine for OCT2 and OCT3) were determined as described in the Experimental Procedures. Briefly, (A) MDCK cells were incubated in the antibiotic-free medium containing cisplatin (3 μM), carboplatin (15 μM) or oxaliplatin (3 μM) at 37°C and 5% CO_2 for 2 hours. For the inhibitor studies, the incubation medium also contained disopyramide (150 μM). (B) HEK 293 cells were incubated in the antibiotic-free medium containing cisplatin (0.3 μM), carboplatin (10 μM) or oxaliplatin (0.3 μM) at 37°C and 5% CO_2 for 2 hours. For the inhibitor studies, the incubation medium also contained cimetidine (1.5 mM). (C) The study was performed similarly as (B) except that the concentrations of cisplatin, carboplatin and oxaliplatin in the incubation medium were 2 μM, 10 μM and 2 μM, respectively. After drug exposure, the cells were washed with ice-cold PBS three times and harvested by scraping and centrifugation. The cell-associated platinum was determined by ICP-MS and normalized for protein content. Data are expressed as mean ± SD from a single experiment performed in triplicate. Experiments were replicated for OCT1 and OCT2, and similar results were obtained.

8.53 ± 0.52 vs. 4.04 ± 0.04 pmol / (mg protein-hr), $p < 0.001$) with little effect in

MDCK-MOCK cells (control vs. disopyramide-treated; 2.94 ± 0.11 vs. 3.23 ± 0.31

pmol / (mg protein-hour), $p > 0.05$) (Figure 2.3A). However, the cellular accumulation rates of platinum after 2-hr exposure to cisplatin (3 μM) or carboplatin (15 μM) in MDCK-hOCT1 cells (cisplatin: 3.88 ± 0.15 pmol / (mg protein-hr)); carboplatin: 2.77 ± 0.36 pmol / (mg protein-hr)) were not significantly different from those in MDCK-MOCK cells (cisplatin: 3.70 ± 0.45 pmol / (mg protein-hr)); carboplatin: 2.22 ± 0.07 pmol / (mg protein-hr)) and were not inhibited by disopyramide (Figure 2.3A). These results indicate that human OCT1 contributes substantially to the uptake of oxaliplatin, but not cisplatin or carboplatin in OCT1-transfected cells. The platinum accumulation rate in HEK-hOCT2 (20.2 ± 1.54 pmol / (mg protein-hr)) was markedly higher (21.7-fold, $p < 0.001$) than that in HEK-MOCK cells and was substantially reduced in the presence of cimetidine (control vs. cimetidine; 20.2 ± 1.54 vs. 1.80 ± 0.13 pmol / (mg protein-hr)). However, the cellular accumulation rate of platinum in HEK-hOCT2 cells after 2-hr exposure to cisplatin (0.3 μM) or carboplatin (10 μM) (cisplatin: 0.738 ± 0.055 pmol / (mg protein-hr); carboplatin: 4.17 ± 0.18 pmol / (mg protein-hr)) was only modestly higher (1.38-fold for carboplatin, $p < 0.001$; 2.08-fold for cisplatin, $p < 0.01$) than that in HEK-MOCK cells. Co-incubation with cimetidine (1.5 mM) produced only a small decrease (less than 1.5-fold, $p < 0.01$) in platinum accumulation rate after exposure of HEK-hOCT2 cells to either cisplatin or carboplatin with little effect in HEK-MOCK cells. These results indicate that OCT2 plays a critical role in the uptake of oxaliplatin in the transfected cells with a much lower effect on the uptake of cisplatin or

carboplatin. In contrast to OCT1 and OCT2, OCT3 overexpression did not affect the uptake of any of these platinum drugs (Figure 2.3C).

Platinum-DNA Adduct Formation after 2-hr Exposure to Oxaliplatin

To determine whether the oxaliplatin taken up by cells via the human OCT1 and OCT2 transporters was available for DNA binding, we also measured platinum-DNA adduct formation after a 2-hr exposure to oxaliplatin (Figure 2.4). The platinum-DNA adduct level in MDCK-hOCT1 cells (0.0457 ± 0.0011pmol / μg DNA, r_b (ratio of bound platinum atoms per nucleotide) = 1.51 ± 0.04 × 10^{-5}) was 4.15-fold greater ($p < 0.001$) than that in MDCK-MOCK cells (0.0110 ± 0.0010 pmol / μg DNA, r_b = 3.63 ± 0.33 × 10^{-6}) after exposure to oxaliplatin (Figure 2.4A).

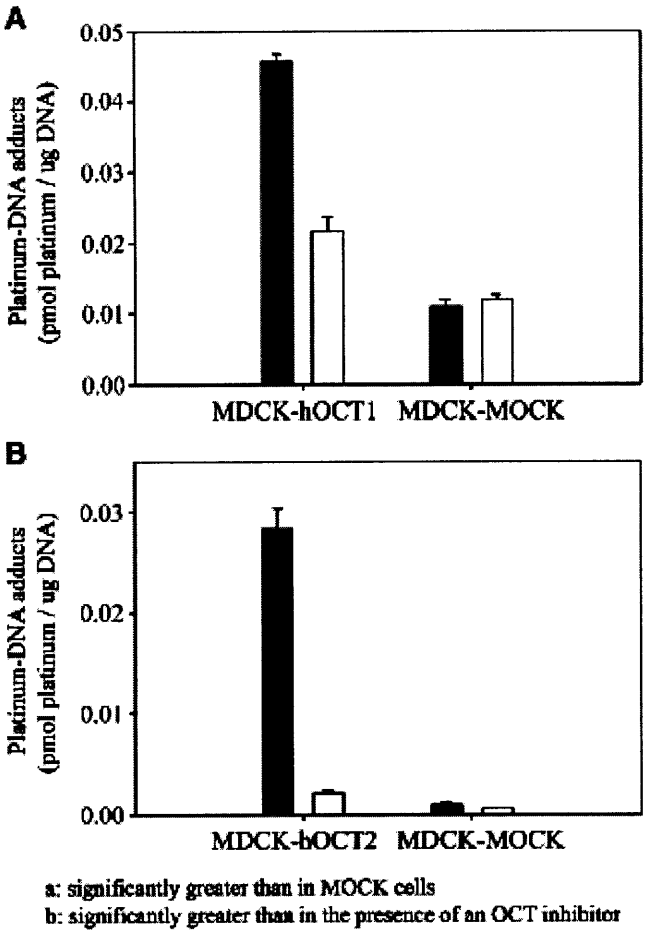

Figure 2.4. The content of platinum bound to DNA after 2-hr exposure to oxaliplatin in the presence (open bars) or absence (solid bars) of an OCT inhibitor (disopyramide for OCT1, cimetidine for OCT2) was determined as described in the Experimental Procedures. Briefly, (A) Transfected MDCK cells were incubated in the antibiotic-free medium containing oxaliplatin (10 μM) with or without disopyramide (150 μM). (B) Transfected HEK 293 cells were incubated in the antibiotic-free medium containing oxaliplatin (0.6 μM) with or without cimetidine (1.5 mM). After incubation at 37°C and 5% CO_2 for 2 hours, the cells were washed with ice-cold PBS three times and harvested. The genomic DNA was isolated from the cells and the platinum content associated with DNA was determined by ICP-MS and normalized for DNA content. Data are expressed as mean ± SD from a typical experiment performed in triplicate. Two independent experiments were conducted and similar results were obtained.

Co-incubation with disopyramide (150 μM) significantly decreased (2.11-fold, $p < 0.001$) platinum-DNA adduct formation in MDCK-hOCT1 cells (control vs. disopyramide-treated; 0.0457 ± 0.0011 pmol / μg DNA, r_b = 1.51 ± 0.04 × 10^{-5} vs. 0.0217 ± 0.0019 pmol / μg DNA, r_b = 7.16 ± 0.63 × 10^{-6}) with no effect in MDCK-MOCK cells. The platinum-DNA adduct level in HEK-hOCT2 cells (0.0284

± 0.0020 pmol / µg DNA, r_b = 9.37 ± 0.66 × 10^{-6}) was 28.8-fold higher ($p < 0.001$) than that in HEK-MOCK after exposure to oxaliplatin (Figure 2.4B) and was markedly reduced by cimetidine (0.00216 ± 0.00031 pmol / µg DNA, r_b = 9.37 ± 0.66 × 10^{-6} vs. 7.13 ± 1.02 × 10^{-7}). Cimetidine produced only a small decrease (1.70-fold, $p < 0.05$) in HEK-MOCK cells.

Structure-Activity Relationships (SAR) for Platinum-OCT1 Interaction

To investigate the SAR for platinum-OCT1 interactions, the drug sensitivities (IC_{50}) and RF values of 9 platinum complexes (Figure 2.1) in both MDCK-MOCK and MDCK-hOCT1 cells were determined (Table 2.2A): the higher the RF value, the higher the interaction.

1. *Nature of the non-leaving group(s):* RF values less than two were obtained for platinum complexes with diammine non-leaving groups including cisplatin, carboplatin and [$Pt(NH_3)_2$(*trans*-1,2-$(OCO)_2C_6H_{10}$], indicating that platinum compounds with this purely inorganic non-leaving unit are poorly recognized by OCT1 (Table 2.2A). However, when the non-leaving group(s) contained an organic component as in [$PtCl_2$(en)], which has two methylene groups between the amine functionalities, the RF value increased to 3.26. Moreover, with increasing size of the organic component of the non-leaving group(s), the interaction of a platinum compound with OCT1 increased. For example, the platinum compounds *cis*-[$Pt(NH_3)$(Cy)Cl_2], the *R,R*- and *S,S*-isomers of oxaliplatin and

[Pt(DACH)Cl_2], which all have a 6-C cyclohexyl moiety as part of their non-leaving group, had high RF values (9.02-28.4) (Table 2.2A). Therefore, it appears that the structure of the non-leaving group(s) of a platinum compound is an important determinant of its interaction with OCT1. Lastly, different isomers of the 1,2-diaminocyclohexane-substituted platinum complexes appear to interact similarly with OCT1. The *R,R*- and *S,S*-isomers of oxaliplatin (*R,R* vs. *S,S*: 22.4 vs. 20.7) and [Pt(DACH)Cl_2] (*R,R* vs. *S,S*: 22.9 vs. 28.4) have similar RF values (Table 2.2A).

Table 2.2. Drug sensitivity of platinum compounds.
Table 2.2(A) Drug sensitivity of structurally diverse platinum complexes in OCT1-transfected cells. The IC_{50} values (μM) of all the 9 platinum complexes, except for carboplatin, in MDCK-MOCK and MDCK-hOCT1 after 7 hours of drug exposure were determined in parallel using an MTT assay as described in the Experimental Procedures. Briefly, MDCK cells were seeded at a density of 5,000 cells/well in 96-well plates and exposed to the test compounds for 7 hours on the following day. After incubation for a total of 72 hours, the cell growth was determined by an MTT assay. The data for carboplatin was taken from Table 2.1A and was not determined simultaneously with the other compounds. The resistance factor (RF) was defined as the ratio of the mean IC_{50} value in MDCK-MOCK cells to that in MDCK-hOCT1 cells.

Platinum Complexes	MDCK-MOCK (μM)	MDCK-hOCT1 (μM)	RF
cisplatin	6.32 ± 0.74	3.58 ± 0.30	1.76**
carboplatin	258 ± 86.3	227 ± 85.8	1.13
[$Pt(NH_3)_2$(*trans*-1,2-$(OCO)_2C_6H_{10}$]	21.4 ± 2.94	10.8 ± 2.66	1.97***
[$Pt(Cl_2)$(en)]	33.2 ± 11.5	10.2 ± 4.76	3.26**
cis-[$Pt(NH_3)(Cy)Cl_2$]	1.42 ± 0.15	0.16 ± 0.03	9.02***
oxaliplatin	10.9 ± 3.66	0.48 ± 0.19	22.4***
[Pt(*S,S*-DACH)oxalato]	30.0 ± 14.2	1.45 ± 1.16	20.7***
[Pt(*R,R*-DACH)Cl_2]	15.0 ± 3.24	0.65 ± 0.26	22.9***
[Pt(*S,S*-DACH)Cl_2]	16.2 ± 3.72	0.57 ± 0.18	28.4***

**: $p < 0.01$; ***: $p < 0.001$.

Table 2.2(B) The sensitivity of the colon cancer cell lines to oxaliplatin and cisplatin in the presence and absence of cimetidine. The IC_{50} values (μM) of oxaliplatin and cisplatin in the colon cancer cell lines were determined in the presence or absence (control) of cimetidine (1.5 mM) in a similar fashion. The cell seeding density was 6,000-, 8,000-, 6,000-, 15,000-12,000- and 4,000 cells/well for HCT116, HT29, RKO, SW620, LS180 and DLD cells, respectively. When cimetidine (1.5 mM) was used, it was added to the wells immediately before the addition of the platinum drugs. The resistance factor (RF) was defined as the ratio of the mean IC_{50} value in the presence to that in the absence of cimetidine. Data are expressed as mean ± SD from six measurements for both (A) and (B), and each measurement was performed in quadruplicate.

	Oxaliplatin			Cisplatin		
Cell Lines	Control	Cimetidine-treated	RF	Control	Cimetidine-treated	RF
HCT116[a]	2.37 ± 1.44	18.8 ± 6.19	7.93***	5.42 ± 1.34	10.2 ± 3.23	1.88**
HT29[a]	4.56 ± 1.40	52.1 ± 18.5	11.4***	12.4 ± 3.91	30.8 ± 11.0	2.47**
RKO[a]	1.64 ± 0.56	9.70 ± 2.70	5.92***	8.58 ± 2.38	12.5 ± 4.44	1.46
SW620[a]	2.81 ± 1.00	14.2 ± 2.81	5.04***	12.6 ± 1.95	22.2 ± 4.92	1.76**
LS180[a]	1.30 ± 0.41	8.39 ± 2.77	6.44***	5.72 ± 1.75	8.27 ± 3.35	1.44
DLD	10.6 ± 5.99	71.3 ± 12.9	6.73***	18.4 ± 7.58	32.3 ± 10.3	1.74*

**: $p < 0.05$; **: $p < 0.01$ and ***: $p < 0.001$.*
[a]: The IC_{50} value of oxaliplatin is significantly lower than that of cisplatin in the absence of cimetidine.

2. *Nature of the leaving group(s):* Changes in the leaving group did not induce substantial changes in the RF values of platinum complexes. For example, all the DACH compounds (*R,R*- and *S,S*-isomers of oxaliplatin and [Pt(DACH)Cl_2]) had similar RF values (20.7-28.4, Table 2.2A), although the leaving group of oxaliplatin (oxalate) is very different from that of [Pt(DACH)Cl_2] (chloride) (Table 2.2A). In addition, cisplatin, carboplatin and [$Pt(NH_3)_2$(*trans*-1,2-$(OCO)_2C_6H_{10}$], all of which have different leaving groups but identical non-leaving groups, had similar RF values (1.13-1.97, Table 2.2A). Moreover, a cyclohexane ring, when present in the non-leaving group(s) of a platinum complex, such as in

those DACH compounds, markedly increases OCT1 interaction (RF : 20.7-28.4) in comparison to diammine ligands (RF : 1.13-1.97). However, when the cyclohexane ring was incorporated into the leaving group, as in $[Pt(NH_3)_2(trans\text{-}1,2\text{-}(OCO)_2C_6H_{10}]$, it had no effect on the OCT1 interaction, the RF value of $[Pt(NH_3)_2(trans\text{-}1,2\text{-}(OCO)_2C_6H_{10}]$ being 1.97 (Table 2.2A).

Identification of the Chemical Form of Oxaliplatin that is the Substrate(s) of OCT1

Multiple chemical species exist in equilibrium when platinum complexes are dissolved in an aqueous solution containing high concentrations of chloride ion.[34,35] Therefore, identification of the chemical species that are taken up by OCT1 would contribute to our understanding of the SAR of platinum-OCT1 interactions. In chloride containing media, such as plasma ($[Cl^-]$ ~ 103 mM)[35] and our cell culture medium, the oxalate leaving group of oxaliplatin can be replaced by chloride, resulting in $[Pt(R,R\text{-DACH})Cl_2]$. The latter can be further aquated to form the mono-, $[Pt(R,R\text{-DACH})(H_2O)Cl]^+$, and dicationic, $[Pt(R,R\text{-DACH})(H_2O)_2]^{2+}$, species.[36] The monoaqua and diaqua cations are the active forms of oxaliplatin, which bind to DNA. Considering the general properties of OCT substrates, which are positively charged small organic compounds, it is likely that the mono- and / or diaqua chemical species, having one or two positive charges, are the chemical forms taken up by OCT1.

To investigate experimentally the oxaliplatin-derived species taken up by OCT1, we first measured the platinum-DNA adduct formation in both MDCK-

hOCT1 and MDCK-MOCK cells after incubation with oxaliplatin (20 μM) in chloride free buffer (PB-SO_4). In this buffer, oxaliplatin should remain predominantly intact because the affinity of sulfate for platinum(II) is much lower than that of chloride.[35] Displacement of the oxalate group by water will be a relatively slow process. In addition, we used short incubation times (25 min) to minimize conversion of oxaliplatin to intermediate aquated species. Under these conditions, the Pt-DNA adduct level in MDCK-hOCT1 cells (0.00398 ± 0.00089 pmol / μg DNA, r_b = 1.31 ± 0.29 × 10^{-6}) was similar to ($p > 0.05$) that in MDCK-MOCK cells (0.00320 ± 0.00042 pmol / μg DNA, r_b = 1.05 ± 0.14 × 10^{-6}) (Figure 2.5), suggesting that unmodified oxaliplatin is not an OCT1 substrate. Secondly, to determine whether an aquated form of oxaliplatin was taken up by OCT1, we

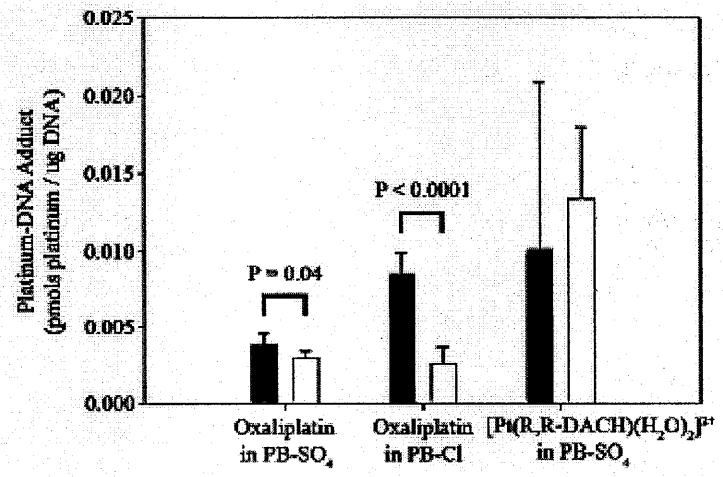

Figure 2.5. Platinum-DNA adduct formation after incubation with oxaliplatin or [Pt(*R,R*-DACH)$(H_2O)_2]^{2+}$ in PB-Cl or PB-SO_4 buffer. Transfected MDCK cells were incubated with oxaliplatin (20 μM) or [Pt(*R,R*-DACH)$(H_2O)_2]^{2+}$ (1 μM) in PB-Cl or PB-SO_4 buffer at 37°C and 5% CO_2 for 25 min. Oxaliplatin was freshly prepared and was added to PB-SO_4 buffer immediately, and to PB-Cl buffer half an hour before cell incubation. After incubation, the cells were washed with ice-cold PBS three times and harvested. Genomic DNA was isolated from the harvested cells and the DNA-associated platinum content was determined by ICP-MS and normalized for the DNA content. Data are expressed as mean ± SD of three measurements.

measured platinum-DNA adduct formation after incubation with oxaliplatin (20 μM) in the chloride-containing buffer, PB-Cl, for 25 min. Under these conditions, it is likely that conversion to the monochloro/monoaqua cation will occur, with displacement of the oxalate ligand. The DNA-associated platinum level was substantially higher (2.74-fold, $p < 0.01$) in MDCK-hOCT1 cells (0.00933 ± 0.00124 pmol / μg DNA, $r_b = 3.08 \pm 0.41 \times 10^{-6}$) than that in MDCK-MOCK cells (0.00340 ± 0.00087 pmol / μg DNA, $r_b = 1.12 \pm 0.29 \times 10^{-6}$) (Figure 2.5) consistent with this expectation. We also determined platinum-DNA adduct formation after direct incubation with the diaqua compound, $[Pt(R,R\text{-}DACH)(H_2O)_2]^{2+}$ (1 μM), in the PB-SO_4 buffer for 25 min. Under these conditions, the platinum complex will be a mixture of diaqua (82.8 %) and aqua/hydroxo (17.1%) species. Here the percentage was calculated based on the pK_a values of 6.14 and 7.56 for the diaqua and aqua/hydroxo forms of oxaliplatin, respectively,[37] and the pH value of 7.4 for the incubation buffer). The DNA-associated platinum level in MDCK-hOCT1 cells (0.0139 ± 0.0020 pmol / μg DNA, $r_b = 4.59 \pm 0.66 \times 10^{-6}$) was similar to ($p > 0.05$) that in MDCK-MOCK cells (0.0142 ± 0.0028 pmol / μg DNA, $r_b = 4.69 \pm 0.92 \times 10^{-6}$) (Figure 2.5), suggesting that the diaqua form is not an OCT1 substrate. Whether or not the aqua/hydroxo form, which carries one positive charge, can be taken up by OCT1 remains unclear. Taken together, these studies suggest that a monoaquated form of oxaliplatin, either the chloro or hydroxo species, both of which carry one positive charge, is the actual substrate of OCT1.

Expression of OCT1 and OCT2 in Colon Cancer Cell Lines and Tissue Samples

Since oxaliplatin is currently approved for advanced colon cancer therapy, we determined the expression of OCT1 and OCT2 in colon cancer cell lines and tumor samples. As shown in Figure 2.6, expression of OCT1 mRNA was detected in the six colon cancer cell lines tested in this study (LS180, DLD, SW620, HCT116, HT29 and RKO) with the highest expression level in HT29 cells. Four normal colon tissue samples and twenty colon tumor samples exhibited variable OCT1 expression levels. OCT2 was not detected in any of the cell lines or in the normal colon tissue samples; however, 11 of the 20 tumor samples demonstrated significant OCT2 expression (Figure 2.6).

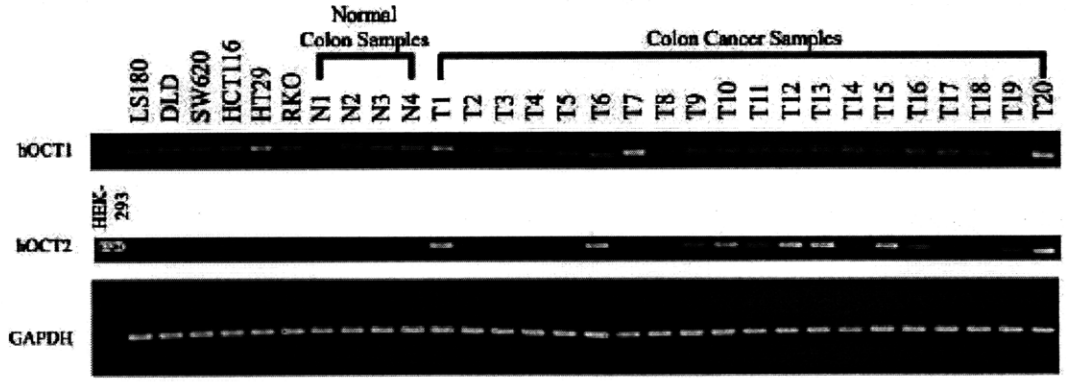

Figure 2.6. Expression of OCT1 and OCT2 in colon cancer cell lines and colon tissue samples. Total RNA was isolated from colon cancer cells and normal or cancerous colon tissues. The expression of OCT1 and OCT2 in these samples was detected by RT-PCR as described in the Experimental Procedures. A PCR cycle number of 40 was used in all the samples. Human GAPDH expression was used as a loading control and a PCR cycle number of 30 was used for its amplification.

Effect of an OCT Inhibitor, Cimetidine, on Colon Cancer Cell Line Sensitivity to Cisplatin and Oxaliplatin

To evaluate the potential role of OCT1 in the cytotoxicity of oxaliplatin and to determine whether OCT1 contributes to the differences in activities of cisplatin

and oxaliplatin, we determined the sensitivities (IC_{50}) of both oxaliplatin and cisplatin in the colon cancer cells in the presence and absence of an OCT inhibitor, cimetidine (1.5 mM). The resistance factor (RF) due to the presence of cimetidine was defined as the ratio of the IC_{50} value in the presence of cimetidine to that in the absence of cimetidine. As shown in Table 2.2B, the sensitivity of oxaliplatin was higher (lower IC_{50}) than that of cisplatin in each of the tested colon cancer cell lines in the absence of cimetidine (control, the mean ± SE of IC_{50} in the six cell lines: 3.88 ± 1.42 μM (oxaliplatin) vs. 10.5 ± 2.02 μM (cisplatin)). However, in the presence of cimetidine, oxaliplatin sensitivity was substantially decreased in each of the cell lines (RF values ranged from 5.04 to 11.4 ($p < 0.001$)), resulting in IC_{50} values comparable to, or even higher than those of cisplatin (mean ± SE of IC_{50} in the six cell lines: 29.1 ± 10.7 μM (oxaliplatin) vs. 19.4 ± 4.32 μM (cisplatin)). The effect of cimetidine on cisplatin sensitivity was small (range of RF values: 1.44-2.47, Table 2.2B).

Discussion

The striking activity of cisplatin in otherwise fatal disease, testicular cancer, has been established by thirty years of clinical experience. However, acquired and intrinsic resistance limits its application to a relatively narrow range of tumor types. To broaden the anticancer spectrum of this platinum agent, thousands of structural analogs have been tested. Cisplatin analogs with two ammine ligands, such as carboplatin and nedaplatin (approved in Japan), are cross-resistant with cisplatin.[38] Analogues with different ligands display more

diverse activity profiles. [4] Notably, oxaliplatin, with DACH in place of the two ammine ligands, in combination with 5-fluoruracil/leucovorin produced response rates twice that of 5-fluoruracil/leucovorin regimens alone in the treatment of colorectal cancer,[39] against which cisplatin is inactive.[6] Efforts to understand the differences in oxaliplatin versus cisplatin antitumor activity have focused mainly on the cellular processing of cisplatin- and oxaliplatin-DNA adducts.[13,14,40] Defects in MMR cause modest to moderate resistance to cisplatin but not to oxaliplatin.[40,41] Differences in the mechanism(s) controlling cellular uptake and efflux of these platinum compounds, although rarely studied, can also contribute to their disparate activities considering the nature of their chemical structures.

In the present study, we observed that the influx transporters, OCT1 and OCT2, play a critical role in the cellular uptake and consequent cytotoxicity of oxaliplatin (Table 2.1 and Figure 2.2). In contrast, the two transporters were relatively unimportant in mediating the uptake and cytotoxicity of cisplatin and carboplatin (Table 2.1). Overexpression of OCT1 and, more strikingly, OCT2 in transfected cells not only increased the rate of cellular platinum accumulation but also elevated the level of platinum-DNA adducts after oxaliplatin exposure (Figure 2.3 and Figure 2.4). These effects were blocked by known OCT inhibitors. The data strongly suggest that oxaliplatin is an excellent substrate of human OCT1 and OCT2, and the cellular uptake of platinum mediated by these transporters has ready access to the key pharmacological target (DNA). These results are in contrast to platinum uptake mediated by human Ctr1, which appears to sequester the drug in some intracellular compartment, rendering it

inaccessible to the pharmacological target [18]. It should be noted that a modest increase in cisplatin uptake (Figure 2.3B) and sensitivity (2.23-fold, $p < 0.001$, Table 2.1B) was observed in HEK-hOCT2 cells in comparison to HEK-MOCK cells, suggesting that cisplatin is a weak substrate of OCT2, consistent with previous work [33].

It is noteworthy that expression of OCT1 or OCT2, even at low levels, may play a significant role in the cytotoxicity of oxaliplatin. We consistently observed a more than three-fold increase (3.18-fold) in the IC_{50} value of oxaliplatin in HEK-MOCK cells in the presence of the OCT inhibitor, cimetidine (Figure 2.2E), but not for cisplatin or carboplatin (data not shown). The decrease in oxaliplatin sensitivity in HEK-MOCK cells by the OCT inhibitor is most likely due to inhibition of intrinsic OCT1 and/or OCT2 activity in HEK 293 cells. Both transporters were detected in HEK-MOCK cells in PCR studies using a cycle number of 40 (data not shown). Furthermore, cimetidine consistently produced a significant decrease in the cellular uptake of oxaliplatin, but not of cisplatin or carboplatin in HEK-MOCK cells (Figure 2.3B, 2.3C). Although it might be possible that cimetidine reacts with the platinum compounds and therefore inactivates them, this explanation is unlikely to be of the primary importance since we would have expected to observe similar effects of cimetidine on the cellular uptake and cytotoxicity of cisplatin and carboplatin. Taken together, the data suggest that low levels of expression of OCT1 and OCT2 play a significant role in sensitizing cells to oxaliplatin.

Structure-activity relationship studies revealed that the nature of the amine ligand bound to platinum is important for interaction with OCT1, with an organic component being required for effective interaction. On the other hand, the structure of the leaving ligand seems to be unimportant. We showed that a monoaqua derivative of oxaliplatin, either the chloro or hydroxo species, not a divalent diaqua complex, was likely to be the preferred substrate of OCT1 (Figure 2.5). These results are consistent with previous work showing that OCTs interact with small molecular weight monovalent organic cations [25]. Although the structure-activity relationships were established for platinum-OCT1 interactions, it is likely that the conclusions will apply to platinum-OCT2 interactions because the two transporters have largely overlapping substrate specificities. These studies establish the basis for the design of additional platinum complexes to facilitate the development of an even more detailed structure-activity relationship, which could be used to predict their interaction with OCTs. We anticipate the potential to target platinum complexes for therapy against tumors that express OCT1 and OCT2.

Our structure-activity relationship studies further suggest that OCTs do not play a major role in determining the cytotoxicity of platinum compounds with two ammine ligands, such as cisplatin, carboplatin and nedaplatin. In contrast, OCTs may be important for mediating cytotoxicity of platinum compounds with organic amine ligands (Table 2.2B). Cell lines that are resistant to cisplatin are cross-resistant to the diammine complexes, carboplatin and nedaplatin, but not to the DACH compounds, oxaliplatin and tetraplatin, which share a similar activity

profile [4,38]. Differences in the activity profiles of these compounds parallel the differences in their interaction with OCTs, suggesting that interactions with OCT1 and OCT2 may explain, at least in part, differences in the activities and tumor specificities of platinum complexes.

It is likely that the activity of oxaliplatin in colorectal cancer can be explained, at least in part, by the selective uptake via OCTs. In this study, we detected OCT1 expression in all twenty human colon cancer tissue samples and OCT2 expression in 11 out of 20 tissue samples (Figure 2.6). Similar levels of OCT1 were also detected in the six tested human colon cancer cell lines although OCT2 was not detectable (Figure 2.6). However, both OCT1 and OCT2 expression have been detected in another human colon cancer cell line, Caco-2 [28,31]. As has been observed previously [4], drug sensitivity to oxaliplatin was greater than that of cisplatin in each of the six colon cancer cell lines (Table 2.2B). The higher activity of oxaliplatin in comparison to that of cisplatin in these colon cancer cells is probably a consequence of the selective uptake of oxaliplatin mediated by the intrinsic OCT1 in these cells, since similar activities of oxaliplatin and cisplatin were observed in these cells when OCT1 was blocked by cimetidine (Table 2.2B).

Based on the expression of OCT1 and OCT2 in the colon cancer tissue samples and the OCT-dependent activity of oxaliplatin in the cell lines, it is reasonable to speculate that these transporters are important determinants of oxaliplatin activity in colorectal cancer. Also, it is possible that variable expression of OCTs, especially OCT2, may account for the variability in response

to oxaliplatin treatment. Further studies are required to determine whether expression levels of OCT1 and OCT2 may be used as markers for the rational selection of oxaliplatin-based versus irrinotecan-based combination therapies for treatment of individuals with colorectal cancer. Such selection is now primarily based on side-effect profiles or clinical experience [42]. Oxaliplatin-based therapy may be a better choice for patients with high levels of OCT1 and OCT2 in their tumor samples. In addition, genotyping for non-functional and reduced function polymorphisms of OCT1 and OCT2 may be incorporated in the decision-making process.[43,44].

Currently, platinum based therapies are used in the treatment of a variety of tumors including testicular cancer, ovarian cancer, small cell lung cancer and head and neck cancers [38]. In these therapies, cisplatin is often the drug of choice because other platinum compounds such as oxaliplatin are not superior. However, our studies suggest that when OCT1 or OCT2 is expressed in the tumor, oxaliplatin may be a better choice. Recently, OCT1 and OCT2 expression has been observed in a number of human cancer cell lines [31], suggesting that these transporters may be expressed in the corresponding tumors. The results of this study clearly suggest the need for further investigations to determine whether expression of OCTs can provide a basis for the rationale selection of platinum based therapies.

Experimental Procedures

Drugs and Reagents

Cisplatin, carboplatin, oxaliplatin, cimetidine, disopyramide, N-methyl-4-phenylpyridinium (MPP^+) and thiazolyl blue tetrazolium bromide were purchased from Sigma (St. Louis, MO). Solutions of carboplatin (10 mM) and oxaliplatin (5 mM) were freshly prepared in water. A solution of cisplatin (2 mM) was made in 1× phosphate buffered saline (PBS). These stock solutions were immediately aliquoted and stored frozen at -20°C and discarded one month after preparation. [methyl-^{3}H]-MPP^+ was from Perkin Elmer (Boston, MA) and tetraethylammonium (TEA) bromide [ethyl-1-^{14}C] was from American Radiolabeled Chemicals (St. Louis, MO). Hygromycin B and G418 were from Invitrogen (Carlsbad, CA). The cell culture medium Dubecco's Modified Eagle Medium (DMEM), RPMI and fetal bovine serum (FBS) were from the Cell Culture Facility of University of California, San Francisco (San Francisco, CA).

Cell Lines and Transfection

Madin-Darby canine kidney (MDCK) cells stably transfected with the full length human OCT1 cDNA (MDCK-hOCT1) and with the empty vector (MDCK-MOCK) were established previously in our laboratory [43], Human embryonic kidney (HEK) 293 cells transfected with pcDNA5/FRT vector (Invitrogen) containing the full length human OCT2 cDNA (HEK-hOCT2) and with the empty vector (HEK-MOCK) were established using Lipofectamine™ 2000 (Invitrogen) per manufacturer's instructions. The stable clones were selected with 75 µg / ml of hygromycin B. HEK 293 cells transfected with pcDNA3 vector containing the full length human OCT3 cDNA (HEK-hOCT3) and with the empty vector (HEK-

MOCK) were also established using Lipofectamine™ 2000. The stable clones were selected with 600 μg / ml G418. The pcDNA3 vector containing the full length human OCT3 cDNA was a kind gift from Dr. Bonisch (Institute of Pharmacology and Toxicology, University of Bonn, Germany). All the colon cancer cell lines (LS180, SW620, DLD, HCT116, HT20 and RKO) used in the present study were from American Type Culture Collection (Manassas, VA).

Cell Culture

The culture medium for stably transfected MDCK and HEK 293 cells is DMEM supplemented with 10% FBS and 100 units / ml penicillin and 100 μg / ml streptomycin (Invitrogen). To maintain the transgene expression, G418 (Invitrogen, 600 μg / ml) was added to the culture medium for MDCK transfected cells, human OCT3 transfected HEK 293 cells (HEK-hOCT3) and the corresponding HEK-MOCK cells; Hygromycin B (Invitrogen, 75 μg / ml) was added to the culture medium for human OCT2 transfected HEK 293 cells (HEK-hOCT2) and the corresponding HEK-MOCK cells. The culture medium for all the colon cancer cell lines (RKO, DLD, HT29, HCT116, LS180 and SW620) is RPMI containing 10% FBS, 100 units / ml penicillin and 100 μg / ml streptomycin. All the cells were grown at 37^0C in a humidified atmosphere with 5 % CO_2/ 95 % air.

Drug Sensitivity Assay

Cytotoxicity of the platinum compounds was measured by MTT (thiazolyl blue tetrazolium bromide) assay. Cells were seeded in 100 μl of the culture

medium without any antibiotics in 96-well plates at a predetermined cell density. For HEK 293 cells, poly-D-lysine coated plates were used. After overnight incubation, the platinum compounds were then added to the culture medium to give the indicated final concentrations. For the OCT inhibitor studies, the inhibitors (disopyramide or cimetidine) were added to the medium at a specified concentration immediately before the addition of the platinum compounds. After incubation for a specified time period, the drug-containing medium was replaced with fresh, drug-free medium and the incubation was continued for a total of 72 hours (start from the addition of platinum compounds). Then the MTT assay was performed similarly as previously described [45]. The IC_{50} (the drug concentration which inhibits 50% of cell growth) values were obtained by fitting the percent of the maximal cell growth at different drug concentrations (F) with the equation, $F=100\times(1-C^{\gamma}/(IC_{50}^{\gamma}+C^{\gamma}))$, using WinNonlin (Pharsight, Mountain View, CA). The maximal cell growth was the cell growth in the medium without any platinum compounds; C is the concentration of the platinum compound and γ is the slope factor.

Cellular Uptake of TEA or MPP^+

MDCK or HEK 293 Cells were grown in 24-well plates to > 90% confluence in the culture medium without any antibiotics. The poly-D-lysine coated plates were used for HEK 293 cells. The cells were washed with 1 × PBS first and then incubated in the uptake buffer (1 × PBS) containing 10 μM ^{14}C-TEA or 2 μM ^{3}H-MPP^+ as specified. For the OCT inhibitor studies, the indicated OCT

inhibitor (disopyramide or cimetidine) was added to the uptake buffer at specified concentration together with the radioactive substrate. The uptake was performed at room temperature for 2 min (^{14}C-TEA uptake) or 5 min (^{3}H-MPP^{+}) and then the cells were washed with ice-cold PBS for three times. The cells were then lysed with the lysis buffer (0.1 N NaOH, 0.1% SDS) for scintillation counting and BCA protein assay (Pierce, Rockford, IL) to determine the uptake.

Cellular Accumulation of Platinum

The cellular accumulation of platinum was determined as previous described[18] with some modifications. Briefly, the cells were grown in 100 mm × 20 mm dishes in the culture medium without any antibiotics to over 90% confluence. For HEK 293 cells, poly-D-lysine coated dishes were used. For platinum accumulation, the cells were incubated in the culture medium containing the indicated concentrations of the platinum compounds at 37°C in 5% CO_2 for 2 hr unless specified. After incubation, the dishes were immediately placed on ice and the cells were washed with 6 ml of ice-cold PBS for three times and collected with a rubber policeman. The cell pellets were obtained by centrifugation at 400 x g and at 4°C for 15 min. For the OCT inhibitor studies, the incubation medium also contained the indicated inhibitor (disopyramide or cimetidine) in addition to the platinum compounds. The resulting cell pellets were then dissolved into 200 µl of 70% nitric acid at 65°C for at least 2.5 hours, and then distilled water containing 10 ppb of iridium (Sigma) and 0.1% Triton X-100 was added to the samples to dilute nitric acid to 7%. The platinum content was measured by

inductively plasma coupled mass spectrometry (ICP-MS) in the Analytical Facility at University of California at Santa Cruz (Santa Cruz, CA). Cell lysates from a set of identical cultures were used for BCA protein assay.

Platinum-DNA Adduct Formation

The platinum content associated with genomic DNA was determined as previously described[20] with some modifications. Briefly, the cells were grown in 100 mm × 20 mm dishes in the culture medium without any antibiotics to over 90% confluence. For HEK 293 cells, poly-D-lysine coated dishes were used. Then, the cells were incubated in the culture medium containing the specified concentrations of the platinum compounds at 37°C in 5% CO_2 for 2 hours (or 25 min as specified). In some experiments, phosphate buffer (PB: 1.06 mM KH_2PO_4, 2.97 mM Na_2HPO_4, pH 7.4) containing 155 mM NaCl (PB-Cl buffer) or 103 mM Na_2SO_4 (PB-SO_4 buffer) was used instead of the culture medium as specified. For the OCT inhibitor study, the incubation medium (buffer) also contained disopyramide or cimetidine). If PB-Cl or PB-SO_4 buffer was used, the cells were washed with the same buffer once before drug incubation. After incubation, the cells were washed with ice-cold PBS, scraped and pelleted. Genomic DNA was isolated from the cell pellets using Wizard® Genomic DNA Purification Kit (Promega, Madison, WI) following the manufacturer's instruction. Briefly, the cells were lysed with Nuclei Lysis Solution. After RNA digestion and protein precipitation, the lysates were centrifuged and the resulting supernatant was aliquoted. The genomic DNA prepared from two different aliquots of the

supernatant was used for platinum and DNA content determination, respectively. For the determination of platinum, the DNA samples were treated with 70% nitric acid at 65°C and diluted in the same way as described above. The platinum content was analyzed using ICP-MS and the DNA content was measured by absorption spectroscopy.

RNA Isolation

Cultured cells were grown in 100 mm × 20 mm dishes to 70-80% confluence. Total RNA was isolated using RNeasy® Mini Kit (Qiagen, Valencia, CA) following manufacturer's instruction, quantified by spectroscopy and stored at -80°C until use. Samples of tumor and normal colon mucosa were collected from colon cancer resection from Department of Surgery, Queen Mary Hospital, University of Hong Kong. Tissues were frozen in liquid nitrogen within half an hour after they were resected. Nonneoplastic mucosa from colon was dissected free of muscle and histologically confirmed to be tumor free by frozen section. Total RNA was extracted using Trizol (Invitrogen, Carlsbad, CA). This study was approved by the Ethics Committee of the University of Hong Kong and the Internal Review Board of University of California, San Francisco.

RT-PCR

The first-strand cDNA was synthesized from 2 μg of total RNA using SuperScript™ III First-Strand Synthesis System for RT-PCR kit (Invitrogen) in a 20 μl reaction mixture, and the random hexamers were used as the primer. The

sense and antisense primers for human OCT1 were 5'-CTG TGT AGA CCC CCT GGC TA-3' and 5'-GTG TAG CCA GCC ATC CAG TT-3', corresponding to the nucleotide positions 408-427 and 751-770 (accession number: NM_003057), respectively, and the size of the expected PCR product is 363 bp. The sense and antisense primers for human OCT2 were 5'-CCT GGT ATG TGC CAA CTC CT-3' and 5'-CAC CAG GAG CCC AAC TGT AT-3', corresponding to the nucleotide positions 590-609 and 904-923 (accession number: NM_003058), respectively, and the size of the expected PCR product is 334 bp. The sense and antisense primers for human OCT3 were 5'-ATC GTC AGC GAG TTT GAC CT-3' and 5'-TTG AAT CAC GAT TCC CAC AA-3', corresponding to the nucleotide positions 445-464 and 749-768 (accession number: NM_021977), respectively, and the size of the expected PCR product is 324 bp. The sense and antisense primers for human GAPDH were 5'-AAT CCC ATC ACC ATC TTC CA-3' and 5'-TGT GGT CAT GAG TCC TTC CA-3', corresponding to the nucleotide positions 289-308 and 587-606 (accession number: NM_002046), respectively, and the size of the expected PCR product is 318 bp. The sense and antisense primers for dog GAPDH were 5'-GGT GAT GCT GGT GAG TA-3' and 5'-GTG GAA GCA GGG ATG ATG TT-3', corresponding to the nucleotide positions 256-275 and 607-626 (accession number: AB038240), respectively, and the size of the expected PCR product is 371 bp. All sets of primers were designed to anneal with sequences in different exons of the genes. An annealing temperature of 58°C was used for PCR amplification. A cycle number of 40 was used for the detection of human OCT1 and OCT2 in the colon cancer cell lines and colon tissue samples. A cycle

of 30 was used to detect human OCT1, OCT2 or OCT3 in the corresponding OCT-transfected cells and the MOCK cells. For the detection of human or dog GAPDH, a PCR cycle number of 30 was used in all the conditions.

Synthesis of Platinum Analogs

Potassium tetrachloroplatinate(II) was a gift from Engelhard Corp. and the starting materials cisplatin and potassium amminetrichloroplatinate(II) were synthesized as reported [46,47]. ^{1}H NMR spectra were acquired on a Varian 300 MHz spectrometer. FT-IR spectra were measured on an Avatar 380 FT-IR (Thermo Nicolet, Waltham, MA). ESI-MS spectra were obtained on an Agilent Technologies 1100 Series LCMS instrument. Previously reported procedures were used to prepare [Pt(Cl_2)(en)] [46], *cis*-[Pt(NH_3)(cy)Cl_2] [47], and [Pt(*R,R*-DACH)Cl_2] [48]. The [Pt(*S,S*-DACH)Cl_2] and [Pt(*S,S*-DACH)oxalato] were synthesized as described [49]. FTIR and ^{1}H NMR spectra of all compounds matched literature spectra.

Preparation of [Pt(NH_3)$_2$(trans-1,2-(OCO)$_2$$C_6H_{10}$)]: The compound was prepared as described for the Pt-DACH derivative [50]. Solubility problems, similar to those reported for the DACH compound, prevented analysis by NMR spectroscopy. IR (KBr, cm^{-1}) 3266 (sh), 2920 (s), 2850 (s), 1618 (s), 1556 (sh), 1384 (vs), 1279 (w), 1222 (m), 1111 (w), 1030 (w), 772 (w), 719 (w), 588 (b). ESI-MS: $[M+H]^+$ = 400.2 amu (observed), 400.3 amu (calculated).

Preparation of [Pt(R,R-DACH)(H_2O)$_2$]$^{2+}$: [Pt(*R,R*-DACH)Cl_2] was dissolved in distilled water (200 μM) and incubated with silver nitrate (400 μM) in dark for 10

hours. $[Pt(R,R\text{-DACH})(H_2O)_2]^{2+}$ was obtained by filtering the reaction mixture to remove the silver chloride precipitate.

Statistical Analysis

The differences between the mean values were analyzed for significance using Student's t test. P values < 0.05 were considered statistically significant.

Acknowledgements

This work was supported by grants from the National Institutes of Health, GM36780 and GM61390. Work at MIT was supported by research grant CA 34992 from the National Cancer Institute. K.S.L. acknowledges the support of a National Science Foundation Graduate Research Fellowship. We would like to thank Drs. SY Leung and ST Yuen from the University of Hong Kong for providing the colon cancer samples.

References

(1) S. Zhang, K. S. Lovejoy, J. E. Shima, L. L. Lagpacan, Y. Shu, A. Lapuk, Y. Chen, T. Komori, J. W. Gray, X. Chen, S. J. Lippard and K. M. Giacomini (2006). Organic Cation Transporters Are Determinants of Oxaliplatin Cytotoxicity. *Cancer Res.*, **66**, 8847-8857.

(2) E. Wong and C. M. Giandomenico (1999). Current Status of Platinum-Based Antitumor Drugs. *Chem. Rev.*, **99**, 2451-2466.

(3) R. B. Weiss and M. C. Christian (1993). New cisplatin analogs in development: a review. *Drugs*, **46**, 360-377.

(4) O. Rixe, W. Ortuzar, M. Alvarez, R. Parker, E. Reed, K. Paull and T. Fojo (1996). Oxaliplatin, tetraplatin, cisplatin, and carboplatin: spectrum of activity in drug-resistant cell lines and in the cell lines of the National Cancer Institute's Anticancer Drug Screen panel. *Biochem. Pharmacol.*, **52**, 1855-1865.

(5) E. Raymond, S. G. Chaney, A. Taamma and E. Cvitkovic (1998). Oxaliplatin: a review of preclinical and clinical studies. *Ann. Oncol.*, **9**, 1053-1071.

(6) J. L. Misset, H. Bleiberg, W. Sutherland, M. Bekradda and E. Cvitkovic (2000). Oxaliplatin clinical activity: a review. *Crit. Rev. Oncol. Hematol.*, **35**, 75-93.
(7) A. L. Pinto and S. J. Lippard (1985). Sequence-dependent termination of in vitro DNA synthesis by cis- and trans-diamminedichloroplatinum(II). *Proc. Natl. Acad. Sci. U. S. A.*, **82**, 4616-4619.
(8) D. B. Zamble and S. J. Lippard (1995). Cisplatin and DNA repair in cancer chemotherapy. *Trends Biochem. Sci.*, **20**, 435-439.
(9) D. Wang and S. J. Lippard (2005). Cellular processing of platinum anticancer drugs. *Nature Reviews Drug Discovery*, **4**, 307-320.
(10) J. M. Woynarowski, W. G. Chapman, C. Napier, M. C. Herzig and P. Juniewicz (1998). Sequence- and region-specificity of oxaliplatin adducts in naked and cellular DNA. *Mol. Pharmacol.*, **54**, 770-777.
(11) J. D. Page, I. Husain, A. Sancar and S. G. Chaney (1990). Effect of the diaminocyclohexane carrier ligand on platinum adduct formation, repair, and lethality. *Biochemistry*, **29**, 1016-1024.
(12) M. M. Jennerwein, A. Eastman and A. Khokhar (1989). Characterization of adducts produced in DNA by isomeric 1,2-diaminocyclohexaneplatinum(II) complexes. *Chem. Biol. Interact.*, **70**, 39-49.
(13) A. Vaisman, S. E. Lim, S. M. Patrick, W. C. Copeland, D. C. Hinkle, J. J. Turchi and S. G. Chaney (1999). Effect of DNA polymerases and high mobility group protein 1 on the carrier ligand specificity for translesion synthesis past platinum-DNA adducts. *Biochemistry*, **38**, 11026-11039.
(14) S. Chaney, G., S. Campbell, L., E. Bassett and Y. Wu (2005). Recognition and processing of cisplatin- and oxaliplatin-DNA adducts. *Crit. Rev. Oncol. Hematol.*, **53**, 3-11.
(15) D. P. Gately and S. B. Howell (1993). Cellular accumulation of the anticancer agent cisplatin: A review. *Br. J. Cancer*, **67**, 1171-1176.
(16) R. Safaei and B. Howell Stephen (2005). Copper transporters regulate the cellular pharmacology and sensitivity to Pt drugs. *Crit. Rev. Oncol. Hematol.*, **53**, 13-23.
(17) G. Zhao, X. Hu, P. Yu and H. Lin (2004). Synthesis and DNA-binding properties of binuclear platinum complexes with two trans-[Pt(NH3)2Cl]+ units bridged by 4,4'-dipyridyl sulfide or selenide. *Transition Metal Chemistry*, **29**, 607-612.
(18) A. K. Holzer, G. Samimi, K. Katano, W. Naerdemann, X. Lin, R. Safaei and S. B. Howell (2004). The copper influx transporter human copper transport protein 1 regulates the uptake of cisplatin in human ovarian carcinoma cells. *Mol. Pharmacol.*, **66**, 817-823.
(19) M. Komatsu, T. Sumizawa, M. Mutoh, Z. S. Chen, K. Terada, T. Furukawa, X. L. Yang, H. Gao, N. Miura, T. Sugiyama and S. Akiyama (2000). Copper-transporting P-type adenosine triphosphatase (ATP7B) is associated with cisplatin resistance. *Cancer Res.*, **60**, 1312-1316.
(20) G. Samimi, K. Katano, A. K. Holzer, R. Safaei and S. B. Howell (2004). Modulation of the Cellular Pharmacology of Cisplatin and Its Analogs by the Copper Exporters ATP7A and ATP7B. *Mol. Pharmacol.*, **66**, 25-32.

(21) N. Aissat, C. Le Tourneau, A. Ghoul, M. Serova, I. Bieche, F. Lokiec, E. Raymond and S. Faivre (2008). Antiproliferative effects of rapamycin as a single agent and in combination with carboplatin and paclitaxel in head and neck cancer cell lines. *Cancer Chemother. Pharmacol.*, **62**, 305-313.
(22) K. Nakayama, A. Kanzaki, K. Terada, M. Mutoh, K. Ogawa, T. Sugiyama, S. Takenoshita, K. Itoh, N. Yaegashi, K. Miyazaki, N. Neamati and Y. Takebayashi (2004). Prognostic value of the Cu-transporting ATPase in ovarian carcinoma patients receiving cisplatin-based chemotherapy. *Clin. Cancer Res.*, **10**, 2804-2811.
(23) H. Miyashita, Y. Nitta, S. Mori, A. Kanzaki, K. Nakayama, K. Terada, T. Sugiyama, H. Kawamura, A. Sato, H. Morikawa, K. Motegi and Y. Takebayashi (2003). Expression of copper-transporting P-type adenosine triphosphatase (ATP7B) as a chemoresistance marker in human oral squamous cell carcinoma treated with cisplatin. *Oral Oncol.*, **39**, 157-162.
(24) G. Samimi, N. M. Varki, S. Wilczynski, R. Safaei, D. S. Alberts and S. B. Howell (2003). Increase in expression of the copper transporter ATP7A during platinum drug-based treatment is associated with poor survival in ovarian cancer patients. *Clin. Cancer Res.*, **9**, 5853-5859.
(25) J. W. Jonker and A. H. Schinkel (2004). Pharmacological and physiological functions of the polyspecific organic cation transporters: OCT1, 2, and 3 (SLC22A1-3). *J. Pharmacol. Exp. Ther.*, **308**, 2-9.
(26) L. Zhang, M. J. Dresser, A. T. Gray, S. C. Yost, S. Terashita and K. M. Giacomini (1997). Cloning and functional expression of a human liver organic cation transporter. *Mol. Pharmacol.*, **51**, 913-921.
(27) V. Gorboulev, J. C. Ulzheimer, A. Akhoundova, I. Ulzheimer-Teuber, U. Karbach, S. Quester, C. Baumann, F. Lang, A. E. Busch and H. Koepsell (1997). Cloning and characterization of two human polyspecific organic cation transporters. *DNA Cell Biol.*, **16**, 871-881.
(28) J. Müller, K. S. Lips, L. Metzner, R. H. H. Neubert, H. Koepsell and M. Brandsch (2005). Drug specificity and intestinal membrane localization of human organic cation transporters (OCT). *Biochem. Pharmacol.*, **70**, 1851-1860.
(29) S. Verhaagh, N. Schweifer, D. P. Barlow and R. Zwart (1999). Cloning of the mouse and human solute carrier 22a3 (Slc22a3/SLC22A3) identifies a conserved cluster of three organic cation transporters on mouse chromosome 17 and human 6q26-q27. *Genomics*, **55**, 209-218.
(30) D. Grundemann, B. Schechinger, G. A. Rappold and E. Schomig (1998). Molecular identification of the corticosterone-sensitive extraneuronal catecholamine transporter. *Nat. Neurosci.*, **1**, 349-351.
(31) M. Hayer-Zillgen, M. Bruss and H. Bonisch (2002). Expression and pharmacological profile of the human organic cation transporters hOCT1, hOCT2 and hOCT3. *Br. J. Pharmacol.*, **136**, 829-836.
(32) O. Briz, M. A. Serrano, N. Rebollo, B. Hagenbuch, P. J. Meier, H. Koepsell and J. J. G. Marin (2002). Carriers involved in targeting the cytostatic bile acid-cisplatin derivatives cis-diammine-chloro-cholylglycinate-platinum(II)

and cis-diammine-bisursodeoxycholate-platinum(II) toward liver cells. *Mol. Pharmacol.*, **61**, 853-860.

(33) G. Ciarimboli, T. Ludwig, D. Lang, H. Pavenstaedt, H. Koepsell, H.-J. Piechota, J. Haier, U. Jaehde, J. Zisowsky and E. Schlatter (2005). Cisplatin nephrotoxicity is critically mediated via the human organic cation transporter 2. *Am. J. Pathol.*, **167**, 1477-1484.

(34) B. Desoize and C. Madoulet (2002). Particular aspects of platinum compounds used at present in cancer treatment. *Crit. Rev. Oncol. Hematol.*, **42**, 317-325.

(35) M. E. Howe-Grant and S. J. Lippard In *Metal Ions in Biological Systems*, 1980; Vol. 11, pp 63-125.

(36) A. M. Di Francesco, A. Ruggiero and R. Riccardi (2002). Cellular and molecular aspects of drugs of the future: Oxaliplatin. *Cell. Mol. Life Sci.*, **59**, 1914-1927.

(37) D. S. Gill and B. Rosenberg (1982). Syntheses, kinetics, and mechanism of formation of polynuclear hydroxo-bridged complexes of (trans-1,2-diaminocyclohexane)platinum(II). *J. Am. Chem. Soc.*, **104**, 4598-4604.

(38) D. Lebwohl and R. Canetta (1998). Clinical development of platinum complexes in cancer therapy: an historical perspective and an update. *Eur. J. Cancer*, **34**, 1522-1534.

(39) H. Kelly and R. M. Goldberg (2005). Systemic therapy for metastatic colorectal cancer: current options, current evidence. *J. Clin. Oncol.*, **23**, 4553-4560.

(40) D. Fink, S. Nebel, S. Aebi, H. Zheng, B. Cenni, A. Nehme, R. D. Christen and S. B. Howell (1996). The role of DNA mismatch repair in platinum drug resistance. *Cancer Res.*, **56**, 4881-4886.

(41) D. Fink, H. Zheng, S. Nebel, P. S. Norris, S. Aebi, T. P. Lin, A. Nehme, R. D. Christen, M. Haas, C. L. MacLeod and S. B. Howell (1997). In vitro and in vivo resistance to cisplatin in cells that have lost DNA mismatch repair. *Cancer Res.*, **57**, 1841-1845.

(42) R. M. Goldberg, D. J. Sargent, R. F. Morton, C. S. Fuchs, R. K. Ramanathan, S. K. Williamson, B. P. Findlay, H. C. Pitot and S. R. Alberts (2004). A randomized controlled trial of fluorouracil plus leucovorin, irinotecan, and oxaliplatin combinations in patients with previously untreated metastatic colorectal cancer. *J. Clin. Oncol.*, **22**, 23-30.

(43) Y. Shu, M. K. Leabman, B. Feng, L. M. Mangravite, C. C. Huang, D. Stryke, M. Kawamoto, S. J. Johns, J. DeYoung, E. Carlson, T. E. Ferrin, I. Herskowitz, K. M. Giacomini, L. Z. Benet, C. M. Brett, E. G. Burchard, R. Castro, M. de la Cruz, R. H. Edwards, J. Gitschier, C. E. Glatt, C. Ho, D. L. Kroetz, E. T. Lin, V. I. Reus, W. Sadee, M. Salazar, C. Schaefer, L. B. Sheiner, C. Tran, T. J. Urban, C. Vulpe and E. M. Wright (2003). Evolutionary conservation predicts function of variants of the human organic cation transporter, OCT1. *Proc. Natl. Acad. Sci. U. S. A.*, **100**, 5902-5907.

(44) M. K. Leabman, C. C. Huang, M. Kawamoto, S. J. Johns, D. Stryke, T. E. Ferrin, J. DeYoung, T. Taylor, A. G. Clark, I. Herskowitz and K. M.

Giacomini (2002). Polymorphisms in a human kidney xenobiotic transporter, OCT2, exhibit altered function. *Pharmacogenetics*, **12**, 395-405.

(45) M. C. Alley, D. A. Scudiero, A. Monks, M. L. Hursey, M. J. Czerwinski, D. L. Fine, B. J. Abbott, J. G. Mayo, R. H. Shoemaker and M. R. Boyd (1988). Feasibility of drug screening with panels of human tumor cell lines using a microculture tetrazolium assay. *Cancer Res.*, **48**, 589-601.

(46) S. C. Dhara (1970). A rapid method for the synthesis of *cis*-$[Pt(NH_3)_2Cl_2]$. *Indian J. Chem.*, **8**, 193-194.

(47) C. M. Giandomenico, M. J. Abrams, B. A. Murrer, J. F. Vollano, M. I. Rheinheimer, S. B. Wyer, G. E. Bossard and J. D. Higgins (1995). Carboxylation of kinetically inert platinum(IV) hydroxy complexes. An entree into orally active platinum(IV) antitumor agents. *Inorg. Chem.*, **34**, 1015-1021.

(48) J. D. Hoeschele, N. Farrell, W. R. Turner and C. D. Rithner (1988). Synthesis and characterization of diastereomeric (substituted iminodiacetato)(1,2-diaminocyclohexane)platinum(II) complexess. *Inorg. Chem.*, **27**, 4106-4113.

(49) Y. I. Kidani, K. (1978). Antitumor activity of 1,2-diaminocyclohexane-platinum complexes against Sarcoma-180 ascites Form. *J. Med. Chem.*, **21**, 1315-1318.

(50) T. A. K. Al-Allaf, L. J. Rashan, D. Steinborn, K. Merzweiler and C. Wagner (2003). Platinum(II) and palladium(II) complexes analogous to oxaliplatin with different cyclohexyldicarboxylate isomeric anions and their in vitro antitumour activity. Structural elucidation of [Pt(C2O4)(cis-dach)]. *Transition Met. Chem.*, **28**, 717-721.

Chapter 3

Synthesis of Pt(II) and Pt(IV) Compounds for Uptake by the Organic Cation Transporters: Extension of Structure-activity Relationship

Introduction

The structure-activity relationship developed in chapter 2[2] was used to inform design of new compounds as drugs for colorectal cancer and other cancers that contain the organic cation transporters. Compounds were characterized with respect to cytotoxicity in MDCK cells that were stably overexpressing hOCT1.[2]

In addition to studying compounds in cells with overexpressed transporters, it is interesting to study the response of cells in the absence of these genes. Silencing of genes by RNAi works by introducing a plasmid that codes for short (21-28 nucleotides) double-stranded RNA. Longer precursors are processed into small interfering RNAs (siRNAs) by a cytoplasmic ribonuclease called Dicer.[3] Using the antisense strand of the siRNA as a template, the RNA-induced silencing complex (RISC) recognizes and cleaves any mRNA that is complementary to the template, resulting in rapid degradation of mRNA for the target protein.[3]

The original structure-activity relationship for platinum-based antitumor drug candidates dictates that complexes should bear no net charge and have two amine or ammine groups plus two relatively labile groups that can be aquated under physiological conditions.[4] The structure-activity relationship developed for the treatment of tumor cells containing organic cation transporters (OCTs)[2] indicates that platinum-based OCT substrates 1) have a sizeable organic component, such as a diaminocyclohexyl ligand, suggesting an non-covalent interaction between protein and substrate (π-π stacking, hydrogen bonds, hydrophobic interactions);[5] and 2) be in a cationic state prior to uptake, possibly due to a cation-π interaction between the protein and the platinum complex.[6] Based on these findings, we synthesized compounds that were a) cationic

due to structure, specifically ([Pt(dien)Cl]Cl, [Pt(*R,R*-DACH)(acac)]Cl, *cis*-[$Pt(NH_3)_2$(pyridine)Cl]Cl, and *trans*-[$PtCl_2(NH_3)$(piperazine)]Cl); b) neutral compounds expected to be aquated quickly, namely (*trans*-[$PtCl_2$(pyridine)$_2$], *trans*-[Pt(cyclopentylamine)$_2Cl_2$]); and c) aromatic compounds that could take potentially take part in π-π stacking interactions, including ([Pt(*R,R*-DACH)(acac)]Cl, *cis*-[$Pt(NH_3)_2$(pyridine)Cl]Cl, *cis*-[$Pt(NH_3)$(benzylamine)Cl_2], and *trans*-[$PtCl_2$(pyridine)$_2$]). Additionally, we synthesized one cationic compound with an aromatic component, *cis*-[$Pt(NH_3)_2$(2-amino-3-picoline)Cl]Cl, based on a hit from a high-throughput screen of platinum(II) compounds for antitumor activity.[7]

Finally, we used drugs currently undergoing clinical trials to inform the design of new compounds as OCT substrates. We synthesized *cis*-[$Pt(NH_3)_2$(2-picoline)Cl]Cl based on picoplatin, *cis*-[$Pt(NH_3)$(2-picoline)Cl_2] (also known as AMD473), a drug that recently entered clinical trials under the control of Poniard Pharmaceuticals. Picoplatin was designed with additional steric bulk around the platinum center to reduce inactivation by cellular thiols, such as glutathione.[8,9] The phase III trial of picoplatin, SPEAR (Study of Picoplatin Efficacy After Relapse) is underway in Europe and India and is also focused on patients with small cell lung cancer. A phase I trial in colorectal cancer (combination therapy with 5-fluorouracil) and a phase II trial in prostate cancer (combination therapy with docetaxel and prednisone) are also underway.

The compounds were characterized for cellular cytotoxicity and accumulation in cells overexpressing OCT1 and cells that had endogenous levels of OCT1 knocked down by RNAi.

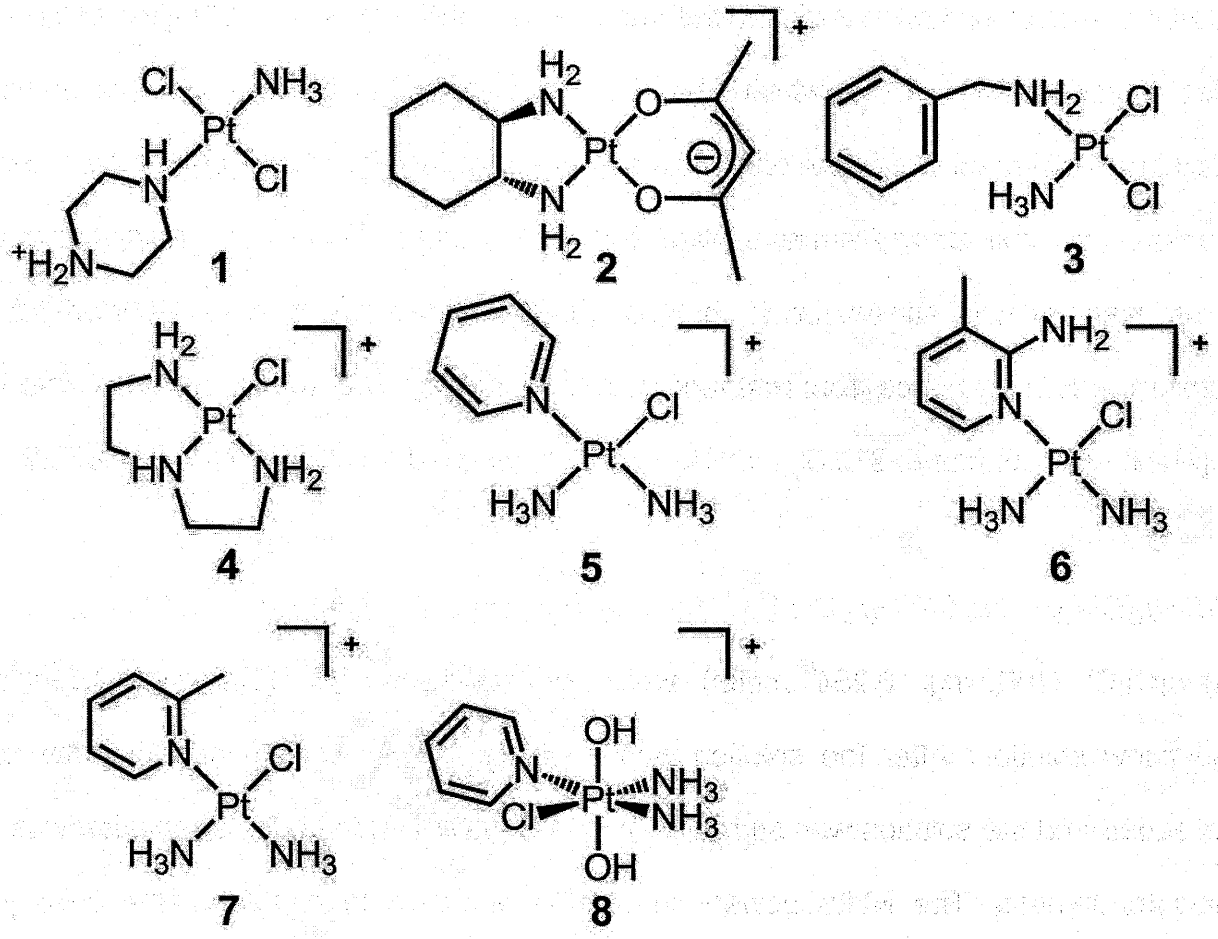

Chart 3.1 Cationic platinum compounds.

Experimental

Materials

Potassium tetrachloroplatinum(II) was a gift from Engelhard Corp. Both cisplatin and oxaliplatin were synthesized as reported previously.[10,11] The known compounds *trans*-[$PtCl_2$(pyridine)$_2$],[12] *trans*-[Pt(cyclopentylamine)$_2Cl_2$],[12] *trans*-[$Pt(NH_3)$(pz)Cl_2]Cl (**1**),[13] [Pt(R,R-DACH)(acac)]Cl (**2**),[14] [Pt(dien)Cl]Cl (**4**),[15,16] *cis*-[$Pt(NH_3)_2$(pyridine)Cl]Cl (**5**),[17] and *cis*-[$Pt(NH_3)_2$(2-picoline)Cl]Cl (**7**)[18] were synthesized as described. All other chemicals and solvents were from commercial sources. ^{1}H NMR and ^{195}Pt NMR spectra were obtained on Varian 300 and 500 MHz spectrometers, respectively. NMR

spectra are supplied as Figures 3.11-3.23. Electrospray ionization-MS (ESI-MS) spectra were obtained on an Agilent Technologies 1100 Series liquid chromatography/MS instrument. Fourier transform-IR (FT-IR) spectra were measured on an Avatar 380 FT-IR. Cyclic voltammetry experiments were performed on a 263 EG&G Princeton Applied Research electrochemical analyzer using a three-electrode setup with a glassy carbon working electrode, a platinum wire auxiliary electrode and an Ag/AgCl reference electrode. Electrochemical data were uncorrected for junction potentials. DNA concentrations were measured by UV-Vis absorption spectroscopy at 260 nm on a Cary 50 Bio UV-Visible spectrometer equipped with a microprobe from C Technologies Inc.

Synthesis of cis-[Pt(NH_3)(benzylamine)Cl_2] ***(3)***

The *trans* isomer of this complex has been synthesized previously.[19] To a solution of $[Et_4N][PtNH_3Cl_3]$[20] (1.11 mmol) in 4 mL H_2O was added a solution of benzylamine in 0.5 mL H_2O. The orange mixture was stirred for 9 h in the dark at room temperature, although an orange precipitate was observed after only 30 min. The orange precipitate was collected by filtration and washed with water (4x), ethanol (3x) and ethyl ether (2x) to yield an orange solid (73 mg, 17%). ^{1}H-NMR (*d*-DMF, 300 MHz) δ 4.034 (m, 2H), 4.292 (s, 3H), 5.315 (s, 2H), 7.376 (m, 3H), 7.473 (dd, 2H, J=1.5 Hz, 6.6 Hz); ^{195}Pt NMR (CD_3OD, 500 MHz) δ -2163.4. ESI-MS m/z calculated (M+Na): 412.9901, found: 412.9905.

Synthesis of cis-[Pt(NH_3)$_2$(2-amino-3-picoline)Cl]Cl ***(6)***

One equivalent of cDDP (200 mg, 0.668 mmol) was dissolved in 2 mL of DMF, to which $AgNO_3$ (100 mg, 0.596 mmol) was added dropwise. After 4 h, at which time an aliquot of the supernatant added to NaCl produced no AgCl precipitate, the reaction was centrifuged (10 min, 10,000 x g). The supernatant was collected, 2-amino-3-picoline (0.532 mmol, 0.79 equiv) was added, and the reaction was stirred for 12 h. The lyophilized powder was recrystallized twice from 0.1 N HCl and once from methanol to yield 41.1 mg (18.9%). ESI-MS m/z calculated (M+H): 372.06, found: 372.0.

*Synthesis of cis,cis,trans-[Pt(NH$_3$)$_2$(pyridine)Cl(OH)$_2$]Cl (**8**)*

One equivalent of *cis*-[Pt(NH_3)$_2$(pyridine)Cl]Cl (100 mg, 0.264 mmol) was dissolved in 3.4 mL water to make a faintly yellow solution. After the solution was heated to 50°C, 1.4 mL of H_2O_2 (50% w/v) was added and the solution was stirred for 2 h. The colorless solution was then lyophilized to dryness. The white powder was washed with acetonitrile (5 times) to produce the product (21.4 mg, 0.05 mmol, 21.50%) ^{1}H-NMR (*d*-methanol, 300 MHz) δ 7.691 (t, 2H, J=7.5 Hz), 8.157 (t, 1H, J=7.5 Hz), 8.946 (m, 2H); ^{195}Pt NMR (H_2O, 500 MHz) δ 678.6. ESI-MS m/z calculated (M+): 377.03, found: 377.0. Elemental analysis for platinum content by AAS: calculated 51.66%, found 51.65 ± 2.17%.

Electrochemical Studies of cis,cis,trans-[Pt(NH$_3$)$_2$(pyridine)Cl(OH)$_2$]Cl

Cyclic voltammetry measurements were performed at 25 °C at pH 6.0 or pH 7.4 on 2 mM solutions of complex **8** in 0.1 M KCl and 10 mM sodium phosphate buffer. Nitrogen was bubbled through the solutions and measurements were performed under

a nitrogen atmosphere. Measurements were carried out at six different scan rates from 50 to 300 mV s^{-1}.

Elemental Analysis of Platinum

Platinum was quantified by atomic absorption (AA) spectroscopy (Aanalyst 300, HGA-800 graphite furnace, AAWinLab software version 3.0, Perkin Elmer, Wellesley, MA). A hollow cathode platinum lamp with 265.9 nm emission was used with a slit width of 0.70 nm. Pyrolysis was performed at 1200 °C for 20 s and atomization at 2650 °C for 5 s. Samples in water were diluted to 100 μg/L and two dilutions were each measured in triplicate and all data were averaged. The instrument was calibrated over a range of 50-150 μg/L and an r value of $\geq$ 0.998 was obtained for the linear fit in all cases.

Plasmids for RNAi Silencing of OCT1

The pSicoR-GFP plasmid (Figure 3.1) was chosen for generation of shRNA against hOCT1 in human colorectal cells and was generously provided by the Tyler Jacks lab at MIT. Three different shRNA-encoding DNA sequences were designed according to previously derived principles,[3,21] with siRNA sequences beginning at 803, 806, and 1142 nucleotides from the origin of the sequence NM_003057, as found in the PubMed Nucleotide database. Cloning into pSicoR was performed as previously described.[1] Three positive clones per sequence were identified by digestion with XhoI and XbaI, which, for positive clones, yields a fragment ~50 bp larger than the empty vector. All plasmids were sequenced by the Genewiz GC-rich template sequencing service.

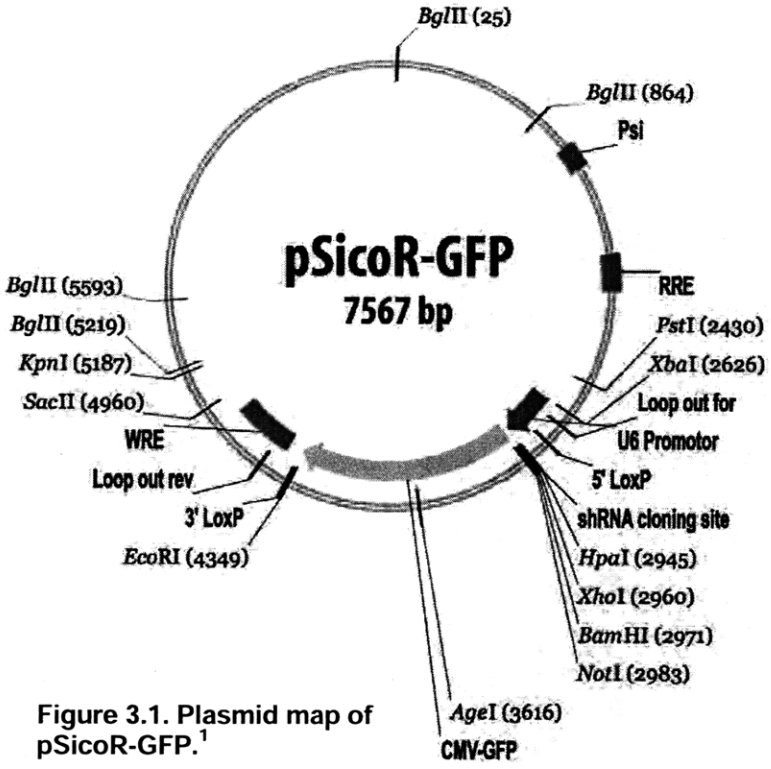

Figure 3.1. Plasmid map of pSicoR-GFP.[1]

Generation of OCT1-knockdown Cells

Human kidney 293T/17 cells were transfected using Fugene 6, pSicoR-GFP, and three viral packaging plasmids (ViraPower, Invitrogen). Six hours after transfection, the medium was replaced with fresh, antibiotic-free medium. After 48 h, GFP expression was examined by fluorescence microscopy and the virus-containing medium was removed for the purpose of infecting the target cell line. The medium was passed through a 0.45 μm syringe filter and used to replace the medium of HT-29 cells. Twenty-four hours after infection, the virus-containing medium on the HT-29 cells was replaced with fresh medium and discarded after treatment with bleach. Cells were grown to confluence in T-75 flasks and GFP-expressing cells were collected by FACS.

RT-PCR

RNA was isolated from 1-2 x 10^6 cells in the presence of β-mercaptoethanol and was purified on a Qiagen silica column following digestion with DNase I. RNA was primed using an oligo d(T)18 primer and cDNA was generated with ImProm_II reverse

transcriptase (Promega) for 60 min at 42°C. PCR was performed using specific primers for GADPH and hOCT1 as described.[2]

DNA-Platinum Adducts in Live Cells

Cells were plated in two 175 cm^2 flasks per cell line. Either 400 μM **5** or 3 μM oxaliplatin (approximate IC_{80} for each) was added one day later, at 90% confluence. The platinum-containing medium was removed after 2 h and cells were collected using trypsin/EDTA, washed twice with ice-cold PBS and resuspended in a digestion buffer (100 mM NaCl, 10 mM Tris-HCl pH 8.0, 25 mM EDTA pH 8.0, 0.5% SDS, 0.1 mg/mL proteinase K) for lysis over 15 h at 50°C. Protein was extracted in phenol/chloroform/isoamyl alcohol and the aqueous layer was ethanol precipitated twice. Approximately 40 μg DNA was obtained per 175 cm^2 flask. DNA concentration was determined by absorption at 260 nm and the A_{260}/A_{280} ratio was 1.9 or greater for all samples. Platinum concentration was determined by atomic absorption spectroscopy and r_b values were calculated as bound Pt atoms per nucleotide.

Results

Synthesis of Cationic Complexes for OCT-Containing Tumors

The known compounds, *trans*-[$PtCl_2$(pyridine)$_2$],[12] *trans*-[Pt(cyclopentylamine)$_2Cl_2$],[12] *trans*-[Pt(NH_3)(piperazine)Cl_2]Cl (**1**),[13] [Pt(R,R-DACH)(acac)]Cl (**2**),[14] [Pt(dien)Cl]Cl (**4**),[15,16] *cis*-[Pt(NH_3)$_2$(pyridine)Cl]Cl (**5**),[17] and *cis*-[Pt(NH_3)$_2$(2-picoline)Cl]Cl (**7**)[18] were synthesized as described in the literature. The compounds *cis*-[Pt(NH_3)(benzylamine)Cl_2] (**3**), *cis*-[Pt(NH_3)$_2$(2-amino-3-picoline)Cl]Cl (**6**), and

cis,cis,trans-[Pt(NH_3)$_2$(pyridine)Cl(OH)$_2$]Cl (**8**) had not been synthesized previously. The use of one equivalent of $AgNO_3$ to activate cisplatin at one position only followed by introduction of the selected amine ligand is a preferred method of producing platinum triamines.[17,22] An alternate method, heating cisplatin and the selected amine ligand in water at 50-60 °C for several days, leads to a large proportion of disubstituted products (*cis*-[Pt(NH_3)$_2$(Am)$_2$]$^{2+}$.[17] Performing the reaction without heat produces a more favorable product distribution, but is overall low-yielding. The large amount of disubstituted products may be due to the low solubility of cisplatin in water, which results in much more available amine than platinum in the initial stages of the reaction. Moreover, the reaction with $AgNO_3$ replaces a chloride ligand with either *O1*-DMF or NO_3^-, either of which is relatively more labile.[17]

Redox Properties of cis,cis,trans-[Pt(NH_3)$_2$(pyridine)Cl(OH)$_2$]Cl (**8**)

The reduction potential of **8** is critical to its function in the body, because only the platinum(II) form of the compound will readily bind DNA. The electrochemical behavior of **8** indicates irreversible loss of axial ligands upon reduction. At a pH value of 7.4 (Figures 3.4 and 3.5), a value chosen because it reflects the pH in the bloodstream, the reduction potential of **8,** extrapolated to 0.0 mV s^{-1} is -0.228 V vs. NHE. At a pH of 6.0 (Figures 3.2 and 3.3), a value that reflects the pH in endosomes and lysosomes, the reduction potential of **8** shifts to -0.195 V vs. NHE. The complex is more readily reduced due to protonation of the axial ligands as they dissociate.

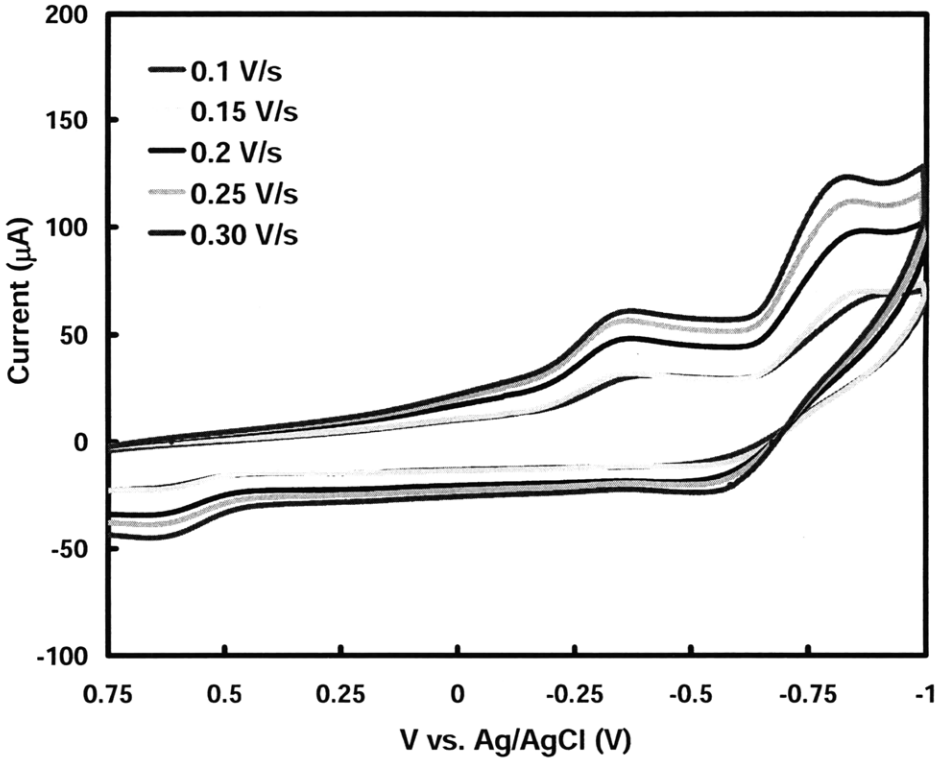

Figure 3.2. Cyclic voltammetry measurements of complex 8 at pH 6.0. Measurements were made at 25 °C on compound 8 dissolved to a final concentration of 2.0 mM in 0.1 M aqueous KCl buffered with 10 mM phosphate. The scan rate was varied as shown.

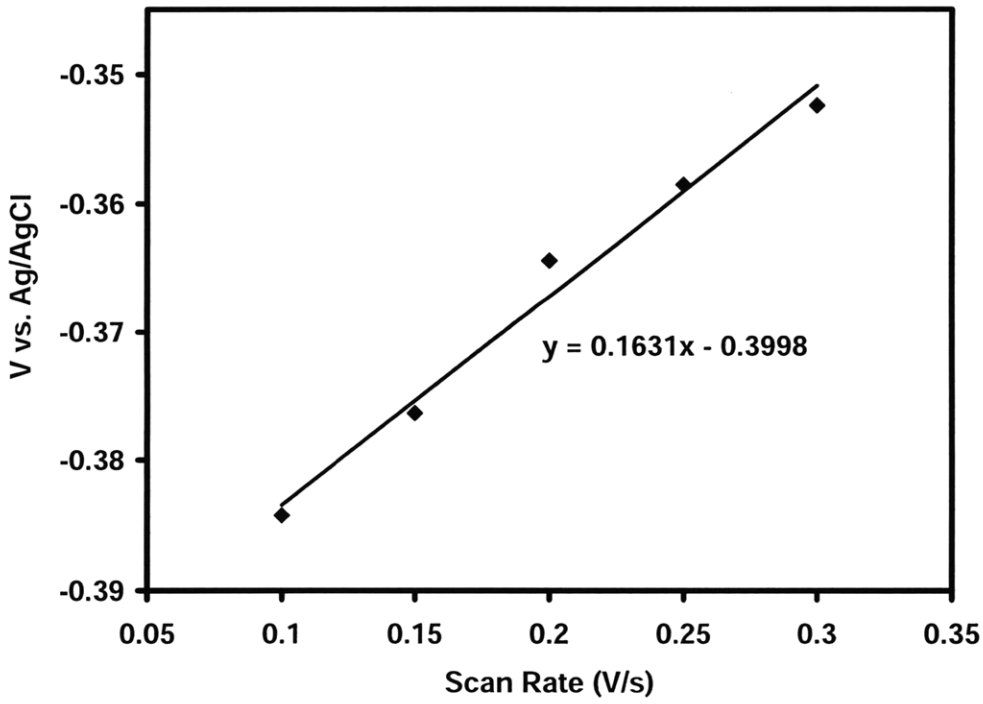

Figure 3.3. Scan rate vs. potential at pH 6.0. Measurements were made at 25 °C on compound 8 dissolved to a final concentration of 2.0 mM in 0.1 M aqueous KCl buffered with 10 mM phosphate.

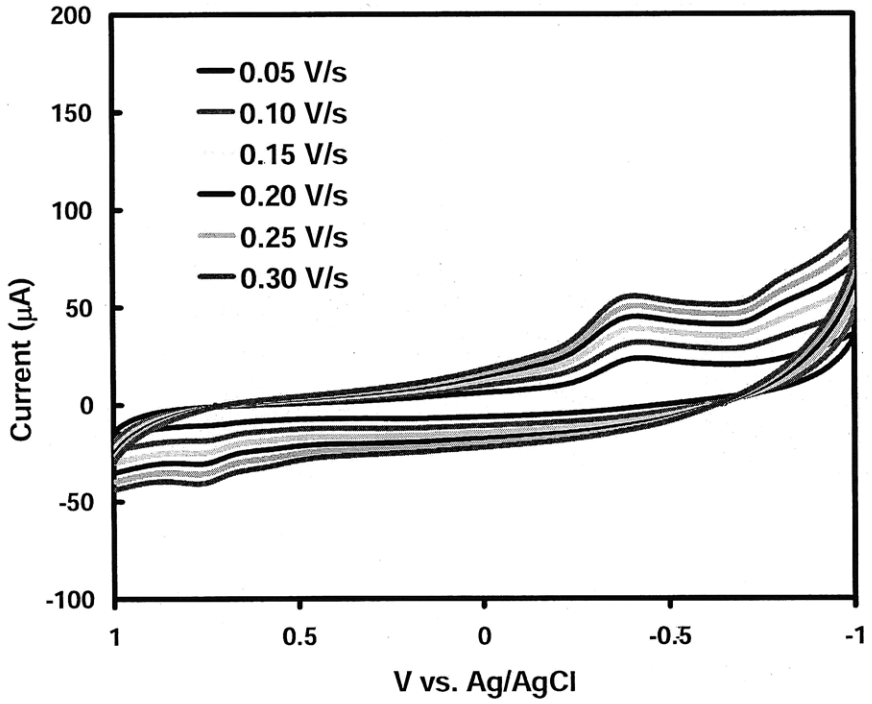

Figure 3.4. Cyclic voltammetry of compound 8 at pH 7.4. Measurements were made at 25 °C on compound 8 dissolved to a final concentration of 2.0 mM in 0.1 M aqueous KCl buffered with 10 mM phosphate. The scan rate was varied as shown.

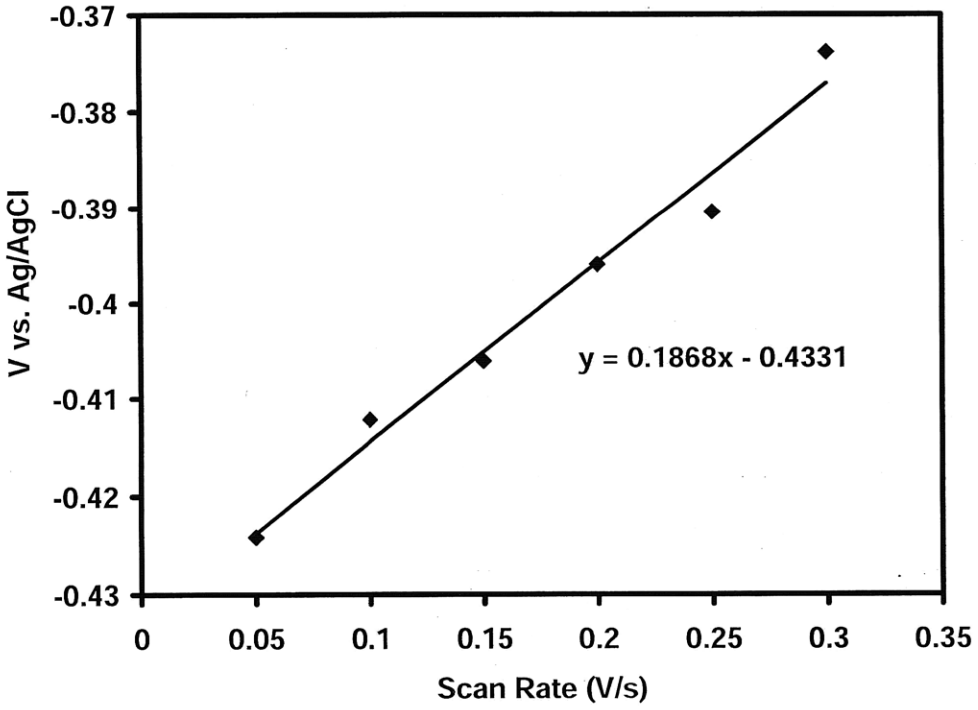

Figure 3.5. Scan rate vs. potential at pH 7.4. Measurements were made at 25 °C on compound 8 dissolved to a final concentration of 2.0 mM in 0.1 M aqueous KCl buffered with 10 mM phosphate.

Cytotoxicity in OCT1(+) vs. hOCT1(-) Cell Lines

Compounds were evaluated for cytotoxicity in hOCT1(+) and hOCT1(-) cell lines by Shuzhong Zhang in the lab of Kathy Giacomini at UCSF. Cytotoxicity was measured in MDCK cells by the MTT assay. Cells were exposed to the compounds in DMEM for 7 h, after which the drug-containing medium was replaced with fresh DMEM. Following a 72-hour incubation, cytotoxicity was evaluated by the MTT method as previously described.[23] The data, reported in Table 3.1 and Figure 3.6, show improved cytotoxicity in the hOCT1(+) cell line for five of the seven "second generation" compounds tested. The *cis*-[Pt(NH_3)(benzylamine)Cl_2] compound is as toxic as oxaliplatin in this line and shows a greater difference between OCT1(+) and OCT(-) cells (24.5-fold vs. 22-fold difference). The [Pt(*R,R*-DACH)(acac)]Cl compound also exhibits a large difference in OCT + vs – cytotoxicities (21.2-fold), although it is two to three times less cytotoxic than oxaliplatin. The *cis*-[Pt(NH_3)$_2$(pyridine)Cl]Cl compound displayed the greatest improvement in cytotoxicity of 87-fold (Table 3.1, Figure 3.6), although it is also about two-fold less cytotoxic than oxaliplatin in the OCT1(+) cell line. One other tested compound with a single labile ligand is **4**, a compound regarded as inactive in much of the platinum literature that showed a 10-fold improvement in cytotoxicity in MDCK-OCT1 cells.

Platinum(II) compounds of the form *trans*-[Pt(Am1)(Am2)Cl_2], where Am1 and Am2 are am(m)ine ligands, aquate four times faster than the corresponding *cis* compounds.[24] The facile aquation, which leads to faster formation of a cationic form as compared with oxaliplatin, was not sufficient for activation of the traditionally inactive

trans geometry. Neither *trans*-[$PtCl_2$(pyridine)$_2$] nor *trans*-[Pt(cyclopentylamine)$_2Cl_2$] showed activity in the MDCK-OCT1 cells.

Table 3.1. IC_{50} values for MDCK with overexpressed hOCT1.

Compound	IC_{50} hOCT1(+) (μM)	fold decrease for OCT1 + vs. -
trans-[$PtCl_2$(pyridine)$_2$]	>400	NA
trans-[Pt(cyclopentylamine)$_2Cl_2$]	>400	NA
trans-[$PtCl_2(NH_3)$(piperazine)]Cl (1)	94	5.1
cis-[$Pt(NH_3)$(benzylamine)Cl_2] (3)	1.15	24.5
[Pt(dien)Cl]Cl (4)	62 ± 16.8	10
[Pt(*R,R*-DACH)(acac)]Cl (2)	8.68 ± 1.39	21.2
cis-[$Pt(NH_3)_2$(pyridine)Cl]Cl (5)	8.09 ± 1.62	87
oxaliplatin	3.9 ± 1.3	22
cisplatin	3.6 ± 0.3	1.7

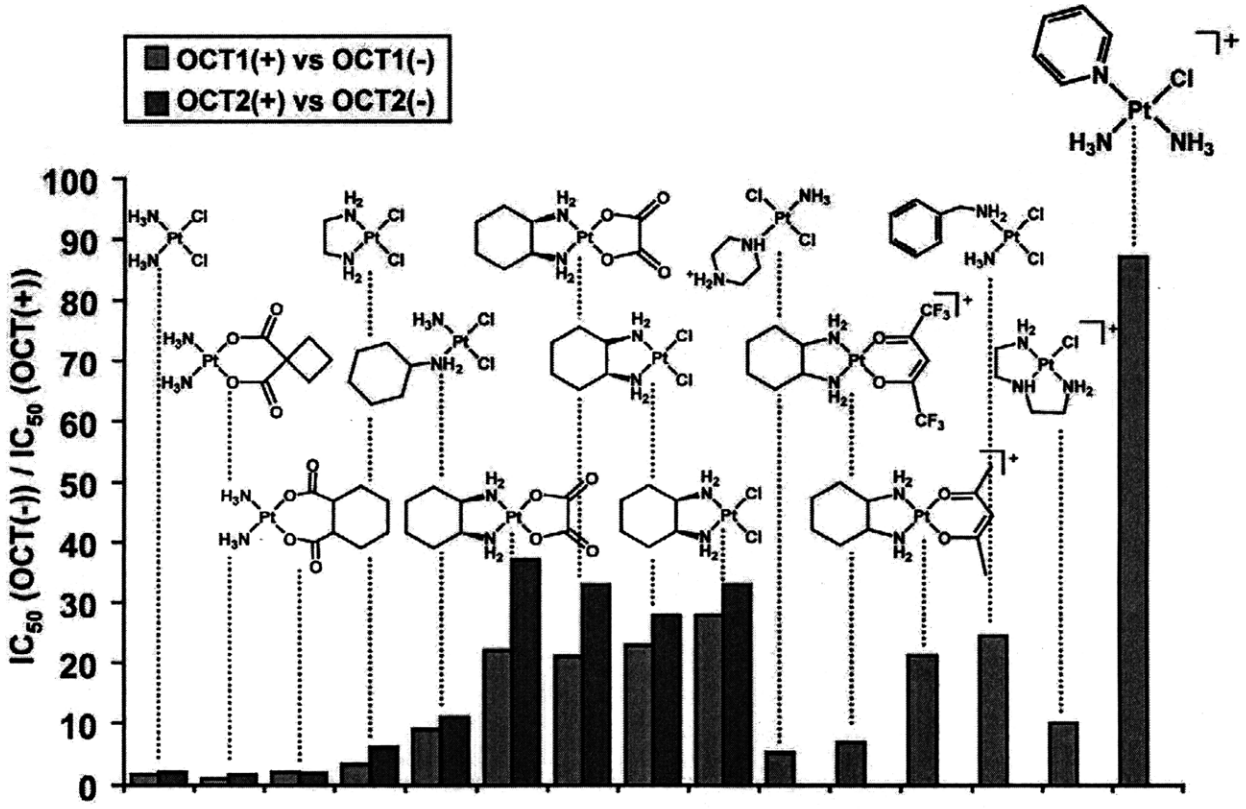

Figure 3.6. Plot of improvement in cytotoxicity for compounds studied (IC_{50} in OCT(-) divided by IC_{50} in OCT(+) cells).

Knockdown of hOCT1 in Human Colorectal Cancer Cells

Generation of shRNA against OCT1 in human colorectal cells was achieved using a versatile plasmid platform designed by Andrea Ventura in the Jacks lab at MIT. The plasmid pSicoR-GFP (Figure 3.1) contains the U6 promoter for RNA polymerase III, which has been widely used to generate shRNAs. The Lox-STOP-Lox element in this promoter allows conditional turn-off of shRNA expression upon addition of Cre recombinase.[1] GFP is also expressed by the plasmid, allowing verification of transfection and infection by fluorescence microscopy.

Three DNA sequences coding for shRNA against hOCT1 were successfully cloned into pSicoR-GFP and those plasmids, along with the requisite viral packaging vectors, were transfected into 293T/17 cells. Virus generation was robust and a high viral titer was obtained, as observed by fluorescence microscopy (Figure 3.7).

Human colorectal HT-29 cells were successfully infected by incubation with the virus-containing medium produced by the 293T/17 cells, as detected by fluorescence microscopy (Figure 3.7). The GFP-expressing cells, which comprised 76.2%, 92.4%, and 0.07% of the cells infected with the 1142, 806, and 803 clones, respectively, were collected by FACS (fluorescence-assisted cell sorting).

293T/17 in virus generation. HT-29 cells after infection.

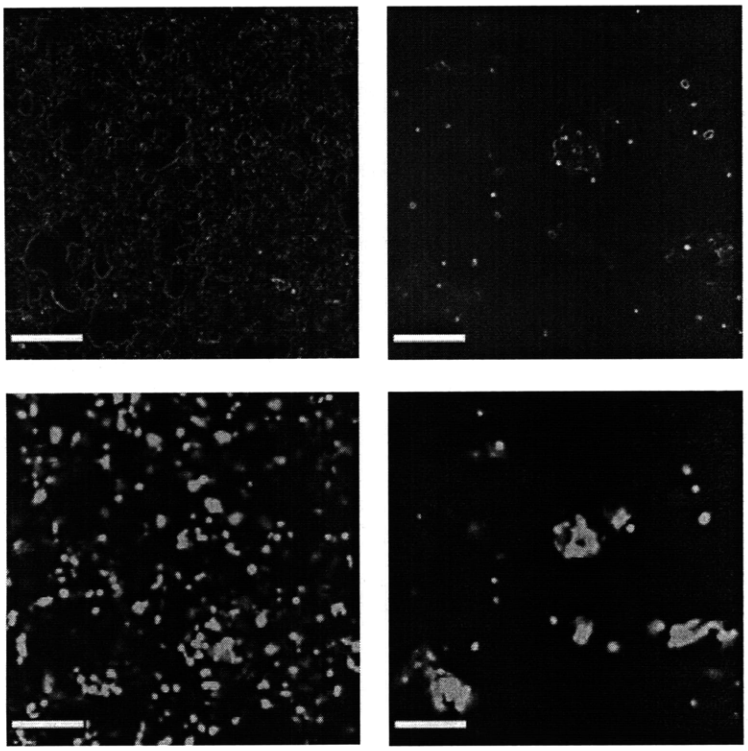

Figure 3.7. Fluorescence microscopy (10x magnification) of 293T/17 cells in the virus-generation stage (left column) and in infected HT-29 cells (right column), 4 weeks after successful infection. The number of cells showing fluorescence is nearly 100%, as verified by fluorescence-assisted cell sorting.

Validation of OCT1 Knockdown

RT-PCR was performed using previously described primers.[2] Analysis of gene silencing by RT-PCR is an accepted method of validation (See Table 3.2). Expression of OCT1 mRNA was reduced by 28% in the HT-29/pSicoR-1142_3 line, 53% in HT-29/pSicoR-803_6, and 86% in HT-29/pSicoR-806_4 (Figures 3.8 and 3.9).

Method	Detection Level	Advantage	Disadvantage	Throughput
Northern blot	Endogenous mRNA	Easy	RNA isolation	Low
qRT-PCR (TaqMan® or SYBR® Green	Endogenous mRNA	Sensitive, quantitative	RNA isolation, primer design	High
QuantiGene® www.genospectra.com	Endogenous mRNA	Sensitive, quantitative, works on crude lysate	Cost	High
Western blot, IF, ELISA, FACS, etc.	Endogenous protein	Easy	Antibody availability	Low
Western blot, IF, etc., on epitope tag	Exogenous fusion protein	Same antibody for detection	In-frame cloning, restricted target region	High
Fluorescent/enzymatic reporter assay	Exogenous protein (translated from chimeric mRNA)	Entire cDNA can be targeted, only reporter is translated		High

mRNA, messenger RNA; qRT-PCR, quantitative reverse transcription PCR; IF, immunofluorescence; ELISA, enzyme-linked immunosorbent assay; FACS, fluorescence-activated cell sorting.

Table 3.2. Table of commonly used functional validation methods for mammalian RNAi.[3] Table reproduced from Jacks, T.; *et. al.*, *Biotechniques*, 2005.

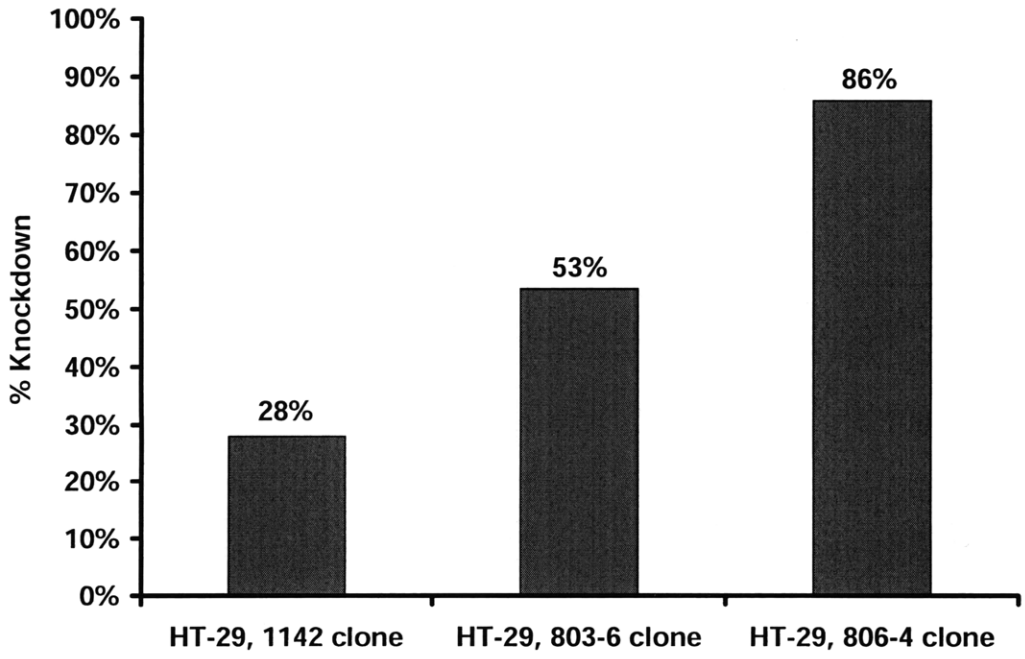

Figure 3.8. Plot of percent knockdown of hOCT1 by shRNA relative to native HT-29 mRNA for OCT1 (0% knockdown).

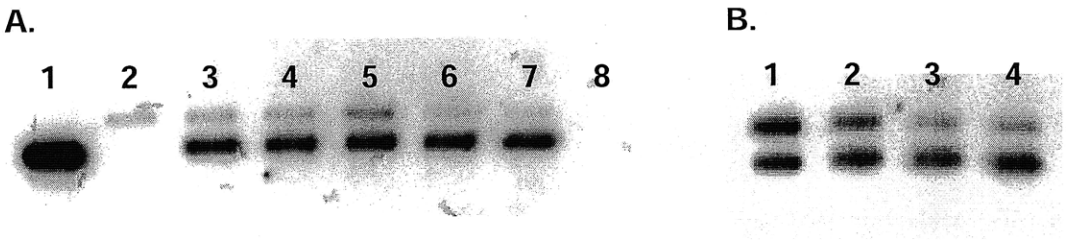

Figure 3.9. Agarose gel showing bands resulting from detection of mRNA of hOCT1 and GADPH in human colorectal cell lines. A: Semi-quantitative RT-PCR. Lane 1: GADPH primers only, lane 2: hOCT1 primers only, lane 3: HCT-116, lane 4: 293T/17, lane 5: HT-29 wild-type, lane 6: HT-29 with pSicoR-803_6, lane 7: HT-29 with pSicoR-806_4, lane 8: no DNA control reaction. B: Comparison of knockdown from three plasmids. Lane 1: HT-29 wild-type, lane 2: HT-29 with pSicoR-1142_3, lane 3: HT-29 with pSicoR-806_4, lane 4: HT-29 with pSicoR-803_6.

Cytotoxicity of Platinum Compounds in hOCT-Knockdown Cell Lines

The response of hOCT1-knockdown cells to varying doses of either oxaliplatin or **5** was evaluated in two separate experiments, each performed in triplicate for each compound. The IC_{50} values for **5** and **6** were evaluated in the control cell line as well and both values were on the same order of magnitude as **4** and much less toxic than oxaliplatin. The IC_{50} values for both oxaliplatin and **5** were directly related to the level of OCT knockdown, as shown in Table 3.3, which is the inverse of what would be expected if OCT1 were implicated in cellular accumulation.

The lowest IC_{50} values of 133 μM and 0.81 μM for **5** and oxaliplatin, respectively, were obtained for the HT-29/pSicoR-806_4 cell line, the cells with the lowest level of OCT1 mRNA. The trend was pronounced for **5**, which showed IC_{50} values of 260, 287, and 719 μM in cells with the second lowest, second highest, and highest (wild-type) level of OCT1 mRNA. The corresponding results for oxaliplatin were 1.62, 1.75, and 3.22 μM.

Table 3.3. IC_{50} values for knockdown cell lines.

	5	oxaliplatin	**6**	**7**
HT-29	719 μM	3.22 μM	770 μM	460 μM
HT-29/pSicoR-1142_3	260 μM	1.62 μM		
HT-29/pSicoR-803_6	287 μM	1.75 μM		
HT-29/pSicoR-806_4	133 μM	0.81 μM		

Uptake in hOCT1(+) vs. hOCT1(-) Cell Lines

DNA platination levels were measured in HT-29 and HT-29/pSicoR-806_4 cells, which allowed comparison of lines with the highest and lowest levels of OCT1. The r_b values for **5** were $1.9 \times 10^{-4} \pm 7.2 \times 10^{-6}$ and $2.4 \times 10^{-4} \pm 1.6 \times 10^{-5}$ in HT-29 and HT-29/pSicoR-806_4, respectively.(Table 3.4, Figure 3.10) The r_b values for oxaliplatin were $9.4 \times 10^{-6} \pm 1.7 \times 10^{-6}$ and $6.1 \times 10^{-6} \pm 1.2 \times 10^{-6}$.

Table 3.4. DNA Platination Levels in Normal and OCT1-knockdown Cell Lines (r_b)

	5	oxaliplatin
HT-29 control (CD8)	$1.9 \times 10^{-4} \pm 7.2 \times 10^{-6}$	$9.4 \times 10^{-6} \pm 1.7 \times 10^{-6}$
HT-29 with pSicoR-806_4	$2.4 \times 10^{-4} \pm 1.6 \times 10^{-5}$	$6.1 \times 10^{-6} \pm 1.2 \times 10^{-6}$

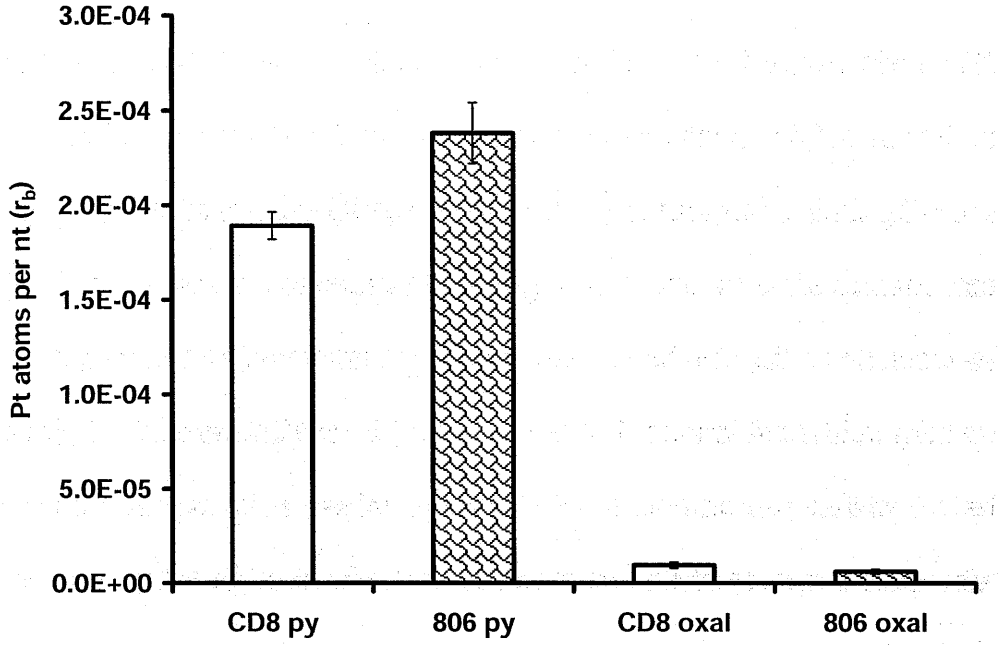

Figure 3.10. Uptake in HT-29 vs. HT-29 OCT1-knockdown cells expressed as platinum atoms bound per nucleotide (r_b) Compounds tested were oxaliplatin (oxal) and compound 5 (py).

Discussion

Synthesis of Compounds as OCT Substrates

Using the previously developed structure-activity relationship as a starting point,[2] a variety of new compounds were designed as potential OCT substrates. The synthesis and investigation of cationic compounds that do not require aquation prior to OCT uptake was of particular interest. A more inert cationic Pt(IV) complex was also synthesized for the purpose of tuning activation of the complex. The synthesis of *cis*-[$Pt(NH_3)_2$(2-amino-3-picoline)Cl]Cl was motivated by results of a high-throughput screen of platinum(II) compounds in which *cis*-[$Pt(NH_3)$(2-amino-3-picoline)Cl_2] was one of four hits.[7] The related compound *cis*-[$Pt(NH_3)_2$(2-picoline)Cl]Cl was synthesized to probe the behavior of a cationic, monofunctional form of "picoplatin," or *cis*-[$Pt(NH_3)$(2-

picoline)Cl_2], a compound designed to overcome cisplatin resistance that is currently in clinical development.[8]

Redox Properties of a Cationic Pt(IV) Compound

The redox properties of **8** indicate the complex is less readily reduced than satraplatin (*c,c,t*-[$Pt(NH_3)_2$(cyclohexylamine)$Cl(OH)_2$], also known as JM216), the first orally active platinum compound to undergo clinical investigation. The ease of reduction of satraplatin and similar Pt(IV) complexes is related to the electron-withdrawing nature of the axial ligands and the steric bulk of all ligands.[25] Satraplatin has a relatively bulky cyclohexylamine ligand and relatively electron-withdrawing acetate axial ligands, both of which contribute to its high redox potential of -0.053 V vs. NHE.[25] This high redox potential renders it readily reducible in the bloodstream. Hemoglobin in red blood cells are implicated as a key catalyst in the NADH-dependent reduction and contribute to the rapid (<30 min) reduction of satraplatin in blood.[26]

The redox potential of **8** is lower than that of satraplatin, but higher than those of *c,c,t*-[Pt(ipa)$Cl_2(OH)_2$] (-530 mV vs. NHE)[25] and [Pt(en)$Cl_2(OH)_2$] (-684 mV vs. NHE)[27] because of its cationic nature. Because only one Pt(IV) complex has ever been tested in humans, the ideal reduction potential for an orally bioavailable platinum drug remains to be determined. The redox behavior of **8** suggests that it will remain intact for a longer period than satraplatin, which has a shorter-than-desirable half-life in blood, but will be reduced in cells over time to bind DNA, its cytotoxic target.

Cytotoxicity of Platinum(II) Compounds in MDCK-HOCT1 Cells

A comparison of the difference in IC_{50} values in MDCK-MOCK cells and MDCK-hOCT1 cells is plotted in Figure. 3.6. This figure includes data from chapter 2.[2] Absolute values for IC_{50} are shown in Table 3.1. Comparing absolute values for IC_{50} for the seven drug candidates, only compound **3**, has a potency equal to or greater than oxaliplatin or cisplatin. Compound **3** has about half the IC_{50} of oxaliplatin and cisplatin in MDCK-OCT1 cells and has about the same IC_{50} as oxaliplatin (but not cisplatin) in MDCK cells without the transporter. The stability of this compound in biological milieu may be related to its potency, although the *trans* isomer of this complex was stable enough to undergo reflux in water and H_2O_2 for 2 h.[19]

Of the seven second generation compounds, five show improved cytotoxicity in OCT1 (+) as compared with OCT1(-) cell lines. The best improvement was seen for *cis*-$[Pt(NH_3)_2(pyridine)Cl]Cl$, **5**, a monofunctional compound with only one leaving group and three neutral am(m)ine ligands, The absolute IC_{50} value of **5** is about 2-fold higher than oxaliplatin, even in the MDCK-hOCT1 line. Because of this high IC_{50}, a relatively high load of **5** might need to be delivered to patients for it to be effective even though **5** is likely to be much more potent in tumors expressing OCT1 than in cells without OCT1. This compound has previously shown activity without overt toxic side effects in a i.p./i.p. mouse model,[17] suggesting potential viability as a drug.

Another compound with a single leaving group is **4**, a compound often used in the platinum literature to model the "inactive" monofunctional adduct. The 10-fold improvement in cytotoxicity of this compound in MDCK-OCT1 cells suggests that its inactivity arises in part from low cellular accumulation and not from the cell killing ability

of the monofunctional platinum-DNA adduct. Compound **5** will be investigated in more detail as "pyriplatin" in chapters 4 and 6.

Knock-down of OCT1 in a Colorectal Cancer Cell Line

Studies in cells with overexpression of organic cation transporters have provided results relevant for the transporter community regarding whether platinum compounds could be substrates for OCTs. More relevant to the cancer community is the issue of whether these transporters will be an important factor in cancer therapy. The hOCT1 is expressed in human colorectal tumors,[2] but we did not know whether the organic cation transporters would be relevant to platinum drug potency in cells with normal levels of the transporter. Initial studies of oxaliplatin cytotoxicity using an inhibitor of OCT1 (disopyramide) in HT-29 cells, a colorectal cell line only expressing OCT1 (and no OCT2[2]), showed no difference in oxaliplatin potency between cells treated with the inhibitor and control cells. We resolved to generate cells that lacked OCT1 to eliminate all transport by OCTs. Among the three sequences used to knock down OCT1, a sequence that started at position 806 in the gene produced the best knockdown of OCT1 in HT-29 cells.

Cytotoxicity of Platinum(II) Compounds in HT-29 and hOCT1-Depleted Cell Lines

The IC_{50} values for both oxaliplatin and **5** increased as the level of OCT knockdown increased. The compounds were more potent in cell lines with low levels of OCT1, which is the inverse of what should be expected if OCT1 were implicated in uptake of these compounds.

DNA Binding in Cells with Depleted hOCT1

DNA binding experiments comparing **5** in HT-29 and HT-29/pSicoR-806_4 showed a 125% increase in DNA-bound platinum for the HT-29/pSicoR-806_4 line (Figure 3.10, Table 3.4), which corresponds to the decrease in IC_{50} seen in the knockdown line. In contrast, oxaliplatin experiments showed only 65% DNA-bound platinum in the HT-29/pSicoR-806_4 as compared with HT-29 cells. Because oxaliplatin forms many fewer adducts on DNA than other platinum compounds,[28] the background on these measurements was very high and the difference between the control and knockdown samples were within the error of measurement. This was not the case for the pyriplatin measurements, which reinforce the trend seen in the IC_{50} values.

Conclusion

The conflicting results regarding the organic cation transporter studies indicate that the mechanism of uptake for **5** and oxaliplatin may be too complex to attribute to a single transporter. The cell may increase transcription of genes coding for other transporters to compensate for the lack of hOCT1, a plausible theory because of the multitude of cation transporters in the cell.[29] The compound **5** is still of strong scientific interest because it is a cytotoxic, cationic compound that binds in a monofunctional manner with DNA. The interest of drug companies in compounds that differ significantly from cisplatin, carboplatin, and oxaliplatin in their mechanisms of action is strong. The well-developed talent of our lab in structural characterizations of platinum-DNA interactions suggests we should pursue compounds, including compound **5**, that

interact in novel ways with DNA. The focus on single proteins within the cell, such as hOCT1, hOCT2, or HMGB1 can yield highly relevant information for the respective protein communities, but may not always produce useful insight into the design of anticancer drugs. In the case of **5**, a representative of a class of compounds that has been investigated by our lab previously and tested for use in leukemia,[30,31] we have identified a valuable exception that will be evaluated in detail in Chapters 4 and 6.

References

(1) A. Ventura, A. Meissner, C. P. Dillon, M. McManus, P. A. Sharp, L. Van Parijs, R. Jaenisch and T. Jacks (2004). Cre-lox-regulated conditional RNA interference from transgenes. *Proc. Natl. Acad. Sci. U. S. A.*, **101**, 10380-10385.

(2) S. Zhang, K. S. Lovejoy, J. E. Shima, L. L. Lagpacan, Y. Shu, A. Lapuk, Y. Chen, T. Komori, J. W. Gray, X. Chen, S. J. Lippard and K. M. Giacomini (2006). Organic Cation Transporters Are Determinants of Oxaliplatin Cytotoxicity. *Cancer Res.*, **66**, 8847-8857.

(3) P. Sandy, A. Ventura and T. Jacks (2005). Mammalian RNAi: A practical guide. *Biotechniques*, **39**, 215-224.

(4) M. J. Cleare and J. D. Hoeschele (1973). Studies on the Antitumor Activity of Group VIII Transition Metal Complexes. Part I. Platinum(II) Complexes. *Bioinorg. Chem.*, **2**, 187-210.

(5) B. Feng, Y. Shu and K. M. Giacomini (2002). Role of Aromatic Transmembrane Residues of the Organic Anion Transporter, rOAT3, in Substrate Recognition. *Biochemistry*, **41**, 8941-8947.

(6) D. A. Dougherty (1996). Cation-p interactions in chemistry and biology: a new view of benzene, Phe, Tyr, and Trp. *Science*, **271**, 163-168.

(7) C. J. Ziegler, A. P. Silverman and S. J. Lippard (2000). High throughput synthesis and screening of platinum drug candidates. *J. Biol. Inorg. Chem.*, **5**, 774-783.

(8) L. Kelland (2007). The resurgence of platinum-based cancer chemotherapy. *Nat. Rev. Cancer*, **7**, 573-584.

(9) J. Holford, S. Y. Sharp, B. A. Murrer, M. Abrams and L. R. Kelland (1998). In vitro circumvention of cisplatin resistance by the novel sterically hindered platinum complex AMD473. *Br. J. Cancer*, **77**, 366-373.

(10) S. C. Dhara (1970). A rapid method for the synthesis of *cis*-$[Pt(NH_3)_2Cl_2]$. *Indian J. Chem.*, **8**, 193-194.

(11) Y. I. Kidani, K. (1978). Antitumor activity of 1,2-diaminocyclohexane-platinum complexes against Sarcoma-180 ascites Form. *J. Med. Chem.*, **21**, 1315-1318.

(12) L. K. Thompson (1980). Trans platinum(II) complexes with pyridine and substituted pyridines. *Inorg. Chim. Acta*, **38**, 117-119.

(13) Y. Najajreh, J. M. Perez, C. Navarro-Ranninger and D. Gibson (2002). Novel Soluble Cationic trans-Diaminedichloroplatinum(II) Complexes that Are Active

against Cisplatin Resistant Ovarian Cancer Cell Lines. *J. Med. Chem.*, **45**, 5189-5195.
(14) P. Schwartz, S. J. Meischen, G. R. Gale, L. M. Atkins, A. B. Smith and E. M. Walker, Jr. (1977). Preparation and antitumor evaluation of water-soluble derivatives of dichloro(1,2-diaminocyclohexane)platinum(II). *Cancer Treat. Rep.*, **61**, 1519-1525.
(15) J. H. Price, A. N. Williamson, R. F. Schramm and B. B. Wayland (1972). Palladium(II) and platinum(II) alkyl sulfoxide complexes. Examples of sulfur-bonded, mixed sulfur- and oxygen-bonded, and totally oxygen-bonded complexes. *Inorg. Chem.*, **11**, 1280-1284.
(16) G. Annibale, M. Brandolisio and B. Pitteri (1995). New routes for the synthesis of chloro(diethylenetriamine)platinum(II) chloride and chloro(2,2':6',2''-terpyridine)platinum(II) chloride dihydrate. *Polyhedron*, **14**, 451-453.
(17) L. S. Hollis, A. R. Amundsen and E. W. Stern (1989). Chemical and biological properties of a new series of cis-diammineplatinum(II) antitumor agents containing three nitrogen donors: cis-[Pt(NH3)2(N-donor) Cl]+. *J. Med. Chem.*, **32**, 128-136.
(18) V. X. Jin, S. I. Tan and J. D. Ranford (2005). Platinum(II) triammine antitumour complexes: structure-activity relationship with guanosine 5'-monophosphate (5'-GMP). *Inorg. Chim. Acta*, **358**, 677-686.
(19) L. R. Kelland, F. J. Barnard, I. G. Evans, B. A. Murrer, B. R. C. Theobald, S. B. Wyer, P. M. Goddard, M. Jones, M. Valenti and et al. (1995). Synthesis and in vitro and in vivo antitumor activity of a series of trans platinum antitumor complexes. *J. Med. Chem.*, **38**, 3016-3024.
(20) A. J. Kraker, J. D. Hoeschele, W. L. Elliott, H. D. H. Showalter, A. D. Sercel and N. P. Farrell (1992). Anticancer activity in murine and human tumor cell lines of bis(platinum) complexes incorporating straight-chain aliphatic diamine linker groups. *J. Med. Chem.*, **35**, 4526-4532.
(21) A. Reynolds, D. Leake, Q. Boese, S. Scaringe, W. S. Marshall and A. Khvorova (2004). Rational siRNA design for RNA interference. *Nat. Biotechnol.*, **22**, 326-330.
(22) B. Lippert, R. Pfab and D. Neugebauer (1979). The role of N(1) coordinated thymine in 'platinum thymine blue'. *Inorg. Chim. Acta*, **37**, L495-L497.
(23) M. C. Alley, D. A. Scudiero, A. Monks, M. L. Hursey, M. J. Czerwinski, D. L. Fine, B. J. Abbott, J. G. Mayo, R. H. Shoemaker and M. R. Boyd (1988). Feasibility of drug screening with panels of human tumor cell lines using a microculture tetrazolium assay. *Cancer Res.*, **48**, 589-601.
(24) M. E. Howe-Grant and S. J. Lippard In *Metal Ions in Biological Systems*, 1980; Vol. 11, pp 63-125.
(25) S. Choi, C. Filotto, M. Bisanzo, S. Delaney, D. Lagasee, J. L. Whitworth, A. Jusko, C. Li, N. A. Wood, J. Willingham, A. Schwenker and K. Spaulding (1998). Reduction and Anticancer Activity of Platinum(IV) Complexes. *Inorg. Chem.*, **37**, 2500-2504.
(26) J. L. Carr, M. D. Tingle and M. J. McKeage (2006). Satraplatin activation by haemoglobin, cytochrome C and liver microsomes in vitro. *Cancer Chemother. Pharmacol.*, **57**, 483-490.

(27) L. T. Ellis, H. M. Er and T. W. Hambley (1995). The influence of the axial ligands of a series of platinum(IV) anti-cancer complexes on their reduction to platinum(II) and reaction with DNA. *Aust. J. Chem.*, **48**, 793-806.
(28) E. Raymond, S. Faivre, S. Chaney, J. Woynarowski and E. Cvitkovic (2002). Cellular and molecular pharmacology of oxaliplatin. *Mol Cancer Ther*, **1**, 227-235.
(29) H. Koepsell (2004). Polyspecific organic cation transporters: their functions and interactions with drugs. *Trends Pharmacol. Sci.*, **25**, 375-381.
(30) L. S. Hollis, W. I. Sundquist, J. N. Burstyn, W. J. Heiger-Bernays, S. F. Bellon, K. J. Ahmed, A. R. Amundsen, E. W. Stern and S. J. Lippard (1991). Mechanistic studies of a novel class of trisubstituted platinum(II) antitumor agents. *Cancer Res.*, **51**, 1866-1875.
(31) S. F. Bellon and S. J. Lippard (1990). Bending studies of DNA site-specifically modified by cisplatin, trans-diamminedichloroplatinum(II) and cis-[Pt(NH3)2(N3-cytosine)Cl]+. *Biophys. Chem.*, **35**, 179-188.

NMR Spectra

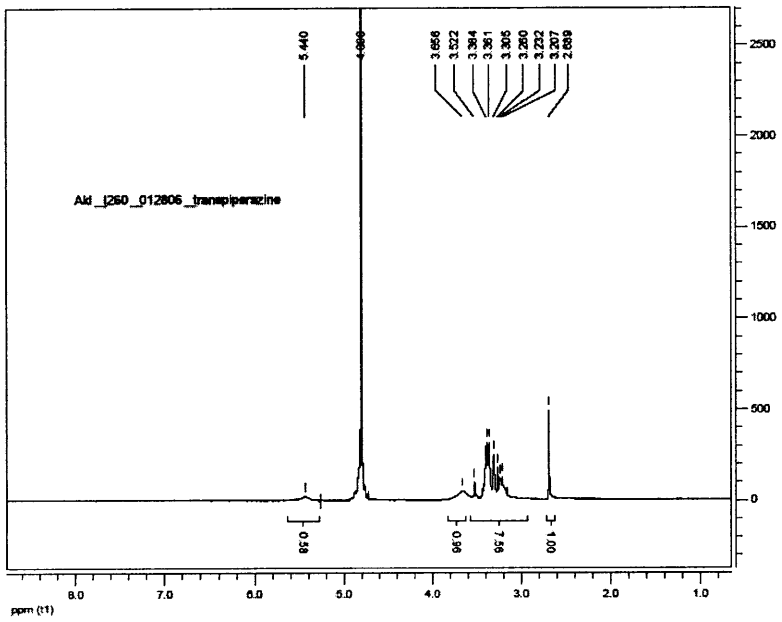

Figure 3.11. ^{1}H NMR of *trans*-[Pt(NH_3)(piperazine)Cl_2]Cl in D_2O.

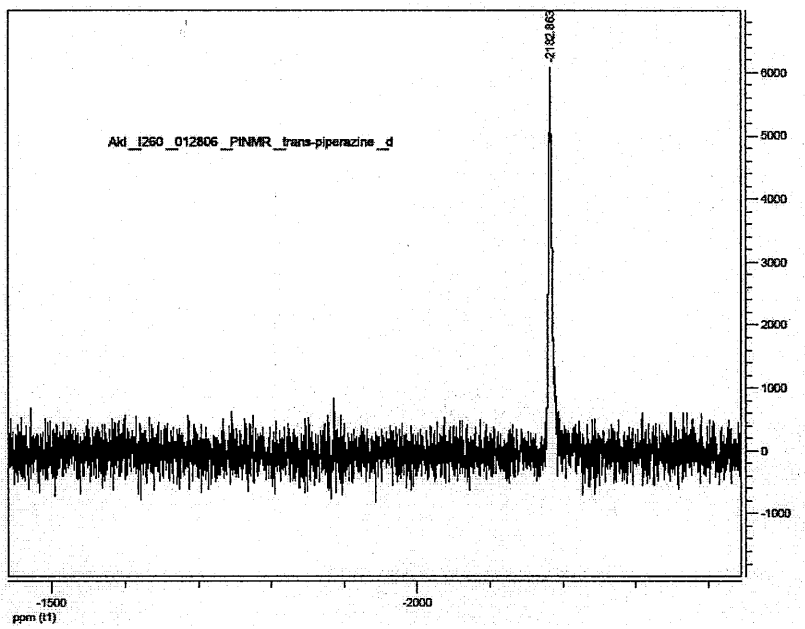

Figure 3.12. ^{195}Pt NMR of *trans*-[Pt(NH_3)(piperazine)Cl_2]Cl in D_2O.

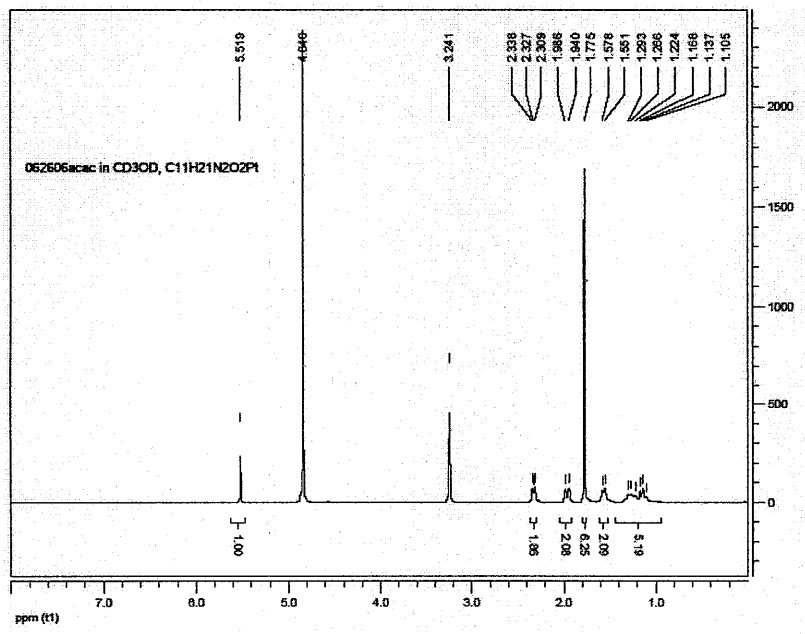

Figure 3.13. ^{1}H NMR of [Pt(*R,R*-DACH)(acac)]Cl in CD_3OD.

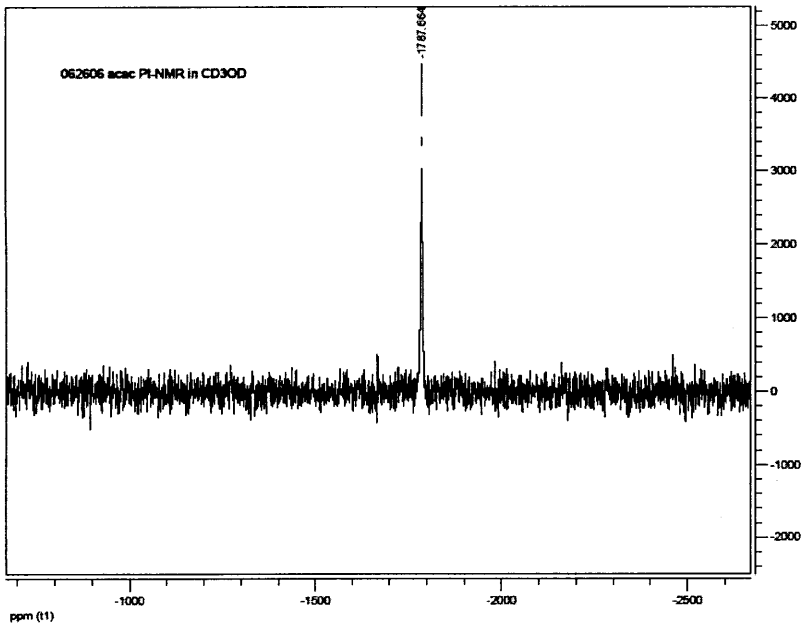

Figure 3.14. ^{195}Pt NMR of [Pt(*R,R*-DACH)(acac)]Cl in CD_3OD.

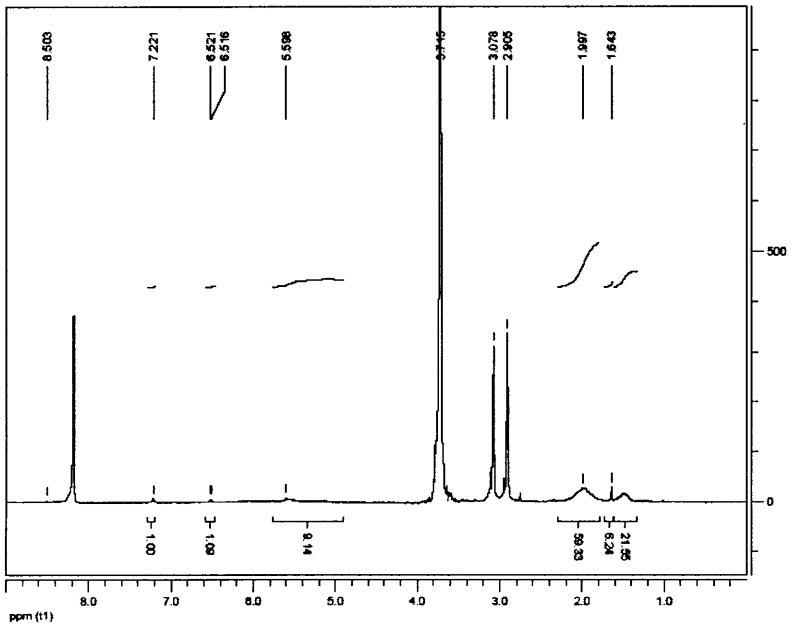

Figure 3.15. ^{1}H NMR of [Pt(*R,R*-DACH)(F6-acac)]Cl in *d*-DMF.

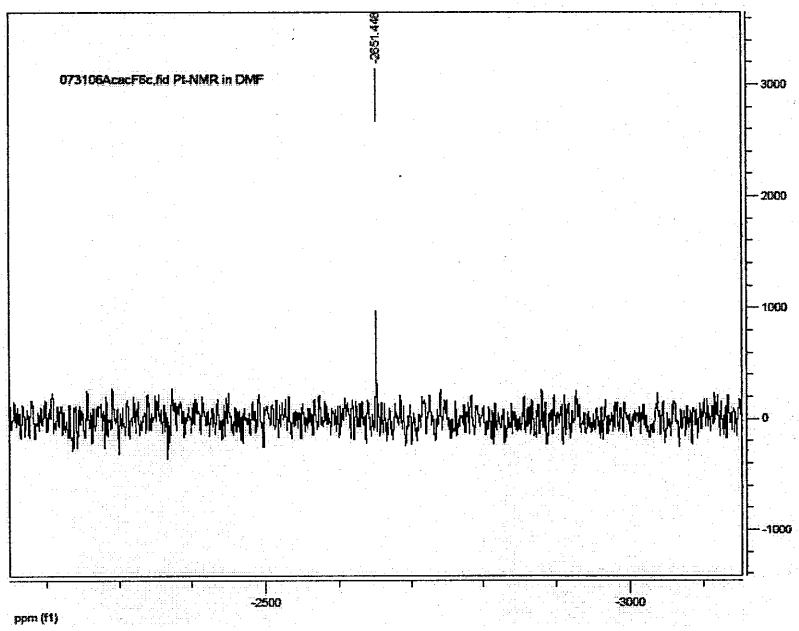

Figure 3.16. ^{195}Pt NMR of [Pt(*R,R*-DACH)(F6-acac)]Cl in DMF.

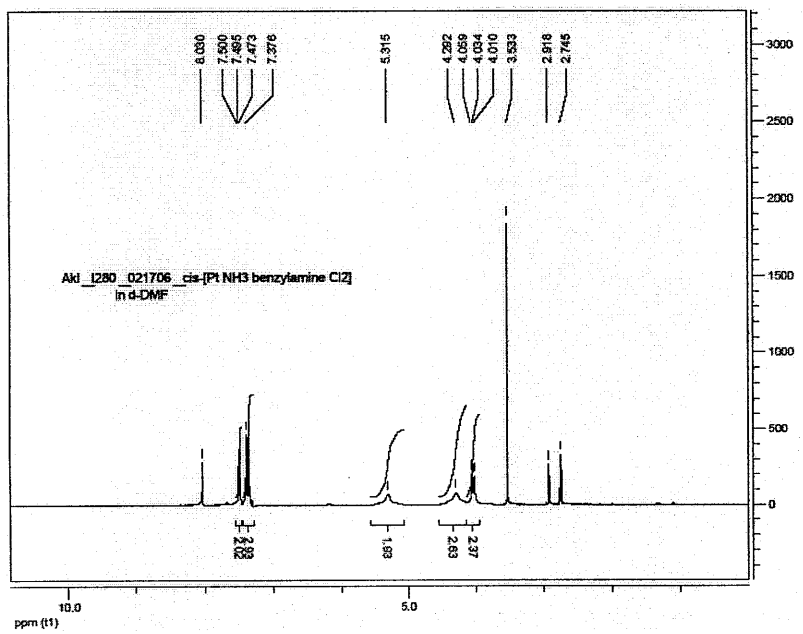

Figure 3.17. ^{1}H NMR of *cis*-[Pt(NH_3)(benzylamine)Cl_2] in *d*-DMF.

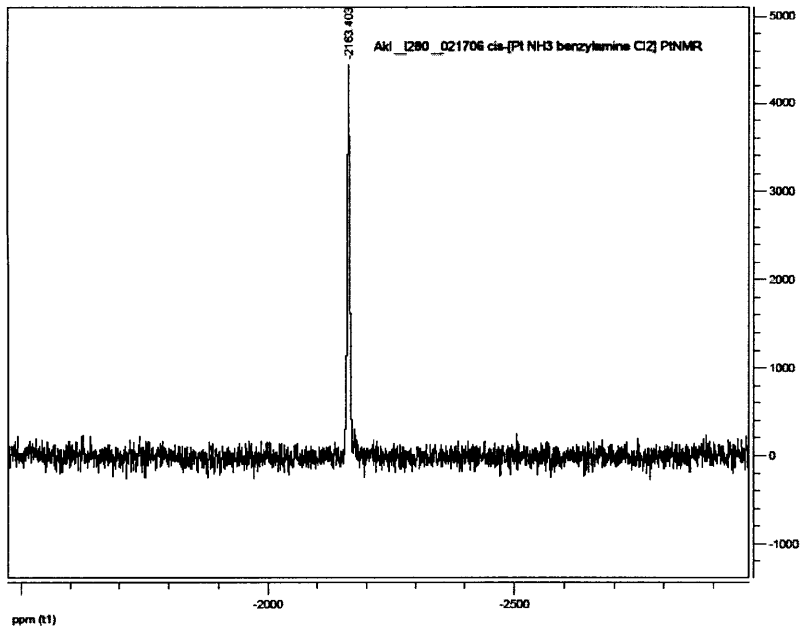

Figure 3.18. ^{195}Pt NMR of *cis*-[Pt(NH_3)(benzylamine)Cl_2] in CH_3OH.

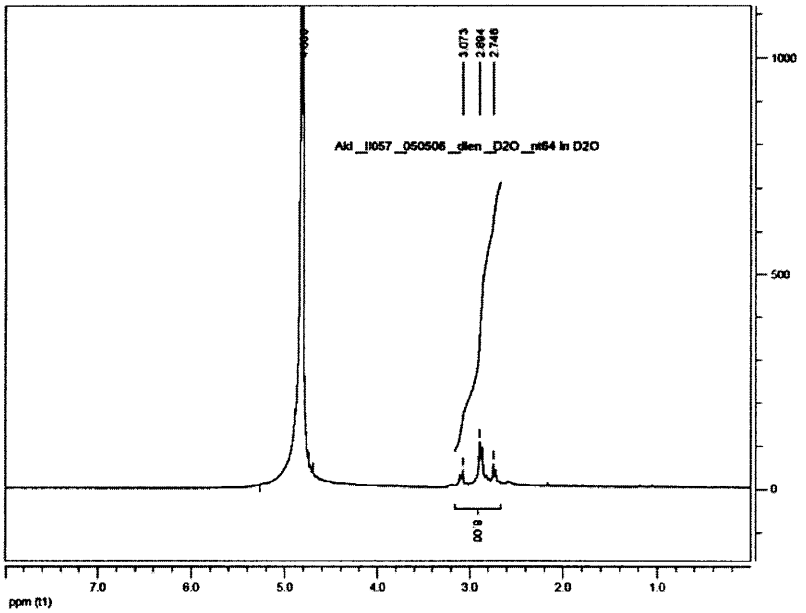

Figure 3.19. ^{1}H NMR of [Pt(dien)Cl]Cl in D_2O.

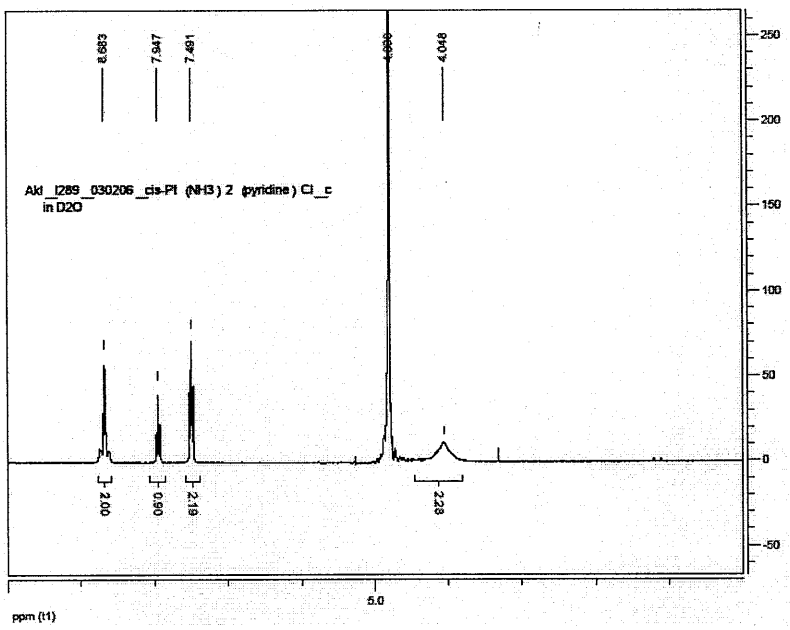

Figure 3.20. ^{1}H NMR of *cis*-[$Pt(NH_3)_2$(pyridine)Cl]Cl in D_2O.

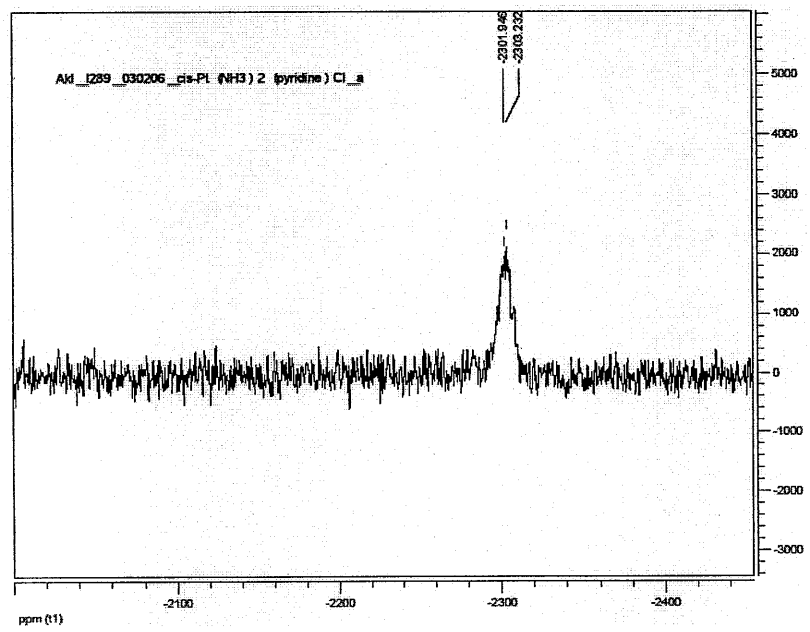

Figure 3.21. ^{195}Pt NMR of *cis*-[$Pt(NH_3)_2$(pyridine)Cl]Cl in CD_3OD.

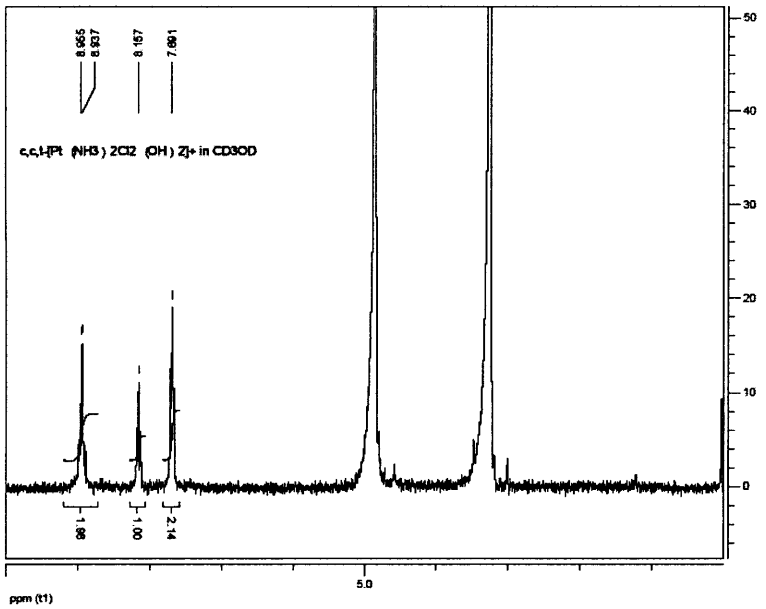

Figure 3.22. ^{1}H NMR of *cis,cis,trans*-$[Pt(NH_3)_2(pyridine)Cl(OH)_2]Cl$ in CD_3OD.

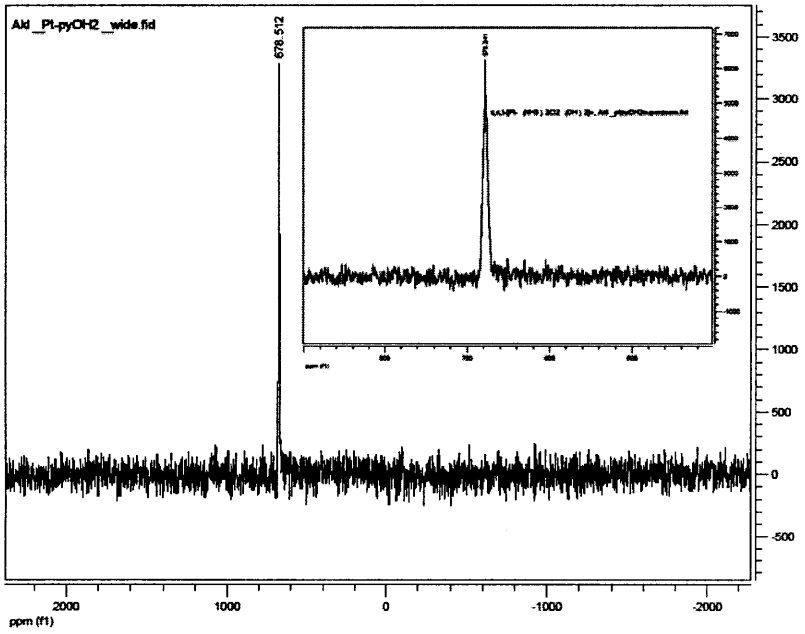

Figure 3.23. ^{195}Pt NMR of *cis,cis,trans*-$[Pt(NH_3)_2(pyridine)Cl(OH)_2]Cl$ in H_2O.

Chapter 4

Pyriplatin, *cis*-[Pt(NH_3)$_2$(pyridine)Cl]Cl, a Monofunctional, Cationic Platinum(II) Antitumor Agent

This chapter is composed, in part, of material from a published work (*Proc Natl Acad Sci USA* **2008**, *105*, 8902-8907).[1]

Introduction

The three FDA-approved platinum-based anticancer drugs, cisplatin, carboplatin, and oxaliplatin, form similar adducts on DNA, although only oxaliplatin is active in colorectal cancer. Organic cation transporters OCT1 and OCT2 have been implicated in the uptake of oxaliplatin by colorectal tumors.[2] We discovered *cis*-diammine-(pyridine)chloroplatinum(II), pyriplatin, as a highly effective organic cation transporter substrate that shows 80-fold increased cytotoxicity in OCT(+) mammalian cell lines.

The recent surge in clinical trials involving platinum anticancer drugs reflects the underlying potency and success rate of cisplatin. Most recent is the success of oxaliplatin in treating colorectal cancer.[3] Several platinum compounds that violate the classical structure-activity relationships for cisplatin are now in the clinic, including platinum(IV),[4] polyplatinum,[5] and platinum complexes with a trans stereochemistry.[6-13] Inspired by recent work[2] that identified the organic cation transfer receptors OCT1 and OCT2 as mediators of oxaliplatin entry into cells, we discovered *cis*-diammine-(pyridine)chloroplatinum(II), pyriplatin, to be a viable candidate for anticancer drug development. The anticancer activity of pyriplatin was established in rodents over 20 years ago[14,15] but, perhaps because unlike cisplatin it forms monofunctional rather than bifunctional cross-links with target DNA, the compound was never tested in humans. In the present report we describe the remarkable properties of pyriplatin including (i) its ability to block transcription and elude nucleotide excision repair, two mechanistic features that endow cisplatin with its anticancer activity; (ii) accumulation mediated by the OCT1/OCT2 receptors significantly better than that of oxaliplatin; and (iii) the X-ray crystal structure of a DNA dodecamer duplex containing a monofunctional adduct of the

complex bound to a central guanosine residue. Features of the structure bear a remarkable resemblance to those of the cisplatin intrastrand d(GpG) cross-link in DNA, which may account for the properties of pyriplatin.

Goals of the Chapter

The aim of the work described in chapter 4 is to characterize the interaction of a cationic, monofunctional platinum compound, pyriplatin, with DNA in cells and in vitro. Based on work in chapters 2 and 3, the hypothesis that the antitumor activity and accumulation of pyriplatin in cancer cells is due to organic cation transporters was also investigated.

Results

Cytotoxicity in Cells Expressing hOCT1 or hOCT2

Mammalian cells stably expressing human OCT1 or OCT2 or a control plasmid were used to study the cellular accumulation and cytotoxicity of pyriplatin and oxaliplatin. Pyriplatin is 87-fold more cytotoxic in cells expressing hOCT1 than in cells that lack the transporter, whereas oxaliplatin was only 12-fold more effective. The cytotoxicity of pyriplatin in cells expressing hOCT2 is 137-fold improved over the corresponding control cells, compared with a 53-fold increase with oxaliplatin (Figure 4.1). The outstanding improvement in cytotoxicity and large therapeutic window seen in the response of cells containing either OCT1 or OCT2 to pyriplatin immediately set this compound apart from the others tested (Chapter 3). The potency of pyriplatin is much lower than that of oxaliplatin in all four cell lines in Table 4.1.

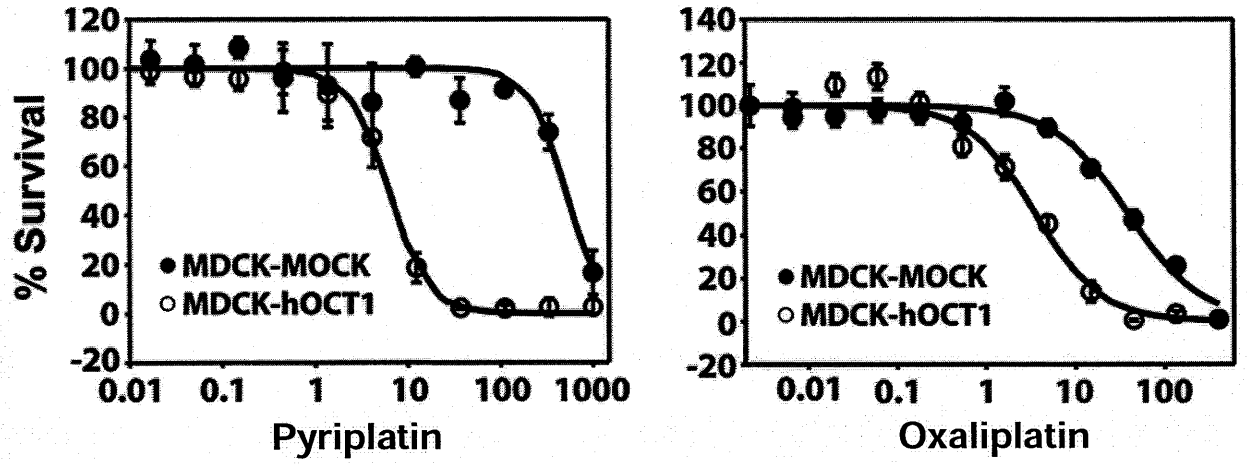

Figure 4.1. Antiproliferative effects of pyriplatin and oxaliplatin evaluated in MDCK cells expressing either hOCT1 or a control plasmid.

Table 4.1. Comparison of IC_{50} values for pyriplatin and oxaliplatin in cells with and without hOCT1 and hOCT2. IC_{50} values are expressed as mean±SD from three experiments and quadruplicate measurements were obtained in each experiment.

IC_{50} values (μM)

	MDCK-MOCK	MDCK-hOCT1	Fold Change
Pyriplatin	704 ± 280	8.1 ± 1.2	87
Oxaliplatin	40.5 ± 1.6	3.3 ± 1.0	12
	HEK-MOCK	HEK-hOCT2	
Pyriplatin	206 ± 56	1.50 ± 0.22	137
Oxaliplatin	4.0 ± 1.3	0.075 ± 0.009	53

Accumulation of Pyriplatin in Cells Expressing hOCT1 or hOCT2

Examination of treated cells for platinum content revealed that accumulation of pyriplatin is 68-fold higher in hOCT2-containing cells than in cells not expressing the transporter. Cells expressing hOCT1 accumulated 23-fold more platinum than the corresponding MOCK-transfected cells. Treatment of cells with oxaliplatin resulted in a 4.7-fold increase in hOCT1 cells than in control cells (Table 4.2) and a 23-fold increased

Table 4.2. Platinum accumulation in hOCT1 cells—cells were incubated with 10 μM platinum for 2 h and assayed for platinum content by ICP-MS. Units are in pmol/mg protein. Data are expressed as the mean of six measurements ± one standard deviation.

	MDCK-MOCK	MDCK-hOCT1	Fold Change
Oxaliplatin	13.9±0.94	65.6±4.1	4.7
Pyriplatin	33.1±0.5	779±67.2	23

Table 4.3. Platinum accumulation in hOCT2 cells—cells were incubated with 2 μM platinum for 2 h and assayed for platinum content by ICP-MS. Units are in pmol/mg protein. Data are expressed as the mean of six measurements ± one standard deviation.

	HEK-MOCK	HEK-hOCT2	Fold Change
Oxaliplatin	5.65±0.72	130±11	23
Pyriplatin	18.7±1.6	1278±69.4	68

platinum accumulation in hOCT2 cells than in control (Table 4.3). Measurements of platinum levels on DNA after pyriplatin treatment were not obtained, but DNA platination by oxaliplatin closely tracks its accumulation in cells expressing hOCT1 and hOCT2. Increases in cellular accumulation as well as DNA platination are reversible by OCT1 and OCT2 inhibitors.[2] The level of pyriplatin bound to DNA of cancer cells that are not overexpressing OCTs has been determined for other purposes (Chapter 3, Chapter 6). In those cases, DNA platination levels achieved by pyriplatin are generally greater than those found for oxaliplatin when cells are treated with the compounds at the IC_{50} concentrations.

Platination of Plasmid DNA

Plasmid (pBR322) DNA was incubated with pyriplatin or cisplatin for 24 h in Hepes buffer and platination levels were measured by atomic absorption spectroscopy. The results were plotted (Figure 4.2) as platinum atoms bound per nucleotide (r_b) vs. the formal ratio of platinum added per nucleotide (r_f). The plot indicates that the level of

plasmid-bound platinum is, within experimental error, the same for cisplatin and pyriplatin.

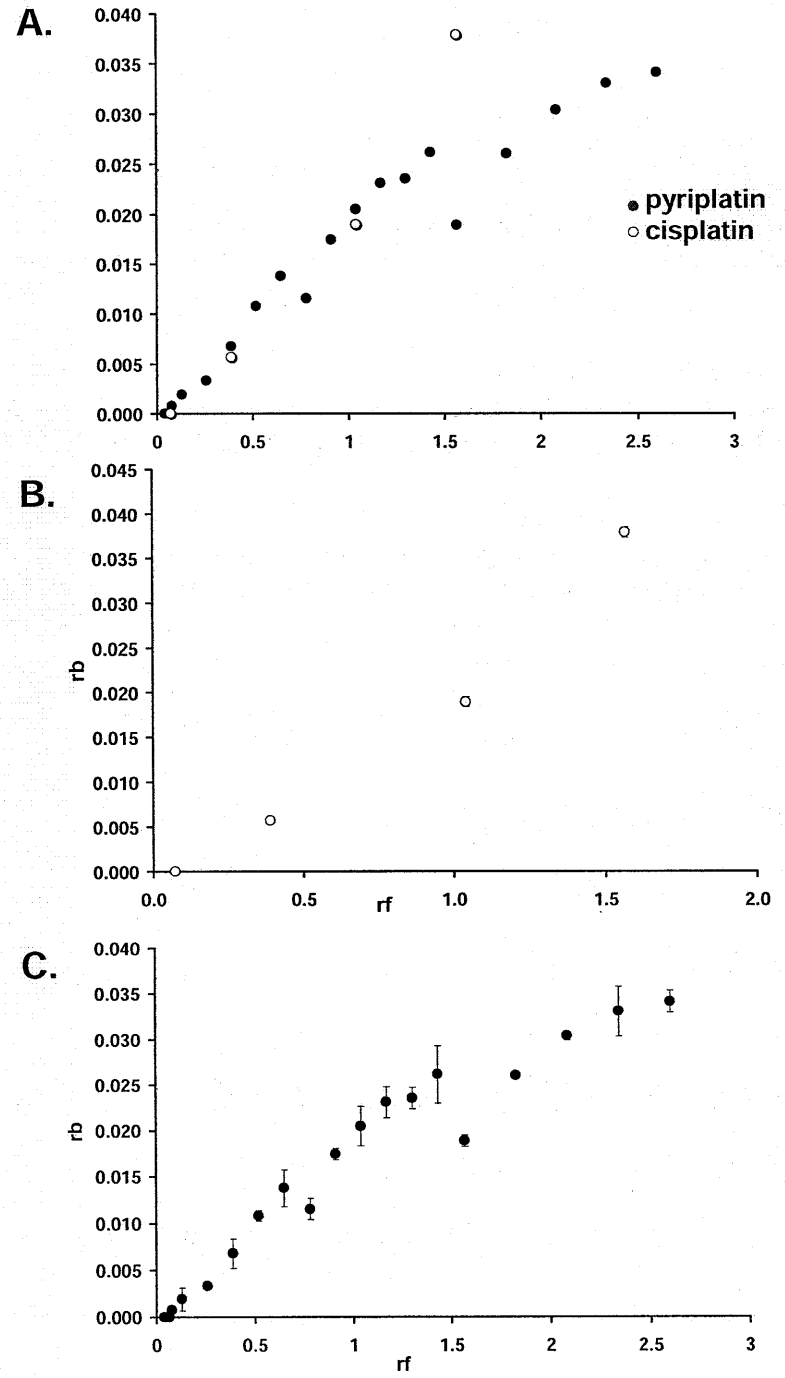

Figure 4.2. Results of r_f vs. r_b determination. A) Combined plot with cisplatin and pyriplatin overlaid. B) R_f vs. r_b for cisplatin only. C) R_f vs. r_b for pyriplatin only. Error bars show one standard deviation of data points measured in triplicate.

Agarose gel electrophoresis to analyze the unwinding of pBR322 DNA globally platinated with pyriplatin (Figure 4.3) was performed concurrently with atomic absorption spectroscopy on the samples plotted in Figure 4.2. This method of analysis of the

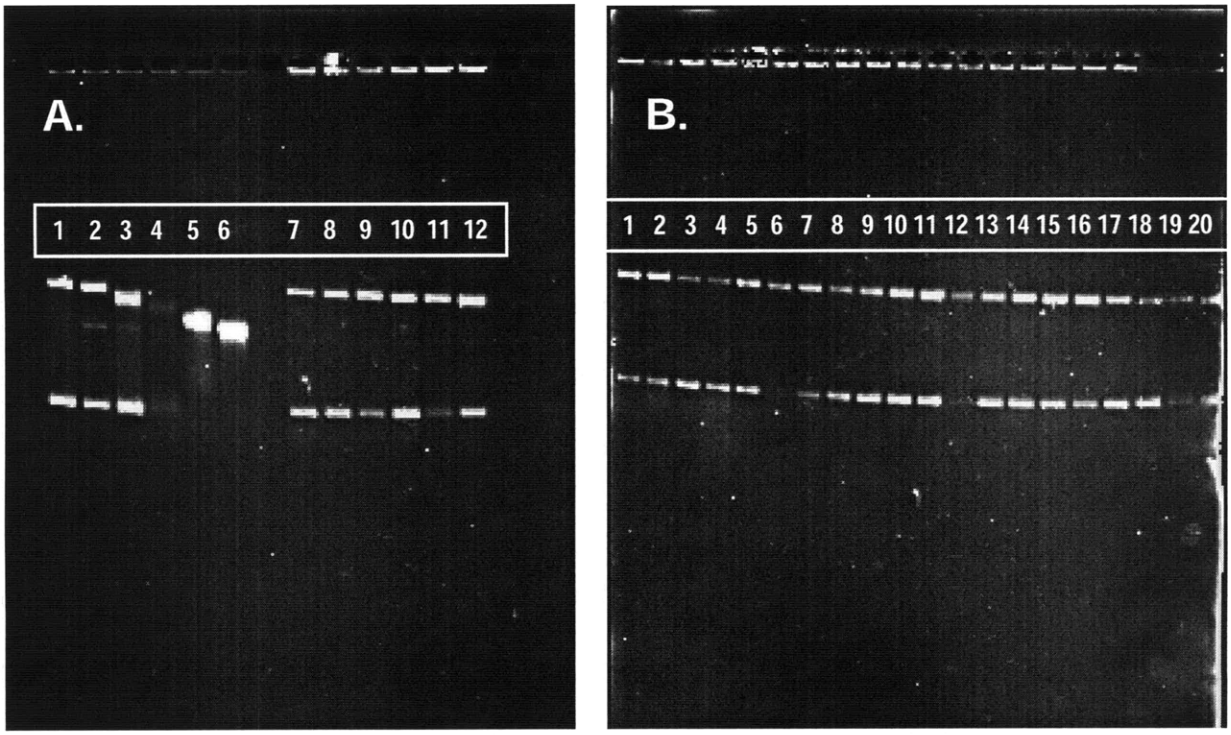

Figure 4.3. Analysis of DNA unwinding by agarose gel. Lanes as follows, wherein values are reported as r_f, then r_b (r_f/r_b): A) cisplatin: 1) 0.072/0; 2) 0.13/0.085; 3) 0.39/.006; 4) 0.65/0.005; 5) 1.04/0.019; 6) 1.57/0.038; pyriplatin: 7) 0.072/0; 8) 0.13/0.002; 9) 0.39/0.007; 10) 0.65/0.014; 11) 1.04/0.020; 12) 1.57/0.019. B) pyriplatin: 1) 0.039/0; 2) 0.052/0; 3) 0.065/0; 4) 0.078/0.001; 5) 0.13/0.002; 6) 0.26/0.003; 7) 0.39/0.007; 8) 0.52/0.011; 9) 0.65/0.014; 10) 0.78/0.012; 11) 0.91/0.017; 12) 1.04/0.020; 13) 1.17/0.023; 14) 1.3/0.024; 15) 1.43/0.026; 16) 1.57/0.019; 17) 1.83/0.026; 18) 2.08/0.030; 19) 2.34/0.033; 20) 2.6/0.034

unwinding of plasmid DNA is based on the principle that negatively supercoiled circular DNA becomes positively wound when the duplex is locally unwound, a phenomenon encountered upon the formation of intrastrand crosslinks by cisplatin. Each intrastrand Pt-DNA adduct formed by cisplatin unwinds the DNA duplex by 13°, whereas the monofunctional adducts formed by compounds such as $[Pt(dien)Cl]^+$ and $[Pt(NH_3)_3Cl]^+$

unwind the DNA duplex by only 6°.[16,17] Treatment of plasmid DNA with pyriplatin did not induce measurable unwinding of the superhelix at r_b (platinum bound per nucleotide) values of up to 0.034. This observation is consistent with the formation of monofunctional platinum-DNA adducts in solution.

Repair of DNA Damage Induced by Pyriplatin

We further examined the cellular response to pyriplatin by launching an investigation into cellular repair of the DNA damage caused upon the formation of DNA adducts. Nucleotide excision repair (hereafter "excision repair") is the repair pathway by which the major product of cisplatin-induced DNA damage, the intrastrand d(GpG) lesion,[18,19] is repaired.[20] The vitality of the excision repair pathway in human cells is a key indicator of the sensitivity of the tissue, and the entire patient, to platinum-based chemotherapy. Human cells from disorders in which nucleotide excision repair deficiency is a phenotype, such as xeroderma pigmentosum,[21] and Cockayne syndrome,[22] are exquisitely sensitive to cisplatin damage. A test for the presence of a key protein in the excision repair pathway, ERCC1, is in FDA Phase III trials for use as a predictive factor in tailoring chemotherapy to patients with non-small cell lung cancer.[23] Conversely, increased efficiency of the excision repair pathway leads to rapid removal of cisplatin adducts and the upregulation of ERCC1 is associated with cisplatin resistance in human tumor cells.[24,25]

In comparing the repair of three different site-specifically platinated 156mer probes, prepared as described[26,27] (Figure 4.4 and 4.5) we obtained 3.5% repair of the cisplatin-modified DNA, 1% repair of the pyriplatin adduct, and 0.3% repair of the

[Pt(dien)Cl]Cl adduct after 60 min reactions (Figure 4.6 and 4.7). This rate and amount of repair is comparable to the 1% repair previously observed for d(GpG) probes platinated with cisplatin,[20,26,28] and is less than the 10% repair observed for cisplatin-modified d(GpTpG) probes.[28]

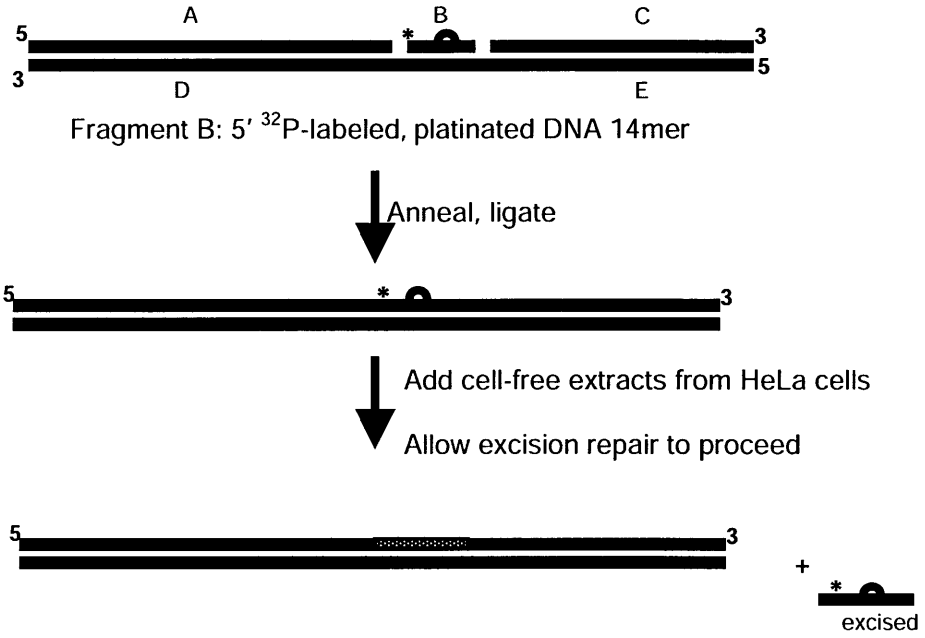

Figure 4.4. Preparation of site-specifically platinated probe and diagram of *in vitro* nucleotide excision repair assay.

63mer:
5′-ATCAATATCCACCTGCAGATTCTACCAAAAGTGTATTTGGAAACTGCTCCA
TCAAAAGGCATG-3′

14mer-G strand
5′-TTCACC**G**CAATTCC-3′

14mer-GG strand
5′-TTCACC**GG**AATTCC-3′
79mer
5′-CCTCAACATCGGAAAACTACCTCGTCAAAGGTTTATGTGAAAACCATCTTA
GACGTCCACCTATAACTACCTGGGAACC-3′

86mer-C strand
5′-ATGTTGAGGGGAATTG**C**GGTGAACATGCCTTTTGATGGAGCAGTTTCCAAA
TACACTTTTGGTAGAATCTGCAGGTGGATATTGAT-3′

86mer-CC strand
5′-ATGTTGAGGGGAATT**CC**GGTGAACATGCCTTTTGATGGAGCAGTTTCCAAA
TACACTTTTGGTAGAATCTGCAGGTGGATATTGAT-3′

70mer
5′-GGTTCCCAGGTAGTTATAGGTGGACGTCTAAGATGGTTTTCACATAAACCT
TTGACGAGGTAGTTTTCCG-3′

Figure 4.5. DNA oligomer components of 156mer repair probe.

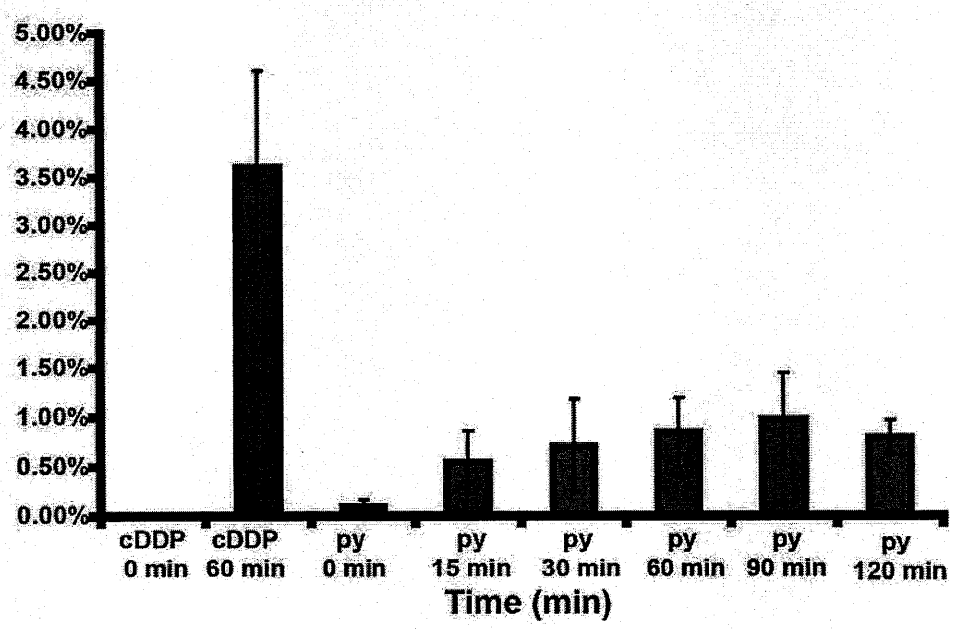

Figure 4.6. Kinetics of repair for pyriplatin-modified-DNA (py) reported as % repair relative to the 156mer band (CHO extracts).

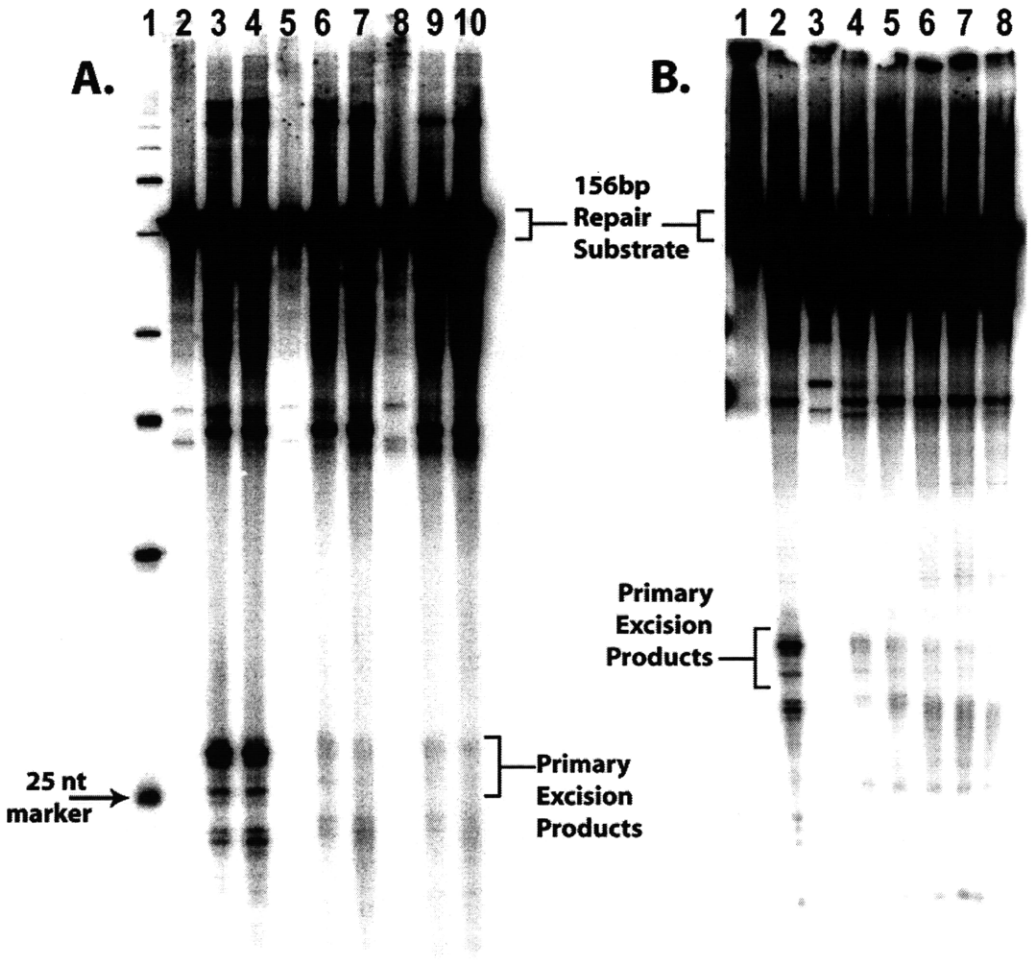

Figure 4.7. Representative gels showing nucleotide excision repair products. Lane assignments: A. Comparison of three probes. (1)100 bp ladder, (2) cisplatin 0 min, (3) cisplatin 30 min, (4) cisplatin 60 min, 5-7) pyriplatin 0/30/60 min, 8-10) [Pt(dien)Cl]Cl 0/30/60 min. B. Kinetics of repair for pyriplatin. (1) cisplatin 0 min, (2) cisplatin 60 min, 3-(8) pyriplatin 0/15/30/60/90/120 min.

A decrease in repair due to shielding by the nuclear structure-specific DNA binding protein HMGB1[29] was also observed, suggesting that some perturbation of the DNA structure does occur upon binding of the monofunctional pyriplatin. Repair of the 1,2-d(GpG) cisplatin adduct was inhibited by 77% upon addition of full length, fully reduced HMGB1 to 3.2 μM, whereas repair of the pyriplatin and [Pt(dien)Cl]Cl adducts was reduced by 65% and 32%, respectively (Figures 4.8, 4.9).

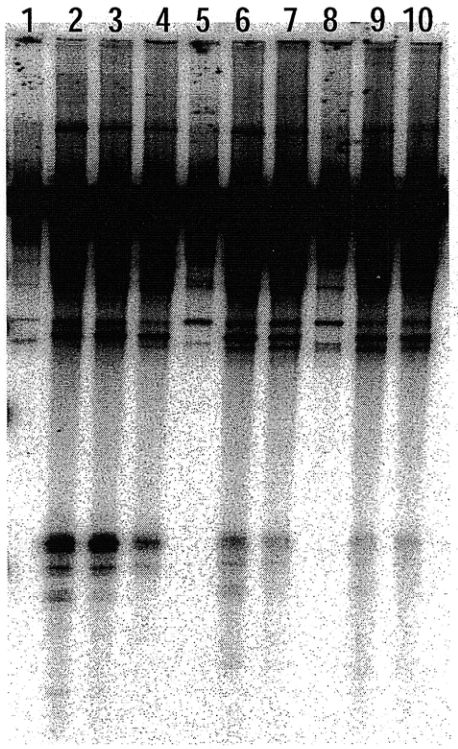

Figure 4.9. Comparison of 3 probes +/- $HMGB1_{full}$. 1) cisplatin 0 min, 2) cisplatin 30 min, 3) cisplatin + .06 mM DTT 30 min, 4) cisplatin, DTT, 4 μM $HMGB1_{full}$, 5) pyriplatin 0 min, 6) pyriplatin, DTT 30 min, 7) pyriplatin, DTT, HMGB1 30 min, 8) [Pt(dien)Cl]Cl, 0 min, 9) [Pt(dien)Cl]Cl, DTT, 30 min, 10) [Pt(dien)Cl]Cl, DTT, HMGB1, 30 min

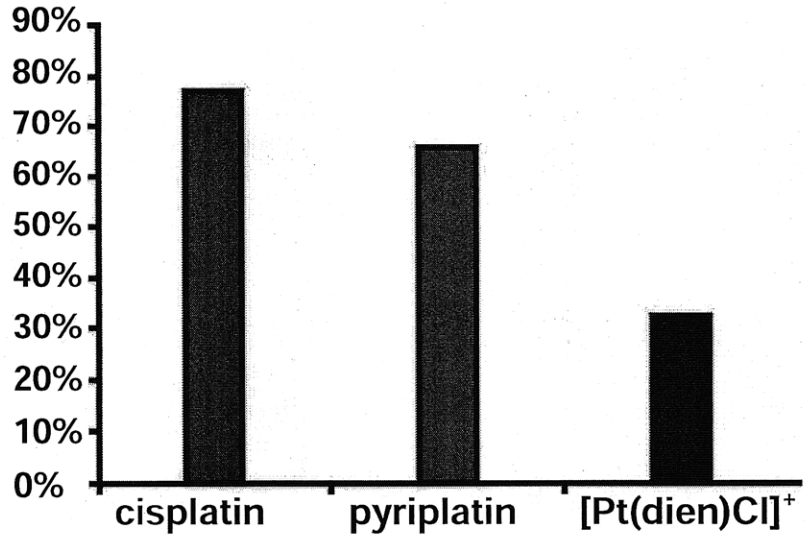

Figure 4.8. Decrease in repair due to repair shielding by HMGB1. Percentages are expressed as % reduction of repair due to HMGB1, where the control reaction (no HMGB1 was set to 0% inhibition).

The pyriplatin adduct is clearly recognized by the excision repair machinery, possibly because of a noncovalent interaction between the pyridine ring and DNA, suggesting that the transcription inhibition/nucleotide excision repair pathway involved in cellular processing of cisplatin-DNA adducts is also relevant to pyriplatin-DNA adducts. Conversely, the reduced repair of pyriplatin relative to that of cisplatin suggests that DNA damage caused by pyriplatin is able to elude the cellular repair machinery, rendering those adducts more persistent and potentially more cytotoxic to tumor cells.

Inhibition of Transcription Induced by Pyriplatin in HeLa Cells

Among the proteins and protein complexes that encounter cisplatin–DNA adducts is the transcription apparatus. Unlike DNA polymerases, which briefly pause at, and then bypass, cisplatin cross-links, presumably without major downstream effects, [30] RNA polymerases are greatly affected by the presence of these adducts. The progression of human RNA polymerase II (Pol II) along the DNA strand is almost completely blocked by cisplatin-DNA adducts,[31] and the arrest and subsequent ubiquitylation of Pol II initiate transcription-coupled repair, a subpathway of nucleotide excision repair, and programmed cell death, or apoptosis.[32] Plasmids containing the *lac*Z gene downstream of an SV40 promoter were modified with cisplatin, pyriplatin, or $[Pt(dien)Cl]^+$ at r_b levels from 0 to 0.13 (Figure 4.10) and transfected into HeLa cells. The products of β-galactosidase activity were assayed colorimetrically after 24 h by addition of *ortho*-nitrophenyl-β-galactoside (ONPG). Bypass of platinum adducts by the Pol II

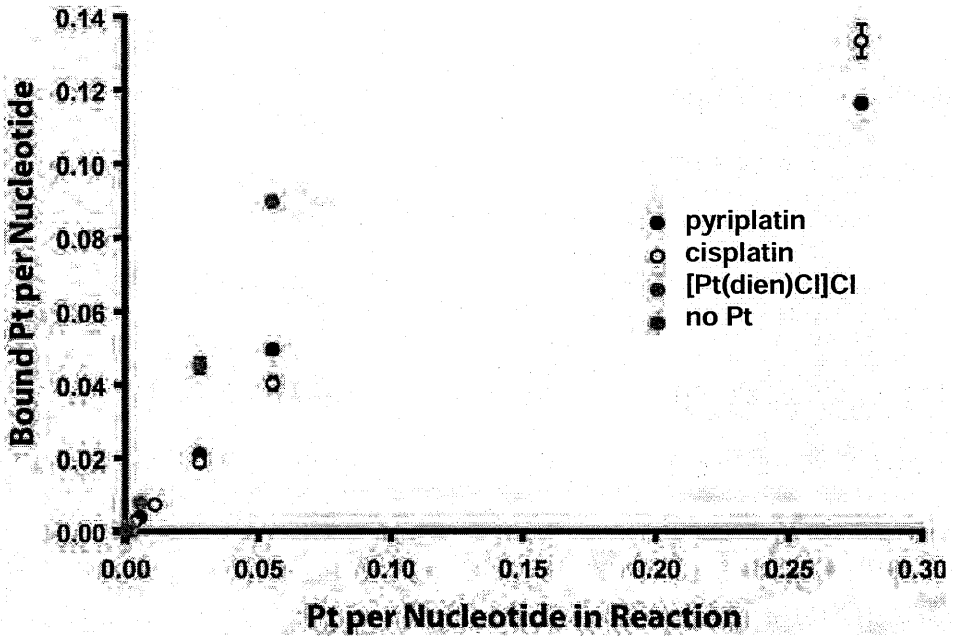

Figure 4.10. Results of r_b vs. r_f determination for platination with pyriplatin and cisplatin on pSV-b-galactosidase plasmid DNA. Error bars show one standard deviation.

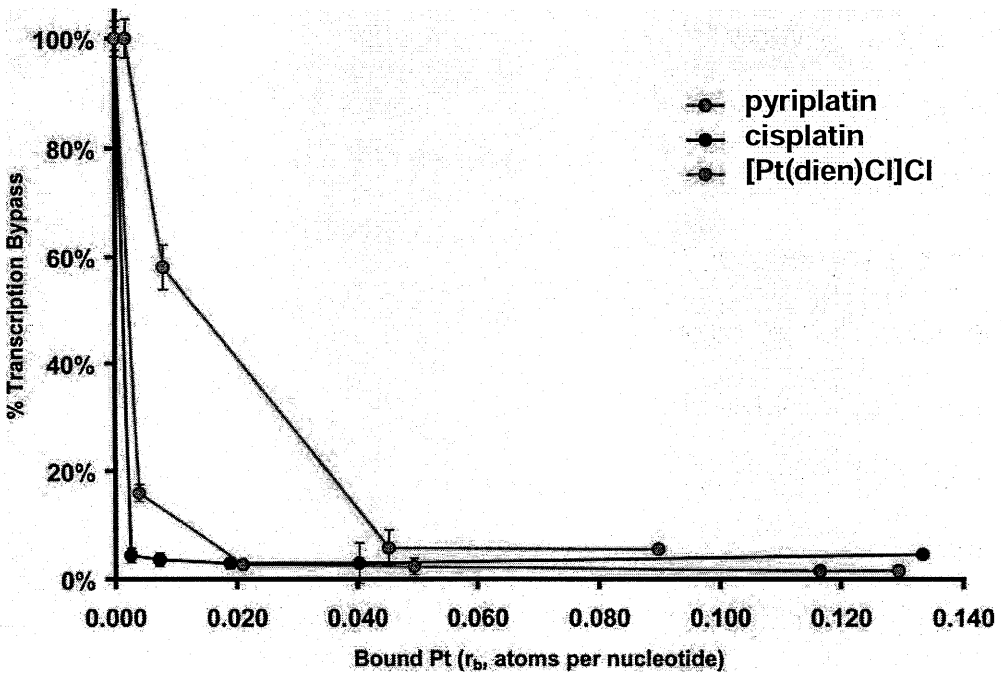

Figure 4.11. Bypass of various platinum adducts by the transcribing complex as assayed in live cells using a platinated pSV-β-galactosidase reporter plasmid. The percent transcription bypass relative to cells treated with unplatinated plasmid is plotted vs. platination level (r_b value). A bypass percentage of 100% indicates that there was no decrease in transcription of the reporter protein due to platination. Error bars represent the standard deviation of three samples from the same cell preparation and the experiment was repeated twice.

complex led to increased transcription of the *lacZ* gene and absorbance at 420 nm arising from ONPG cleavage by β-galactosidase. There was a clear difference between Pol II bypass of cisplatin vs. $[Pt(dien)Cl]^+$ adducts, relative to that for the unplatinated control plasmids (Figures 4.11, 4.12), with $[Pt(dien)Cl]^+$ requiring 5 times the platination level as cisplatin to block progression of RNA Pol II completely. In contrast, transcription inhibition by the monofunctional pyriplatin adducts very nearly matched that of cisplatin and was much more effective than inhibition by $[Pt(dien)Cl]^+$. Transcription of the cisplatin-modified plasmid was effectively inhibited at an r_b value of 2.5×10^{-3}.

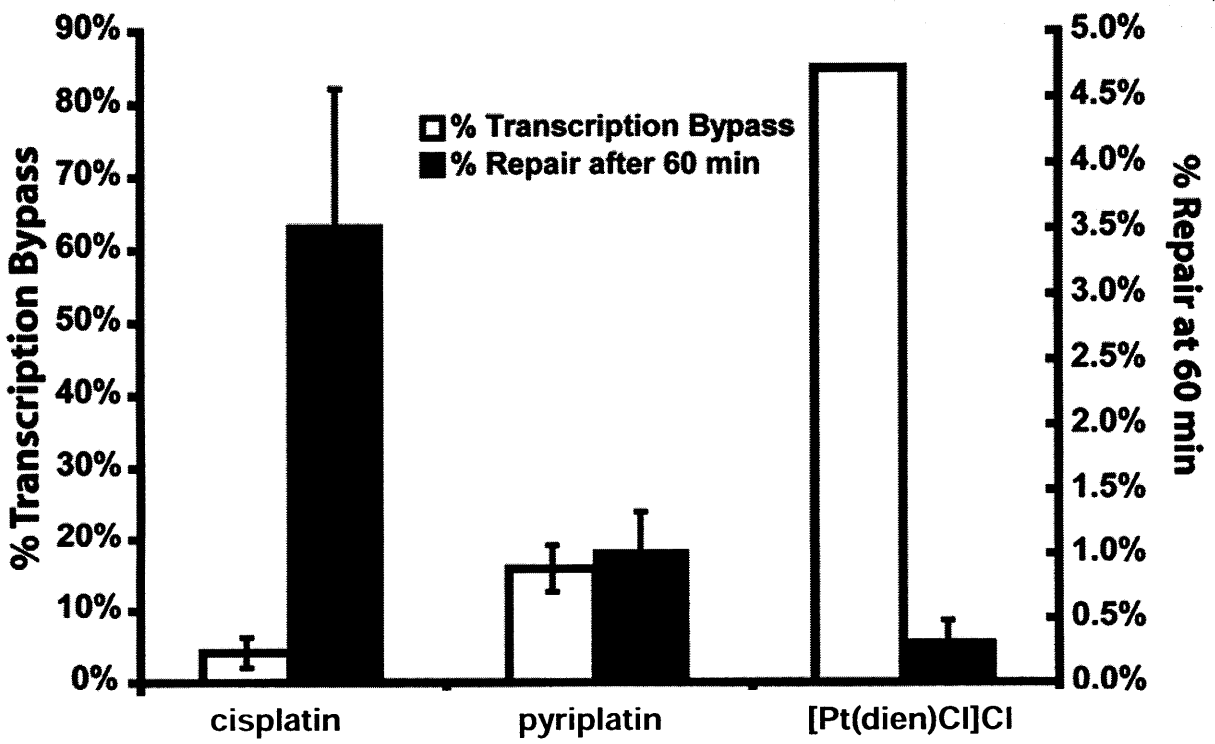

Figure 4.12. Comparison of successful transcription bypass and repair of various Pt-DNA adducts. Adducts of pyriplatin, much like those of cisplatin, allow minimal bypass by RNA pol II, but are inefficiently repaired. The level of repair of pyriplatin adducts is comparable to that of [Pt(dien)Cl]Cl adducts. Repair values report percent excision products detected after 60 min and transcription bypass values are given at r_b = 0.0039 for the β-gal live-cell assay. Repair error bars are the standard deviation of five, five, and two separate experiments for cisplatin, pyriplatin, and [Pt(dien)Cl]Cl, respectively. Absence of an error bar indicates very small deviation between experiments. Transcription error bars are the standard deviation of samples prepared in triplicate.

Inhibition by $[Pt(dien)Cl]^+$-modified plasmids was the same as that of the unplatinated control at $r_b = 7.8 \times 10^{-3}$ whereas transcription from the pyriplatin-modified plasmid was reduced to 16% that of the control at an r_b value of 3.9×10^{-3} (Figure 4.12).

Discussion and Conclusions

Identification of *cis*-$[Pt(NH_3)_2(pyridine)Cl]Cl$ as a highly cytotoxic agent in tumor cells transfected with organic cation transporters led us to question the mechanism of its cytotoxicity. Pyriplatin is an excellent substrate for OCT1 and OCT2, as revealed by its increased accumulation in cells that overexpress these transporters. The fact that cells expressing OCT1 or OCT2 are up to two orders of magnitude more sensitive to pyriplatin than control cells suggests that pyriplatin could be used to target OCT-expressing cancers, such as colorectal, liver, or kidney cancers. Pyriplatin has a greater tumor-targeting potential than oxaliplatin, the colorectal cancer agent that owes its unique antitumor properties to specific uptake by OCT1 and OCT2. Compared with oxaliplatin, cDPCP is much less toxic to cells that do not express OCT1 or 2. This property suggests that, like oxaliplatin, cDPCP will be able to target colorectal or liver cancer but with a reduction in the severity of side effects for tissues that do not express OCT1 or OCT2. The presence of these transporters in certain organs, most notably kidney and liver, may require the use of cotreatments to mitigate toxic side effects. Nephrotoxicity, the dose-limiting side effect for cisplatin therapy, is less problematic in oxaliplatin treatment.[33] Liver toxicity is a non-dose-limiting side effect of cisplatin and oxaliplatin.[34]

Although pyriplatin forms a monofunctional adduct on DNA, as shown by DNA unwinding studies, adducts of pyriplatin are repaired by the nucleotide excision repair pathway at a reduced rate than those of cisplatin and pyriplatin binds plasmid DNA as readily as cisplatin. Because pyriplatin can escape repair, the DNA damage induced by pyriplatin should endure longer than DNA damaged by cisplatin, thereby increasing the cytotoxic potential of pyriplatin. The repair of pyriplatin adducts is inhibited by the DNA damage recognition protein HMGB1, suggesting an interaction between components of the repair machinery and the platinum complex beyond that observed for other monofunctional compounds, such as [Pt(dien)Cl]Cl.

The cytotoxic effect of pyriplatin may be linked with its ability to inhibit Pol II, which it does significantly better than a model monofunctional compound, [Pt(dien)Cl]Cl. Like cisplatin, transcription is strongly inhibited by pyriplatin both in cell extracts and in live cells.

Pyriplatin largely escapes the nucleotide excision repair pathway and yet inhibits transcription very effectively. The combination of these effects suggest that its adducts will persist longer than those of cisplatin yet produce substantial downstream consequences that might raise the therapeutic potential of pyriplatin relative to cisplatin. The design of anticancer agents specifically as transcription inhibitors has been proposed, based on the premise that an extended delay in the restoration of transcription would induce apoptosis by p53- dependent and -independent pathways.[35] If true, persistence of transcription blocks would promote cell death and enhance the potency of pyriplatin. Combined with the high selectivity of pyriplatin for cells expressing hOCT1 and hOCT2, which are broadly expressed in human colorectal cancer,[2] these

findings support the candidacy of this unique monofunctional cationic complex as an anticancer drug with a mechanism of action that is likely to differ from that of cisplatin. Preclinical trials of pyriplatin are ongoing.

Materials and Methods

Materials

Potassium tetrachloroplatinum(II) was a gift from Engelhard Corp. (now BASF, Iselin, NJ) and cisplatin[36] and *cis*-$[Pt(NH_3)_2(py)Cl]Cl$ were synthesized as described.[14] Phosphoramidites and other reagents for DNA synthesis were purchased from Glen Research. Enzymes were purchased from New England Biolabs. Plasmids pBR322 and pSV-β-galactosidase were purchased from New England Biolabs and Promega, respectively, and were amplified in 100 mL LB cultures of *E. coli* XL1-Blue cells containing ampicillin as a selecting agent and purified on Maxi-prep columns (Qiagen). Plasmids were analyzed for purity by agarose gel electrophoresis and used for platination reactions. [γ-^{32}P]ATP was obtained from Perkin Elmer. All other chemicals and solvents were purchased from commercial suppliers.

Instrumentation

^{1}H NMR and ^{195}Pt NMR spectra were obtained on Varian 300 and 500 MHz spectrometers, respectively. Electrospray ionization-MS (ESI-MS) spectra were obtained on an Agilent Technologies 1100 Series liquid chromatography/MS instrument. Fourier transform-IR (FT-IR) spectra were measured on an Avatar 380 FT-IR.

Cell Lines and Transfection

Madin-Darby canine kidney (MDCK) cells stably transfected with the full-length human OCT1 cDNA (MDCK-hOCT1) and with the empty vector (MDCK-MOCK) were previously established.[37] Human embryonic kidney (HEK) 293 cells stably transfected with the full-length OCT2 cDNA (HEK-hOCT2) and with the empty vector (HEK-MOCK) were also previously described.[2]

Cell Culture

The stably transfected MDCK and HEK 293 cells were cultured in DMEM supplemented with 10% FBS, 100 units/mL penicillin, 100 μg/mL streptomycin (Invitrogen), and the respective selection antibiotics and grown at 37°C in a humidified atmosphere with 5% CO_2.

Drug Sensitivity

Cytotoxicities of the compounds were determined by plating cells in 96-well plates at a predetermined cell density. Cells were then incubated overnight and platinum complexes with or without an OCT inhibitor (cimetidine or disopyramide) were added to the culture medium. After drug exposure for 7 h, the medium was replaced with fresh, drug-free medium and the incubation was continued for a total of 72 h (starting from addition of platinum compounds). MTT assays were performed as previously described[38] and IC_{50} values were obtained by fitting *F*, the percentage of the maximal cell growth at different drug concentrations, to the equation

$F = 100 \times [1-C^{\gamma} / IC_{50}^{\gamma} + C^{\gamma})]$ using WinNonlin (Pharsight, Mountain View, CA). The maximal cell growth was set to the cell growth in the absence of platinum compounds; C is the concentration of the platinum compound and γ is the slope factor.

Cellular Accumulation of Platinum

Studies of cellular accumulation of platinum were based on a previously described protocol.[39] Cells were incubated in medium with either pyriplatin or oxaliplatin at 37°C in 5% CO_2 for 2 h. After incubation, cells were washed with ice-cold PBS, harvested, and pelleted by centrifugation (400 x *g*, 4°C, 15 min). Cell pellets were digested by heating at 65°C in 70% nitric acid for at least 2.5 h. Samples were prepared in distilled water containing 10 ppb of elemental iridium as an internal standard (diluted from Ir standard: 1000 μg/mL in 10% HCl) and 0.1% Triton X-100 to an overall nitric acid concentration of 7%. Platinum content was measured by inductively coupled plasma mass spectrometry in the Analytical Facility at the University of California at Santa Cruz. Cell lysates from a set of identical cultures were used for determination of protein content by the bicinchoninic acid assay.

Plasmid Preparation and Platination for DNA Unwinding Assays

The plasmid pBR322 was allowed to react with cisplatin or *cis*-$[Pt(NH_3)_2(py)Cl]Cl$ in 24 mM HEPES, pH 7.4, and 10 mM NaCl over 24 h at 37 °C in the dark. The DNA concentration was 19.6 μM (in base pairs) and the platinum concentration ranged from 1.5 to 90 μM in 120.4 μL total reaction volume. R_f values varied from 0.039 to 2.6. Platinum still unbound after 24 h was removed by spin microdialysis (Nanosep

cartridges, Pall Biosciences, 30,000 MWCO). After loading the DNA solution, spin cartridges were washed until no further platinum was detected in the wash solution (5 x 100 μL ddH_2O). DNA-bound platinum was quantified by atomic absorption (AA) spectroscopy (Aanalyst 300, HGA-800 graphite furnace, AAWinLab software version 3.0, Perkin Elmer, Wellesley, MA). A hollow cathode platinum lamp with 265.9 nm emission was used with a slit width of 0.70 nm. Pyrolysis was performed at 1200°C for 20 s and atomization at 2650°C for 5 s. AA samples were measured in duplicate using a calibration range of 20-80 μg/L and an r value of $\geq$ 0.998 for all calibration curves. DNA concentrations were measured by UV-Vis absorption spectroscopy at 260 nm (Cary 50 Bio UV-Visible Spectrometer equipped with a microprobe from C Technologies Inc.).

Determination of Pt-Induced DNA Unwinding

Agarose gel electrophoresis was used to determine the extent of DNA unwinding induced by the Pt-DNA adducts. Samples were concentrated by ethanol precipitation and loaded onto an ethidium-free 1 % agarose gel (loading solution: 4 μL ddH_2O plus 6 μL 50% glycerol and 0.002% of each bromophenol blue and xylene cyanol). Gels were electrophoresed for 4 h at 75 V in 1x TAE buffer at room temperature. Gels were then soaked in 1 μg/mL ethidium bromide in ddH_2O for 15 min, destained in ddH_2O for 5 min, and imaged in a Fluor-S gel scanner using QuantityOne software (BioRad).

Repair Probe Preparation for Nucleotide Excision Repair

Repair probes were made by synthesizing, annealing, and ligating five short oligomers to form dsDNA strands of 156 base pairs in length (Figures 4.4, 4.5) and

were purified and radiolabeled with ^{32}P as described.[26,27] For platinated strands, the platination step was performed on the 14mer oligomers prior to assembly of the probe with either cisplatin (14mer, GG strand), *cis*-$[Pt(NH_3)_2(pyridine)Cl]^+$ (14mer, G strand), or $[Pt(dien)Cl]^+$ (14mer, G strand).

Excision Assay

Assays were performed as described[20,26,27] with 10 fmol of the platinated repair probe and 75 μg cell-free HeLa extract. Reactions were allowed to proceed for 60 min at 30°C and were stopped by the addition of SDS and proteinase K to final concentrations of 0.34% and 20 μg/mL, respectively. After phenol extraction, 25:24:1 phenol:chloroform:isoamyl alcohol extraction, and careful ethanol precipitation with 10 μg linear polyacrylamide as co-precipitant, reaction products were analyzed by 10% urea-PAGE. For reactions in the presence of HMGB1, the full length, fully reduced recombinant form of the protein was added to the DNA and reaction buffer *prior* to the addition of the cell extract. After incubation at room temperature for 10 min, cell extract was added to begin the repair reaction, putting the overall $[HMGB1_{full}]$ at 3.2 μM.

Evaluation of Excision Kinetics

Excision reactions were performed as described above, with reaction incubation times of 0, 15, 30, 60, 90, or 120 minutes. After the specified reaction time had elapsed, reactions were quenched with SDS and proteinase K as previously described. Data from three separate experiments were averaged.

Transcription Assay. HeLa cells (ATCC) were cultured in DMEM with 10% fetal bovine serum at 5% CO_2 in a humidified chamber and restarted upon reaching passage number 20. Cells were transfected with platinated or unplatinated control plasmids according to the manufacturer's protocol (Lipofectamine 2000, Invitrogen Corp.). After 24 h incubation, cells were washed twice with PBS, incubated for 15 min in lysis buffer (25mM bicine, pH 7.8, 0.05% Tween 20, 0.05% Tween 80) and scraped from the plate. After 15 s vigorous vortexing and centrifugation (18,000 x g), the supernatant was treated with 2.2 mM *ortho*-nitrophenyl-β-galactoside (ONPG) and 50 mM β-mercaptoethanol in 100 mM sodium phosphate, pH 7.3, and 1 mM $MgCl_2$. Following incubation at 37 °C for 4 h and addition of sodium carbonate to 0.75 M, the absorbance of the solution was measured at 420 nm and values from the cells transfected with platinated plasmid were normalized to those from cells transfected with nonplatinated plasmid.

References

(1) K. S. Lovejoy, R. C. Todd, S. Zhang, M. S. McCormick, J. A. D'Aquino, J. T. Reardon, A. Sancar, K. M. Giacomini and S. J. Lippard (2008). cis-diammine(pyridine)chloroplatinum(II), a monofunctional platinum(II) antitumor agent: uptake, structure, function, and prospects. *Proc. Natl. Acad. Sci. U. S. A.*, **105**, 8902-8907.

(2) S. Zhang, K. S. Lovejoy, J. E. Shima, L. L. Lagpacan, Y. Shu, A. Lapuk, Y. Chen, T. Komori, J. W. Gray, X. Chen, S. J. Lippard and K. M. Giacomini (2006). Organic Cation Transporters Are Determinants of Oxaliplatin Cytotoxicity. *Cancer Res.*, **66**, 8847-8857.

(3) R. M. Goldberg, D. J. Sargent, R. F. Morton, C. S. Fuchs, R. K. Ramanathan, S. K. Williamson, B. P. Findlay, H. C. Pitot and S. R. Alberts (2004). A randomized controlled trial of fluorouracil plus leucovorin, irinotecan, and oxaliplatin combinations in patients with previously untreated metastatic colorectal cancer. *J. Clin. Oncol.*, **22**, 23-30.

(4) M. D. Hall, H. R. Mellor, R. Callaghan and T. W. Hambley (2007). Basis for Design and Development of Platinum(IV) Anticancer Complexes. *J. Med. Chem.*, **50**, 3403-3411.
(5) N. Farrell In *Metal Ions in Biological Systems.*; Sigel, H., Ed.; Marcel Dekker Inc., New York: New York, 2004; Vol. 42, pp 251-296.
(6) N. Farrell (1996). Current status of structure-activity relationships of platinum anticancer drugs: activation of the trans geometry. *Metal Ions in Biological Systems*, **32**, 603-639.
(7) J. M. Perez, L. R. Kelland, E. I. Montero, F. E. Boxall, M. A. Fuertes, C. Alonso and C. Navarro-Ranninger (2003). Antitumor and cellular pharmacological properties of a novel platinum(IV) complex: trans-[PtCl2(OH)2(dimethylamine)(isopropylamine)]. *Mol. Pharmacol.*, **63**, 933-944.
(8) L. R. Kelland, F. J. Barnard, I. G. Evans, B. A. Murrer, B. R. C. Theobald, S. B. Wyer, P. M. Goddard, M. Jones, M. Valenti and et al. (1995). Synthesis and in vitro and in vivo antitumor activity of a series of trans platinum antitumor complexes. *J. Med. Chem.*, **38**, 3016-3024.
(9) M. Coluccia, A. Boccarelli, M. A. Mariggio, N. Cardellicchio, P. Caputo, F. P. Intini and G. Natile (1995). Platinum(II) complexes containing iminoethers: a trans platinum antitumor agent. *Chemico-Biological Interactions*, **98**, 251-266.
(10) Y. Najajreh, E. Khazanov, S. Jawbry, Y. Ardeli-Tzaraf, J. M. Perez, J. Kasparkova, V. Brabec, Y. Barenholz and D. Gibson (2006). Cationic Nonsymmetric Transplatinum Complexes with Piperidinopiperidine Ligands. Preparation, Characterization, in Vitro Cytotoxicity, in Vivo Toxicity, and Anticancer Efficacy Studies. *J. Med. Chem.*, **49**, 4665-4673.
(11) S. Zorbas-Seifried, M. A. Jakupec, N. V. Kukushkin, M. Groessl, C. G. Hartinger, O. Semenova, H. Zorbas, V. Y. Kukushkin and B. K. Keppler (2007). Reversion of structure-activity relationships of antitumor platinum complexes by acetoxime but not hydroxylamine ligands. *Mol. Pharmacol.*, **71**, 357-365.
(12) A. Boccarelli, F. P. Intini, R. Sasanelli, M. F. Sivo, M. Coluccia and G. Natile (2006). Synthesis and in Vitro Antitumor Activity of Platinum Acetonimine Complexes. *J. Med. Chem.*, **49**, 829-837.
(13) F. P. Intini, A. Boccarelli, V. C. Francia, C. Pacifico, M. F. Sivo, G. Natile, D. Giordano, P. Rinaldis and M. Coluccia (2004). Platinum complexes with imino ethers or cyclic ligands mimicking imino ethers: synthesis, in vitro antitumour activity, and DNA interaction properties. *J. Biol. Inorg. Chem.*, **9**, 768-780.
(14) L. S. Hollis, A. R. Amundsen and E. W. Stern (1989). Chemical and biological properties of a new series of cis-diammineplatinum(II) antitumor agents containing three nitrogen donors: cis-[Pt(NH3)2(N-donor) Cl]+. *J. Med. Chem.*, **32**, 128-136.
(15) L. S. Hollis, W. I. Sundquist, J. N. Burstyn, W. J. Heiger-Bernays, S. F. Bellon, K. J. Ahmed, A. R. Amundsen, E. W. Stern and S. J. Lippard (1991). Mechanistic studies of a novel class of trisubstituted platinum(II) antitumor agents. *Cancer Res.*, **51**, 1866-1875.
(16) M. V. Keck and S. J. Lippard (1992). Unwinding of supercoiled DNA by platinum-ethidium and related complexes. *J. Am. Chem. Soc.*, **114**, 3386-3390.

(17) G. L. Cohen, W. R. Bauer, J. K. Barton and S. J. Lippard (1979). Binding of cis- and trans-dichlorodiammineplatinum(II) to DNA: Evidence for unwinding and shortening of the double helix. *Science*, **203**, 1014-1016.
(18) A. M. Fichtinger-Schepman, A. T. van Oosterom, P. H. Lohman and F. Berends (1987). cis-Diamminedichloroplatinum(II)-induced DNA adducts in peripheral leukocytes from seven cancer patients: quantitative immunochemical detection of the adduct induction and removal after a single dose of cis-diamminedichloroplatinum(II). *Cancer Res.*, **47**, 3000-3004.
(19) A. M. J. Fichtinger-Schepman, R. A. Baan, A. Luiten-Schuite, M. Van Dijk and P. H. M. Lohman (1985). Immunochemical quantitation of adducts induced in DNA by cis-diamminedichloroplatinum(II) and analysis of adduct-related DNA-unwinding. *Chem. Biol. Interact.*, **55**, 275-288.
(20) J.-C. Huang, D. B. Zamble, J. T. Reardon, S. J. Lippard and A. Sancar (1994). HMG-domain proteins specifically inhibit the repair of the major DNA adduct of the anticancer drug cisplatin by human excision nuclease. *Proc. Natl. Acad. Sci. U. S. A.*, **91**, 10394-10398.
(21) M. F. Pera, F. Friedlos, J. Mills and J. J. Roberts (1987). Inherent sensitivity of cultured human embryonal carcinoma cells to adducts of cis-diamminedichloroplatinum(II) on DNA. *Cancer Res.*, **47**, 6810-6813.
(22) D. B. Bregman, R. Halaban, A. J. von Gool, K. A. Henning, E. C. Friedberg and S. L. Warren (1996). UV-induced ubiquitination of RNA polymerase II: A novel modification deficient in Cockayne syndrome cells. *Proc. Natl. Acad. Sci. U. S. A.*, **93**, 11586-11590.
(23) M. Cobo, D. Isla, B. Massuti, A. Montes, J. M. Sanchez, M. Provencio, N. Vinolas, L. Paz-Ares, G. Lopez-Vivanco, M. A. Munoz, E. Felip, V. Alberola, C. Camps, M. Domine, J. J. Sanchez, M. Sanchez-Ronco, K. Danenberg, M. Taron, D. Gandara and R. Rosell (2007). Customizing cisplatin based on quantitative excision repair cross-complementing 1 mRNA expression: a phase III trial in non-small-cell lung cancer. *J. Clin. Oncol.*, **25**, 2747-2754.
(24) K. B. Lee, R. J. Parker, V. Bohr, T. Cornelison and E. Reed (1993). Cisplatin sensitivity/resistance in UV repair-deficient Chinese hamster ovary cells of complementation groups 1 and 3. *Carcinogenesis*, **14**, 2177-2180.
(25) R. Rosell, F. Cecere, M. Santarpia, N. Reguart and M. Taron (2006). Predicting the outcome of chemotherapy for lung cancer. *Current Opinion in Pharmacology*, **6**, 323-331.
(26) D. B. Zamble, D. Mu, J. T. Reardon, A. Sancar and S. J. Lippard (1996). Repair of Cisplatin-DNA Adducts by the Mammalian Excision Nuclease. *Biochemistry*, **35**, 10004-10013.
(27) J. T. Reardon and A. Sancar (2006). Purification and characterization of Escherichia coli and human nucleotide excision repair enzyme systems. *Methods in Enzymology*, **408**, 189-213.
(28) D. Wang, R. Hara, G. Singh, A. Sancar and S. J. Lippard (2003). Nucleotide Excision Repair from Site-Specifically Platinum-Modified Nucleosomes. *Biochemistry*, **42**, 6747-6753.

(29) I. E. Dumitriu, P. Baruah, A. A. Manfredi, M. E. Bianchi and P. Rovere-Querini (2005). HMGB1: guiding immunity from within. *Trends in Immunology*, **26**, 381-387.

(30) K. M. Comess, J. N. Burstyn, J. M. Essigmann and S. J. Lippard (1992). Replication inhibition and translesion synthesis on templates containing site-specifically placed cis-diamminedichloroplatinum(II) DNA adducts. *Biochemistry*, **31**, 3975-3990.

(31) Y. Jung and S. J. Lippard (2006). RNA Polymerase II Blockage by Cisplatin-damaged DNA: stability and polyubiquitylation of stalled polymerase. *J. Biol. Chem.*, **281**, 1361-1370.

(32) K.-B. Lee, D. Wang, S. J. Lippard and P. A. Sharp (2002). Transcription-coupled and DNA damage-dependent ubiquitination of RNA polymerase II in vitro. *Proc. Natl. Acad. Sci. U. S. A.*, **99**, 4239-4244.

(33) T. Ludwig, C. Riethmueller, M. Gekle, G. Schwerdt and H. Oberleithner (2004). Nephrotoxicity of platinum complexes is related to basolateral organic cation transport. *Kidney Int.*, **66**, 196-202.

(34) D. Zorzi, A. Laurent, T. M. Pawlik, G. Y. Lauwers, J. N. Vauthey and E. K. Abdalla (2007). Chemotherapy-associated hepatotoxicity and surgery for colorectal liver metastases. *Br. J. Surg.*, **94**, 274-286.

(35) M. Ljungman and D. P. Lane (2004). Opinion: Transcription - guarding the genome by sensing DNA damage. *Nat. Rev. Cancer*, **4**, 727-737.

(36) S. C. Dhara (1970). A rapid method for the synthesis of *cis*-$[Pt(NH_3)_2Cl_2]$. *Indian J. Chem.*, **8**, 193-194.

(37) Y. Shu, M. K. Leabman, B. Feng, L. M. Mangravite, C. C. Huang, D. Stryke, M. Kawamoto, S. J. Johns, J. DeYoung, E. Carlson, T. E. Ferrin, I. Herskowitz, K. M. Giacomini, L. Z. Benet, C. M. Brett, E. G. Burchard, R. Castro, M. de la Cruz, R. H. Edwards, J. Gitschier, C. E. Glatt, C. Ho, D. L. Kroetz, E. T. Lin, V. I. Reus, W. Sadee, M. Salazar, C. Schaefer, L. B. Sheiner, C. Tran, T. J. Urban, C. Vulpe and E. M. Wright (2003). Evolutionary conservation predicts function of variants of the human organic cation transporter, OCT1. *Proc. Natl. Acad. Sci. U. S. A.*, **100**, 5902-5907.

(38) M. C. Alley, D. A. Scudiero, A. Monks, M. L. Hursey, M. J. Czerwinski, D. L. Fine, B. J. Abbott, J. G. Mayo, R. H. Shoemaker and M. R. Boyd (1988). Feasibility of drug screening with panels of human tumor cell lines using a microculture tetrazolium assay. *Cancer Res.*, **48**, 589-601.

(39) A. K. Holzer, G. Samimi, K. Katano, W. Naerdemann, X. Lin, R. Safaei and S. B. Howell (2004). The copper influx transporter human copper transport protein 1 regulates the uptake of cisplatin in human ovarian carcinoma cells. *Mol. Pharmacol.*, **66**, 817-823.

Chapter 5

Characterization of the Role of HMGB1 in the Cellular Response to Cisplatin

Introduction

HMGB1 and the Repair Shielding Hypothesis

The finding that the DNA-binding high mobility group protein HMGB1 recognizes and binds the major cisplatin-DNA adduct[1,2] led to the hypothesis that these proteins shield the damaged DNA from excision repair, thereby significantly contributing to the cytotoxic effect of cisplatin. Subsequent studies investigating the repair-shielding effect have focused on methods of increasing the amount of HMGB1 in cancer cells to potentiate the activity of cisplatin. The observation that estrogen and progesterone upregulate HMGB1 in MCF-7 and Evsa-T cell lines, respectively,[3] opened up a new line of inquiry for the study of cisplatin. The discovery that treatment of MCF-7 cells with estrogen or progesterone causes a two-fold increase in the sensitivity of the cells to cisplatin[4] was followed up by the synthesis of estrogen-tethered platinum(IV) complexes for potential use in breast-cancer patients.[5] These compounds were also shown to upregulate HMGB1 in cancer cells and one of the compounds sensitized cells to cisplatin.

Upregulation of HMGB1 by Hormones

The biological connection between the estrogen receptor and HMGB1 is related to the estrogen receptor—DNA interaction. The estrogen receptor binds tightly to specific DNA sequences, called estrogen response elements, and this binding is enhanced by the presence of other accessory nuclear factors, including HMGB1.[6] The interaction between the progesterone receptor and the progesterone response element occurs in a similar manner. The androgen receptor also binds to a specific DNA

sequence, but the role of HMGB1 in this interaction has not been completely elucidated. Although androgens have not yet been shown to upregulate HMGB1, the transient expression of HMGB1 or HMGB2 in HeLa cells has been shown to increase the apparent DNA binding affinity of the androgen receptor.[6] The central DNA binding domains of all three of these steroid hormone receptors are similar and are composed of two highly conserved zinc fingers.[7]

We evaluated the effect of androgens on the upregulation of HMGB1 and on the cytotoxicity of cisplatin, focusing on the LNCaP human prostate cancer cell line. This cell line, unlike many prostate cancer cell lines, continues to expresses the androgen receptor under the conditions required for tissue culture. The choice of the androgen dehydroepiandrosterone (DHEA) for these cell experiments was partially motivated by the fact that it was the only androgen receptor substrate directly upstream of dihydrotestosterone (DHT) in the biosynthetic pathway (Scheme 5.1) that was obtainable without a DEA license. The exception from the DEA list is due to political circumstances,[8] not scientific reasons. Although it is converted into testosterone and DHT in the body, DHEA itself is an inferior substrate for the androgen receptor. Testosterone has a binding affinity over 1800 times that of DHEA and DHT has a binding affinity over 10,000 fold higher than DHEA.[9] Besides avoiding DEA-controlled substances, another motivation for the use of DHEA was its common use as a dietary supplement for the treatment of age-related ailments[8,10] and the implication of DHEA in the prevention of prostate cancer.[11] Additionally, cancer cells treated with DHEA do not exhibit the increased proliferation that is a characteristic of treatment with DHT or

testosterone.[12] Upon obtaining the DEA license, the more potent DHT (Scheme 5.1) was also used in cell studies.

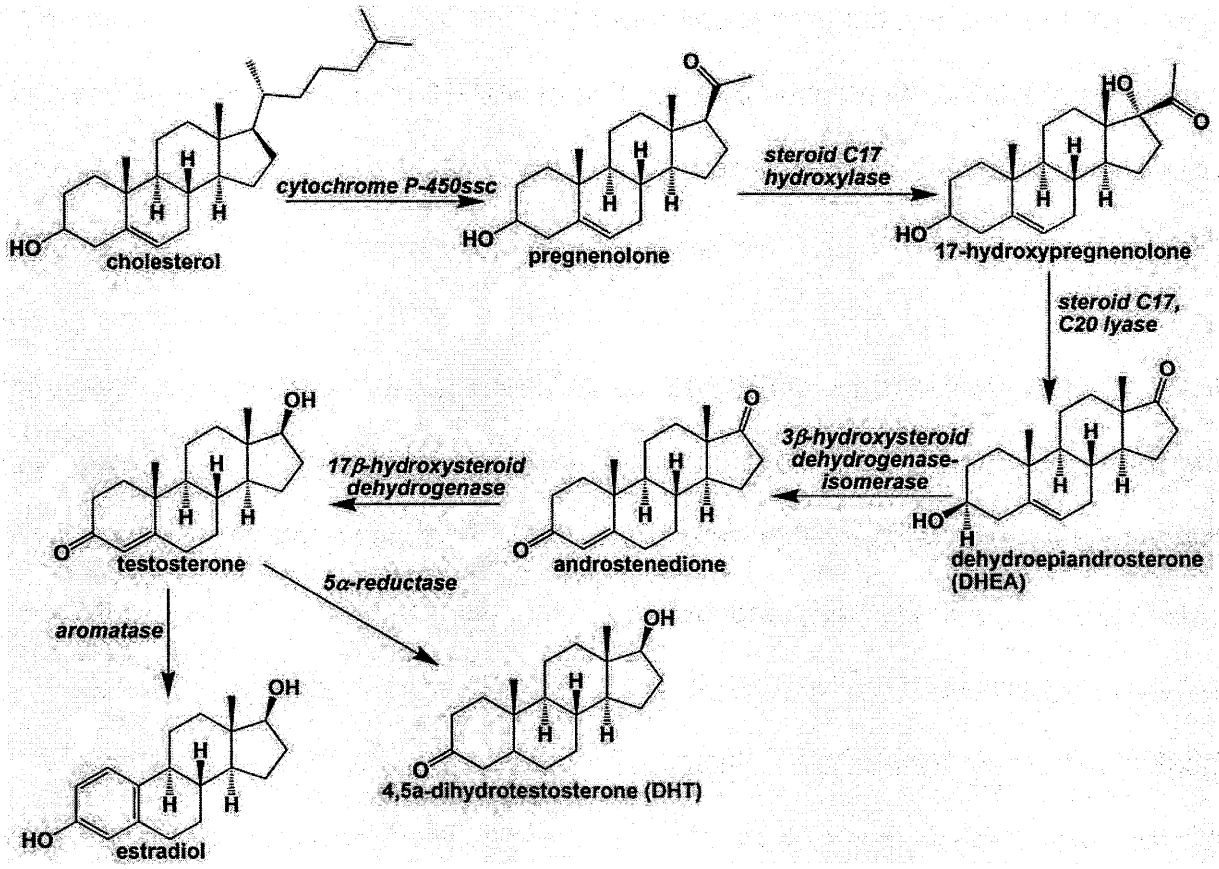

Scheme 5.1. Steroid biosynthetic pathway starting from cholesterol

Retinoic Acid and HMGB1

Along with progesterone, estrogen, and androgen receptors, the retinoic acid receptor (RAR) is a member of the steroid receptor superfamily. Unlike androgens and estrogen, the proliferative effects of which have been implicated in exacerbating the problems of cancer, all-*trans*-retinoic acid (ATRA, Chart 5.1) has been shown to have

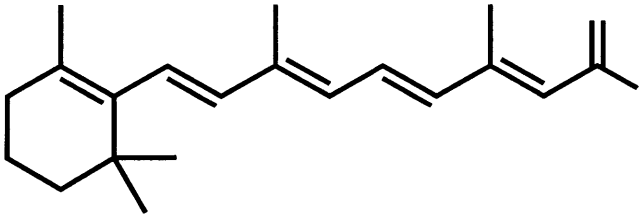

Chart 5.1. all-*trans*-retinoic acid.

an antiproliferative effect on cancer cells.[13] For this reason, ATRA is used to treat cancer patients, particularly those suffering from prostate cancer and leukemia. Three subtypes of RAR exist, RARα, RARβ, and RARγ, all of which are receptors for ATRA. The expression of RARβ, a subtype that has been implicated in the antiproliferative effect of ATRA, is often downregulated in human cancers[14] The human breast cancer cell line MCF-7 expresses all three types of RAR.[14]

The connection between retinoic acid and the study of cisplatin drugs is based on the observation that, like estrogen and progesterone, retinoic acid can also cause the upregulation of HMGB1. Specifically, embryonal carcinoma cells of the P19 murine cell line show increased amounts of HMGB1 beginning six days after treatment with 500 nM retinoic acid.[15]

Studies in patients and in human cancer cell lines have indicated that the combination of cisplatin and ATRA has anti-cancer effects. Phase II clinical trials of the combination of ATRA, cisplatin, and interferon-α in women with recurrent or metastatic cervical squamous cell carcinoma were carried out in Europe in 2002. The trial was halted due to unacceptable toxicity after three months, although the preliminary results showed a good response to the drug combination.[16] There are other indications that the co-treatment of ATRA and cisplatin could sensitize cells to cisplatin treatment. A phase II trial of the combination plus etoposide in small cell lung carcinoma yielded a 45%

response rate before it too was stopped due to toxic side-effects.[17] Co-treatment of cisplatin and ATRA in the ovarian carcinoma cell lines OVCCR1 and NIH-OVCAR-3 potentiated cisplatin cytotoxicity,[18,19] as did cotreatment in both human ovarian adenocarcinoma and in head and neck squamous carcinoma cell lines.[20]

The possibility that ATRA could be linked to both the upregulation of HMGB1 and increased cisplatin efficacy led us to investigate the nature of HMGB1 upregulation by retinoic acid.

Effect of Reducing and Oxidizing Cellular Potentials on the HMGB1-DNA Interaction

Transcription factors in the nucleus are often activated or disabled according to external signals, such as oxidative stress. Redox-sensitive transcription factors include NF-κB (nuclear factor κB, involved in a pathway activated by HMGB1,[21] p53, AP-1 (activator protein-1, specifically c-Jun and c-Fos), SoxR, OxyR,[22] c-Myb, NF-Y/CBF, SP-1, NFI/CTF, EGR-1, glucocorticoid receptor, Heat Shock Factor, TTF-1, USF, Pax-8, Hox B5, PEBP2, GABPα, HLF, and HIF-1α).[23] (reviewed[24,25]) Redox-related cell signaling involves changes in the oxidation state of cysteines that lead to protein structural changes and modulation of protein activity. The formation of a disulfide bond under oxidative conditions, for example, can dramatically alter protein structure, providing a mechanism for oxidative stress to switch transcription factor activity. In the prototypic switch example, the reduced transcription factor is inactive, whereas the disulfide form of the protein is transcriptionally active.[22] Beyond this on-off switch mechanism, other cysteine modifications that can occur based on the reduction potential of a particular cellular organelle, such as S-NO, S-OH, and S-SG

(SG=glutathione), can more moderately regulate transcription, as has been shown for the transcription factor OxyR, which is the bacterial transcriptional activator of *E. coli*.[22]

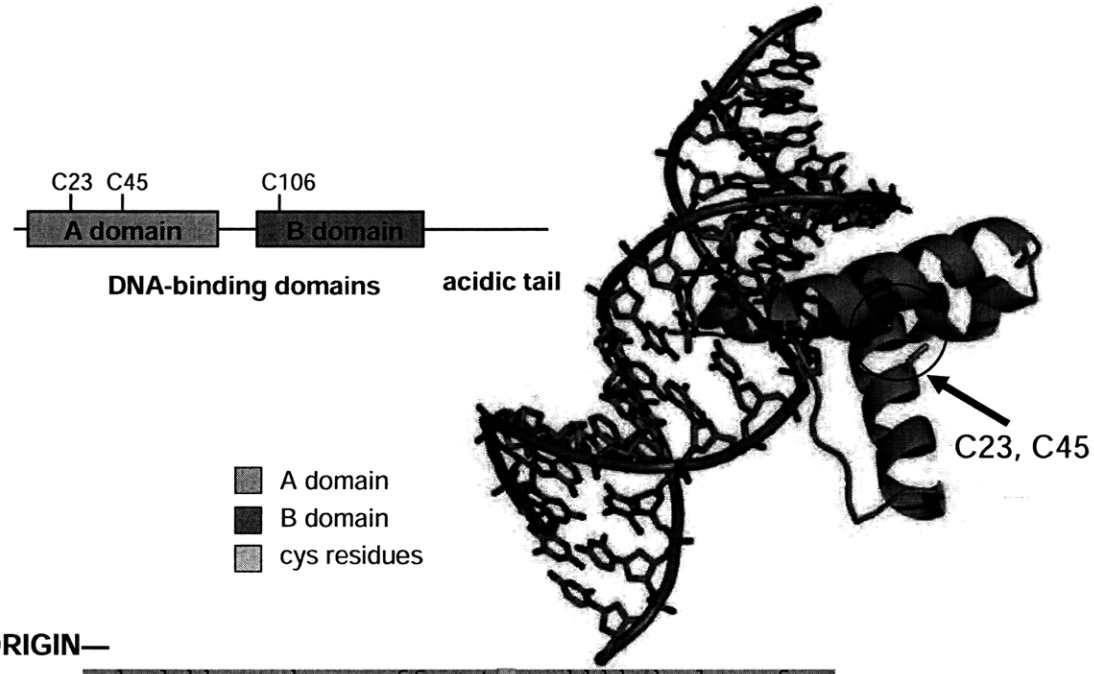

ORIGIN—

```
1    mgkgdpkkpr gkmssyaffv qtcreehkkk hpdasvnfse
41   fskkcserwk tmsakekgkf edmakadkar yeremktyip
81   pkgetkkkfk dpnapkrpps afflfcseyr pkikgehpgl
121  sigdvakklg emwnntaadd kqpyekkaak lkekyekdia
161  ayrakgkpda akkgvvkaek skkkkeeeed eedeedeeee
201  edeededeee dddde
```

Figure 5.1. Sequence of full length HMGB1, diagram of A and B domains, and structure[2] of the A domain on cisplatin-modified 16mer DNA.

The interaction of metallothionein, a metalloprotein consisting of ~33% cysteines, with zinc depends on an interaction of metallothionein with oxidized glutathione (GSSG) to release zinc. The combination of oxidized and reduced glutathione (GSH) then enables the transfer of zinc from metallothionein to an apoenzyme.[26] The difficulty in examining the effect of these various modifications lies in the production of the pure form of oxidized proteins and the retention of these instable species once they are formed. Experiments generally require anaerobic conditions and analysis of tryptic digests of the oxidized or reduced proteins samples by ESI-MS.[22]

Cancer cells are hypoxic, a condition that induces oxidative stress. Oxidative stress causes a large increase in cellular reduction potential, rendering the cellular mediator of oxidative stress, glutathione, less able to reduce proteins. Severe oxidative stress causes cell death. Specifically, moderate stress can trigger apoptosis and more intense oxidative stress can cause necrosis. ROS are produced, which cause cellular damage.

The highly abundant nuclear protein HMGB1 regulates transcription and remodels chromatin by binding and bending DNA in a structure-specific, non-sequence-specific manner.[27] The protein is also released into the cytosol during necrosis and is present at sites of inflammatory diseases. The protein comprises two alpha-helical HMG box domains (A and B domains) of about 80-amino acids each and an acidic C-terminal domain. The HMGB1 gene sequence (Figure 5.1) maps to chromosome 13[28] and sequences from mouse, rat, hamster, bovine, pig, and human are almost identical.[29]

Of the three cysteine residues found in HMGB1, Cys106, on the B box, determines the nuclear or cytoplasmic localization of the protein. The C106S mutant protein is localized in both the cytosol and nucleus of healthy CHO cells, in contrast to the wild-type protein, which is observed only in the nucleus.[23] The two A-box cysteines, Cys23 and Cys45, form a disulfide bond under conditions of oxidative stress, inducing structural changes in the protein and possibly switching its DNA binding ability. Cys23 and Cys45 are separated by 4.25 Å in the HMGB1 A domain-DNA crystal structure, which was performed under reducing conditions (2.5 mM DTT).[2,30] NMR structural information about the interaction of the A domain with DNA was similarly performed under reducing conditions (50 μM DTT) and with a C22S mutated protein.[31,32]

The presence of a Cys23—Cys45 disulfide bond in HMGB1 under oxidizing conditions is not currently disputed.[23,33,34] One outstanding question is whether reversible oxidation of the HMGB1 cysteines occurs *in vivo*. The cytoplasm and nucleus are both reducing environments, as compared with the extracellular milieu. Exact redox potentials in the cytoplasm and organelles of various species depend upon factors such as the concentration of glutathione reductase and NADPH,[35] the presence of renaturation catalysts, such as the eukaryotic protein disulfide isomerase,[36] preferential transport of GSSH over GSH through cell and organelle membranes, and the production of oxidizing equivalents as byproducts of other cellular mechanisms. Generally, favorable conditions for refolding of disulfide-bond-dependent proteins involve a reduced glutathione to glutathione disulfide (GSH:GSSH) ratio of less than 10. The GSH:GSSH ratio is about 60 (-233 mV vs. SHE) in the eukaryotic cytoplasm and about 2 (-180 mV) in the endoplasmic reticulum, as determined for the *Mus musculus* hybridoma cell line CRL-1606.[35]

If we assume that the HMGB1 disulfide bond could form *in vivo*, which is not unreasonable based on western-blot analysis of native HMGB1 from CHO extracts,[23] we additionally wish to understand whether oxidation of this bond switches the binding affinity of HMGB1 for cisplatin-modified and/or naked DNA. A disulfide bond-based switch has been observed in the Ku protein, wherein only the oxidized form of the protein binds cDDP-modified DNA.[37] Existing data on HMGB1 are contradictory and data on HMGB1 and HMGB2 (in which the cysteine sites are conserved) interacting with platinated DNA is based on poorly characterized, globally platinated material.

Mutations and covalent modifications of Cys23 and Cys45 have no effect on nuclear localization of HMGB1,[23] but do modulate HMGB1-DNA binding and alter the overall structure of the protein. Global modification of full-length HMGB1 with Ellman's reagent (DTNB; 5,5'-dithiobis(2-nitrobenzoic acid), hydrogen peroxide, or *N*-ethylmaleimide (NEM) reduces HMGB1 binding to globally platinated DNA by 81%, 90%, and 85%, respectively, whereas incubation with 2-mercaptoethanol has no effect on the protein interaction with platinated DNA binding.[38] DTNB and NEM modify cysteinate thiols and prevent formation of the Cys23-Cys45 disulfide bond. 2-Mercaptoethanol would also ensure the reduced form of the protein. Conversely, hydrogen peroxide is an oxidizing agent that would induce formation of the disulfide bond. The authors conclude that the reduced form of the protein has the higher affinity for Pt-DNA, although, based on the data, this conclusion does not seem obvious.[38] Contrary to these results on full-length HMGB1, NEM does not inhibit the interaction of the AB-only fragment of HMGB1 with unplatinated DNA,[39] indicating that NEM-induced modifications along the C-terminal tail, not around Cys23 or Cys45, are responsible for the observed modulation in DNA binding ability. Supporting evidence for the localization of chemically induced oxidative effects to the C-terminal tail includes the fact that C-domain-induced structural changes, such as induction of DNA looping and compaction, are not observed in the presence of NEM.[40]

The effect of site-specific mutations of the HMGB2 protein, in which the cysteine sites are conserved, on protein affinity to globally platinated DNA add further conflicting data. Mutations C45S and C106S, but not C23S, resulted in significant reductions in protein-platinated DNA binding (25% and 50%, respectively).[41] If a Cys23-Cys45

disulfide bond were somehow involved in the modulation of DNA binding, one might expect similar effects for the C23S mutation as for the C45S mutation. Contrary to this HMGB2 study, an HMGB1 C23A mutant showed reduced binding affinity for unplatinated duplexes and 4WJ DNA. Neither C45A nor C106A mutants were examined.[42]

HMGB1 in the reduced form binds H1 with significantly greater affinity than in the oxidized form, although this interaction may involve a 4:1 HMGB1:H1 complex, a complex that has never been found at the sites of HMGB1/cisplatinated DNA interactions.[43]

In conclusion, a disulfide bond is most definitely formed in HMGB1 under certain *in vitro* conditions and, although the specific redox potential has not been determined, it is likely that the disulfide bond forms *in vivo* under conditions of oxidative stress. Reports on the nature of oxidized and reduced HMGB1 binding to globally platinated DNA are conflicting and no studies on site-specifically platinated DNA have been performed. Definitive experimental work on the relative affinity of oxidized and reduced HMGB1 for site-specifically platinated DNA would greatly improve the current scientific understanding of this protein.

HMGB4

A new member of the mammalian HMGB family, HMGB4 (NCBI Reference Sequence: NP_660206.2), has recently been characterized.[44] The murine form of HMGB4 is isolable from adult mouse testis and a virtually identical protein is found in humans. The protein is of particular interest because of the connection with the testis,

an organ in which the treatment of tumors with cisplatin is extraordinarily effective (over 99% cure rate). Comparison of the human HMGB4 and human HMGB1 sequences (Chart 5.2) reveals that the phenylalanine at position 38 that is critical for the binding of HMGB1 to cisplatin-modified DNA[2] is conserved in the HMGB4 sequence. The sequence alignment further indicates that the disulfide bond formed in HMGB1 between Cys23 and Cys45 cannot be formed in HMGB4 due to the absence of a cysteine at position 23.

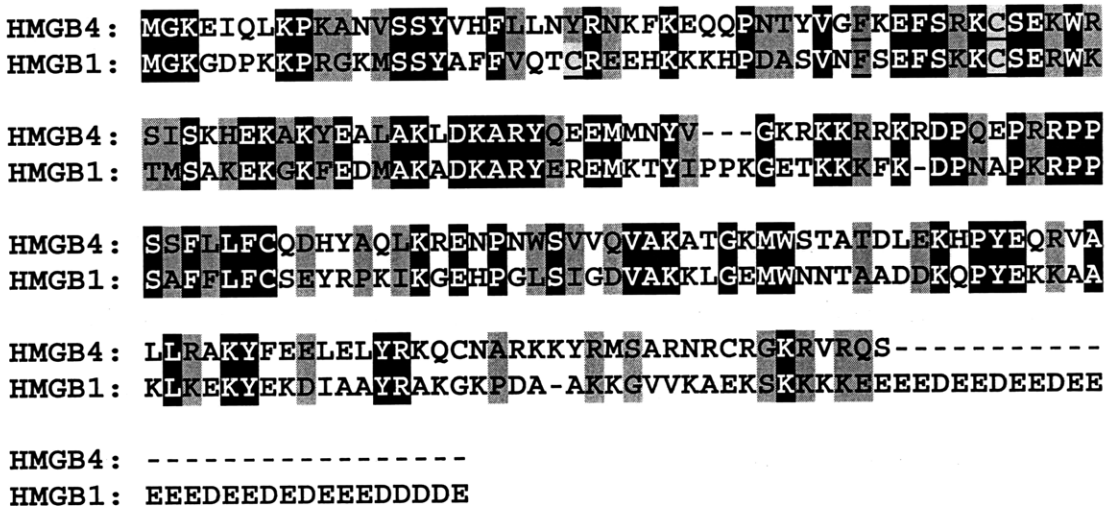

Chart 5.2. Sequence alignment of human HMGB4 and human HMGB1. Identical residues are highlighted in black, similar residues are highlighted in grey, and the Phe38, Cys23, and Cys45 residues are underlined.

The last 34 C-terminal residues of HMGB1 are acidic and wrap around to associate with the N-terminal A-domain of the protein (Chart 5.2).[45] The affinity of HMGB1 for DNA is increased if the tail is removed from the protein.[46] HMGB4 lacks the acidic tail (Chart 5.2), but seems to bind chromatin with less affinity than HMGB1. This preliminary conclusions is based on separate observations that HMGB1 binds chromatin with about the same affinity as the histone linker H1 protein[47,48] and that

HMGB4 binds with less affinity than H1,[44] although the differences in binding affinity for specific DNA structures (cisplatin-modified DNA, cruciform DNA) have yet to be determined.

Goals of this Chapter

The aim of this work is three-fold. The first goal is to investigate the hypothesis that androgens, like estrogen and progesterone, will increase the level of HMGB1 in cell nuclei and potentiate the antitumor activity of cisplatin in cells. If both of these hypotheses are true, inorganic compounds combining platinum(IV) and a modified androgen can be synthesized and used to selectively target and kill prostate cancer. cells The second goal is to show that retinoic acid, an agent already being investigated as an antitumor agent can increase the level of HMGB1 in tumor cell nuclei and that it can potentiate the antitumor activity of cisplatin. The third goal is to determine the effect of reducing or oxidizing conditions on the affinity of HMGB1 for cisplatin-modified DNA.

Experimental

Materials

The prostate cancer cell lines were a gift from the lab of J. M. Essigman (MIT), who had obtained them from the American Type Culture Collection (ATCC). The MCF-7 cell line was obtained from ATCC. 4,5α-Dihydrotestosterone (DHT), dehydroepiandrosterone (DHEA), (Scheme 5.1) and all-*trans* retinoic acid (ATRA) (Chart 5.1) were obtained from Aldrich. DHT and DHEA were kept in strict accordance with all US Drug Enforcement Agency requirements. Specifically, one gram of DHT was stored in a locked cabinet that was permanently built into the wall, usage records were

kept, and all DHT remaining after the completion of the experiments was incinerated (Guaranteed Returns, Holbrook, NY). Cisplatin was synthesized from potassium tetrachloroplatinate as previously reported.[49] Solutions of the androgens and ATRA were prepared fresh daily in dimethylformamide and diluted 10-fold in sterile PBS before use. Cisplatin solutions in PBS were prepared daily and quantitated by atomic absorption spectroscopy (Perkin Elmer, Aanalyst 300, HGA800 graphite furnace). Highly purified sterile water (Milli-Q) was used for the immunofluorescence assay. Recombinant $HMGB1_{full}$ and $HMGB1_{AB}$ was prepared by Yongwon Jung of the Lippard lab.

Cell Culture

LNCaP, a cell line which expresses the androgen receptor (AR+), DU-145 (AR-), and PC-3 (AR-) prostate cancer cells were incubated at 37°C in 5% CO_2 and grown in RMPI medium supplemented with 1% glucose, 10% fetal bovine serum, 1% penicillin/streptomycin, 1% 1M Hepes buffer (pH 7.4), 1% sodium pyruvate, and 1% L-glutamine. MCF-7 cells, which express retinoic acid receptor β (RARβ) were grown in DMEM with 10% FBS and 1% penicillin/streptomycin. Cells were passed every 4 to 5 days and restarted from frozen stock upon reaching pass number 20. Media was changed every three days.

Immunofluorescence

Cells were plated on day 1 in a 25 cm^2 flask and treated with 500 nM ATRA on day 2. The medium was replaced with fresh ATRA-containing medium on day 4. On day

6, cells were treated with trypsin/EDTA and plated in a 24-well plate on microscope cover slips at 30,000 to 50,000 cells per well in ATRA-containing medium. Cells treated with either DHT or DHEA were plated directly in a 24-well plate on microscope cover slips at 30,000 to 50,000 cells per well on day 1. Androgens were added on day 2 to a concentration of 1 μM at time points of 20, 16, 12, 8, 6, 4, 2, and 0.5 hours prior to fixation and permeabilization. Cells treated with either ATRA or androgens were fixed for 10 min in 2% paraformaldehyde/0.1M phosphate buffer (pH 7.4) and washed three times in fresh PBS. Cells were then permeabilized by incubating for 10 minutes in 0.1% Triton-X100, a detergent, in PBS (pH 7.4). The samples were washed six times in PBS and incubated for 15 minutes in a blocking buffer, (PBS, pH 7.4, 0.1% goat serum, 0.075% glycine). The rabbit anti-HMGB1 primary antibody was diluted 1:100 in blocking buffer and the cover slips were placed in a humid container, covered with 35 μL of the diluted antibody, and incubated at 37°C for 1 hr. After washing the samples three times in blocking buffer, the incubation was repeated with a goat anti-rabbit FITC-conjugated secondary antibody (1:100 dilution in blocking buffer). The cover slips were washed twice in blocking buffer and four times in water before mounting with a p-phenylenediamine anti-bleaching solution (9.2 mM p-phenylenediamine in 1:10 10x PBS:glycerol) on microscope slides. Slides were imaged on a Nikon Eclipse TS100 Microscope with a Nikon DXM1200 digital camera.

Cytotoxicity Assays

Cells to be treated with retinoic acid were grown in a 25 cm^2 flask with medium containing 500 nM retinoic acid. The medium was replaced with fresh retinoic acid-

containing medium after two days of growth. After four days of growth, the cells were plated at 2,000 cells per each well of a 96 well plate and grown for one day before adding cisplatin to concentrations of 0, 1, 2, 5, 8, 10, 12, 15, and 20 μM cisplatin (in MCF-7 cells) or 0, 1, 1.5, 2, 2.5, 3, 6, 10, and 15 μM cisplatin (in PC-3 cells).

Cells to be treated with androgen were plated at 2,000 cells per each well of a 96 well plate and grown for one day before adding androgen to a final concentration of 1 μM and cisplatin to concentrations of 0, 1, 2, 5, 8, 10, 12, 15, and 20 μM. Cell survival was quantified by the MTT assay after five days of growth.

Oxidation and Reduction of HMGB1

$HMGB1_{full}$ and $HMGB1_{AB}$ were fully reduced with 10 mM DTT. Oxidizing conditions were produced with diamide (Chart 5.3) (10-500 mM, 4-25°C, 0-30 min), H_2O_2 (0.1-5 mM), or oxidized and reduced glutathione (GSH:GSSG 1:10).

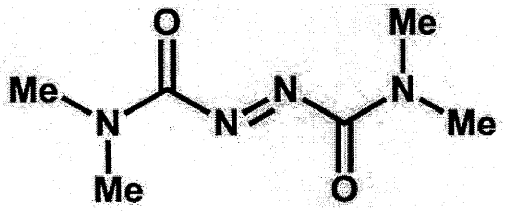

Chart 5.3. Structure of diamide.

Electrophoretic Mobility Shift Assays

EMSAs were performed as diagrammed in Figure 5.2 and as a modification of a previously reported protocol.[50] Radiolabeled, platinated 20mer (~0.5 nM overall) with the top strand sequence (cDDP site in bold):

5′-CCT CTC CTC TCT **GG**A TCT TCT CTC C-3′

was incubated in a buffer (10 mM Hepes, pH 7.5, 50 mM $LiCl_2$, 10 mM $MgCl_2$, 100 mM NaCl, 2 mg/mL BSA, 0.05% Nonidet P40, 1 mM spermidine, carrier poly dGdC DNA at a 10:1 ratio with platinated DNA on a per nucleotide basis). HMGB1 pre-incubated in the same buffer with either 10 mM DTT or 10 mM diamide was added and the reaction was kept at 4°C for 30 minutes. A 10% polyacrylamide gel with a 37.5:1 ratio of acrylamide:bis-acrylamide was pre-run for at least 30 min in an ice bath with recirculating chilled water. Non-denaturing loading buffer (overall 0.7% sucrose (w/v), 0.017% xylene cyanol (w/v), 0.5% Ficoll 400 (v/v)) was added to the protein-DNA reactions and the protein-DNA complexes were electrophoresed at 150 V for 2.67 h.

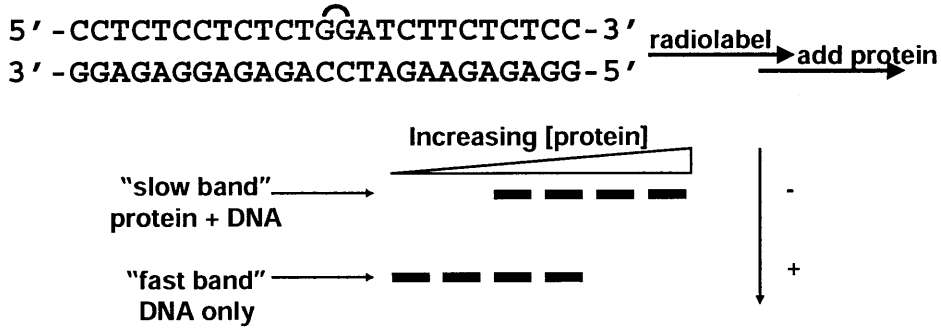

Bandshift Buffer
10 mM Hepes, pH 7.5
50 mM $LiCl_2$,10 mM $MgCl_2$,100 mM NaCl
2 mg/mL BSA
0.05% Nonidet P40
1 mM spermidine (fresh daily)
10:1 (nt basis) poly dGdC DNA
± 10 mM DTT/± 10 mM diamide

Incubate 4°C, 30 min
Add loading buffer:
Sucrose to 0.7% (w/v)
Xylene cyanol to 0.017% (w/v)
Ficoll 400 to 0.5% (v/v)
Low V gel, 150 V, 2.67 h
10% acrylamide, 37.5:1 acrylamide:bis,
ice bath and recirculating chilled water

Figure 5.2. Summary of experimental conditions for the electrophoretic shift mobility assays on HMGB1.

Results and Discussion

Cytotoxicity of Cisplatin in the Presence of an Androgen

Plots of the cytotoxicity data for cisplatin-treated cells grown in the presence or absence of an androgen, DHEA, are shown in Figure 5.3. The concentrations of cisplatin

required for 50% inhibition of cell growth (IC_{50}) are reported in Table 5.1. Percentage survival was determined separately for cells grown in the presence and absence of androgen due to slightly decreased survival for DHEA-treated cells and slightly increased survival for DHT-treated cells. Based on the IC_{50} values, no statistically significant difference in cytotoxicity was observed in any of the experiments.

Table 5.1. Summary of cytotoxicity values from the plots in Figure 5.3.

	LNCaP (AR+)	DU-145 (AR-)	PC-3 (AR-)
cisplatin	2.5 μM	2 μM	2.55 μM
cisplatin+1μM DHT	4.9 μM	—	—
cisplatin+1μM DHEA	2.5 μM	2.5 μM	2.75 μM

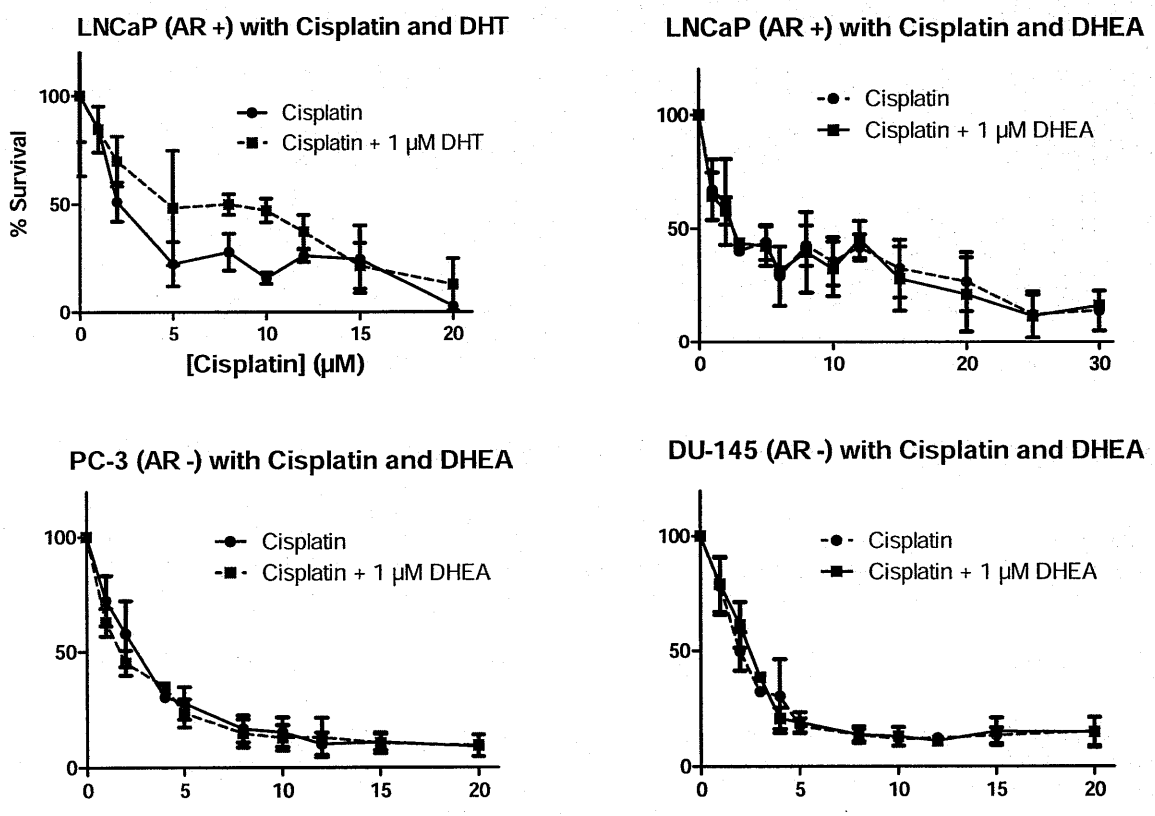

Figure 5.3. Cytotoxicity assays indicating the results of co-treatment of cisplatin with either DHEA or DHT in cells with (LNCaP) and without (DU-145, PC-3) the androgen receptor (AR).

Cytotoxicity of Cisplatin in the Presence of Retinoic Acid

The results of cytotoxicity assays conducted in both the RARβ positive MCF-7 cells and the RARβ negative PC-3 cells are plotted in Figure 5.4 and the IC_{50} values are reported in Table 5.2. Neither RARβ(+) nor RARβ(-) cell lines show cisplatin sensitization after treatment with retinoic acid and cisplatin. An increase of the ATRA treatment time from seven days to eight days did not affect this result. The lack of increased cytotoxicity is unsurprising based on the immunofluorescence results showing the ATRA-upregulated HMGB1 to be localized in the cytosol. Cytosolic HMGB1 would not be available to participate in repair-shielding of cisplatin-DNA adducts and therefore is not expected to sensitize cells to cisplatin.

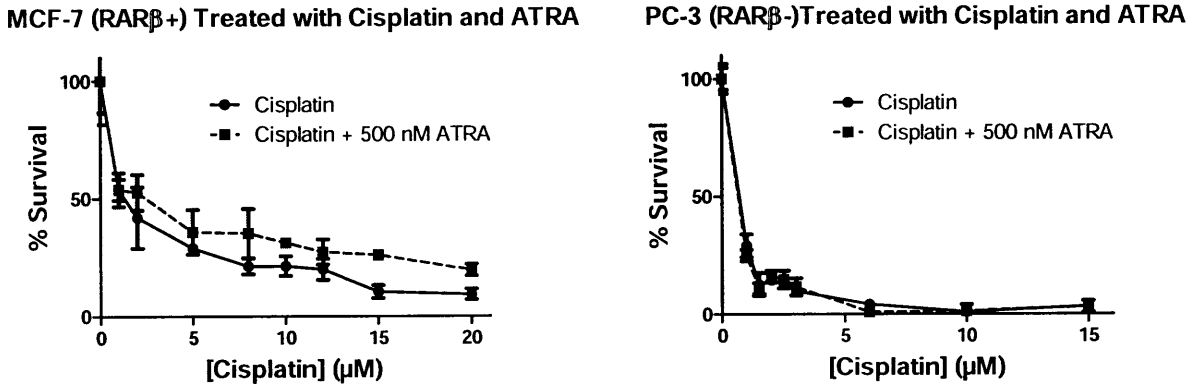

Figure 5.4. Cytotoxicity assays indicating the effect of cisplatin after preincubation of cells in retinoic acid in cells with (MCF-7) and without (PC-3) the retinoic acid receptor (RARβ).

Table 5.2. Summary of cytotoxicity values from plots shown in Figure 5.4

MCF-7 (RARβ+)		PC-3(RARβ-)	
cisplatin	cisplatin+500μM RA	cisplatin	cisplatin+500μM RA
1.4 μM	2.6 μM	0.7 μM	0.7 μM

Immunofluorescence-based Detection of HMGB1 in Cells Treated with Androgens

In the androgen experiments, the upregulation of HMGB1 due to the steroid would have resulted in a marked increase in fluorescence intensity, as was observed in the previously published work on progesterone and estrogen.[5,4] No intensity difference between the androgen-treated and untreated cells was observed. In an effort to allow time for the biosynthetic transformation of DHEA into DHT, the androgen pretreatment time was varied between 0 and 20 hours. None of the timed experiments showed an intensity difference between treated and control cells. Representative samples from two experiments, one with DHEA and one with DHT, in which cells were pretreated with androgen for 4 h are shown in Figure 5.5.

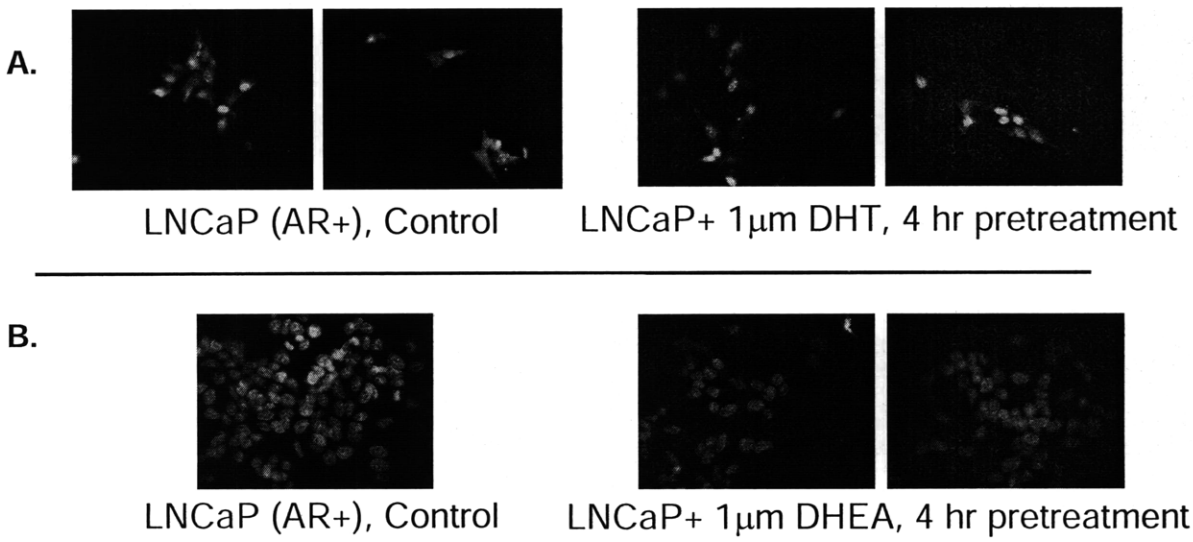

Figure 5.5. Representative immunofluorescence results showing the HMGB1 protein labeled with a FITC-conjugated secondary antibody. Results were invariant, even with varying durations of androgen pretreatment. (A): Results from treatment with DHT. (B): Results from treatment with DHEA.

Immunofluorescence-based Detection of HMGB1 in Cells Treated with Retinoic Acid

For the ATRA experiments, the time course for immunofluorescence was based on the time required for the upregulation of HMGB1 in the P19 (murine embryonal carcinoma) cell line. Images showing the results of the immunofluorescence assay are shown in Figures 5.6 and 5.7. A distinct increase in the level of HMGB1 can be seen in the cells that have been treated with retinoic acid.

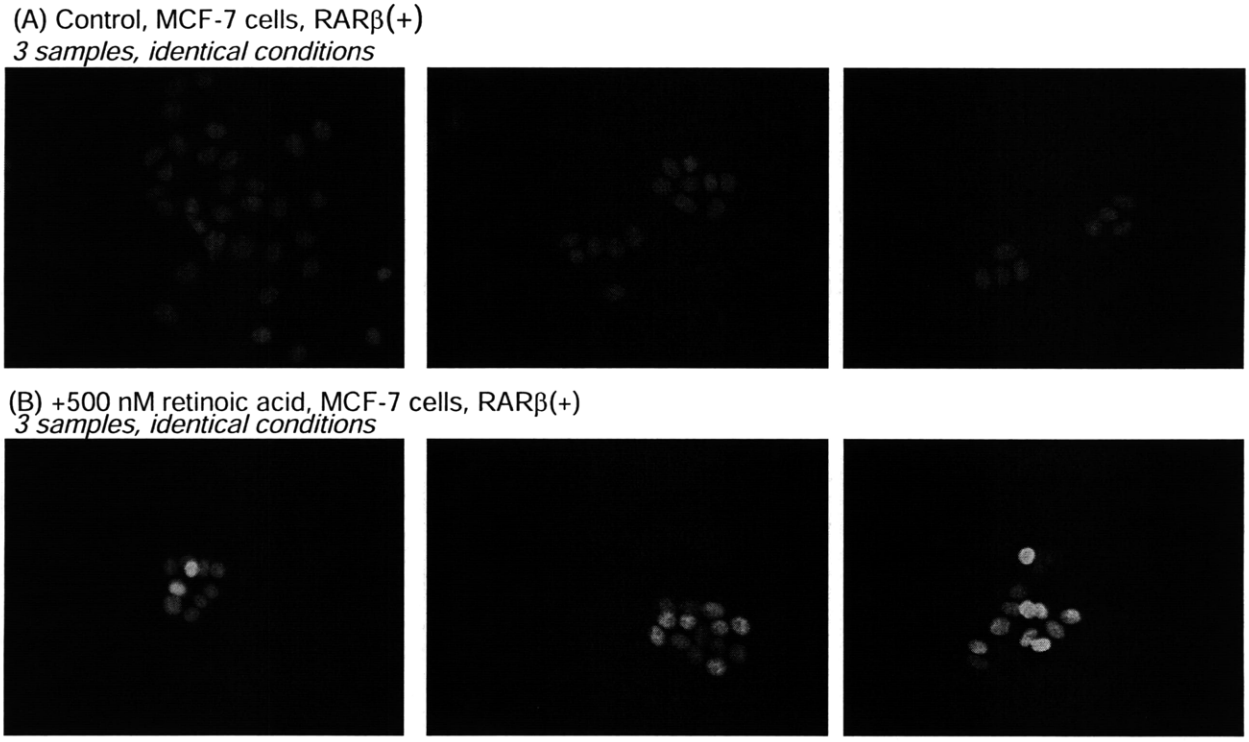

Figure 5.6. Immunofluorescence results showing fluorescence due to an anti-HMGB1 primary antibody and a FITC-conjugated secondary antibody. (A) shows samples photographed in the absence of retinoic acid. (B) shows samples photographed after addition of 500 nM retinoic acid, as stated in the Methods section.

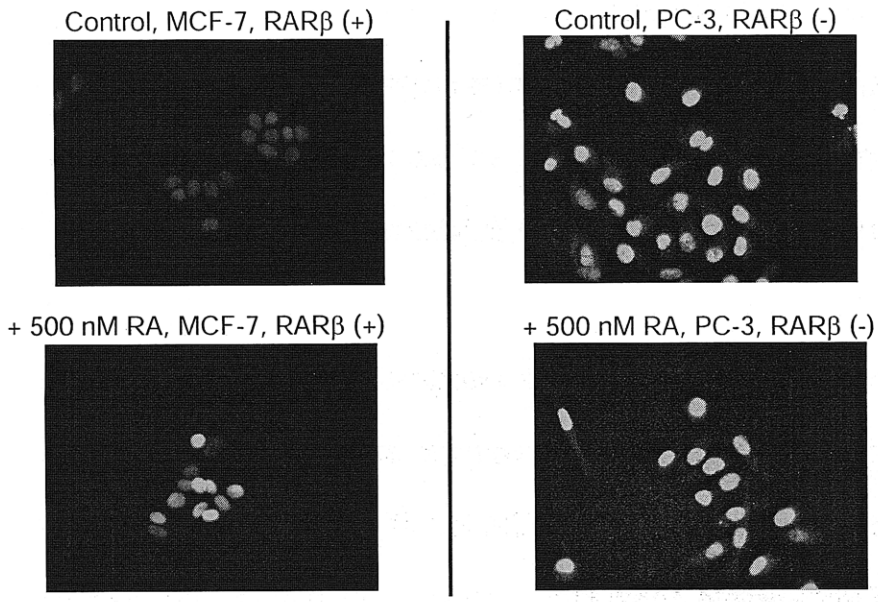

Figure 5.7. Samples showing the difference in upregulation between MCF-7 cells (left), which express the retinoic acid receptor β (RARβ), and PC-3 cells (right), which do not express the receptor.

Oxidation and Reduction of HMGB1

Examination of the interaction of HMGB1 with platinated DNA has been crucial to development of the repair-shielding hypothesis. Previous gel mobility shift assays have been carried out at pH 7.5 with no reducing agent,[30,50-54] pH 7.5 with 1 mM DTT,[55] and pH 7.9 without reducing agent.[56] Because the preparation of recombinant HMGB1 involves expression in *E. coli*, an organism with a reducing cytosol in which disulfide bonds do not commonly form,[57] followed by purification under reducing conditions,[56,58] the proteins used in these previous experiments were probably completely reduced.

Investigation of the relative binding constants of platinated DNA with oxidized and reduced forms of HMGB1 has been completed. Recombinant protein as prepared by Yongwon Jung was 55% oxidized to begin with and could be fully reduced by 10 mM DTT (Figure 5.8). Despite a variety of oxidation strategies, however, HMGB1 could not be oxidized *in vitro*. Diamide concentrations from 10 mM to 500 mM were ineffective.

Variation of the time (0-30 min) and temperature (4°C, 16°C, or 25°C) of incubation with diamide produced no further oxidation than the initial 55% (Figure 5.8). Full reduction with 10 mM DTT followed by treatment with 500 mM diamide yielded only the fully reduced protein, indicating that whatever bond the DTT reduced could not be reformed. "Pre-assembly" of the protein by incubation with salmon sperm DNA, followed by diamide treatment failed to form the disulfide bond. An attempt to oxidize using the GSH:GSSG molar ratio of 10:1 found in the mammalian endoplasmic reticulum yielded no disulfide bond, nor did incubation with [H_2O_2] of 0.1, 0.2, 0.5, 1, or 10 mM. It was finally concluded that some cellular component, such as a disulfide isomerase, is required for the formation of the bond.

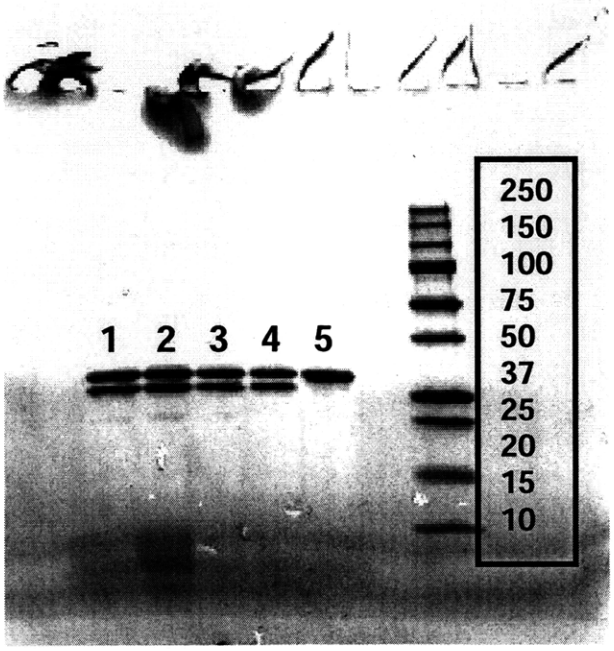

Figure 5.8. SDS-PAGE gel showing complete reduction and attempted complete oxidation of full length HMGB1. A) Lanes: 1) 100 mM diamide, 30 min; 2) 100 mM diamide, 10 min; 3) 10 mM diamide, 30 min; 4) 10 mM diamide, 10 min; 5) 10 mM DTT.

Reexpression of HMGB1 in *E. coli* under oxidizing conditions, such as with the inclusion of a low concentration of diamide in the expression medium, was determined to be the next logical step. The protein in the next experiments was used as purified from *E. coli* under normal conditions, in a 55% oxidized state, or fully reduced by DTT.

Interaction of Oxidized and Reduced HMGB1 with Cisplatin-Modified DNA

The sequence for the bandshift probe was carefully chosen according to previous investigations of the sequence specificity of HMGB1.[50] The 20 bp length is critical. If the probe were too long, the protein could find multiple binding sites and the EMSA would be smeared. Conversely, a shorter probe would not have enough length to accommodate the entire protein footprint. The reduction of voltage and temperature below that normally used for a native gel was also crucial to obtaining clean bandshift data.

Bandshifts with HMGB1domAB and full-length HMGB1 have shown that the reduced form of both the full-length and the AB-truncated protein binds more tightly to cDDP-modified DNA than the 55% oxidized form (Figure 5.9). The binding constant for the AB domain shows on the order of a 10-fold increase for the reduced protein (Figure 5.10).

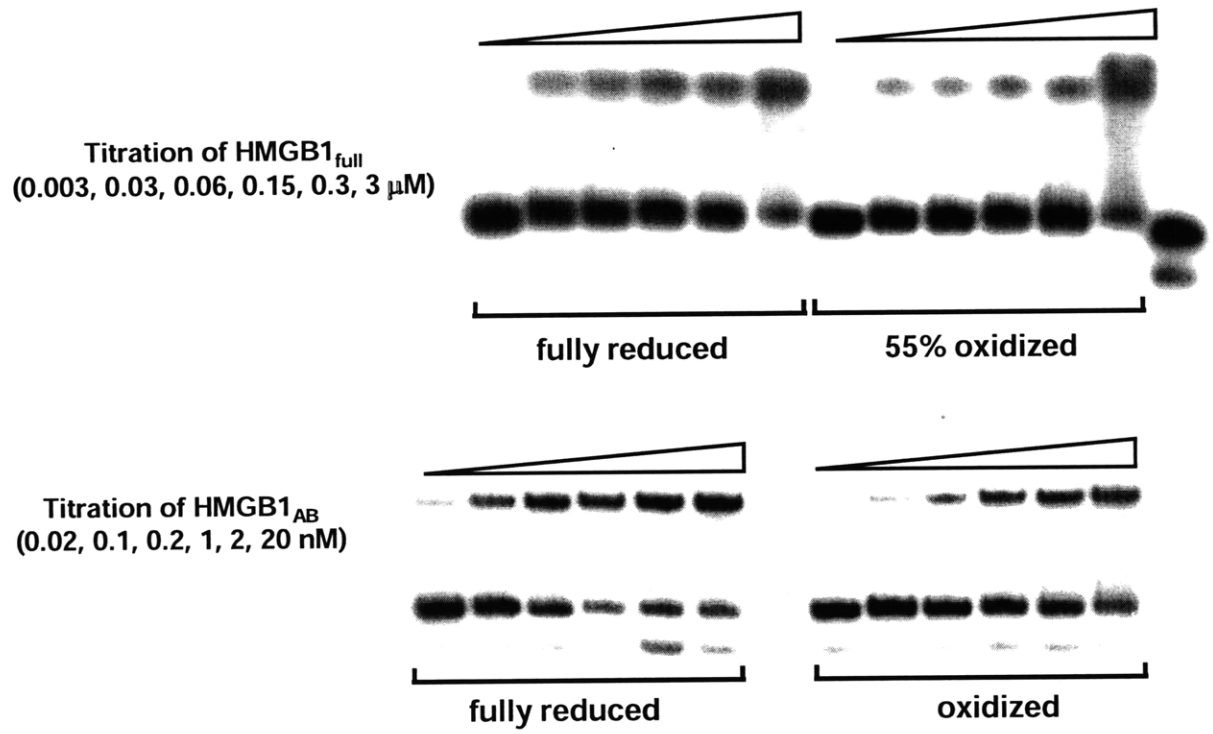

Figure 5.9. EMSAs for HMGB1 in the reduced and oxidized forms. Gels are 10% native PAGE as described in the experimental section. Top gel is full length HMGB1 and bottom gel is for the combined domain AB polypeptide.

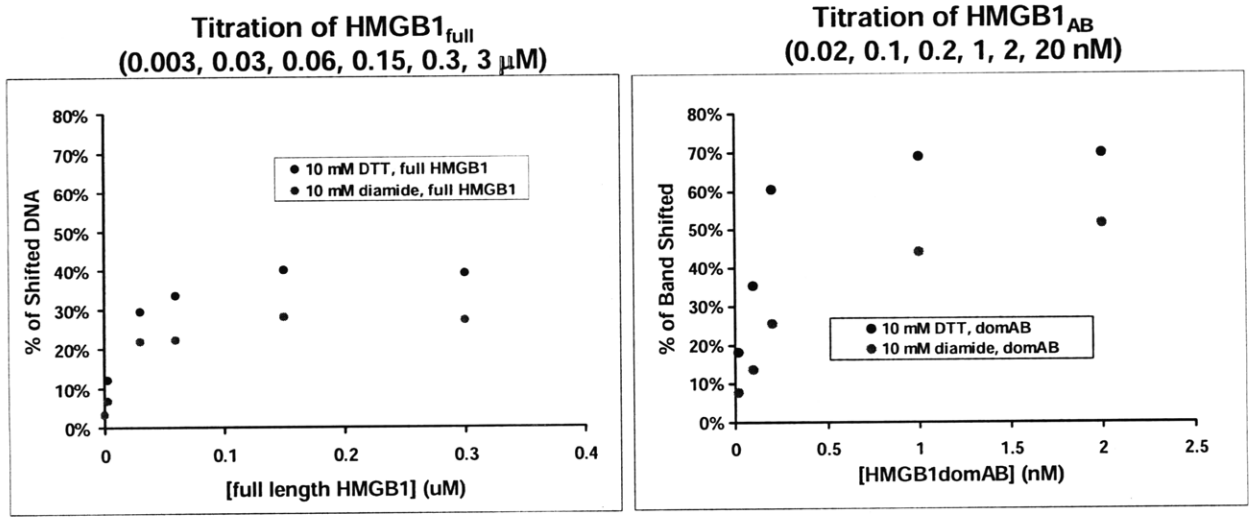

Maximum % shift obtained:

(70.0% at 3 uM HMGB1) **(76.0% at 20 nM domAB)**

Figure 5.10. Analysis of EMSA gels shown as percentage of shifted DNA as a function of increasing HMGB1 concentration. The improvement in binding upon reduction of the full-length protein was 1.5-fold and the improvement upon reduction of the AB-domain protein was 2.4-fold.

Conclusions

The Effect of Androgens on HMGB1 Levels and Cisplatin Potency

HMGB1 is not upregulated upon treatment of LNCaP cells with androgens. Our experiments are not the only evidence for this lack of HMGB1 upregulation. A recent study[59] utilized high-throughput arrays to identify 692 genes upregulated by the treatment of LNCaP cells with dihydrotestosterone. This study also collected results from five similar LNCaP-based experiments performed by other labs, bringing the total of identified upregulated genes to 2118. We obtained this database as a list of mRNA ascension numbers in a searchable Microsoft Excel format and searched using for numbers associated with HMGB1 and HMGB2. Because no reference to either of these high mobility group proteins was found in this extensive database, the conclusion was made that HMGB1 is not involved in the androgen receptor—DNA interaction in LNCaP cells. Other proteins containing the high mobility group box binding domain have been implicated as facilitators in this interaction, including the male sex determining factor SRY.[7]

The Effect of Retinoic Acid on HMGB1 Levels and Cisplatin Potency

All-*trans* retinoic acid does not sensitize the RARβ(+) MCF-7 cells to cisplatin, but does induce an increase in the HMGB1 levels. The interaction of the retinoic acid receptor and HMGB1 is complicated by the observation that the RAR is connected to the RAGE pathway in murine embryonal carcinoma cells.[15,60] Any increase in the cytosolic levels of HMGB1 are likely related to the RAGE pathway and the activity of HMGB1 as a cytokine, although such an increase was not detected by

immunofluorescence. An increase in HMGB1 localized to the nucleus, such as that seen upon treatment with ATRA in this work, indicates a mechanism similar to that seen when cells are treated with either progesterone or estrogen.[4] Of interest for future work would be the study of HMGB1 upregulation in the OVCCR1 or NIH-OVCAR-3 ovarian cancer cell lines, in which the sensitization of cells to cisplatin by ATRA co-treatment has already been proven. [18,19] Interestingly, these cell lines only express RARα and RARγ. [19]

Reducing Conditions and HMGB1 Affinity for Cisplatin-Modified DNA

The large increase in binding constant for the reduced form of HMGB1 provides an exciting chance to expand and develop the theory of repair shielding. The new member of the HMGB family, HMGB4,[44] lacks Cys23 (Chart 5.2). and cannot form the Cys23-Cys45 disulfide bond. HMGB4 therefore permanently resembles the reduced form of HMGB1 that has the higher affinity for cisplatin-modified DNA. The RNAi work of Dong Xu has provided us with a variety of HMGB1 knockdown lines that will allow us to move beyond the *in vitro* EMSA result to *in vivo* proof of concept in human tissue. Using site-directed mutagenesis, we can transfect C23A and C45A mutants of the $HMGB1_A$ domain protein into HMGB1 knockdown cells and look for the potentiation of cisplatin activity. These mutants would prevent the formation of a disulfide bond and should yield a nuclear-bound form of the protein with high affinity for cisplatin-modified DNA. Additionally, a mimic of the oxidized form of the protein could be generated by introducing a salt bridge into the protein, such as C23D and C45K. Finally, tryptophan can be incorporated into the protein as a fluorescent indicator of the folding state of the

protein. The optimal site for such a modification should be determined by examination of the Ohndorf-Lippard structure of $HMBG1_{domA}$ on DNA. Computer-assisted modeling of all of these mutants can be carried out prior to beginning lab work.

In addition to transfection of human cells with plasmids for expression of the mutant proteins *in vivo*, recombinant forms of the proteins can also be produced for the purpose of *in vitro* studies. EMSAs on the mutant proteins will provide information on binding constants. Nucleotide excision repair assays in mammalian cell extracts will yield information on the ability of the mutants to engage in repair shielding of the cisplatin-DNA adduct. Finally, a crystal structure of the protein mutant that shows the most promising behavior in human tissue will lend visual images to complement the *in vitro* and *in vivo* data.

References

(1) P. M. Pil, C. S. Chow and S. J. Lippard (1993). High-mobility-group 1 protein mediates DNA bending as determined by ring closures. *Proc. Natl. Acad. Sci. U. S. A.*, **90**, 9465-9469.

(2) U.-M. Ohndorf, M. A. Rould, Q. He, C. O. Pabo and S. J. Lippard (1999). Basis for recognition of cisplatin-modified DNA by high-mobility-group proteins. *Nature*, **399**, 708-712.

(3) K. Y. Chau, H. Y. P. Lam and K. L. D. Lee (1998). Estrogen treatment induces elevated expression of HMG1 in MCF-7 cells. *Exp. Cell. Res.*, **241**, 269-272.

(4) Q. He, C. H. Liang and S. J. Lippard (2000). Steroid hormones induce HMG1 overexpression and sensitize breast cancer cells to cisplatin and carboplatin. *Proc. Natl. Acad. Sci. USA*, **97**, 5768-5772.

(5) K. R. Barnes, A. Kutikov and S. J. Lippard (2004). Synthesis, characterization, and cytotoxicity of a series of estrogen-tethered platinum(IV) complexes. *Chem. Biol.*, **11**, 557-564.

(6) V. Boonyaratanakornkit, V. Melvin, P. Prendergast, M. Altmann, L. Ronfani, M. E. Bianchi, L. Taraseviciene, S. K. Nordeen, E. A. Allegretto and D. P. Edwards (1998). High-Mobility Group Chromatin Proteins 1 and 2 Functionally Interact with Steroid Hormone Receptors to Enhance Their DNA Binding in Vitro and Transcriptional Activity in Mammalian Cells. *Mol. Cell. Biol.*, **18**, 4471-4487.

(7) X. Yuan, M. L. Lu, T. Li and S. P. Balk (2001). SRY Interacts with and Negatively Regulates Androgen Receptor Transcriptional Activity. *J. Biol. Chem.*, **276**, 46647-46654.
(8) A. E. Kornblut and D. Wilson (2005). How One Pill Escaped Place On Steroid List. *New York Times*, A1.
(9) H. Fang, W. Tong, W. S. Branham, C. L. Moland, S. L. Dial, H. Hong, Q. Xie, R. Perkins, W. Owens and D. M. Sheehan (2003). Study of 202 Natural, Synthetic, and Environmental Chemicals for Binding to the Androgen Receptor. *Chem. Res. Toxicol.*, **10**, 1338-1358.
(10) D. T. Villareal and J. O. Holloszy (2004). Effect of DHEA on Abdominal Fat and Insulin Action in Elderly Women and Men: A Randomized Controlled Trial. *J. Am. Medical Assoc.*, **292**, 2243-2248.
(11) M. Algarte-Genin, O. Cussenot and P. Costa (2004). Prevention of Prostate Cancer by Androgens: Experimental Paradox or Clinical Reality. *Eur. Urol.*, **46**, 285-295.
(12) J. T. Arnold, H. Le, K. K. McFann and M. R. Blackman (2005). Comparative effects of DHEA vs. testosterone, dihydrotestosterone, and estradiol on proliferation and gene expression in human LNCaP prostate cancer cells. *Am. J. Physiol. Endocrinol. Metab.*, **288**, E573-E584.
(13) P. Chambon (2005). The Nuclear Receptor Superfamily: A Personal Retrospect on the First Two Decades. *Mol. Endocrinol.*, **19**, 1418-1428.
(14) A. Arapshain, Y. S. Kuppumbatti and R. Mira-y-Lopez (2000). Methylation of conserved CpG sites neighboring the beta retinoic acid response element may mediate retinoic acid receptor beta gene silencing in MCF-7 breast cancer cells. *Oncogene*, **19**.
(15) D. K. H. Chou, T. R. Henion and F. B. Jungalwala (2003). Regulation of expression of sulfoglucuronyl carbohydrate (HNK-1), Amphoterin and RAGE in retinoic acid-differentiated P19 embryonal carcinoma cells. *J. Neurochem.*, **86**, 917-931.
(16) A. Goncalves, J. Camerlo, H. Bun, G. Gravis, D. Genre, F. Bertucci, M. Resbeut, F. Pech-Gourg, A. Durand, D. Maraninchi and P. Viens (2001). Phase II study of a combination of cisplatin, all-trans-retinoic acid and interferon-alpha in squamous cell carcinoma: Clinical results and pharmacokinetics. *Anticancer Res.*, **21**, 1431-1437.
(17) G. P. Kalemkerian, M. Jiroutek, D. S. Ettinger, J. A. Dorighi, D. H. Johnson and M. Mabry (1998). A Phase II study of all-trans retinoic acid plus cisplatin and etoposide in patients with extensive stage small cell lung carcinoma: an Eastern Cooperative Oncology Group Study. *Cancer*, **83**, 1102-1108.
(18) S. Jozan, S. Paute, M. Courtade-Saidi, S. Julie, S. Vidal, R. Bugat and A. Valette (2002). All trans retinoic acid enhances cDDP-induced apoptosis: modulation of the cDDP effect on cell cycle progression. *Intl. J. Oncology*, **20**, 1289-1295.
(19) M. J. Caliaro, P. Vitaux, C. Lafon, I. Lochon, A. Nehme, A. Valette, P. Canal, R. Bugat and S. Jozan (1997). Multifactorial mechanism for the potentiation of cisplatin (CDDP) cytotoxicity by all-trans retinoic acid (ATRA) in human ovarian carcinoma cell lines. *Br. J. Cancer*, **75**, 333-340.
(20) S. Aebi, R. Kroning, B. Cenni, A. Sharma, D. Fink, G. Los, R. Weisman, S. B. Howell and R. D. Christen (1997). all-trans-Retinoic acid enhances cisplatin-

induced apoptosis in human ovarian adenocarcinoma and in squamous head and neck cancer cells. *Clin. Cancer Res.*, **3**, 2033-2038.
(21) C. Schlueter, H. Weber, B. Meyer, P. Rogalla, K. Roeser, S. Hauke and J. Bullerdiek (2005). Angiogenetic signaling through hypoxia: HMGB1: an angiogenetic switch molecule. *Am. J. Pathol.*, **166**, 1259-1263.
(22) S. O. Kim, K. Merchant, R. Nudelman, W. F. Beyer, Jr., T. Keng, J. DeAngelo, A. Hausladen and J. S. Stamler (2002). OxyR: a molecular code for redox-related signaling. *Cell*, **109**, 383-396.
(23) G. Hoppe, K. E. Talcott, S. K. Bhattacharya, J. W. Crabb and J. E. Sears (2006). Molecular basis for the redox control of nuclear transport of the structural chromatin protein Hmgb1. *Exp. Cell Res.*, **312**, 3526-3538.
(24) H. E. Marshall, K. Merchant and J. S. Stamler (2000). Nitrosation and oxidation in the regulation of gene expression. *FASEB J.*, **14**, 1889-1900.
(25) A.-P. Arrigo (1999). Gene expression and the thiol redox state. *Free Radic. Biol. Med.*, **27**, 936-944.
(26) W. Maret and B. L. Vallee (1998). Thiolate ligands in metallothionein confer redox activity on zinc clusters. *Proc. Natl. Acad. Sci. U. S. A.*, **95**, 3478-3482.
(27) A. Agresti and M. E. Bianchi (2003). HMGB proteins and gene expression. *Curr. Opin. Genet. Dev.*, **13**, 170-178.
(28) S. Ferrari, P. Finelli, M. Rocchi and M. E. Bianchi (1996). The active gene that encodes human high mobility group 1 protein (HMG1) contains introns and maps to chromosome 13. *Genomics*, **35**, 367-371.
(29) M. E. Bianchi In *DNA-Protein: Structural Interactions*, 1995, pp 177-200.
(30) Q. He, U.-M. Ohndorf and S. J. Lippard (2000). Intercalating Residues Determine the Mode of HMG1 Domains A and B Binding to Cisplatin-Modified DNA. *Biochemistry*, **39**, 14426-14435.
(31) C. H. Hardman, R. W. Broadhurst, A. R. C. Raine, K. D. Grasser, J. O. Thomas and E. D. Laue (1995). Structure of the A-Domain of HMG1 and Its Interaction with DNA as Studied by Heteronuclear Three- and Four-Dimensional NMR Spectroscopy. *Biochemistry*, **34**, 16596-16607.
(32) R. W. Broadhurst, C. H. Hardman, J. O. Thomas and E. D. Laue (1995). Backbone Dynamics of the A-Domain of HMG1 As Studied by 15N NMR Spectroscopy. *Biochemistry*, **34**, 16608-16617.
(33) P. N. Cockerill, G. H. Goodwin, P. D. Cary, C. Turner and E. W. Johns (1983). Comparisons of the structures of the chromosomal high mobility group proteins HMG1 and HMG2 prepared under conditions of neutral and acidic pH. *Biochim. Biophys. Acta Protein Struct. Mol. Enzymol.*, **745**, 70-81.
(34) L. A. Kohlstaedt, D. S. King and R. D. Cole (1986). Native state of high mobility group chromosomal proteins 1 and 2 is rapidly lost by oxidation of sulfhydryl groups during storage. *Biochemistry*, **25**, 4562-4565.
(35) C. Hwang, A. J. Sinskey and H. F. Lodish (1992). Oxidized redox state of glutathione in the endoplasmic reticulum. *Science*, **257**, 1496-1502.
(36) M. M. Lyles and H. F. Gilbert (1991). Catalysis of the oxidative folding of ribonuclease A by protein disulfide isomerase: dependence of the rate on the composition of the redox buffer. *Biochemistry*, **30**, 613-619.

(37) B. J. Andrews, J. A. Lehman and J. J. Turchi (2006). Kinetic Analysis of the Ku-DNA Binding Activity Reveals a Redox-dependent Alteration in Protein Structure That Stimulates Dissociation of the Ku-DNA Complex. *J. Biol. Chem.*, **281**, 13596-13603.
(38) P. C. Billings, R. J. Davis, B. N. Engelsberg, K. A. Skov and E. N. Hughes (1992). Characterization of high mobility group protein binding to cisplatin-damaged DNA. *Biochem. Biophys. Res. Commun.*, **188**, 1286-1294.
(39) L. G. Sheflin, N. W. Fucile and S. W. Spaulding (1993). The specific interactions of HMG 1 and 2 with negatively supercoiled DNA are modulated by their acidic C-terminal domains and involve cysteine residues in their HMG 1/2 boxes. *Biochemistry*, **32**, 3238-3248.
(40) M. Stros, J. Reich and A. Kolibalova (1994). Calcium binding to HMG1 protein induces DNA looping by the HMG-box domains. *FEBS Lett.*, **344**, 201-206.
(41) J. E. Cryer, S. W. Johnson, B. N. Engelsberg and P. C. Billings (1996). Analysis of HMG protein binding to DNA modified with the anticancer drug cisplatin. *Cancer Chemother. Pharmacol.*, **38**, 163-168.
(42) S. Taudte, H. Xin and N. R. Kallenbach (2000). Alanine mutagenesis of high-mobility-group-protein-1 box B (HMG1-B). *Biochem. J.*, **347**, 807-814.
(43) L. A. Kohlstaedt and R. D. Cole (1994). Specific interaction between H1 histone and high mobility protein HMG1. *Biochemistry*, **33**, 570-575.
(44) R. Catena, E. Escoffier, C. Caron, S. Khochbin, I. Martianov and I. Davidson (2009). HMGB4, a novel member of the HMGB family, is preferentially expressed in the mouse testis and localizes to the basal pole of elongating spermatids. *Biol. Reprod.*, **80**, 358-366.
(45) S. Knapp, S. Mueller, G. Digilio, T. Bonaldi, M. E. Bianchi and G. Musco (2004). The Long Acidic Tail of High Mobility Group Box 1 (HMGB1) Protein Forms an Extended and Flexible Structure That Interacts with Specific Residues within and between the HMG Boxes. *Biochemistry*, **43**, 11992-11997.
(46) K.-B. Lee and J. O. Thomas (2000). The Effect of the Acidic Tail on the DNA-binding Properties of the HMG1,2 Class of Proteins: Insights from Tail Switching and Tail Removal. *J. Mol. Biol.*, **304**, 135-149.
(47) Y. Ogawa, S. Aizawa, H. Shirakawa and M. Yoshida (1995). Stimulation of transcription accompanying relaxation of chromatin structure in cells overexpressing high mobility group 1 protein. *J. Biol. Chem.*, **270**, 9272-9280.
(48) L. Cato, K. Stott, M. Watson and J. O. Thomas (2008). The Interaction of HMGB1 and Linker Histones Occurs Through their Acidic and Basic Tails. *J. Mol. Biol.*, **384**, 1262-1272.
(49) S. C. Dhara (1970). A rapid method for the synthesis of *cis*-$[Pt(NH_3)_2Cl_2]$. *Indian J. Chem.*, **8**, 193-194.
(50) S. U. Dunham and S. J. Lippard (1997). DNA Sequence Context and Protein Composition Modulate HMG-Domain Protein Recognition of Cisplatin-Modified DNA. [Erratum to document cited in CA127:214676]. *Biochemistry*, **36**, 13972.
(51) J. N. Burstyn, W. J. Heiger-Bernays, S. M. Cohen and S. J. Lippard (2000). Formation of cis-diamminedichloroplatinum(II) 1,2-intrastrand cross-links on DNA is flanking-sequence independent. *Nucleic Acids Res.*, **28**, 4237-4243.

(52) Y. Mikata, Q. He and S. J. Lippard (2001). Laser-Induced Photo-Cross-Linking of Cisplatin-Modified DNA to HMG-Domain Proteins. *Biochemistry*, **40**, 7533-7541.
(53) M. Wei, S. M. Cohen, A. P. Silverman and S. J. Lippard (2001). Effects of spectator ligands on the specific recognition of intrastrand platinum-DNA cross-links by high mobility group box and TATA-binding proteins. *J. Biol. Chem.*, **276**, 38774-38780.
(54) Y. Jung and S. J. Lippard (2003). Nature of Full-Length HMGB1 Binding to Cisplatin-Modified DNA. *Biochemistry*, **42**, 2664-2671.
(55) B. A. Donahue, M. Augot, S. F. Bellon, D. K. Treiber, J. H. Toney, S. J. Lippard and J. M. Essigmann (1990). Characterization of a DNA damage-recognition protein from mammalian cells that binds specifically to intrastrand d(GpG) and d(ApG) DNA adducts of the anticancer drug cisplatin. *Biochemistry*, **29**, 5872-5880.
(56) P. M. Pil and S. J. Lippard (1992). Specific binding of chromosomal protein HMG1 to DNA damaged by the anticancer drug cisplatin. *Science*, **256**, 234-237.
(57) A. I. Derman, W. A. Prinz, D. Belin and J. Beckwith (1993). Mutations that allow disulfide bond formation in the cytoplasm of Escherichia coli. *Science*, **262**, 1744-1747.
(58) L. Falciola, A. I. H. Murchie, D. M. J. Lilley and M. E. Bianchi (1994). Mutational analysis of the DNA binding domain A of chromosomal protein HMG1. *Nucleic Acids Res.*, **22**, 285-292.
(59) A. M. Velasco, K. A. Gillis, Y. Li, E. L. Brown, T. M. Sadler, M. Achilleos, L. M. Greenberger, P. Frost, W. Bai and Y. Zhang (2004). Identification and Validation of Novel Androgen-Regulated Genes in Prostate Cancer. *Endocrinology*, **145**, 3913-3924.
(60) D. K. H. Chou, J. Zhang, F. I. Smith, P. McCaffery and F. B. Jungalwala (2004). Developmental expression of receptor for advanced glycation end products (RAGE), amphoterin and sulfoglucuronyl (HNK-1) carbohydrate in mouse cerebellum and their role in neurite outgrowth and cell migration. *J. Neurochem.*, **90**, 1389-1401.

Chapter 6

Preclinical Evaluation of the Antitumor Properties of Pyriplatin

Introduction

Three platinum compounds in use worldwide, cisplatin, carboplatin, and oxaliplatin, have been developed with crucial support of the National Cancer Institute (NCI) of the United States and based on results of screening done with the NCI's 60-cell line panel.[1] The use of this screen and the NCI COMPARE program has allowed identification of clear differences in activity profile and mechanisms of action among platinum compounds and enabled grouping of platinum compounds according to these differences.[2] The cisplatin activity profile is similar to that of other diammine platinum compounds and to alkylating agents such as melphalan and camptothecin analogs. The oxaliplatin activity profile is similar to that of other platinum compounds with the 1,2-diaminocyclohexane ligand, including the Pt(IV) drug tetraplatin, and also to acridines, organic compounds currently being developed as anticancer drugs.[2]

Other classes have also been defined on the basis of the NCI60 screen. The platinum pyridines are one distinct group, into which the Farrell compounds (including the clinically tested BBR3464) can be grouped,[3,4] and the platinum-silanes are another distinct group. Cells resistant to compounds from one group are commonly not cross-resistant to compounds from another group. Because of the different mechanisms of action for each type of compound, members of different groups can show synergy when combined. For example, synergistic effects upon combination occur for the combination of cisplatin with oxaliplatin.[2]

The aim of present study is to characterize pyriplatin, a novel monofunctional, cationic platinum(II) compound, in vitro with direct comparisons to cisplatin and oxaliplatin as representative members of the cisplatin and dach platinum groups, respectively. The devevlopment of pyriplatin as an antitumor drug is a result of the

structure-activity relationship developed in chapter 2 and explored in chapter 3. Preliminary mechanistic studies and an x-ray structure of pyriplatin bound to a dodecamer of DNA were introduced in chapter 4. builds on work introduced in chapters 2, 3, and 4Pyriplatin has previously shown antitumor activity in mice,[5] despite the fact

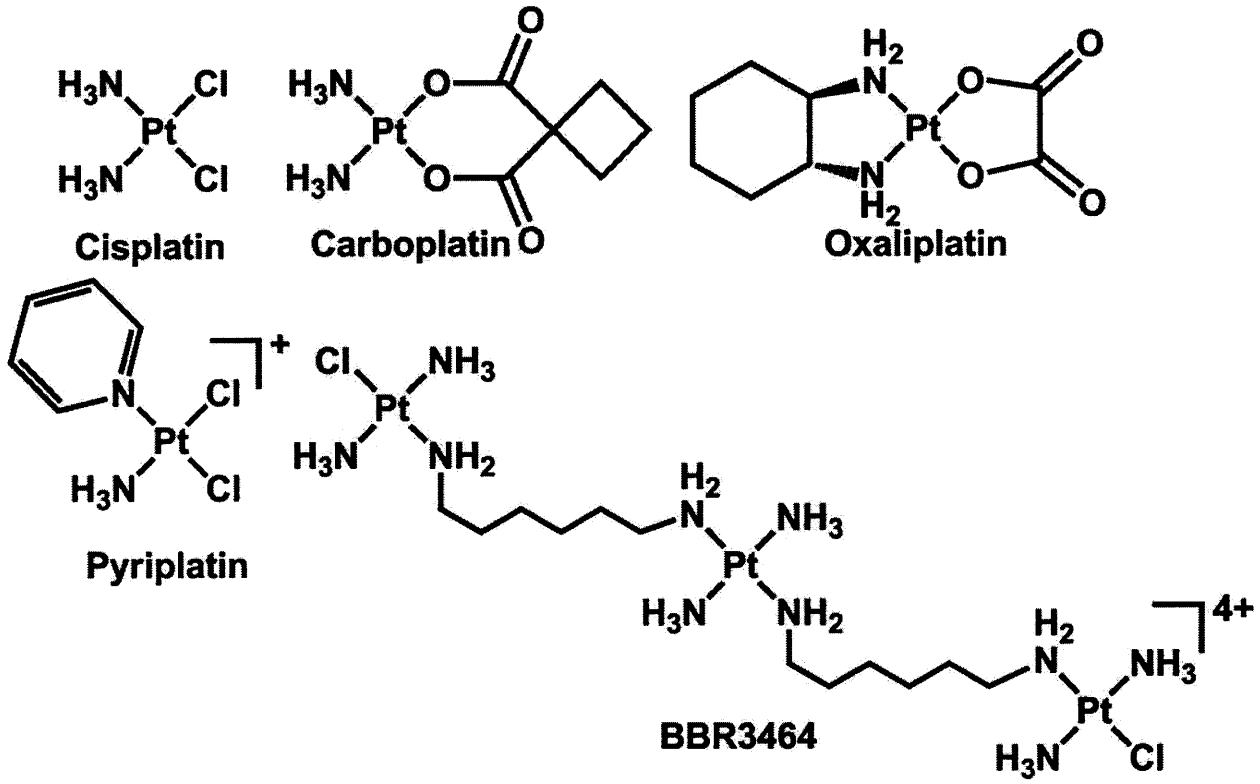

Chart 6.1. Platinum compounds from the cisplatin group (cisplatin, carboplatin), the dach group (oxaliplatin) and, tentatively assigned, the pyridine group (BBR3464, pyriplatin)

that it forms only a single covalent bond with DNA and is cationic. Pyriplatin is similar in some ways to the polynuclear Farrell compounds, including the trinuclear, cationic complex that was tested in phase II clinical trials, BBR3464. The two platinum centers of BBR3464 that bind to DNA each resemble pyriplatin (Chart 6.1), in that they contain three am(m)ine ligands and a single chloro ligand to form one covalent bond with DNA. Both the BBR3464 and pyriplatin have an overall cationic charge and the accumulation of each of these compounds in cells has been attributed to the presence of cell

membrane transporters. Specifically, pyriplatin is an outstanding substrate for the organic cation transporters 1 and 2,[6] and BBR3464 is a substrate for the copper transporter CTR1.[7]

Results of Single-Agent Study of Pyriplatin

Single-Agent Study: Antiproliferative effects of pyriplatin given as a single agent in a panel of human cancer cell lines.

A panel of 10 cancer cell lines of different origins was exposed to pyriplatin for 24 hours and then assessed for cytotoxicity by the MTT assay. Simultaneous assays were performed in the same manner in the 10 cell lines with cisplatin and oxaliplatin. Table 6.1 represents the concentrations required to achieve 50% growth inhibition (IC_{50}) in our panel of cancer cell lines and the standard deviation for at least three experiments, each done in triplicate. A comparison of cytotoxicity for the three drugs is represented in Figure 6.1. Figure 6.2 represents the IC_{50} values in each of the 10 cell lines and Figure 6.3 shows cell survival for the different cell lines at concentrations ranging from 0.1-160 μM of cisplatin (6.3A), oxaliplatin (6.3B), and 0.46-1000 μM pyriplatin (6.3C).

Pyriplatin had a cytotoxicity profile different from that of either cisplatin or oxaliplatin (Figures 6.1 and 6.2). Pyriplatin is roughly 10- or 20-fold less potent than cisplatin or oxaliplatin in all cell lines.

Table 6.1. IC_{50} values for pyriplatin, cisplatin, and oxaliplatin in the 10-cell line panel. Data reflect the mean and standard deviation of results from three separate experiments, each performed in triplicate.

Cell Line	Cancer Type	IC_{50} Cisplatin	IC_{50} Oxaliplatin	IC_{50} Pyriplatin
HT-29	Colorectal	11.9 ± 4.1 μM	6.65 ± 1.0 μM	443 ± 255 μM
MDA-435	Breast /Melanoma	5.81 ± 4.0 μM	12.7 ± 5.6 μM	401 ± 156 μM
HCT-116	Colorectal	4.22 ± 2.5 μM	1.10 ± 0.28 μM	281 ± 50 μM
HCC2998	Colorectal	11.8 ± 4.0 μM	7.27 ± 2.3 μM	381 ± 103 μM
COLO205	Colorectal	16.7 ± 7.2 μM	2.84 ± 0.64 μM	266 ± 57 μM
MCF7	Breast	15.6 ± 6.4 μM	1.70 ± 0.54 μM	335 ± 104 μM
OVCAR3	Ovarian	5.10 ± 3.0 μM	1.24 ± 0.30 μM	328 ± 128 μM
IGROV1	Ovarian	5.64 ± 1.3 μM	8.08 ± 2.9 μM	230 ± 33 μM
HOP92	Non-Small Cell Lung	3.55 ± 3.2 μM	2.70 ± 0.60 μM	171 ± 56 μM
HOP62	Non-Small Cell Lung	3.56 ± 1.4 μM	6.86 ± 0.39 μM	190 ± 36 μM

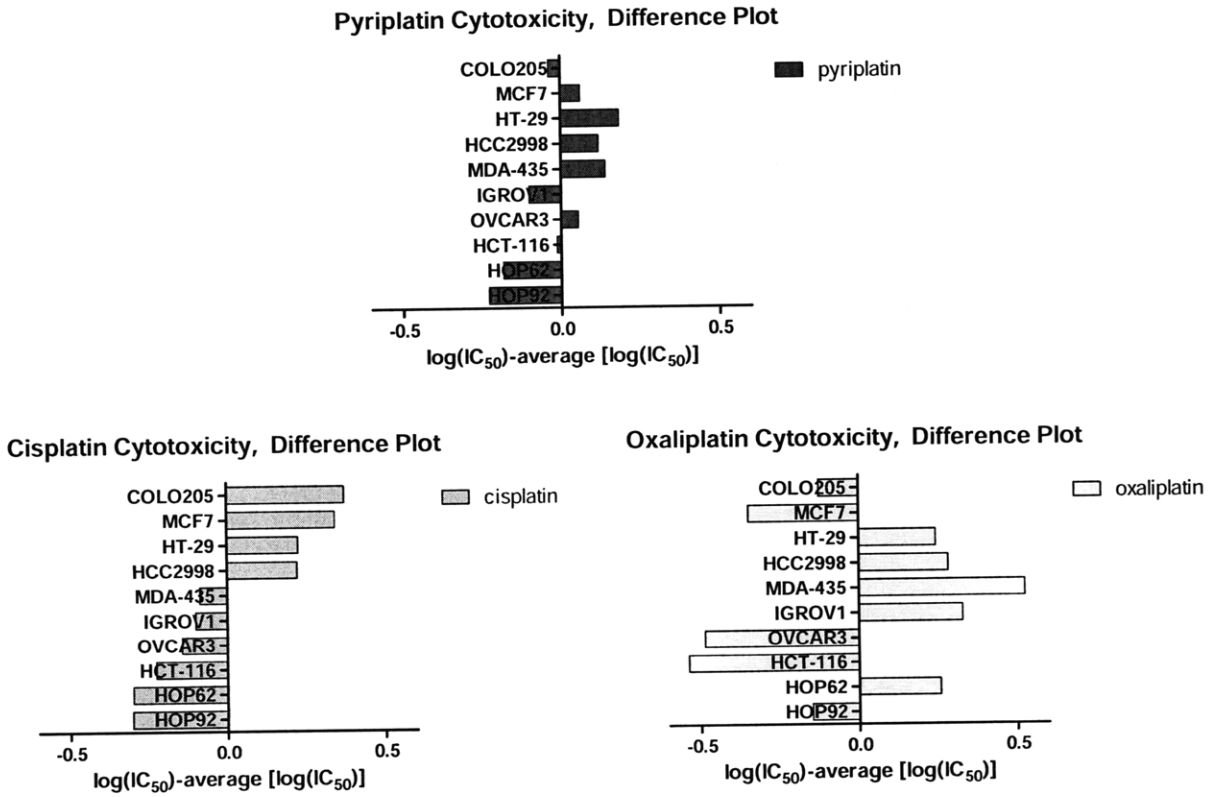

Figure 6.1. Mean graphs for IC_{50}. Bars depict the deviation of individual cell lines from the overall mean value for all the cells tested.

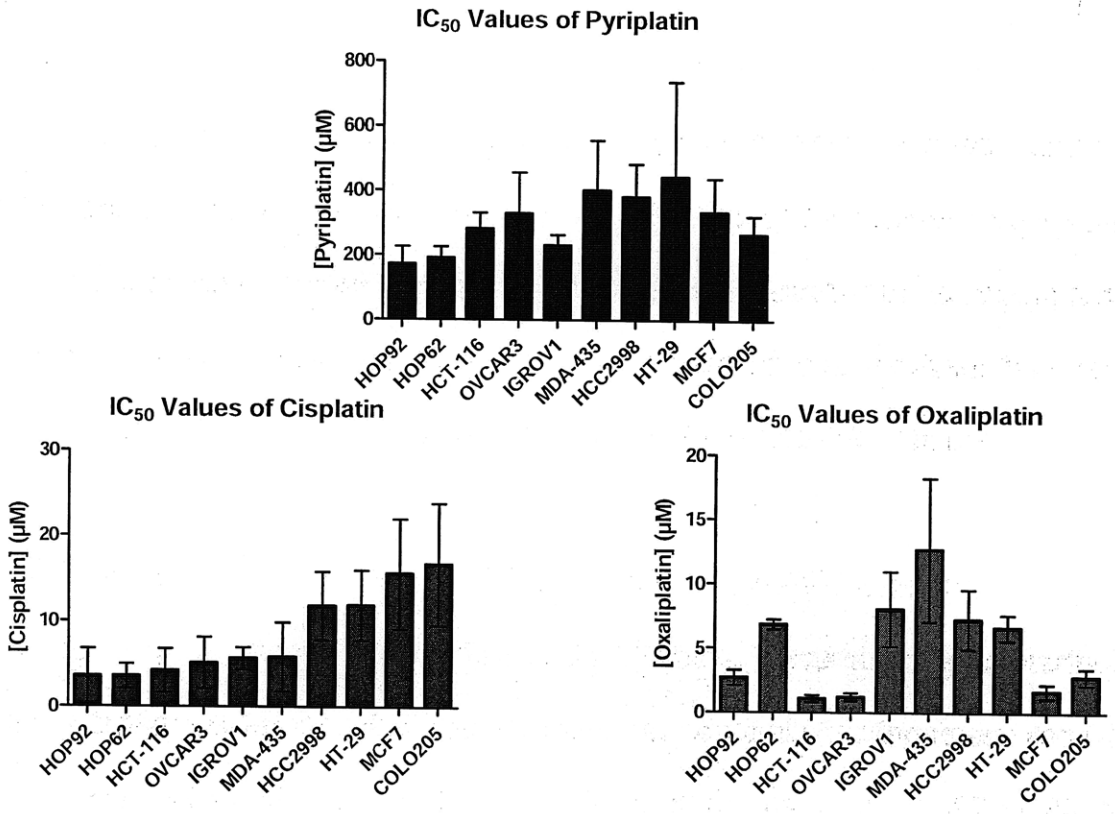

Figure 6.2. IC_{50} values of pyriplatin, cisplatin and oxaliplatin. Plots reflect the mean and standard deviation of results from three separate experiments, each performed in triplicate.

6.3(A) Cisplatin

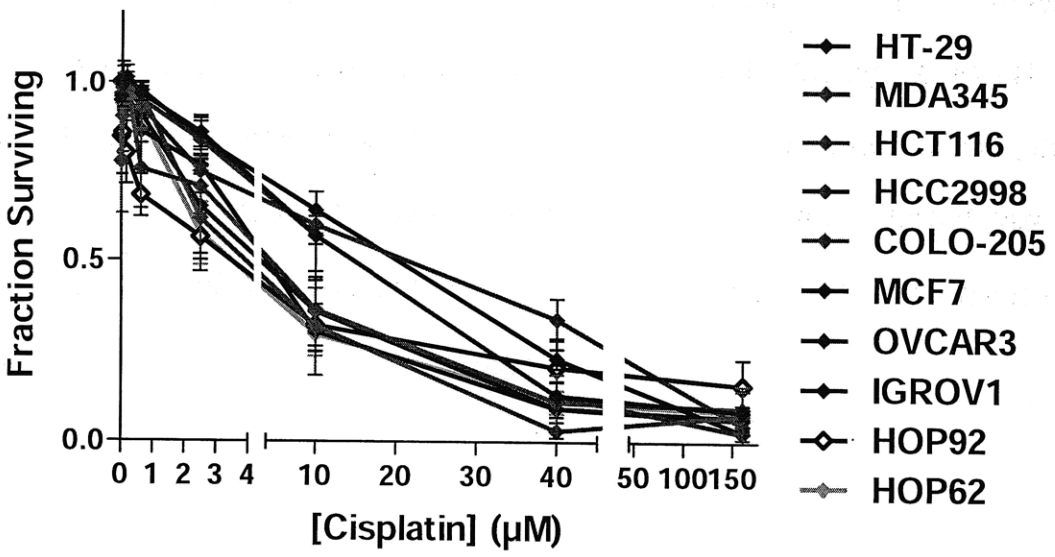

6.3(B) Oxaliplatin

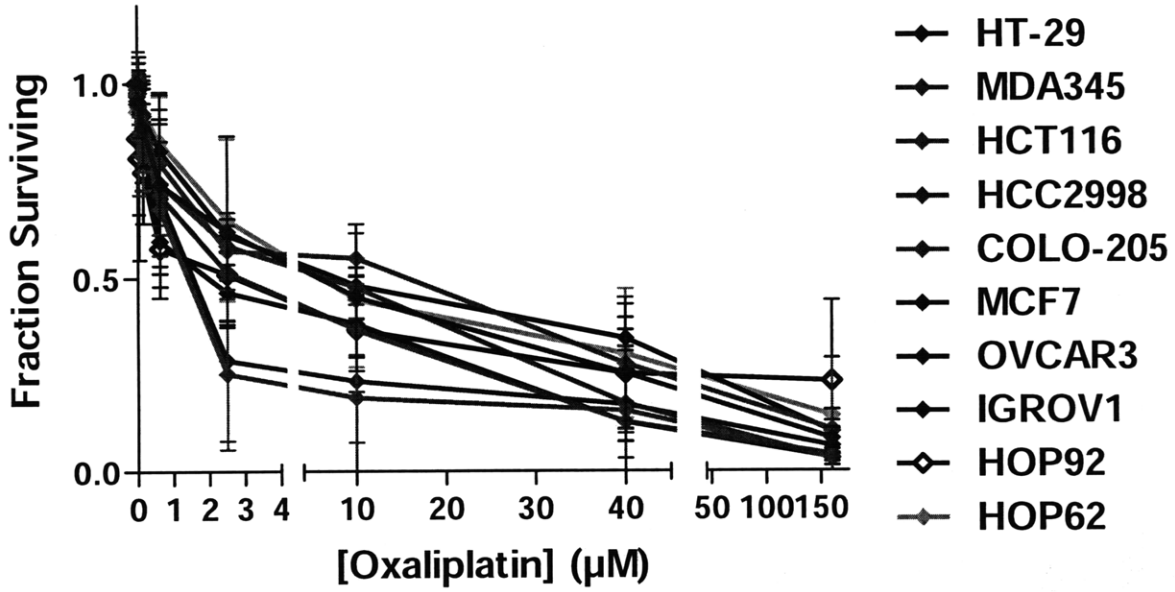

6.3(C) Pyriplatin

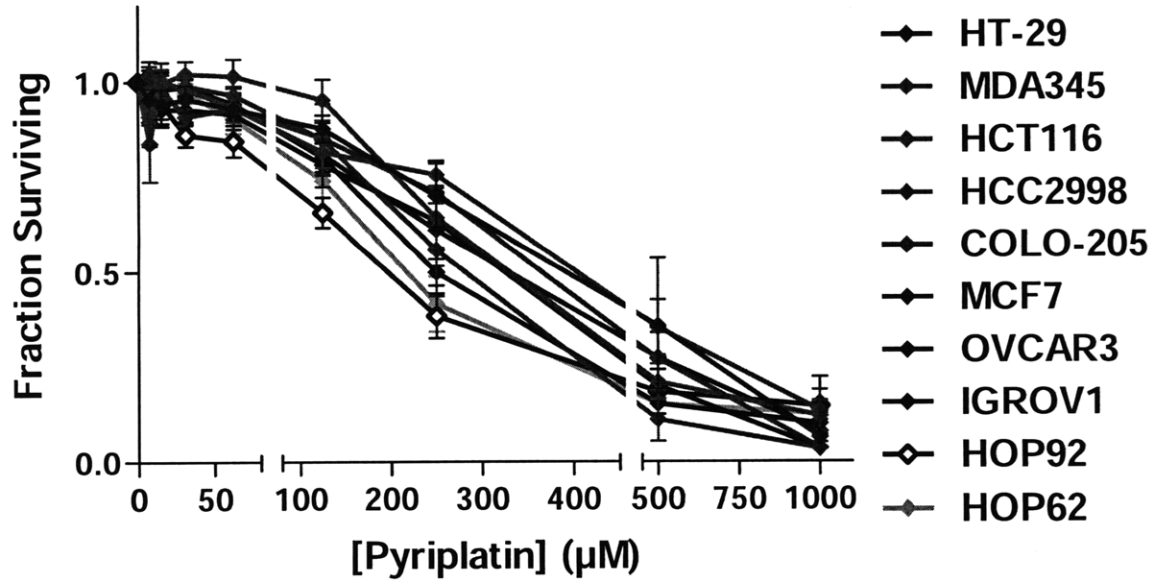

Figure 6.3. Cytotoxicity of cisplatin (A), oxaliplatin (B), and pyriplatin (C) in the studied cancer cell lines given for 24 hours. Plots reflect the mean and standard deviation of results from three separate experiments, each performed in triplicate.

Single-Agent Study: NCI60 Single Dose Study

Pyriplatin was submitted to the National Cancer Institute (USA) for single agent testing in 2008. Analysis by the online COMPARE algorithm revealed that pyriplatin had very little correlation with cisplatin or oxaliplatin. The best correlation with a platinum compound in the NCI database was with an entry titled "(carboxyphthalato) platinum" (NSC # S748451) and a correlation coefficient of 0.396 was found.

Single-Agent Study: Antiproliferative Effects of Pyriplatin Over Time

The non-small cell lung cancer cell line HOP-62 was chosen for further study because it is more sensitive to pyriplatin than the other cell lines in the 10-cell line panel. HOP-62 was treated with pyriplatin, cisplatin, or oxaliplatin for 1, 2, 5, 24, 48, or 72 hours. After the specified time, the plates were washed and the medium replaced with drug-free medium. The MTT assay was performed after 48 hours of incubation in drug-free medium. Results in Figure 6.4 are reported as the mean IC_{50} plus and minus the standard deviation of at least three separate experiments performed in triplicate.

The cytotoxic effects of pyriplatin increased over the entire time period tested, meaning cytotoxicity increased even up to 72 h, indicating that the compound, or biological modifications thereof, retain some cytotoxic characteristics even after extended incubation in cell medium. Similar results were found for both cisplatin and oxaliplatin.

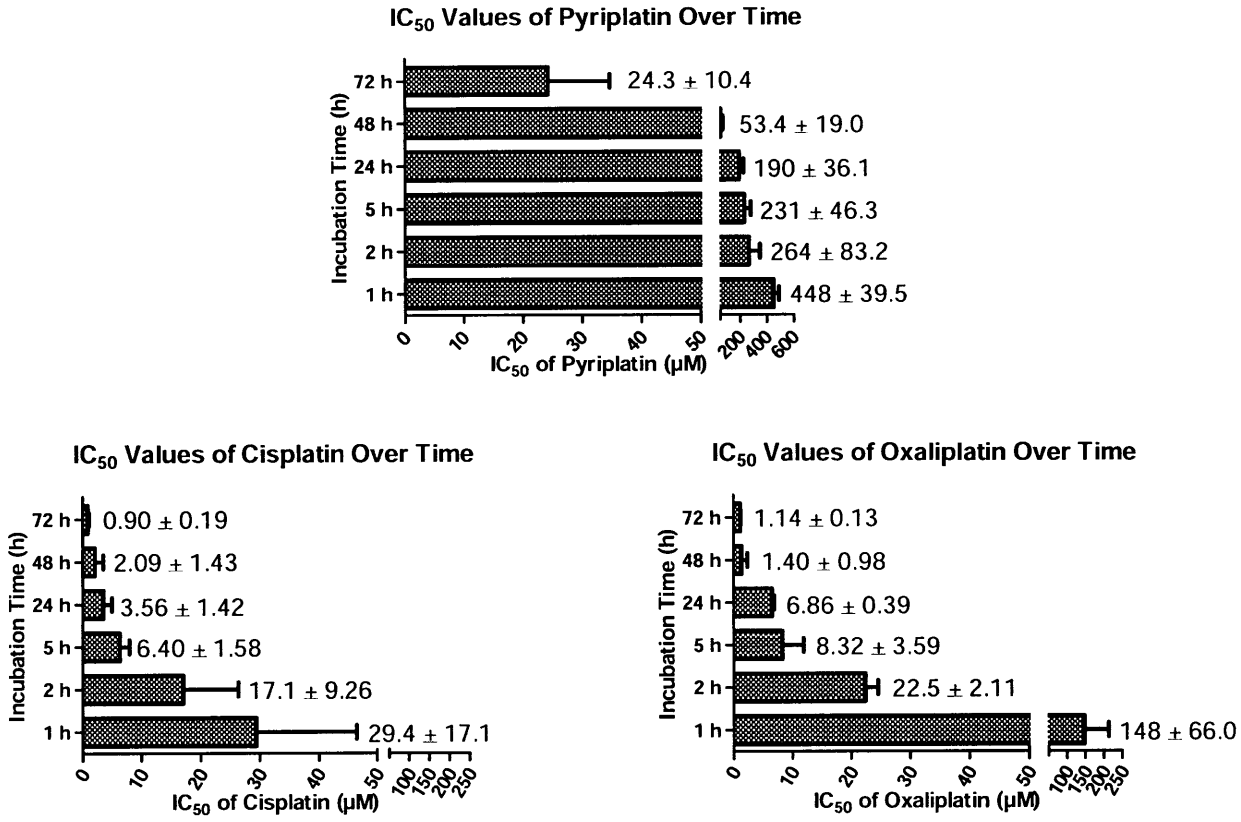

Figure 6.4. Antiproliferative effects of pyriplatin, cisplatin, and oxaliplatin over time.

Single-Agent Study: Cell Cycle

Effects on the cell cycle due to administration of pyriplatin were examined after 24 h incubation with the platinum compound at the IC_{50} value in the MCF-7 breast cancer cell line. Cells were stained with propidium iodide and analyzed immediately by flow cytometry. As shown in Figure 6.5, cisplatin initiates accumulation of cells in the S phase and cells treated with oxaliplatin accumulate in G_0/G_1. The results for pyriplatin show about 10% of the population in a sub-G_1 phase, which can be indicative of cells undergoing apoptosis.

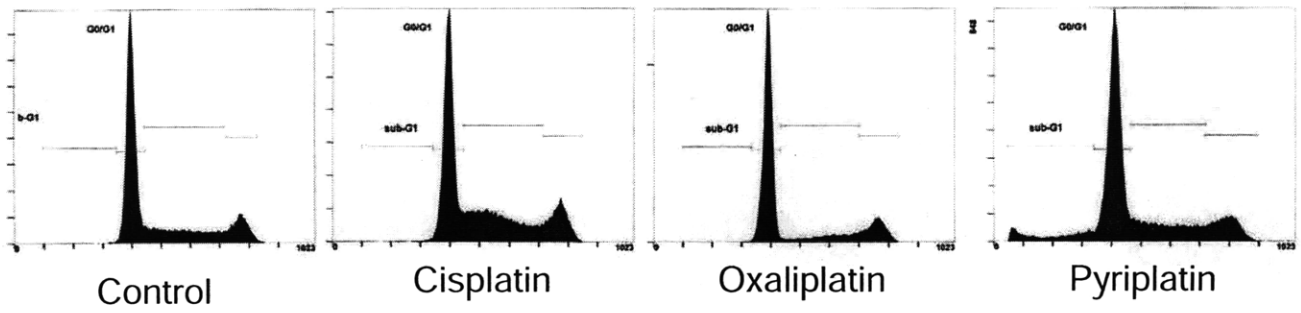

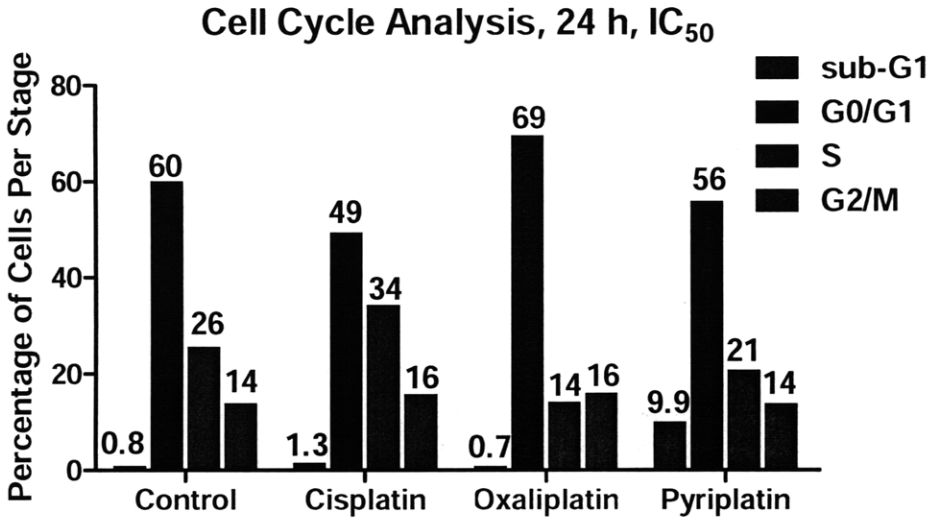

Figure 6.5. Analysis of the effects of platinum drugs on cell cycle progression in MCF-7 cells after treatment at the IC_{50} value for 24 h.

Pyriplatin in Combination with Known Antitumor Agents

Combination assay methodology

The antiproliferative effects of pyriplatin in combination with five known anticancer agents, taxol, gemcitabine, SN38, cisplatin, and 5-fluorouracil, were investigated in two cell lines, the ovarian cancer line OVCAR-3 and the colon cancer cell line HT-29. The combination experiments were performed according to three different schedules as shown in Figure 6.6. Cells were either treated with pyriplatin for 24 h followed by the

combination drug for 24 h, or treated with the drug combination for 24 h followed by pyriplatin for 24 h, or treated with both pyriplatin and the combination drug for 24 h. Antiproliferative effects were evaluated by the MTT assay. Calculation of combinatorial indices and classification of the effects of combination as either additive, synergistic, or antagonistic were done according to the method developed by Chou and Talalay.[8]

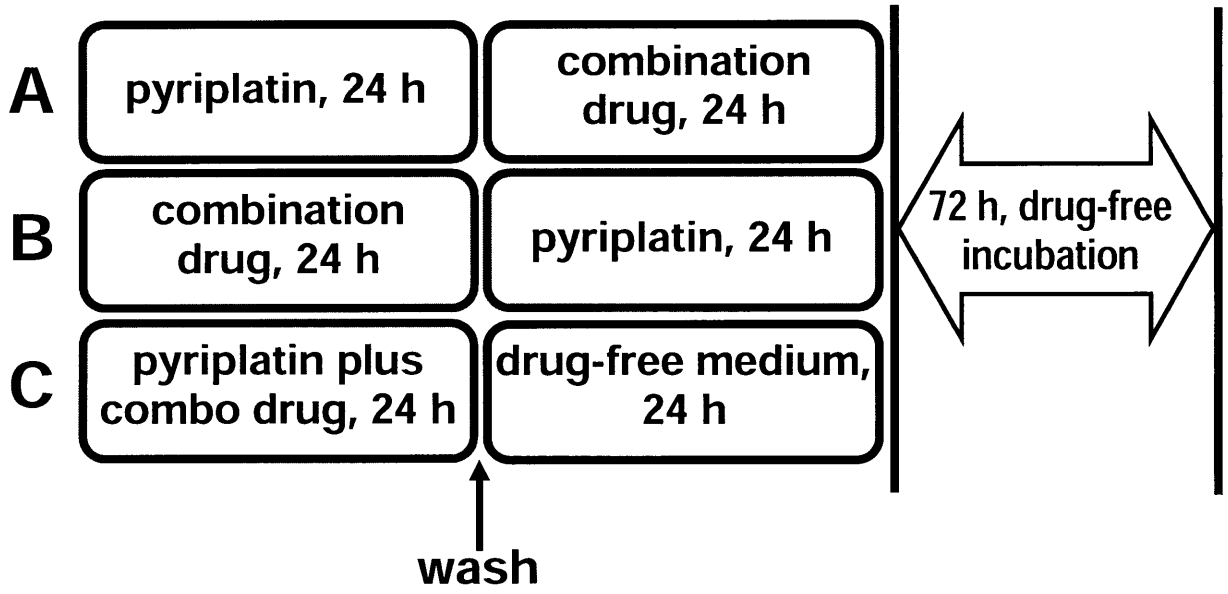

Figure 6.6. The three schedules used for combination experiments.

Combination assay results

Data were analyzed according to the method developed by Chou and Talalay using the CalcuSyn program. A combinatorial index (CI) of 1 indicates that the antiproliferative effects of two drugs are additive. A CI of less than 1 indicates a synergistic effect between the two drugs and a CI of greater than 1 indicates an antagonistic effect. A synergistic effect suggests that two drugs exert antiproliferative effects via separate mechanisms of action. Additive effects indicate that two drugs act via similar mechanisms of action.

Synergistic effects were observed for taxol, especially when pyriplatin and taxol were used simultaneously or when cells were treated with taxol prior to pyriplatin. Synergistic effects were also observed in combination with cisplatin when pyriplatin and cisplatin were added to cells simultaneously.

Table 6.2. Combination experiments in the HT-29 colon cancer cell line. Data are presented as the median CI value and the range represents the 95% confidence interval.

	Taxol	Gemza	SN38	Cisplatin	5-FU
Schedule A	0.87 (0.75-0.98)	1.66 (0.70-2.76)	0.90 (0.72-1.22)	1.11 (0.89-1.23)	0.94 (0.80-1.03)
Schedule B	0.88 (0.69-1.22)	1.09 (0.89-1.38)	2.21 (1.42-3.31)	0.96 (0.94-1.22)	
Schedule C	0.96 (0.55-1.21)	0.86 (0.45-1.49)	0.81 (0.62-1.34)	0.84 (0.83-0.85)	1.02 (0.87-1.20)

Table 6.3. Combination experiments in the OVCAR-3 ovarian cancer cell line. Data are presented as the median CI value and the range represents the 95% confidence interval.

	Taxol	Gemza	SN38	Cisplatin	5-FU
Schedule A	0.89 (0.63-0.99)	1.13 (0.69-1.91)	1.08 (1.51-0.77)	1.09 (0.96-1.19)	0.99 (0.89-1.22)
Schedule B	1.06 (0.63-1.55)	1.31 (0.60-7.22)	0.95 (0.94-0.97)	0.84 (0.72-1.10)	
Schedule C	1.19 (0.87-1.38)	1.21 (1.11-1.44)	1.38 (1.07-1.99)	0.79 (0.74-0.85)	1.32 (1.22-1.55)

Table 6.4. Combinations of pyriplatin and taxol in HT-29, OVCAR-3, HOP 62 and MCF-7 cells.

	HT-29	OVCAR-3	HOP 62	MCF-7
Schedule B	0.88 (0.69-1.22)	1.06 (0.63-1.55)	1.30 (1.08-1.49)	1.43 (1.23-1.49)
Schedule C	0.96 (0.55-1.21)	1.19 (0.87-1.38)	1.42 (1.38-1.58)	0.97 (0.83-1.35)

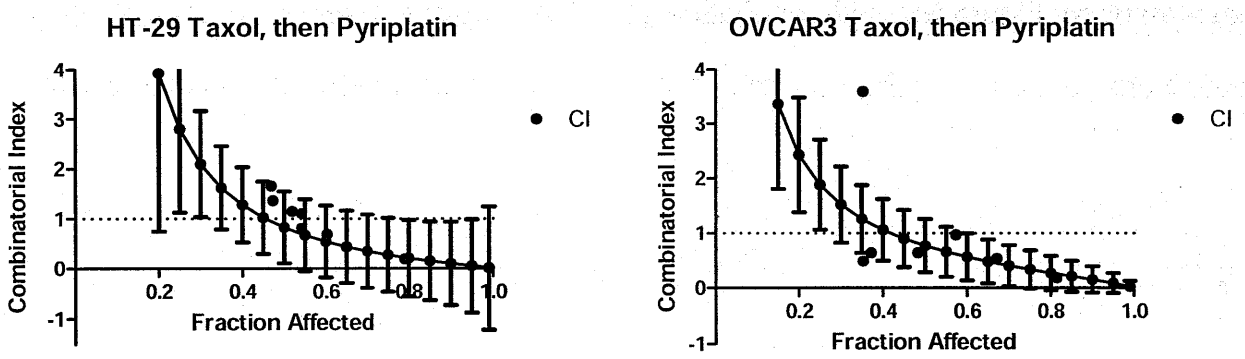

Figure 6.7. Combination data for taxol/pyriplatin in HT-29 and OVCAR-3 on schedule B.

Mechanistic Results

Mechanistic Study: Antiproliferative Effects of Pyriplatin and p53 Status

Cells of the HCT-116 colon cancer cell line were obtained from the Mario Negri Institute for studying the effect of p53 status on pyriplatin cytotoxicity. The p53 status of HCT-116 is wild-type. HCT-116 cells with disrupted p53, a cell line termed E6, were produced by stable transfection of HCT-116 with the human papillomavirus type 16 *E6* gene. As a control, HCT-116 cells transfected with an empty plasmid, termed pcDNA, were included in the study.

Antiproliferative effects of pyriplatin were evaluated by MTT after 24 h treatment with the drug, followed by a 48 h incubation period in drug-free medium. Figure 6.8 reports the results of three experiments, each performed in triplicate.

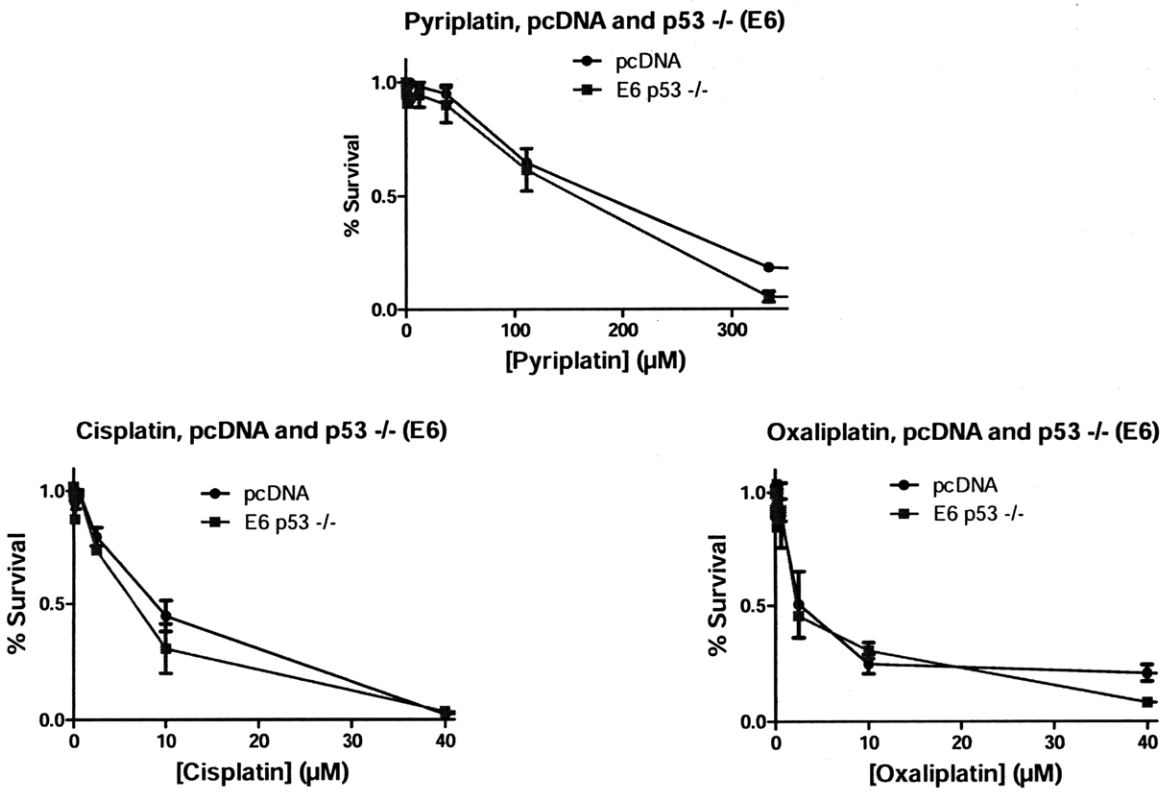

Figure 6.8. Effect of p53 status on pyriplatin, cisplatin and oxaliplatin antiproliferative effects.

Mechanistic Study: Antiproliferative Effects of Pyriplatin and MMR Pathway Status

Cells of the HCT-116 colon cancer cell line were obtained from the Mario Negri Institute for studying the interaction between the mismatch repair (MMR) pathway and pyriplatin cytotoxicity. HCT-116 has a homozygous mutation in the mismatch repair gene *hMLH1* on chromosome 3, which renders the MMR pathway inactive. The p53 status of HCT-116 is wild-type. A cell line with an active MMR pathway, HCT-116 + ch3, was obtained after insertion of a single copy of chromosome 3. HCT-116 cells proficient in MMR and with disrupted p53, a cell line termed N8, were produced by stable transfection of HCT-116+ch3 with the human papillomavirus type 16 *E6* gene. As a control, HCT-116 cells transfected with an empty plasmid, termed pcDNA, were included in the study.

Antiproliferative effects of pyriplatin were evaluated by MTT after 24 h treatment with the drug, followed by a 48 h incubation period in drug-free medium. Figure 6.9 reports the results of three experiments, each performed in triplicate.

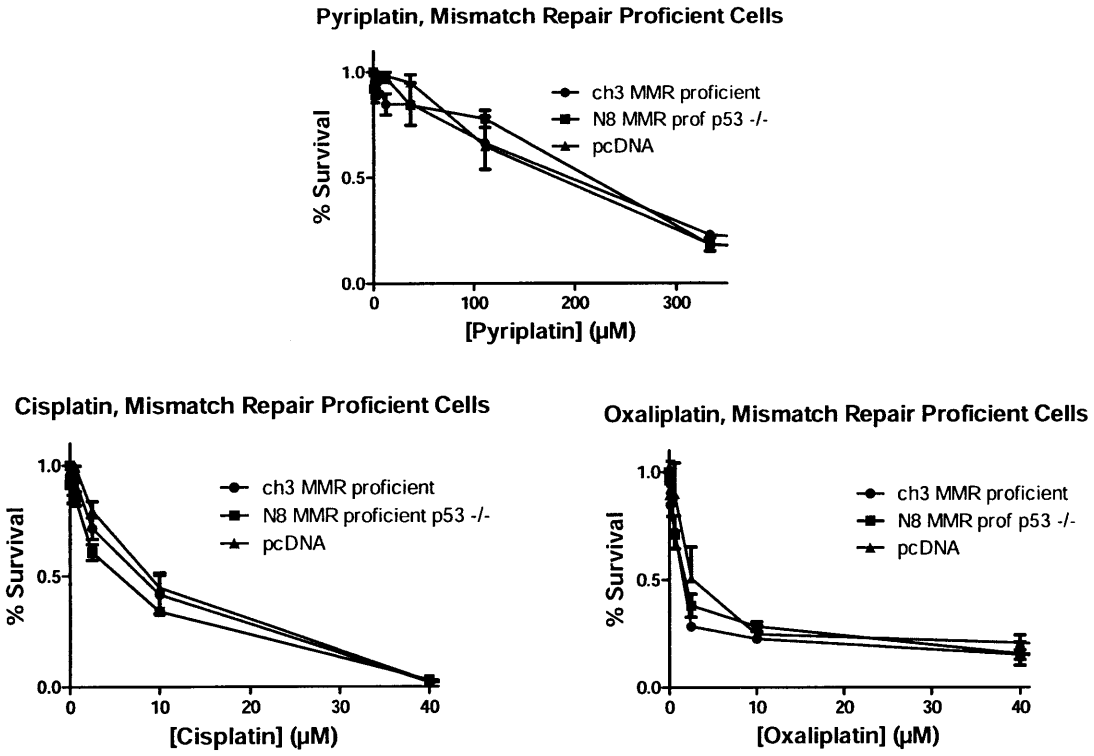

Figure 6.9. Effect of MMR pathway status on antiproliferative effects of pyriplatin, cisplatin and oxaliplatin.

Mechanistic Study: Apoptosis Induction by Pyriplatin and Cisplatin

The induction of apoptosis was detected by treating MCF-7 cells at the IC_{50} and $2*IC_{50}$ (cisplatin) or at the IC_{50} and $½*IC_{50}$ (pyriplatin) for 24 h. Cells were stained with FITC-conjugated Annexin V for apoptosis detection, propidium iodide to detect necrosis, and analyzed by flow cytometry. Annexin V binds to phosphatidylserine, which is present in the cell membrane of apoptotic cells. As shown in Figure 6.10, A higher percentage of cells treated with pyriplatin undergo apoptosis after 24 h as compared with cells treated with cisplatin at an equitoxic dose.

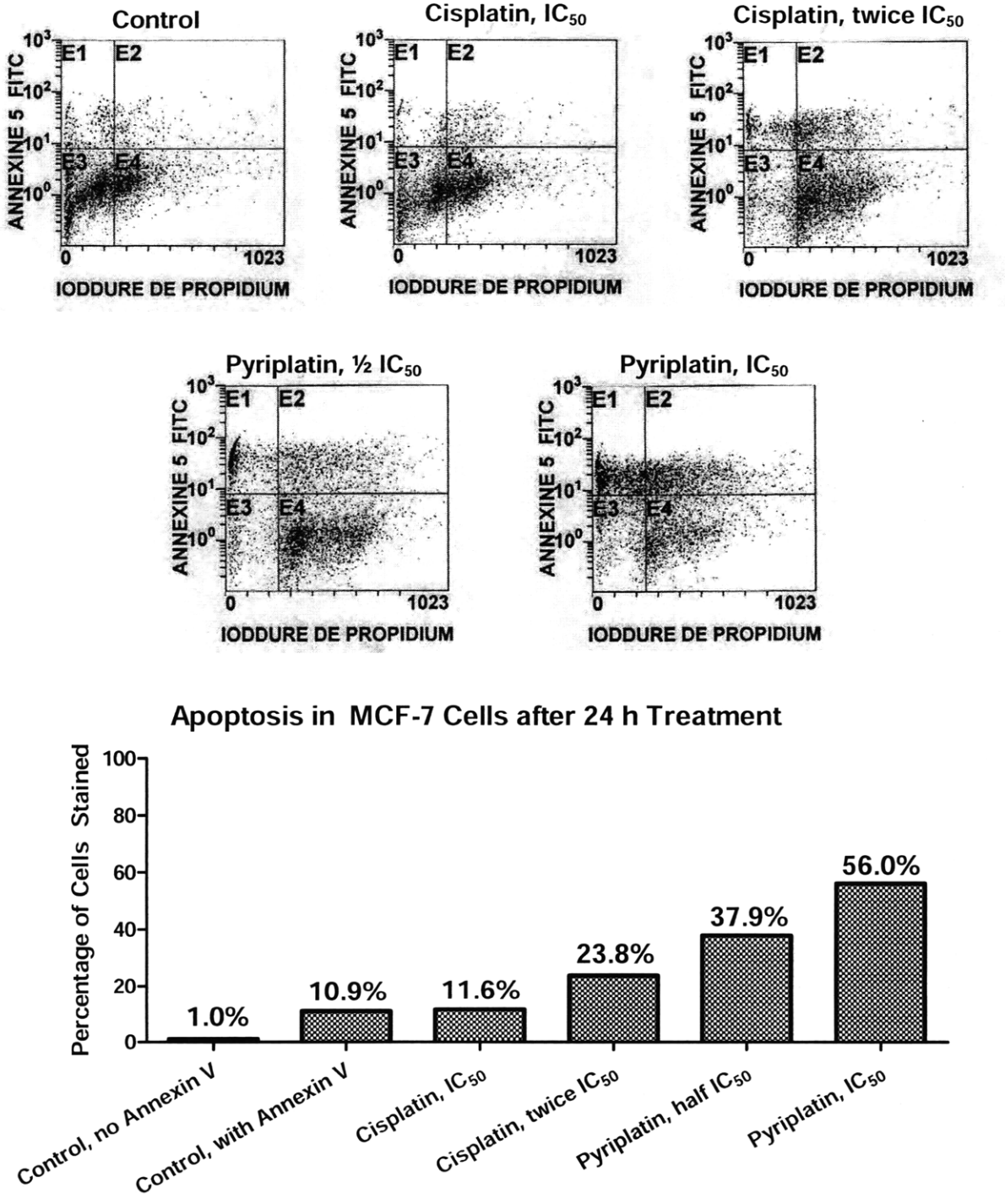

Figure 6.10. Top: Scatter plots of flow cytometry data for cells treated with cisplatin or pyriplatin. Bottom: Plot of all cells detected that were stained with Annexin V after treatment with cisplatin or pyriplatin.

Mechanistic Study: Determination of Factors Predictive of Sensitivity to Pyriplatin

The mRNA expression levels of 21 genes (Table 6.5) in the panel of 10 cell lines were measured by RT-PCR. Levels of gene expression were plotted versus IC_{50} values (Figure 6.11) in order to identify genes that were particularly well-correlated with either resistance or sensitivity to pyriplatin. Cells with high levels of RAD50 mRNA are more resistant to pyriplatin ($r^2 = 0.35$), suggesting that double-strand breaks may play a role in the cellular consequences of pyriplatin-DNA lesions. Cells with high levels of mRNA coding for GSTP1 are also more resistant to pyriplatin ($r^2 = 0.38$), indicating possible cellular inactivation of pyriplatin by modification with glutathione.

Table 6.5. Genes analyzed for correlation of mRNA levels with IC_{50} values.

Gene	Area/Pathway of Interest
ERCC1	Nucleotide Excision Repair
XPA	
XPC	
PARP1	Base Excision Repair
XRCC1	
RAD50	Homologous Recombination
BRCA1	
DNA-PK-cs	Non-homologous end-joining (NHEJ)
XRCC6 (ku70)	
MSH2	Mismatch Repair
MLH1	
BCL2	Apoptosis
PUMA	
COX2	
Ki67	Cell Growth
CDKN1A (p21)	Cell Cycle Regulation
ABCB1	Influx/Export
ABCC1	
GSTP1	

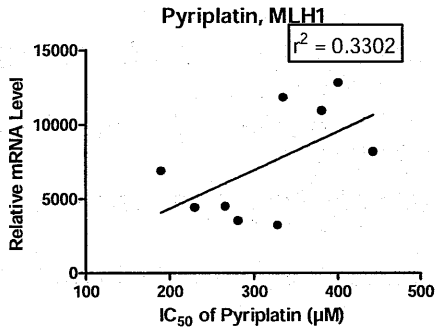
Pyriplatin, MLH1
r² = 0.3302
Relative mRNA Level
15000
10000
5000
0
100
200
300
400
500
IC50 of Pyriplatin (μM)

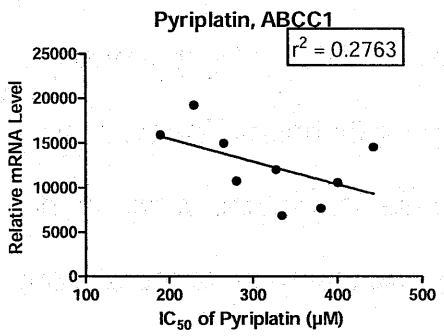
Pyriplatin, ABCC1
r² = 0.2763
Relative mRNA Level
25000
20000
15000
10000
5000
0
100
200
300
400
500
IC50 of Pyriplatin (μM)

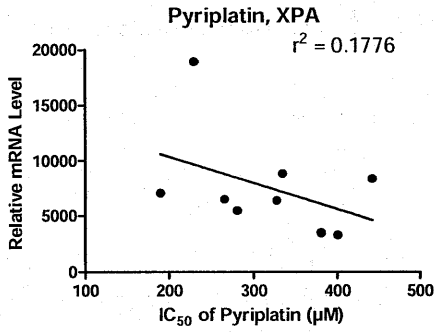
Pyriplatin, XPA
r² = 0.1776
Relative mRNA Level
20000
15000
10000
5000
0
100
200
300
400
500
IC50 of Pyriplatin (μM)

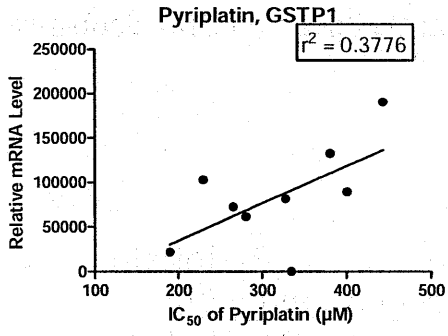
Pyriplatin, GSTP1
r² = 0.3776
Relative mRNA Level
250000
200000
150000
100000
50000
0
100
200
300
400
500
IC50 of Pyriplatin (μM)

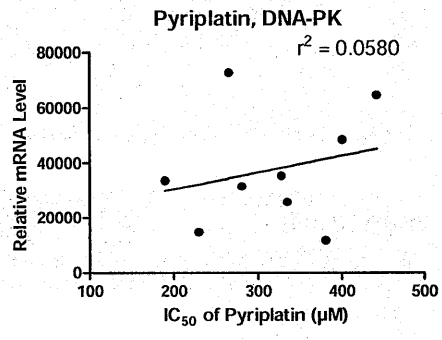
Pyriplatin, DNA-PK
r² = 0.0580
Relative mRNA Level
80000
60000
40000
20000
0
100
200
300
400
500
IC50 of Pyriplatin (μM)

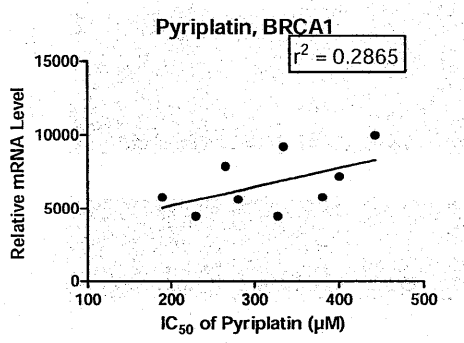
Pyriplatin, BRCA1
r² = 0.2865
Relative mRNA Level
15000
10000
5000
0
100
200
300
400
500
IC50 of Pyriplatin (μM)

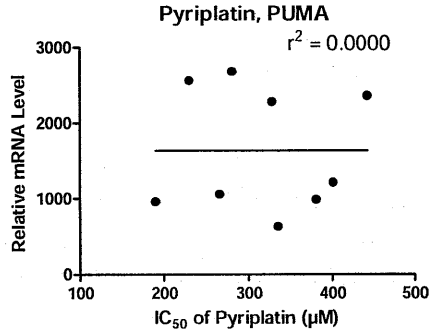
Pyriplatin, PUMA
r² = 0.0000
Relative mRNA Level
3000
2000
1000
0
100
200
300
400
500
IC50 of Pyriplatin (μM)

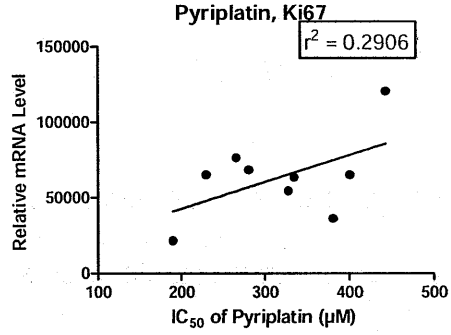
Pyriplatin, Ki67
r² = 0.2906
Relative mRNA Level
150000
100000
50000
0
100
200
300
400
500
IC50 of Pyriplatin (μM)

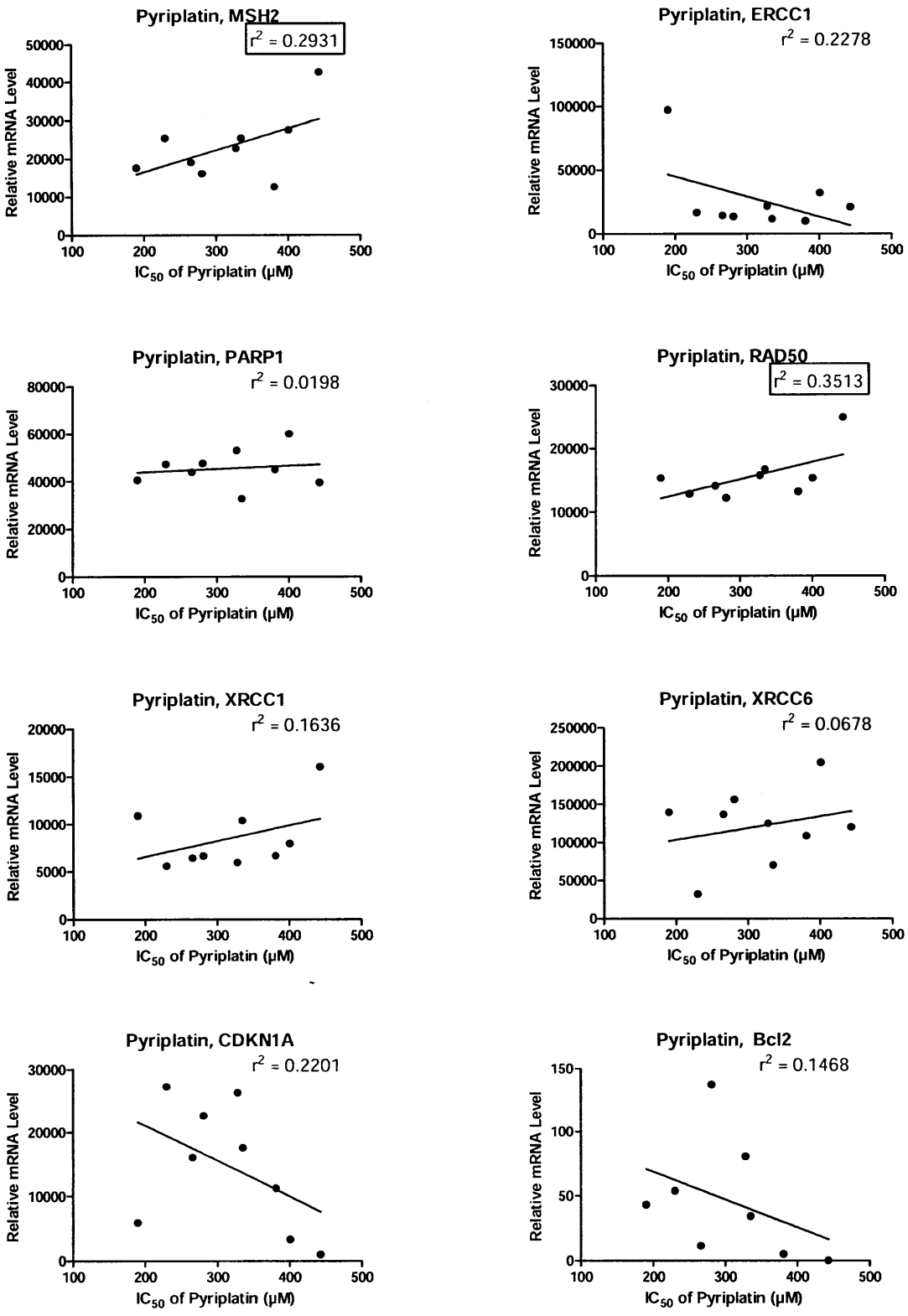

Figure 6.11. Correlation of pyriplatin IC_{50} values and expression levels of genes of interest.

Mechanistic Study: Evaluation of protein markers of apoptosis in HOP 62 cells

Western blots were performed by Shahin Emami at Saint-Antoine to determine the effect of pyriplatin treatment on Chk2 and gamma-H2AX phosphorylation. HOP 62 cells were treated at the IC_{50} values of each drug for 24 hours. The platinum-containing medium was then removed and protein content was determined 0, 24, 48, or 72 hours following removal of the platinum. Figure 6.12 shows the appearance of a band at 25 kDa for cisplatin, oxaliplatin and pyriplatin, which corresponds to the phosphorylated form of γ-H2AX, indicating the induction of apoptosis based on DNA double-strand break formation.

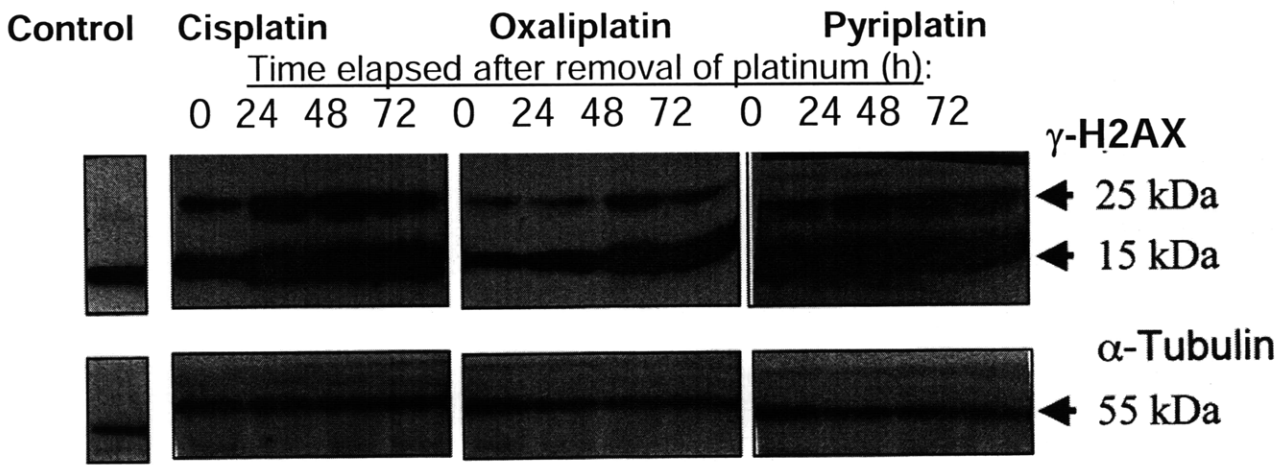

Figure 6.12. Level of γ-H2AX after 24 h treatment at the IC_{50} values with platinum followed by incubation in drug-free medium for 0, 24, 48, or 72 h. The α-tubulin blot is used as a loading control.

Discussion

The antitumor effects of pyriplatin in the 10-cell line panel are significantly different from the effects seen for cisplatin or oxaliplatin. The cytotoxic effects of pyriplatin can be measured after 1 h of incubation with the drug and the potency

increases as the incubation time is increased to 72 h, indicating that pyriplatin or some cytotoxic biological modification of pyriplatin remains potent for extended periods of time in cell medium.

The cell cycle effects of pyriplatin are distinct from those of either cisplatin or oxaliplatin. Pyriplatin does not appear to exert cytotoxic effects by blocking cells in S/G_2 phase, as was observed for cisplatin. Pyriplatin causes a significant, early induction of sub-G_0, or apoptotic, cells that is not seen with either oxaliplatin or cisplatin. This result was confirmed by Annexin V staining and also by western blot for detection of DNA double-strand breaks by measurement of γ-H2AX phosphorylation. Results obtained by RT-PCR to detect mRNA levels of RAD50 suggest that some of the DNA double-strand breaks may be directly due to DNA damage caused by pyriplatin, rather than apoptosis-induced fragmentation of the DNA. Cells with high levels of RAD50 mRNA are more resistant to cisplatin, a result that is being pursued by analysis of pyriplatin-treated cells using the Comet assay.

The effects of treating cells with pyriplatin in combination with other known anticancer drugs have been investigated for four known drugs and three different treatment schedules. The treatment of cells with pyriplatin and cisplatin simultaneously seems to produce a synergistic effect, although these are only preliminary results. Additionally, preliminary results indicate that the treatment of cells with taxol followed by pyriplatin may produce synergistic effects.

Conclusions

Pyriplatin has a unique cytotoxicity profile that is distinct from that of either the platinum dach class of compounds or cisplatin. The distinct profile may suggest a significantly different mechanism of action than either oxaliplatin or cisplatin. Pyriplatin is about 10-fold less potent than either cisplatin or oxaliplatin and shows synergy in combination with taxol or cisplatin in vitro.

Materials and Methods

Cell Lines and Reagents

Colorectal cancer cell lines HT-29, HCT-116, HCC2998, and COLO 205, breast cancer line MCF-7, melanoma line MDA-435, ovarian cancer lines OVCAR-3 and IGROV-1, and non-small cell lung cancer line HOP-92 and HOP-62 were obtained from the American Type Culture Collection (Rockville, MD, USA) and maintained in RPMI medium supplemented with 10% fetal bovine serum. The p53 (-/-) cell lines and MMR proficient cell lines had previously been derived from HCT-116 cells as described[9,10] and were provided by Massimo Broggini of the Mario Negri Institute, Milan. The HCT116-pcDNA, HCT116-ch3, HCT116-E6, and HCT-116-N8 cell lines were maintained in medium supplemented with the antibiotics G418 (Sigma) or G418 and Hygromycin B (HCT116-N8 only, Sigma). All cell lines were regularly tested for mycoplasma contamination by PCR using a Stratagene kit (La Jolla, CA, USA). Cisplatin and oxaliplatin were obtained from the Beaujon University Hospital Pharmacy.

In vitro growth inhibition assays

Cells were plated in 96-well plates at 2 x 10^3 cells per well. Twenty-four hours after plating, the medium was replaced with platinum-containing medium. Cells were incubated with platinum for 24 h, or as indicated in the text. After the 24 h incubation with drug, wells were washed with RPMI and cells were incubated in serum-containing medium for 72 h. Cell viability was determined either by detection of mitochondrial cleavage of the tetrazolium ring of MTT (3-(4,5-dimethylthiazol-2-yl)-2,5-diphenyl tetrazolium bromide) by absorption at 562 nm as described[11] or by detection of sulforhodamine B as described.[12]

Cell Cycle Analysis

Analysis of cell cycle effects of pyriplatin were evaluated after incubation of HOP-62 cells with either pyriplatin, cisplatin, or oxaliplatin at the IC_{50} values (Table 6.1) for 24 h. Immediately after the 24 h incubation, cells were collected, stained with propidium iodide and analyzed by flow cytometry as described.[13]

RT-PCR

Total RNA was extracted from all cell lines at the same passage used for the cytotoxicity studies. The Trizol reagent (Invitrogen), composed of guanidinium thiocyanate, phenol, chloroform, and isoamyl alcohol, was used to facilitate the extraction. RT-PCR was performed as described[14,15] by Ivan Bieche and coworkers to detect mRNA for the genes listed in Table 6.5.

References

(1) R. H. Shoemaker (2006). The NCI60 human tumour cell line anticancer drug screen. *Nat. Rev. Cancer*, **6**, 813-823.

(2) O. Rixe, W. Ortuzar, M. Alvarez, R. Parker, E. Reed, K. Paull and T. Fojo (1996). Oxaliplatin, tetraplatin, cisplatin, and carboplatin: spectrum of activity in drug-resistant cell lines and in the cell lines of the National Cancer Institute's Anticancer Drug Screen panel. *Biochem. Pharmacol.*, **52**, 1855-1865.

(3) J. D. Roberts, J. Peroutka and N. Farrell (1999). Cellular pharmacology of polynuclear platinum anti-cancer agents. *J. Inorg. Biochem.*, **77**, 51-57.

(4) N. Farrell, Y. Qu, U. Bierbach, M. Valsecchi and E. Menta (1999). Structure-activity relationships within di- and trinuclear platinum phase-I clinical anticancer agents. *Cisplatin*, 479-496.

(5) L. S. Hollis, A. R. Amundsen and E. W. Stern (1989). Chemical and biological properties of a new series of cis-diammineplatinum(II) antitumor agents containing three nitrogen donors: cis-[Pt(NH3)2(N-donor) Cl]+. *J. Med. Chem.*, **32**, 128-136.

(6) K. S. Lovejoy, R. C. Todd, S. Zhang, M. S. McCormick, J. A. D'Aquino, J. T. Reardon, A. Sancar, K. M. Giacomini and S. J. Lippard (2008). cis-diammine(pyridine)chloroplatinum(II), a monofunctional platinum(II) antitumor agent: uptake, structure, function, and prospects. *Proc. Natl. Acad. Sci. U. S. A.*, **105**, 8902-8907.

(7) P. Kabolizadeh, J. Ryan and N. Farrell (2007). Differences in the cellular response and signaling pathways of cisplatin and BBR3464 ([[trans-PtCl(NH3)(2)]2mu-(trans-Pt(NH3)(2)(H2N(CH2)(6)-NH2)2)]4+) influenced by copper homeostasis. *Biochem. Pharmacol.*, **73**, 1270-1279.

(8) T. C. Chou and P. Talalay (1984). Quantitative analysis of dose-effect relationships: the combined effects of multiple drugs or enzyme inhibitors. *Adv. Enzyme Regul.*, **22**, 27-55.

(9) G. Colella, S. Marchini, M. D'Incalci, R. Brown and M. Broggini (1999). Mismatch repair deficiency is associated with resistance to DNA minor groove alkylating agents. *Br. J. Cancer*, **80**, 338-343.

(10) F. Vikhanskaya, G. Colella, M. Valenti, S. Parodi, M. D'Incalci and M. Broggini (1999). Cooperation between p53 and hMLH1 in a human colocarcinoma cell line in response to DNA damage. *Clin. Cancer Res.*, **5**, 937-941.

(11) M. C. Alley, D. A. Scudiero, A. Monks, M. L. Hursey, M. J. Czerwinski, D. L. Fine, B. J. Abbott, J. G. Mayo, R. H. Shoemaker and M. R. Boyd (1988). Feasibility of drug screening with panels of human tumor cell lines using a microculture tetrazolium assay. *Cancer Res.*, **48**, 589-601.

(12) V. Vichai and K. Kirtikara (2006). Sulforhodamine B colorimetric assay for cytotoxicity screening. *Nature Protocols*, **1**, 1112-1116.

(13) M. Serova, F. Calvo, F. Lokiec, F. Koeppel, V. Poindessous, A. K. Larsen, E. S. Van Laar, S. J. Waters, E. Cvitkovic and E. Raymond (2006). Characterizations of irofulven cytotoxicity in combination with cisplatin and oxaliplatin in human colon, breast, and ovarian cancer cells. *Cancer Chemother. Pharmacol.*, **57**, 491-499.

(14) I. Bieche, B. Parfait, S. Tozlu, R. Lidereau and M. Vidaud (2001). Quantitation of androgen receptor gene expression in sporadic breast tumors by real-time RT-PCR: evidence that MYC is an AR-regulated gene. *Carcinogenesis*, **22**, 1521-1526.
(15) N. Aissat, C. Le Tourneau, A. Ghoul, M. Serova, I. Bieche, F. Lokiec, E. Raymond and S. Faivre (2008). Antiproliferative effects of rapamycin as a single agent and in combination with carboplatin and paclitaxel in head and neck cancer cell lines. *Cancer Chemother. Pharmacol.*, **62**, 305-313.

Chapter 7

Preclinical Evaluation of the Antitumor Properties of Mitaplatin, a Novel Platinum-based Drug

Introduction

Cancer cells have consistently higher rates of glycolysis than normal cells, a property first identified by Warburg,[1] and the glycolytic phenotype has been associated with suppression of mitochondrial function.[2] This difference between solid tumor cells and cells in healthy tissue offers an appealing target for the design of anticancer drugs, because of the wide therapeutic window potentially available for a drug that targets only cells metabolizing glucose by aerobic glycolysis. If the glycolytic phenotype in affected tumor cells could be reversed, changes in the mitochondria that suppress apoptosis, or programmed cell death, would probably also be reversed. Such a drug would switch on apoptosis in cancer cells, a valuable characteristic for an antitumor agent. The design of such a compound was not previously pursued with much interest because the activation of aerobic glycolosis in many cancers was thought to be a result of cancer and not a cause. Furthermore, it was unknown whether reliance on glycolosis for energy production could be reversed in cancer cells.[3] The connection between the metabolic change in cancer cells and suppression of apoptosis[4] and evidence that apoptosis could be increased by a small molecule kinase inhibitor[5] have recently greatly energized the search for anticancer therapies that exploit the Warburg effect.

The apoptosis resistance that characterizes many human cancers is regulated by hyperpolarization of the mitochondrial membrane and downregulation of the K^+ channel Kv1.5.[3] Dichloroacetate is an existing generic drug that is a small-molecule inhibitor of PDK1, a protein kinase that inactivates pyruvate dehydrogenase (PDH), a mitochondrial enzyme, by phosphorylating its E1 subunit.[6] PDH plays the role of gatekeeper in the

metabolism of glucose by determining whether glucose will undergo glycolysis in the cytoplasm or glucose oxidation in mitochondria.

DCA increases the level of pyruvate in the mitochondria, thereby promoting glucose oxidation and increasing apoptosis in the tumor.[2] The antitumor effect has been proven in rats,[3] and a long-term clinical trial of oral DCA in children with lactic acidosis suggests that DCA will be safe at the doses required for treatment of cancer.[4]

The Lippard lab has modified of cisplatin with two molecules of DCA via a synthetically facile, rapid, high-yielding method.[7] The aim of the work described here has been to characterize this compound, mitaplatin, in vitro and to compare its antitumor properties to those of cisplatin and oxaliplatin. Mitaplatin has the potential for anticancer activity by acting through two distinct pathways. Upon exposure to a reducing agent, mitaplatin is transformed into one molecule of cisplatin plus two molecules of DCA (Scheme 7.1). Cisplatin is a widely used, clinically effective platinum(II) anticancer drug that derives its anticancer activity by forming DNA-platinum adducts and triggering cellular responses to the DNA damage. The anticancer activity of

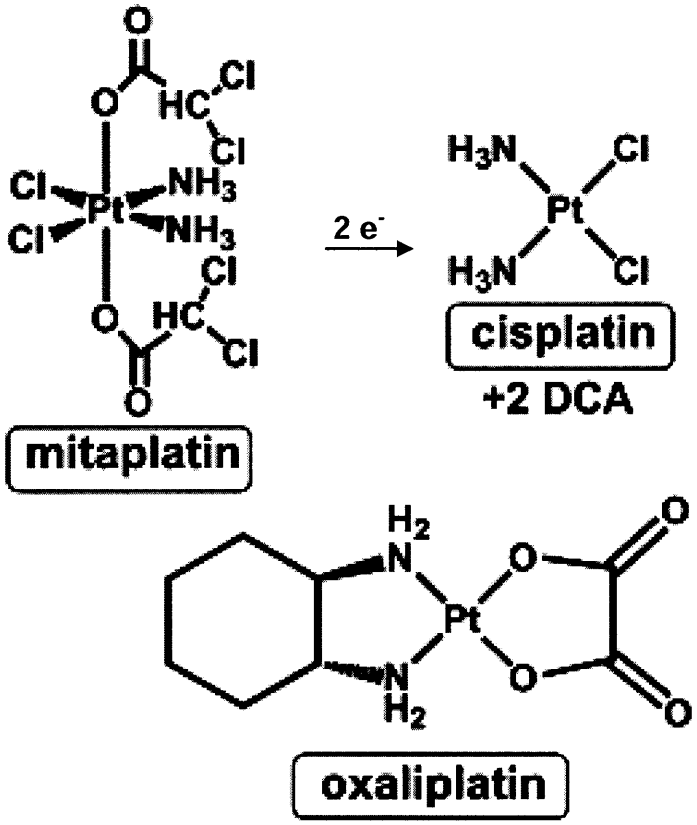

Scheme 7.1. Mitaplatin, cisplatin and oxaliplatin.

DCA is based on its activity in the mitochondrial of cancerous, but not healthy cells, as described above.

Results

Single-Agent Study: Antiproliferative effects of mitaplatin given as a single agent in a panel of human cancer cell lines.

A panel of 10 cancer cell lines of different origins was exposed to mitaplatin for 24 h and then assessed for cytotoxicity by the MTT assay. Simultaneous assays were performed in the same manner in the 10 cell lines with cisplatin and oxaliplatin. Table 7.1 represents the concentrations required to achieve 50% growth inhibition (IC_{50}) in our panel of cancer cell lines and the standard deviation for at least three experiments, each done in triplicate. A comparison of cytotoxicity between the three drugs is represented in Figure 7.1. Figure 7.2 represents the IC_{50} values in each of the 10 cell lines and Figure 7.3 shows cell survival for the different cell lines at concentrations ranging from 0.1-160 μM of cisplatin (7.3A), oxaliplatin (7.3B), and mitaplatin (7.3C).

Mitaplatin had a cytotoxicity profile similar to that of cisplatin in all cell lines (Figures 7.1 and 7.2). The mitochondrial effects of mitaplatin were not apparent in the cytotoxicity profile generated by comparision of IC50 values (Figure 7.1). Mitaplatin was at least as potent as cisplatin and oxaliplatin. It is likely that more DCA per molecule is needed for effect of the mitochondrial activity of the drug to be manifest in IC_{50} values.

Cell Line	Cancer Type	IC_{50} Cisplatin	IC_{50} Oxaliplatin	IC_{50} Mitaplatin
HT-29	Colorectal	11.9 ± 4.1 μM	6.65 ± 1.0 μM	10.1 ± 4.1 μM
MDA-435	Breast /Melanoma	5.81 ± 4.0 μM	12.7 ± 5.6 μM	8.86 ± 4.2 μM
HCT-116	Colorectal	4.22 ± 2.5 μM	1.10 ± 0.28 μM	5.57 ± 3.4 μM
HCC2998	Colorectal	11.8 ± 4.0 μM	7.27 ± 2.3 μM	11.8 ± 4.8 μM
COLO205	Colorectal	16.7 ± 7.2 μM	2.84 ± 0.64 μM	26.0 ± 6.3 μM
MCF7	Breast	15.6 ± 6.4 μM	1.70 ± 0.54 μM	12.3 ± 6.0 μM
OVCAR3	Ovarian	5.10 ± 3.0 μM	1.24 ± 0.30 μM	5.67 ± 1.7 μM
IGROV1	Ovarian	5.64 ± 1.3 μM	8.08 ± 2.9 μM	6.03 ± 2.3 μM
HOP92	Non-Small Cell Lung	3.55 ± 3.2 μM	2.70 ± 0.60 μM	7.24 ± 4.1 μM
HOP62	Non-Small Cell Lung	3.56 ± 1.4 μM	6.86 ± 0.39 μM	2.74 ± 0.8 μM

Table 7.1. IC_{50} values for mitaplatin, cisplatin and oxaliplatin in the 10-cell line panel. Values represent the mean of three independent experiments, each performed in triplicate, and the standard deviation.

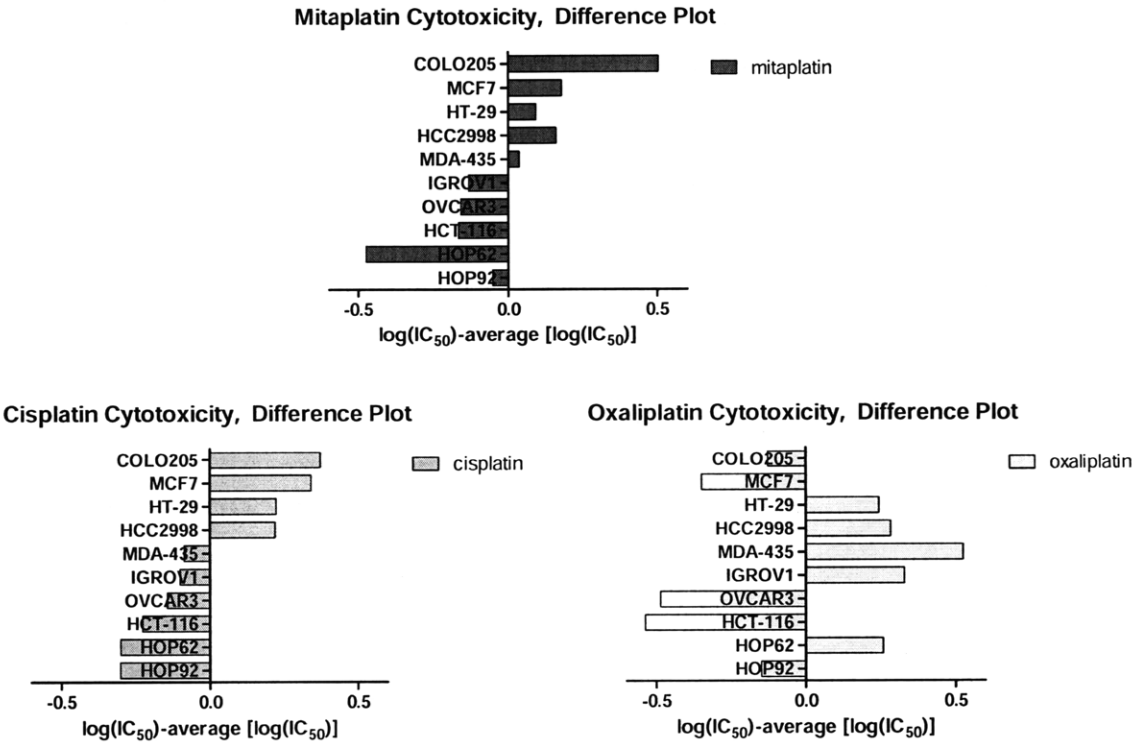

Figure 7.1. Mean graphs for IC_{50}. Bars depict the deviation of individual cell lines from the overall mean value for all the cells tested.

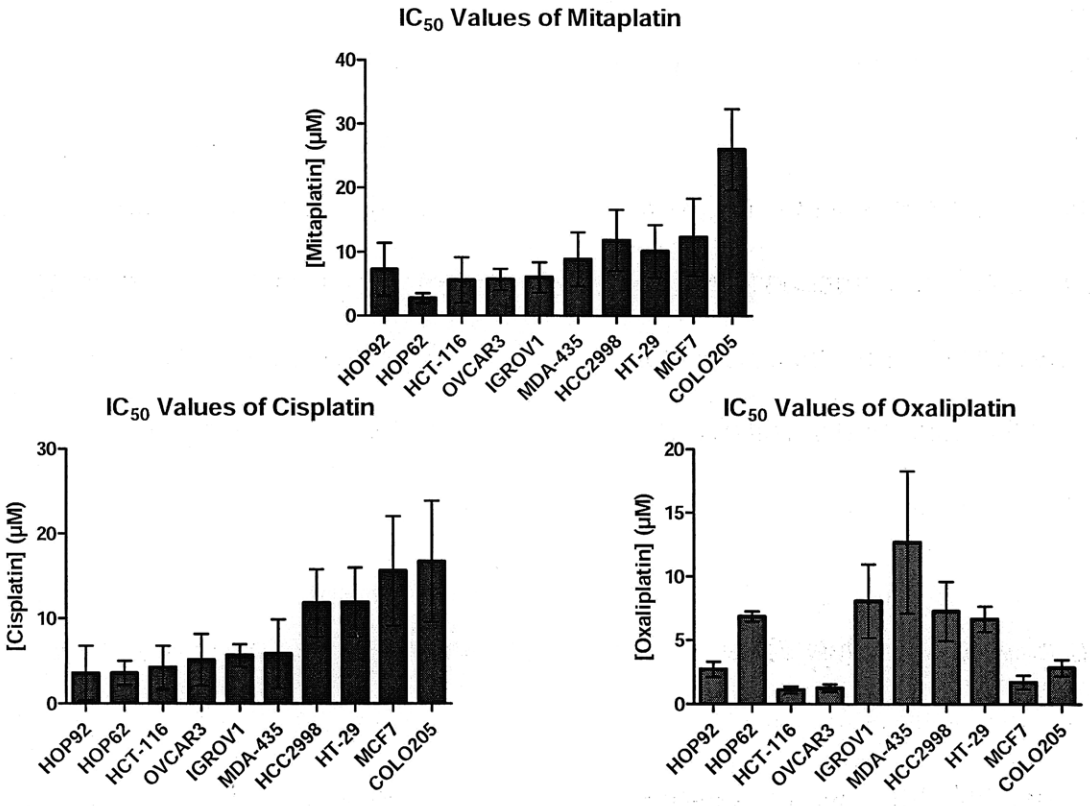

Figure 7.2. IC_{50} values of mitaplatin, cisplatin and oxaliplatin. Values represent the mean of three independent experiments, each performed in triplicate, and the standard deviation

7.3(A) Cisplatin

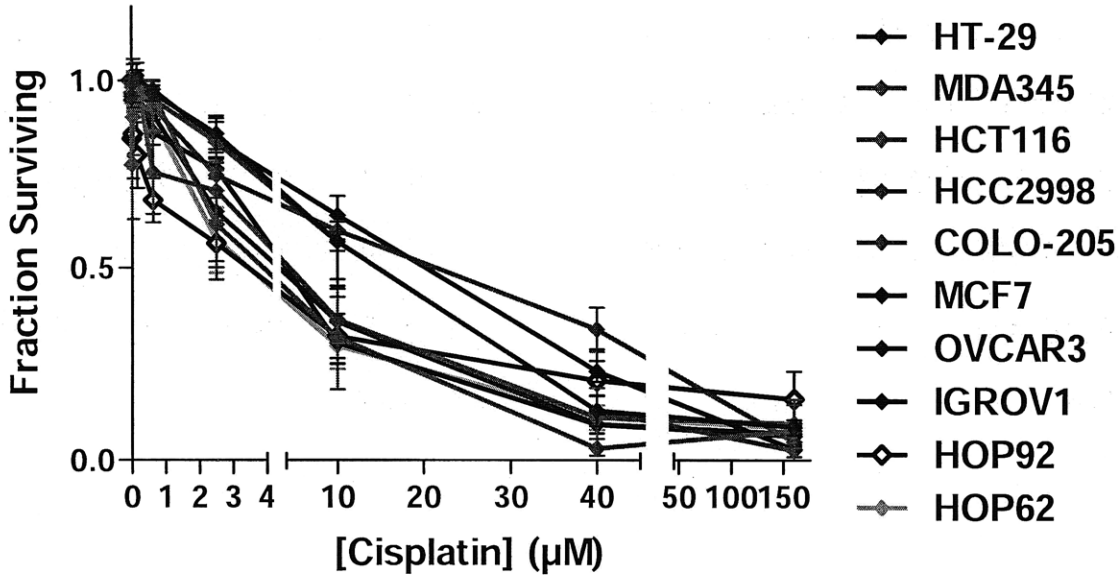

7.3(B) Oxaliplatin

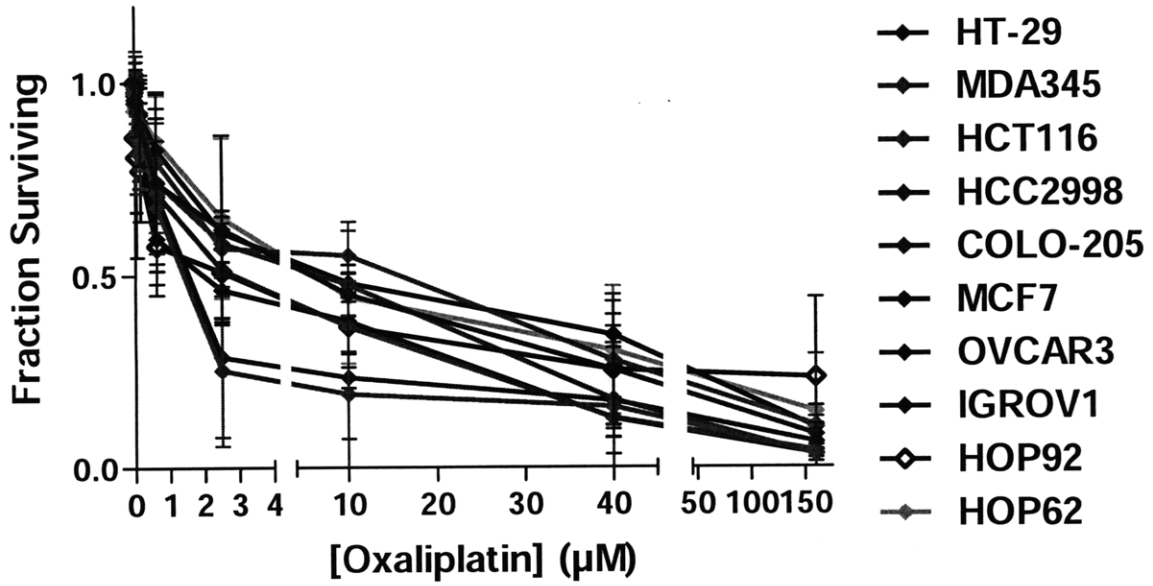

7.3(C) Mitaplatin.

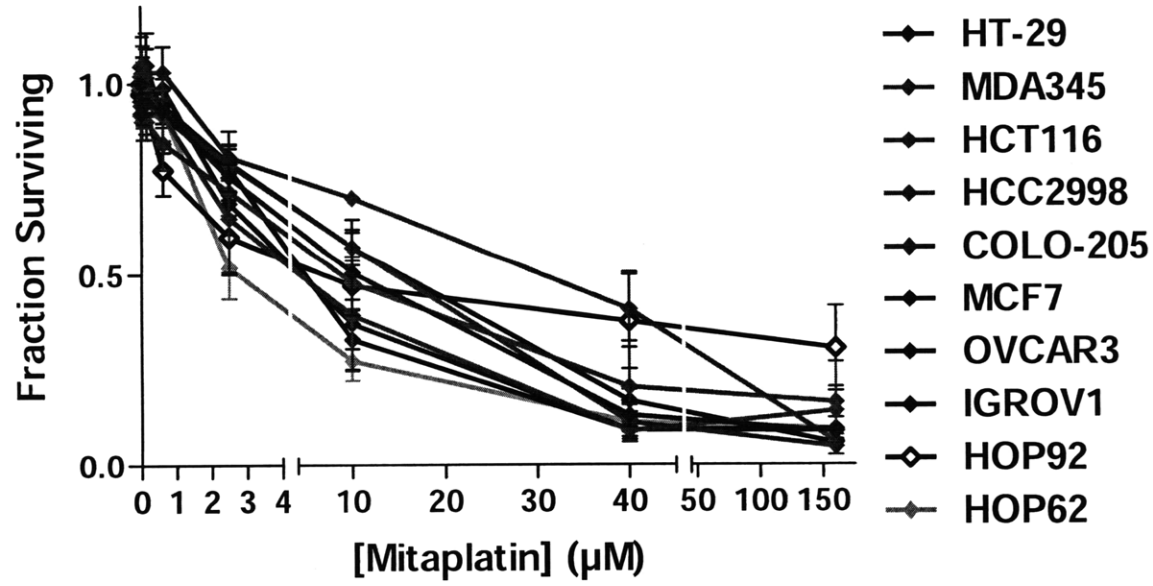

Figure 7.3. Cytotoxicity of cisplatin (A), oxaliplatin (B), and mitaplatin (C) in the studied cancer cell lines given for 24 h. Plots reflect the mean and standard deviation of results from three separate experiments, each performed in triplicate.

Single-Agent Study: NCI60 Single Dose and Five-Dose Study

Mitaplatin was submitted to the National Cancer Institute (USA) for single agent testing in 2008 by Shanta Dhar of the Lippard lab. The compound was tested in a panel of 60 cell lines at a single dose, 10^{-5} M as described.[8] Analysis by the online COMPARE algorithm on January 13, 2009 revealed that mitaplatin had a correlation score of 0.719 with cisplatin.

Single-Agent Study: Antiproliferative Effects of Mitaplatin Over Time

A non-small cell lung cancer cell line, HOP-62, was treated with mitaplatin, cisplatin, or oxaliplatin for 1, 2, 5, 24, 48, or 72 h. After the specified time, the plates were washed and the medium replaced with drug-free medium. The MTT assay was performed after 48 h of incubation in drug-free medium. Results in Figure 7.4 are reported as the mean IC_{50} plus and minus the standard deviation of at least three separate experiments performed in triplicate. The cytotoxic effects of mitaplatin increased over the entire time period tested, meaning cytotoxicity increased even up to 72 h, indicating that the compound or biological modifications thereof, retain some cytotoxic characteristics even after extended incubation in cell medium. Similar results were found for both cisplatin and oxaliplatin.

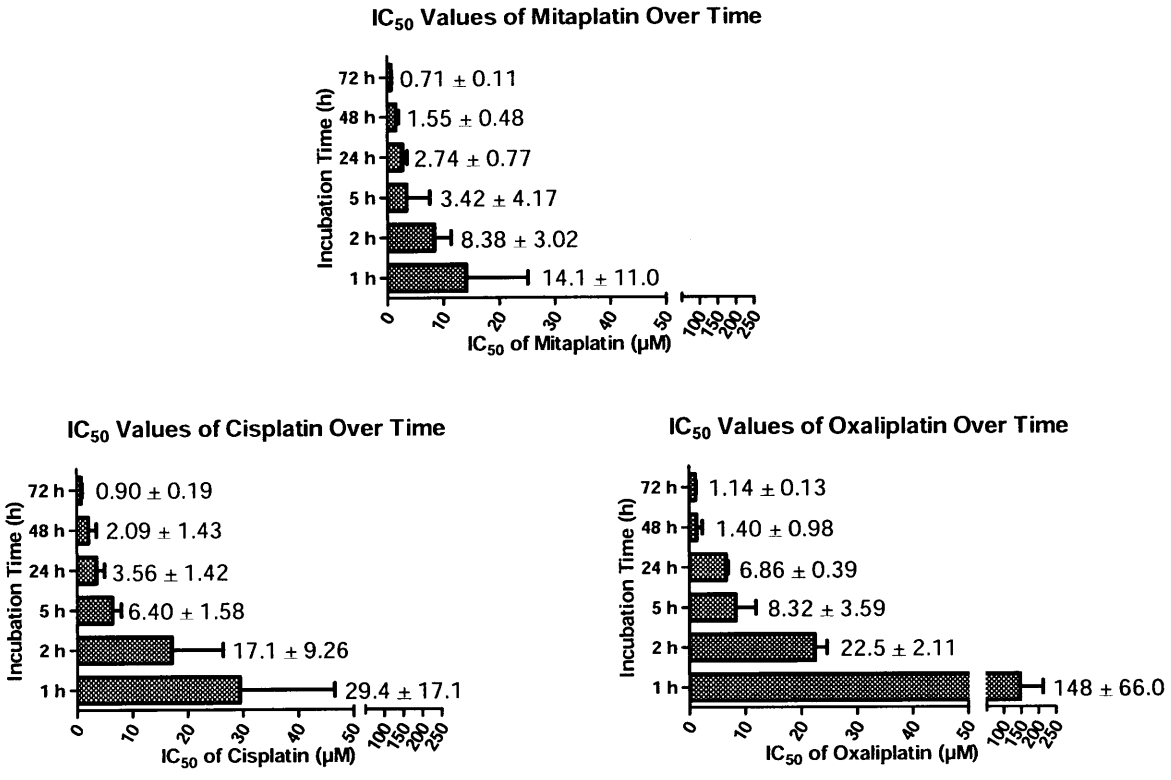

Figure 7.4. Antiproliferative effects of mitaplatin, cisplatin, and oxaliplatin over time.

Single-Agent Study: Antiproliferative Effects of Mitaplatin Evaluated by Cellular Protein Content and by Mitochondrial Activity

Two cell lines, the ovarian cancer line OVCAR-3 and the colon cancer line COLO 205, were used to compare the antiproliferative effects of mitaplatin on the basis of cellular protein content and mitochondrial activity. Cells were treated for 24 h with either mitaplatin or cisplatin, washed, and incubated for 48 h in drug-free medium. Proliferation was assayed by either the MTT assay, which measures mitochondrial activity, or by the SRB assay, which measures cellular protein content. Figure 7.5 shows the similarity of results obtained for either cisplatin or mitaplatin using either the protein content assay or the mitochondria-based tetrazolium assay. The results obtained using the two assays

are very similar. These results suggest that the mitochondrial effect of mitaplatin is not evident, at least at the time points, concentrations, and conditions studied. Additionally, the results reinforce the validity of the MTT assay for use in the evaluation of dose-dependent cell survival after treatment with cisplatin or mitaplatin.

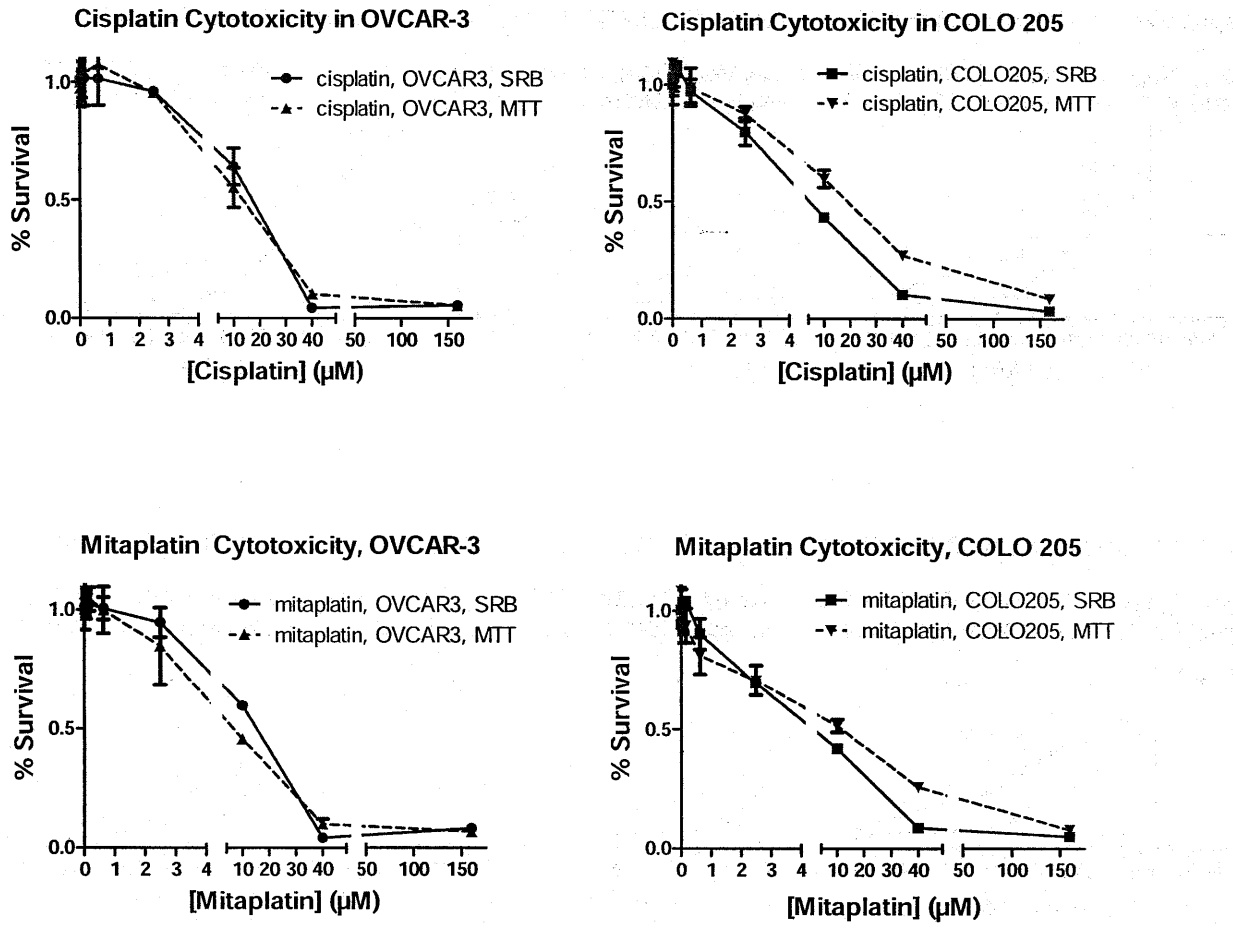

Figure 7.5. Comparison of results obtained by evaluation of protein content or mitochondrial activity for cisplatin (top) and mitaplatin (bottom) in OVCAR-3 (left) and COLO 205 (right).

Mechanism of Action

Mechanistic Study: Cell Cycle

Effects on the cell cycle due to administration of mitaplatin were examined after 24 h incubation with the platinum at the IC_{50} value in the MCF-7 breast cancer cell line. Cells were stained with propidium iodide and analyzed immediately by flow cytometry. As shown in Figure 7.6, both cisplatin and mitaplatin initiate accumulation of cells in the S phase, with the relative percentages of cells in each phase being nearly identical for both drugs.

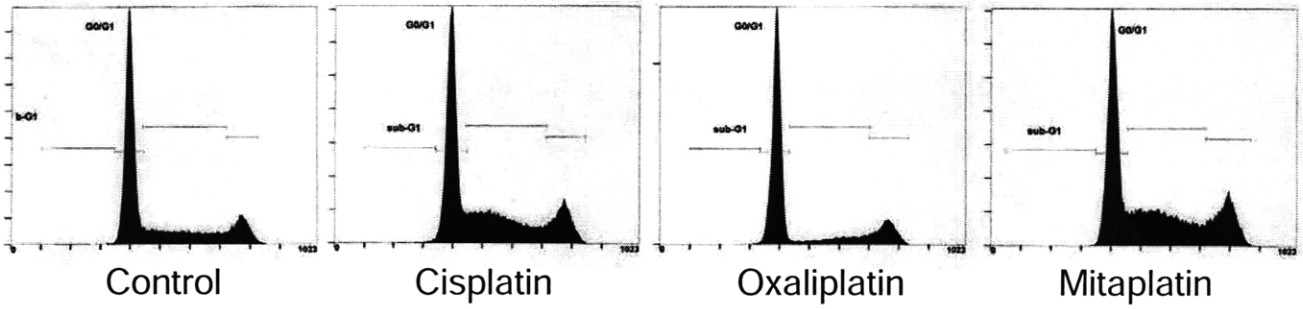

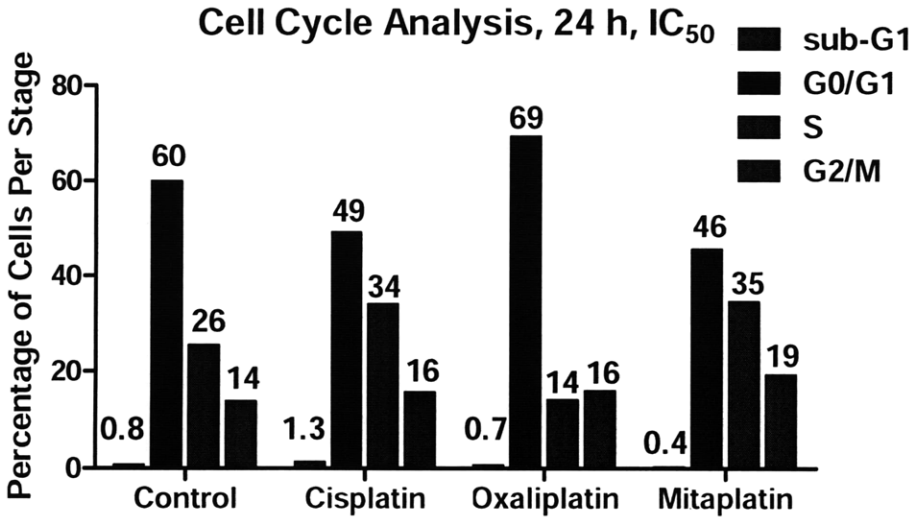

Figure 7.6. Analysis of the effects of platinum drugs on cell cycle progression in MCF-7 after treatment at the IC_{50} value for 24 h.

Mechanistic Study: Antiproliferative Effects of Mitaplatin and p53 Status

Cells of the HCT-116 colon cancer cell line were obtained from the Mario Negri Institute for studying the effect of p53 status on mitaplatin cytotoxicity. The p53 status of HCT-116 is wild-type. HCT-116 cells with disrupted p53, a cell line termed E6, were produced by stable transfection of HCT-116 with the human papillomavirus type 16 *E6* gene. As a control, HCT-116 cells transfected with an empty plasmid, termed pcDNA, were included in the study.

Antiproliferative effects of mitaplatin were evaluated by MTT after 24 h treatment with the drug, followed by a 48 h incubation period in drug-free medium. Figure 7.7 reports the results of three experiments, each performed in triplicate.

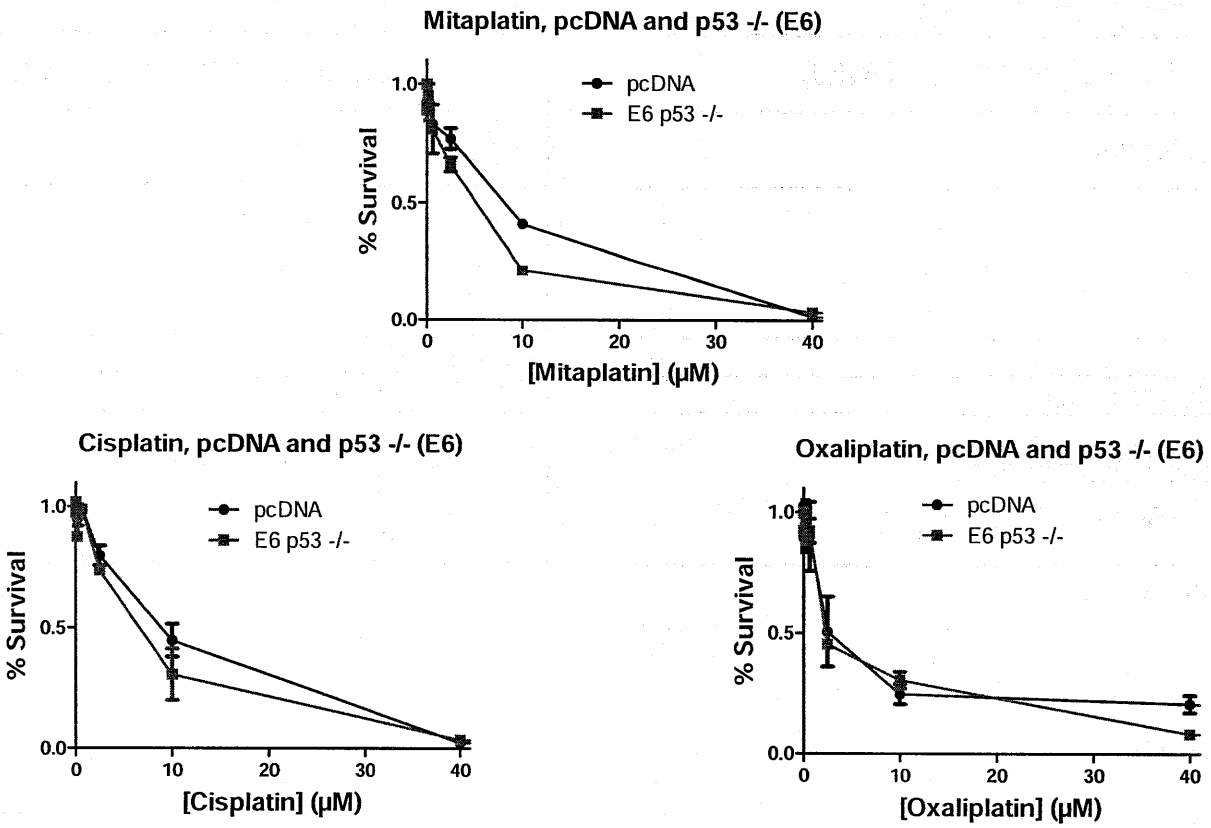

Figure 7.7. Effect of p53 status on mitaplatin, cisplatin and oxaliplatin antiproliferative effects.

Mechanistic Study: Antiproliferative Effects of Mitaplatin and MMR Pathway Status

Cells of the HCT-116 colon cancer cell line were obtained from the Mario Negri Institute for studying the interaction between the mismatch repair (MMR) pathway and mitaplatin cytotoxicity. HCT-116 has a homozygous mutation in the mismatch repair gene *hMLH1* on chromosome 3, which renders the MMR pathway inactive. The p53 status of HCT-116 is wild-type. A cell line with an active MMR pathway, HCT-116 + ch3, was obtained after insertion of a single copy of chromosome 3. HCT-116 cells proficient in MMR and with disrupted p53, a cell line termed N8, were produced by stable transfection of HCT-116+ch3 with the human papillomavirus type 16 *E6* gene. As a control, HCT-116 cells transfected with an empty plasmid, termed pcDNA, were included in the study. Cytotoxicity in these lines was evaluated by MTT after 24 h of drug treatment and 48 h of incubation in drug-free medium (Figure 7.8).

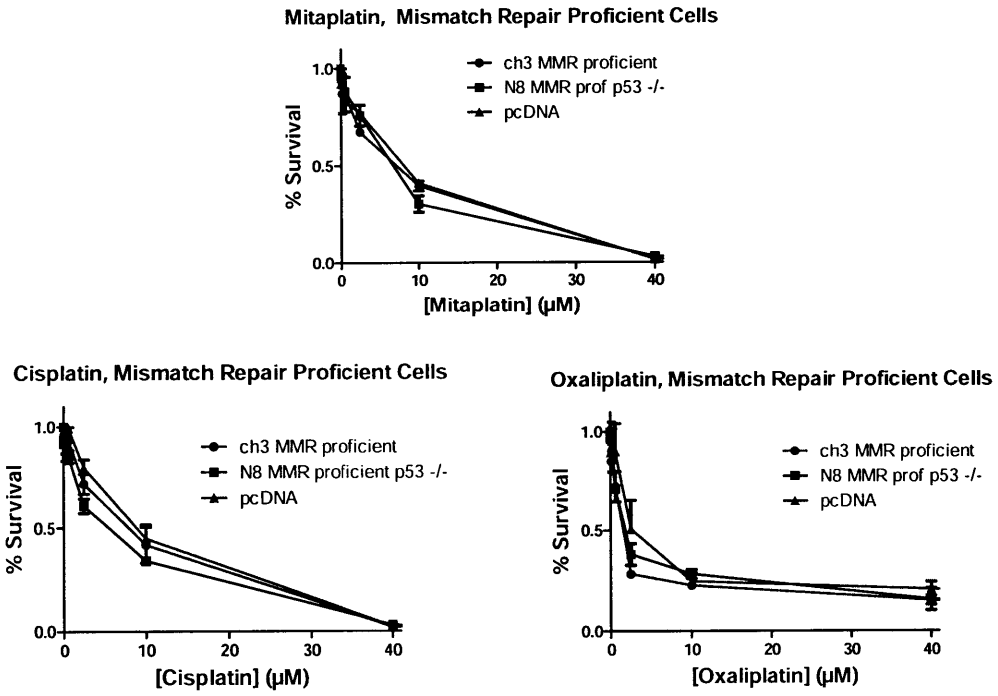

Figure 7.8. Effect of MMR pathway status on antiproliferative effects of mitaplatin, cisplatin and oxaliplatin. Results are the average of three experiments, each performed in triplicate.

Mechanistic Study: Determination of factors predictive of sensitivity to mitaplatin

We have analyzed the correlation of the mRNA levels of 19 genes (Table 7.2) with the IC_{50} values of mitaplatin (Figure 7.9).

Table 7.2. Genes analyzed for correlation of mRNA levels with IC_{50} values.

Gene	Area/Pathway of Interest
ERCC1	Nucleotide Excision Repair
XPA	
XPC (not shown, no correlation)	
PARP1	Base Excision Repair
XRCC1	
RAD50	Homologous Recombination
BRCA1	
DNA-PK-cs	Non-homologous end-joining (NHEJ)
XRCC6 (ku70)	
MSH2	Mismatch Repair
MLH1	
BCL2	Apoptosis
PUMA	
COX2 (not shown, no correlation)	
Ki67	Cell Growth
CDKN1A (p21)	Cell Cycle Regulation
ABCB1 (not shown, no correlation)	Influx/Export Transporters
ABCC1	
GSTP1	

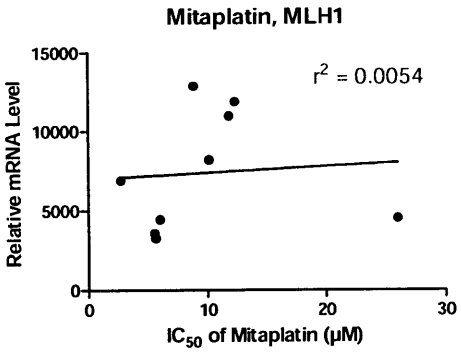
Mitaplatin, MLH1
r² = 0.0054
Relative mRNA Level
15000
10000
5000
0
0
10
20
30
IC50 of Mitaplatin (μM)

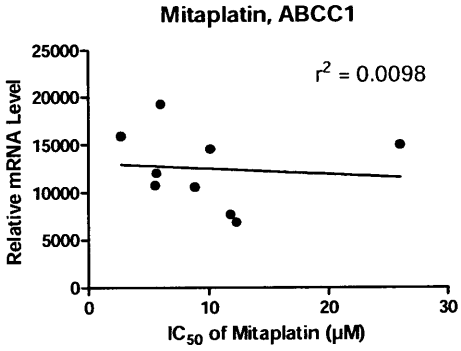
Mitaplatin, ABCC1
r² = 0.0098
Relative mRNA Level
25000
20000
15000
10000
5000
0
0
10
20
30
IC50 of Mitaplatin (μM)

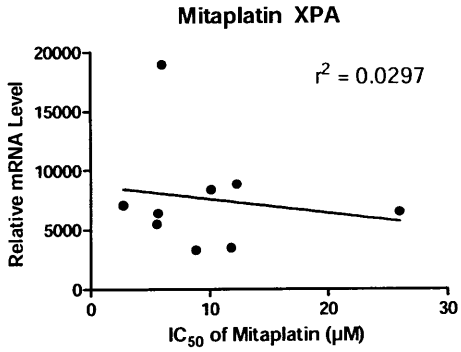
Mitaplatin XPA
r² = 0.0297
Relative mRNA Level
20000
15000
10000
5000
0
0
10
20
30
IC50 of Mitaplatin (μM)

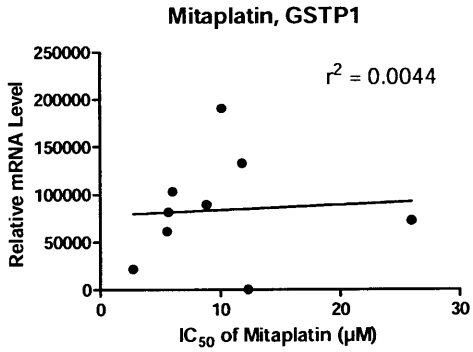
Mitaplatin, GSTP1
r² = 0.0044
Relative mRNA Level
250000
200000
150000
100000
50000
0
0
10
20
30
IC50 of Mitaplatin (μM)

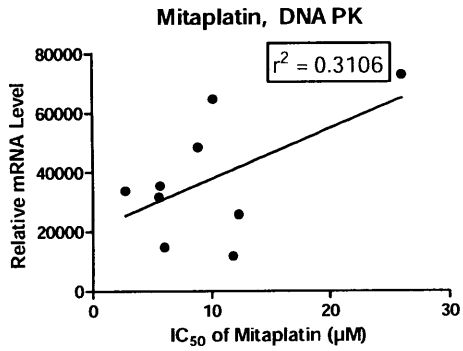
Mitaplatin, DNA PK
r² = 0.3106
Relative mRNA Level
80000
60000
40000
20000
0
0
10
20
30
IC50 of Mitaplatin (μM)

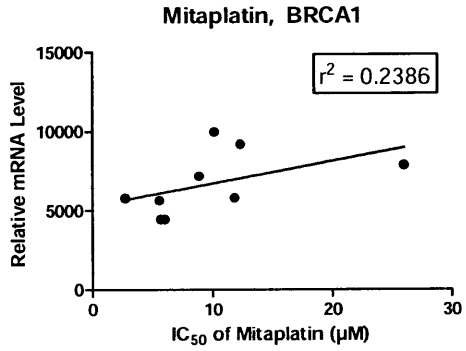
Mitaplatin, BRCA1
r² = 0.2386
Relative mRNA Level
15000
10000
5000
0
0
10
20
30
IC50 of Mitaplatin (μM)

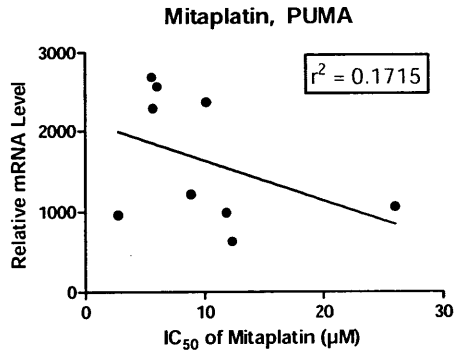
Mitaplatin, PUMA
r² = 0.1715
Relative mRNA Level
3000
2000
1000
0
0
10
20
30
IC50 of Mitaplatin (μM)

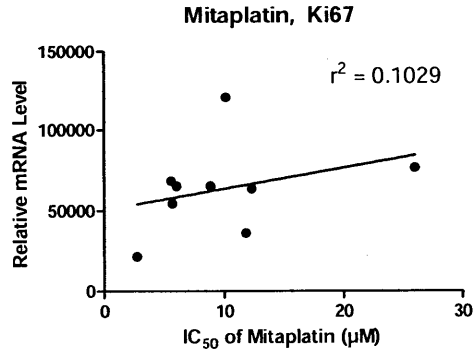
Mitaplatin, Ki67
r² = 0.1029
Relative mRNA Level
150000
100000
50000
0
0
10
20
30
IC50 of Mitaplatin (μM)

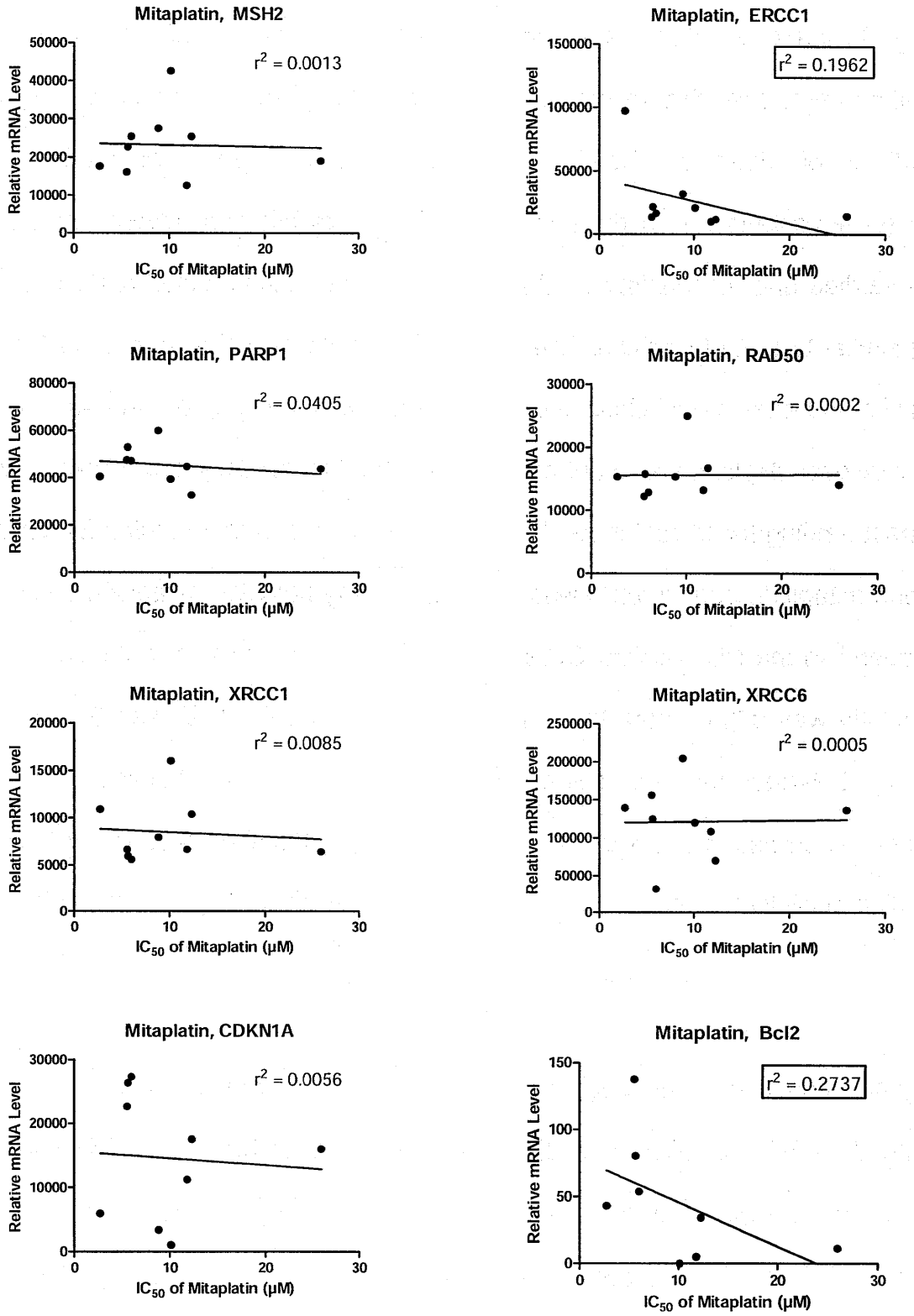

Figure 7.9. Correlation of mitaplatin IC_{50} values and expression levels of genes of interest.

Evaluation of protein markers of apoptosis in HOP 62 cells

Western blots were performed by Shahin Emami at Saint-Antoine to determine the effect of mitaplatin treatment on Chk2 and gamma-H2AX phosphorylation. HOP 62 cells were treated at the IC_{50} values of each drug for 24 h. The platinum-containing medium was then removed and protein content was determined 0, 24, 48, or 72 h following removal of the platinum. The top panel of figure 7.10 tentatively indicates the appearance of a band at 62 kDa for Chk2 in cells treated with either cisplatin, oxaliplatin, or mitaplatin. The bottom panel of Figure 7.10 shows the appearance of a band at 25 kDa for cisplatin, oxaliplatin and mitaplatin, which corresponds to the phosphorylated form of γ-H2AX, indicating the induction of apoptosis based on DNA double-strand break formation.

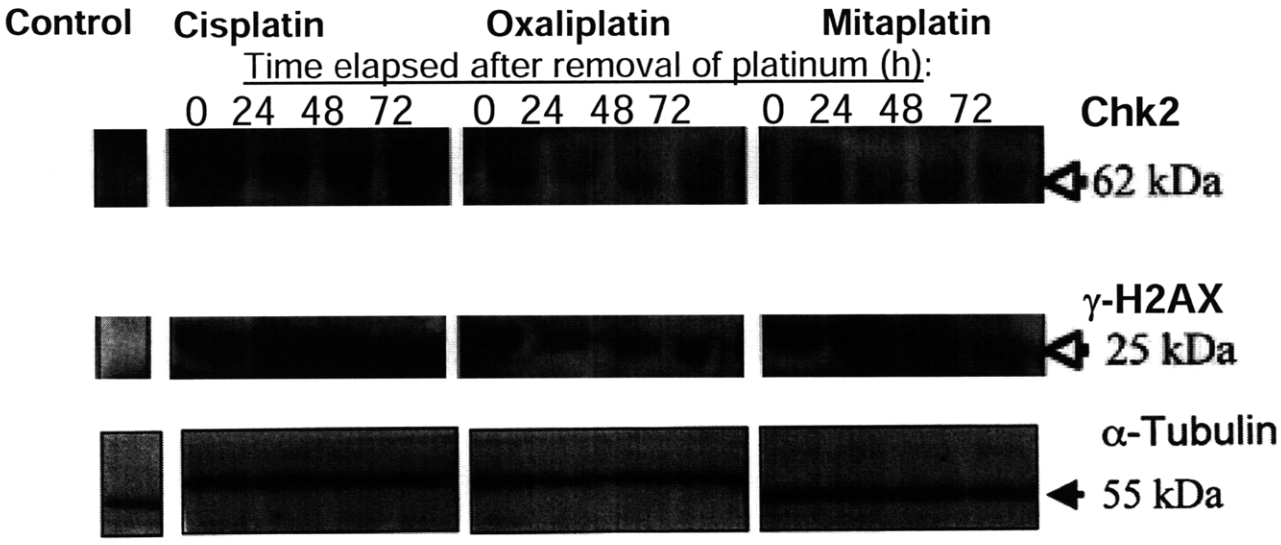

Figure 7.10. Levels of chk2 (top) and γ-H2AX (bottom) after 24 h treatment at the IC50 values with platinum followed by incubation in drug-free medium for 0, 24, 48, or 72 h. The α-tubulin blot is used as a loading control.

Discussion

Mitaplatin is a dual-functional drug designed to affect only the cancer cell mitochondria, not the mitochondria of healthy cells, and also to cause the cytotoxic, DNA-damaging, transcription-inhibiting effects of cisplatin. The fact that it is a platinum(IV)-derivative of cisplatin is both an advantage and a disadvantage. It is at least as potent as cisplatin in all cell lines studied and mechanistic studies reveal that the mitaplatin mechanism of action is very similar to that of cisplatin. The disadvantage is that, because it is an analog of a well-known and well-studied class of drug, mitaplatin should show significantly improved cytotoxicity over cisplatin and proof of a significantly different spectrum of activity in order to attract funding for clinical trials. An independent measure of the difference of activity between mitaplatin and cisplatin was obtained due to the results of the NCI60 single-dose screen.[8] In the NCI's online COMPARE assay, the correlation between cisplatin and mitaplatin was 0.7, a score that, in this context, indicates a very high degree of similarity between the two compounds. Future modifications of mitaplatin should aim to show a correlation of 0.4 or lower in the NCI60 single dose screen to secure interest in funding of clinical trials.

Conclusions

Although it is a promising, intelligently designed dual functional platform for delivery of both cisplatin and dichloroacetate, the dual functional properties of mitaplatin are not apparent in data collected using in vitro models. The cytotoxicity profile, cell cycle results and potential predictive factors (mRNA vs. IC_{50} correlation results) are very similar to that of cisplatin. The results suggesting the similarity of mitaplatin and cisplatin

are supported by the correlation factor between the two compounds of 0.719 found using the NCI's COMPARE algorithm.

Potential strategies to either deliver more DCA per molecule of cisplatin or to ensure that the molecule is not reduced prior to entry into the cell will likely yield compounds of great interest for use in the clinic, especially considering the high potency of this compound relative to other known Pt(IV) compounds.

Materials and Methods

Cell Lines and Reagents

Colorectal cancer cell lines HT-29, HCT-116, HCC2998, and COLO 205, breast cancer line MCF-7, melanoma line MDA-435, ovarian cancer lines OVCAR-3 and IGROV-1, and non-small cell lung cancer line HOP-92 and HOP-62 were obtained from the American Type Culture Collection (Rockville, MD, USA) and maintained in RPMI medium supplemented with 10% fetal bovine serum. The p53 (-/-) cell lines and MMR proficient cell lines had previously been derived from HCT-116 cells as described[9,10] and were provided by Massimo Broggini of the Mario Negri Institute, Milan. The HCT116-pcDNA, HCT116-ch3, HCT116-E6, and HCT-116-N8 cell lines were maintained in medium supplemented with the antibiotics G418 (Sigma) or G418 and Hygromycin B (HCT116-N8 only, Sigma). All cell lines were regularly tested for mycoplasma contamination by PCR using a Stratagene kit (La Jolla, CA, USA). Cisplatin and oxaliplatin were obtained from the Beaujon University Hospital Pharmacy.

In vitro growth inhibition assays

Cells were plated in 96-well plates at 2 x 10^3 cells per well. Twenty-four hours after plating, the medium was replaced with platinum-containing medium. Cells were

incubated with platinum for 24 h, or as indicated in the text. After the 24 h incubation with drug, wells were washed with RPMI and cells were incubated in serum-containing medium for 72 h. Cell viability was determined either by detection of mitochondrial cleavage of the tetrazolium ring of MTT (3-(4,5-dimethylthiazol-2-yl)-2,5-diphenyl tetrazolium bromide) by absorption at 562 nm as described[11] or by detection of sulfrhodamine B as described.[12]

Cell Cycle Analysis

Analysis of cell cycle effects of mitaplatin were evaluated after incubation of HOP-62 cells with either mitaplatin, cisplatin, or oxaliplatin at the IC_{50} values (Table 7.1) for 24 h. Immediately after the 24 h incubation, cells were collected, stained with propidium iodide and analyzed by flow cytometry as described.[13]

RT-PCR

Total RNA was extracted from all cell lines at the same passage used for the cytotoxicity studies. The Trizol reagent (Invitrogen), composed of guanidinium thiocyanate, phenol, chloroform, and isoamyl alcohol, was used to facilitate the extraction. RT-PCR was performed as described[14,15] to detect mRNA for the genes listed in Table 7.2.

References

(1) O. Warburg (1956). On the origin of cancer cells. *Science*, **123**, 309-314.

(2) E. D. Michelakis, L. Webster and J. R. Mackey (2008). Dichloroacetate (DCA) as a potential metabolic-targeting therapy for cancer. *Br. J. Cancer*, **99**, 989-994.

(3) S. Bonnet, S. L. Archer, J. Allalunis-Turner, A. Haromy, C. Beaulieu, R. Thompson, C. T. Lee, G. D. Lopaschuk, L. Puttagunta, S. Bonnet, G. Harry, K. Hashimoto, C. J. Porter, M. A. Andrade, B. Thebaud and E. D. Michelakis (2007). A mitochondria-K+ channel axis is suppressed in cancer and its normalization promotes apoptosis and inhibits cancer growth. *Cancer Cell*, **11**, 37-51.

(4) D. R. Plas and C. B. Thompson (2002). Cell metabolism in the regulation of programmed cell death. *Trends Endocrin. Metab.*, **13**, 74-78.
(5) J. G. Pastorino, J. B. Hoek and N. Shulga (2005). Activation of Glycogen Synthase Kinase 3β Disrupts the Binding of Hexokinase II to Mitochondria by Phosphorylating Voltage-Dependent Anion Channel and Potentiates Chemotherapy-Induced Cytotoxicity. *Cancer Res.*, **65**, 10545-10554.
(6) N. C. Denko (2008). Hypoxia, HIF1 and glucose metabolism in the solid tumor. *Nat. Rev. Cancer*, **8**, 705-713.
(7) S. Dhar and S. J. Lippard: Manuscript sent out for review by *Science*, 2009.
(8) R. H. Shoemaker (2006). The NCI60 human tumour cell line anticancer drug screen. *Nat. Rev. Cancer*, **6**, 813-823.
(9) G. Colella, S. Marchini, M. D'Incalci, R. Brown and M. Broggini (1999). Mismatch repair deficiency is associated with resistance to DNA minor groove alkylating agents. *Br. J. Cancer*, **80**, 338-343.
(10) F. Vikhanskaya, G. Colella, M. Valenti, S. Parodi, M. D'Incalci and M. Broggini (1999). Cooperation between p53 and hMLH1 in a human colocarcinoma cell line in response to DNA damage. *Clin. Cancer Res.*, **5**, 937-941.
(11) M. C. Alley, D. A. Scudiero, A. Monks, M. L. Hursey, M. J. Czerwinski, D. L. Fine, B. J. Abbott, J. G. Mayo, R. H. Shoemaker and M. R. Boyd (1988). Feasibility of drug screening with panels of human tumor cell lines using a microculture tetrazolium assay. *Cancer Res.*, **48**, 589-601.
(12) V. Vichai and K. Kirtikara (2006). Sulforhodamine B colorimetric assay for cytotoxicity screening. *Nature Protocols*, **1**, 1112-1116.
(13) M. Serova, F. Calvo, F. Lokiec, F. Koeppel, V. Poindessous, A. K. Larsen, E. S. Van Laar, S. J. Waters, E. Cvitkovic and E. Raymond (2006). Characterizations of irofulven cytotoxicity in combination with cisplatin and oxaliplatin in human colon, breast, and ovarian cancer cells. *Cancer Chemother. Pharmacol.*, **57**, 491-499.
(14) I. Bieche, B. Parfait, S. Tozlu, R. Lidereau and M. Vidaud (2001). Quantitation of androgen receptor gene expression in sporadic breast tumors by real-time RT-PCR: evidence that MYC is an AR-regulated gene. *Carcinogenesis*, **22**, 1521-1526.
(15) N. Aissat, C. Le Tourneau, A. Ghoul, M. Serova, I. Bieche, F. Lokiec, E. Raymond and S. Faivre (2008). Antiproliferative effects of rapamycin as a single agent and in combination with carboplatin and paclitaxel in head and neck cancer cell lines. *Cancer Chemother. Pharmacol.*, **62**, 305-313.

Appendix A.

Examination of the Platination of Plasmid DNA in Carbonate Buffer

Parts of this material have been published in Todd, R.C.; **Lovejoy, K.S.**; Lippard, S.J. "Understanding the effect of carbonate ion on cisplatin binding to DNA." *J. Am. Chem. Soc.* **2007**, *129*, 20, 6370-6371. The work described below is that of the author of this thesis.

Introduction

Upon IV introduction of cisplatin into the blood of a cancer patient, the electrophilic Pt(II) center is exposed to many nucleophilic species, including carboxylates, amines, and thiols, that are potential reaction partners.[1] Sulfur-containing species such as the tripeptide glutathione and the amino acids cysteine and methionine have a particularly high affinity for platinum(II). The species $Pt(Met)_2$ is one of the few characterized metabolites of cisplatin[2,3] and glutathione, present at mM concentrations in much of the human body, plays a large role in deactivating cisplatin. Besides complexes with sulfur-containing small molecules, many other platinum species exist in the bloodstream and cells of patients receiving cisplatin therapy. Platinum(II) complexes of amino acids as the *N,O*-chelates have been synthesized using combinatorial synthesis.[4,5] Logically, cisplatin also forms complexes with proteins. Much of the Pt(II) found in human blood plasma is bound to serum albumin as a Met-*S,N* chelate, for example.[6] Another example of protein-cDDP complexes is with the iron carrier transferrin, for which a cisplatin binding site has been characterized.[7,8]

Cisplatin also reacts with buffering agents, including carbonate and phosphate.[1] Recent studies on the platinum interaction with carbonate ion should therefore not be of special interest to the cisplatin scientific community. The assertion, based on two-dimensional [^{1}H,^{15}N]HSQC NMR, that the *cis*-$[Pt(NH_3)_2Cl(OCO_2)]^-$ ion is the active adduct-forming species in biological systems[9-11] does require closer scrutiny, however.

We do not propose to have developed a superior method for identifying the multitude of transient $[Pt(NH_3)_2Cl(X)]$ species (X=*O*-coordinating ligand) in complex biological media. We instead intend to use the basic techniques of HPLC, agarose gel

electrophoresis, and measurement of r_b/r_f values to investigate the cisplatin-DNA interaction in carbonate buffer and to correct some recent literature.

Experimental

Platination of Plasmid DNA

Plasmid pBR322 was purchased from New England Biolabs and amplified in a 100 mL LB culture of *e. coli* XL1-Blue cells with ampicillin as a selecting agent. The plasmid was purified on a Maxi-prep column (Qiagen), ethanol precipitated, analyzed by agarose gel electrophoresis, and used for platination reactions. Platination reactions were done in 19.2 μM DNA (with respect to bp), 23.8 mM of buffering agent ($NaHCO_3$, NaH_2PO_4, or Hepes), pH 7.4, and 5 mM NaCl in a total volume of 120.4 μL. Cisplatin concentrations varied from 1.5 μM to 60 μM and r_f values varied from 0.078 to 3.13. Reactions were incubated for 24 h at 37°C in the dark and dialyzed for 24 h against 10 mM Tris-HCl, pH 7.4, 1 mM EDTA to remove excess platinum.

Measurement of r_b Values

DNA concentrations were quantified by measuring the absorbance of the dialyzed solutions at 260 nm on a Cary 50 Bio UV-Visible Spectrometer equipped with a microprobe (C Technologies Inc.). Platinum concentrations were measured by atomic absorption spectroscopy using an AAnalyst 300 equipped with an HGA-800 graphite furnace and operated through the AAWinLab interface, version 3.0 (Perkin Elmer, Wellesley, MA). A hollow cathode platinum lamp with 265.9 nm emission was used with a slit width of 0.70 nm. Pyrolysis was performed at 1200°C for 20 s and atomization at 2650°C for 5 s. AA samples were measured in duplicate using a calibration range of 20-

80 μg/L and an r value of ≥ 0.998 for all calibration curves. For samples requiring dilution, dialysis buffer was used. The dialysis buffer was analyzed by both AA and UV-Vis and no detectable platinum or DNA signals were observed.

Agarose Gel Analysis of Platination

A portion of 8 μL of each of the above samples was removed immediately following the 24 h incubation and 1 μL of a loading solution containing 50% glycerol, 0.05% bromophenol blue, and 0.05% xylene cyanol was added. Samples were loaded in 1% agarose gels prepared with 1x TAE (40 mM Tris-base, pH 8.0, 20 mM acetic acid, 1 mM EDTA) and gels were allowed to run for 4 h at 75 W at room temperature. Gels were stained in 500 mL of deionized water with 1 μg/mL ethidium bromide for 15 min, followed by 60 sec of destaining in deionized water. Imaging was done on a Fluor-S (BioRad) and processed using QuantityOne software (BioRad).

Results and Discussion

Platination of Plasmid DNA

Our measurements of r_b values for platination reactions in phosphate, Hepes and carbonate buffer indicate that significantly less platinum binds to DNA in phosphate or carbonate as compared with Hepes buffer (Figures 1 and 2). Slightly less platinum binds in carbonate than in phosphate buffer.

Agarose gel electrophoresis of platinated plasmid DNA indicates a point at which the unwinding due to platinum has completely removed all supercoils from the DNA (coalescence point) for the platination in Hepes buffer at r_b = 0.138 (Figure 3).

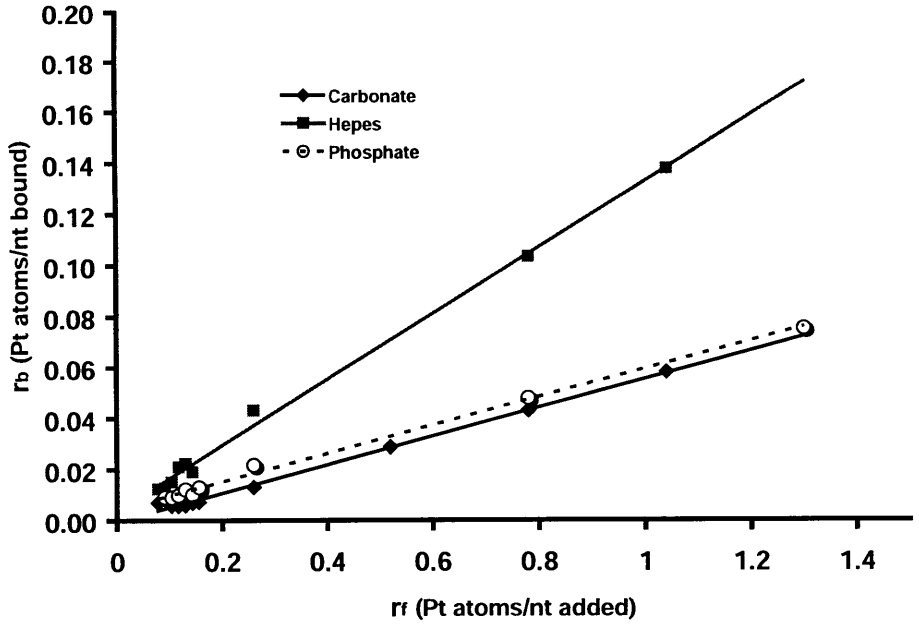

Figure A.1. Platinum bound per nucleotide (r_b) for the platination of plasmid DNA as a function of platinum added per nucleotide (r_f) for reactions at pH 7.4 in Hepes, phosphate, or carbonate buffer.

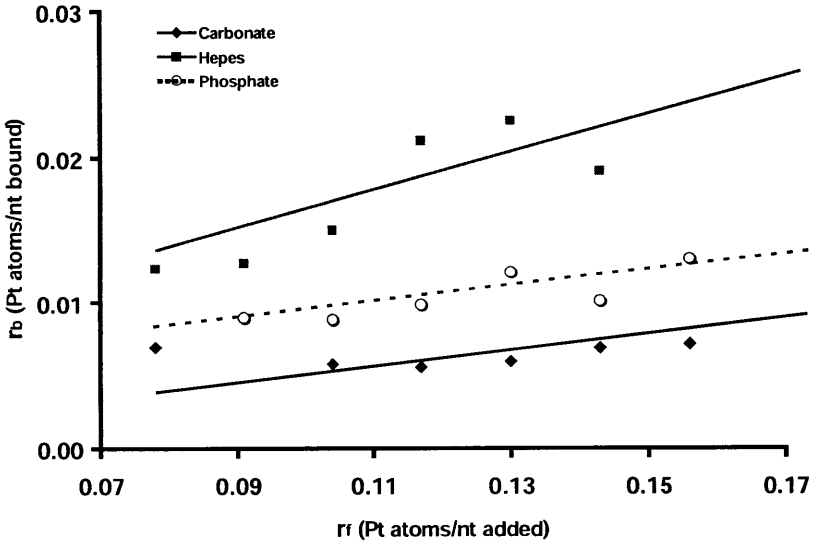

Figure A.2. Plot of (r_b) vs. (r_f) for low platination levels (expansion of Figure A.1).

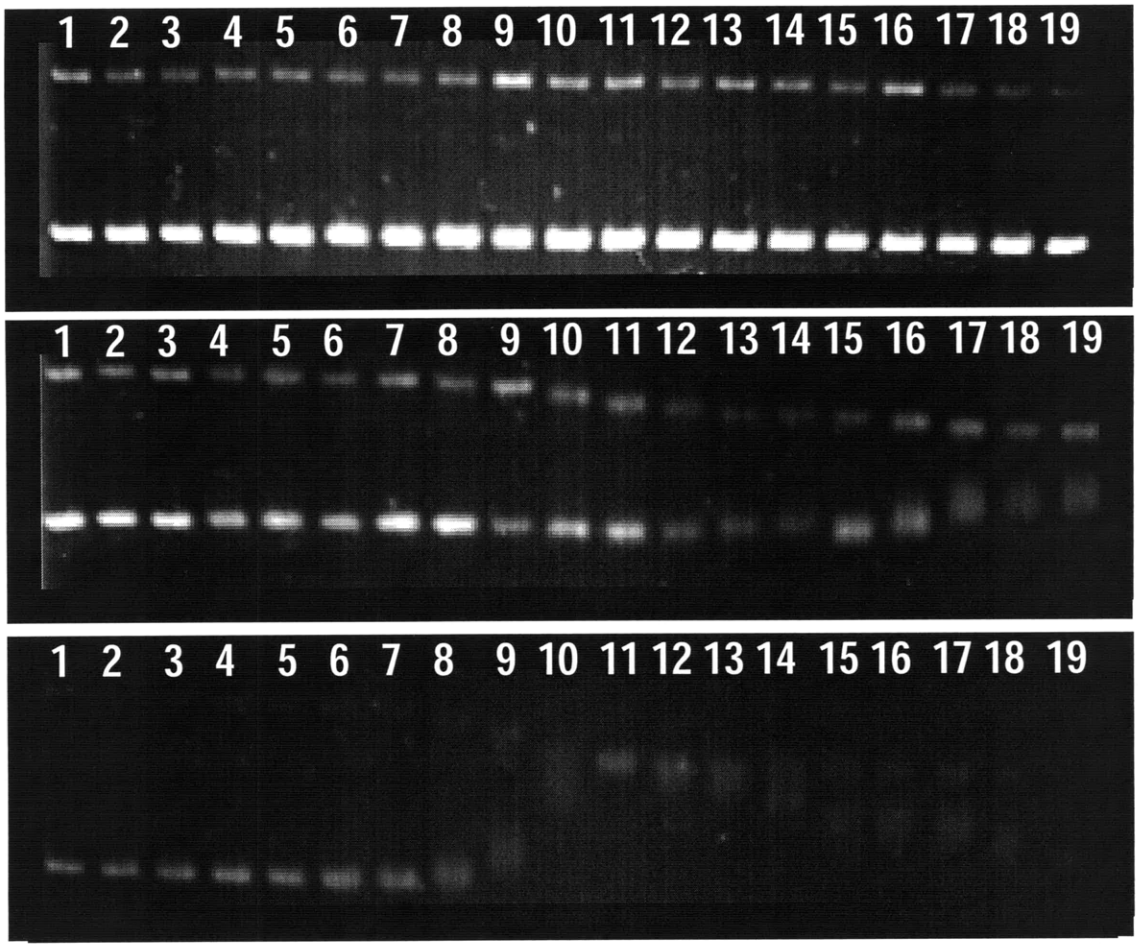

Figure A.3. 1% agarose gels showing DNA platinated at r_f values from 0.078 to 3.13 (r_f increases from left to right). *Top:* platination in carbonate buffer; *Middle*: platination in phosphate buffer; *Bottom*: platination in hepes buffer. Numbers correspond to r_f values: *1*, 0.078; *2*, 0.091; *3*, 0.104; *4*, 0.117; *5*, 0.13; *6*, 0.143; *7*, 0.156; *8*, 0.26; *9*, 0.52; *10*, 0.78; *11*, 1.04; *12*, 1.3; *13*, 1.56; *14*, 1.82; *15*, 2.08; *16*, 2.34; *17*, 2.6; *18*, 2.86; *19*, 3.13.

The coalescence point for platination in phosphate and carbonate buffers is not observed at these r_f values and will be > 0.139 in phosphate buffer and > 0.080 in carbonate buffer. In phosphate buffer, the high r_b value of the coalescence point as compared with Hepes indicates that a greater level of platination is required to achieve DNA unwinding equal to that seen in Hepes buffer. Monofunctional platinum adducts unwind the DNA to a lesser extent than do bifunctional adducts. The complete unwinding of the DNA supercoil, marked by the coalescence point on the agarose gel, is therefore reached for compounds forming monofunctional adducts at a higher r_b value

than for bifunctional adducts.[12] Assuming that only bifunctional cisplatin-DNA adducts are formed in Hepes buffer, the reduced unwinding-per-Pt seen in phosphate buffer indicates that some monofunctional adducts are formed. Similar information about adducts formed in carbonate buffer was not obtained. Despite repeated attempts, the persistently low level of platination in carbonate buffer always precluded any possibility of observing a coalescence point.

Conclusions

Numerous side reactions occur upon the introduction of cisplatin into biological matrices. These side-reactions, which are mostly deactivating, include interactions with ions such as phosphate and carbonate, as well as interactions with proteins, small molecules, and RNA.

Recent reports of the interaction of cisplatin with carbonate suggest that platinum carbonato species are the active species in reactions of cisplatin and carboplatin with DNA,[9] that carbonate activates carboplatin ([$Pt(NH_3)_2$(CBDCA)] by displacing one side of the chelating ligand,[11] and that a monocarbonato Pt(II) species enters Jurkat cells.[10] Although carbonate does displace bidentate dicarboxylate ligands from the Pt(II) center,[13] there is no evidence to support a persistent Pt(II)-carbonato species in biological matrices, nor is there evidence suggesting the existence of long-lived monodentate adducts on DNA *in vivo*.

Monofunctional adducts on DNA in 0.2 M carbonate have been detected immunochemically[14] and ^{195}Pt-NMR studies of aquated cisplatin in 10 mM sodium phosphate buffer shows the presence of a peak at -1736 ppm that does not appear

when the reaction is done in pure water.[15] These and other results suggest that monofunctional DNA-platinum adducts can exist in various buffers under highly controlled, *in vitro* conditions. However, strong evidence exists for the formation of predominantly bifunctional adducts on DNA under biological conditions[16,17] and for the facile deactivation of cisplatin by carbonate and phosphate, among other buffering agents.[1] Furthermore, cells grown in 5% CO_2 show the same sensitivity to cisplatin as cells grown in 10% CO_2 (Hepes-buffered to pH 7.4 in both cases), a preliminary indication that cytotoxicity is independent of [CO_2] in the culture medium.[18]

Also interesting is a review of ^{15}N-NMR and ^{1}H-NMR spectroscopy on cisplatin in various buffering systems. Plots from three figures in papers spanning 11 years attribute the peak at ($\delta(^1H)$, $\delta(^{15}N)$) = ~(3.6,-85) in the two-dimensional [^{1}H,^{15}N]HSQC NMR spectrum of cisplatin to *cis*-[Pt($^{15}NH_3)_2$(OH)Cl][19] (Figure 5, in RPMI medium, later ascribed to the monocarbonato form[9]), either *cis/trans*-[Pt($^{15}NH_3)_2$(OH)Cl] or *cis/trans*-[Pt($^{15}NH_3)_2$(OH_2)Cl]$^+$ (Figure 1, 10 mM sodium phosphate),[20] or *cis*-[Pt($NH_3)_2$Cl(OCO_2)]$^-$ (Figure 2, 5 mM sodium bicarbonate).

Our measurements of r_b values for platination reactions in phosphate, Hepes and carbonate buffer indicate that significantly less platinum binds to DNA in phosphate or carbonate as compared with Hepes buffer. Slightly less platinum binds in carbonate than in phosphate buffer. Agarose gel electrophoresis of platinated plasmid DNA suggests that predominantly bifunctional adducts form during platination reactions in Hepes or phosphate buffers. In carbonate buffer, agarose gels could not yield information about the mode of binding because the highest platination levels achieved were too low for observation of supercoil unwinding behavior. It is noted that the

experiments performed do not directly address the nature of the platinum adducts formed in biological matrices. The results may instead be useful for researchers platinating DNA *in vitro*.

References

(1) M. E. Howe-Grant and S. J. Lippard In *Metal Ions in Biological Systems*, 1980; Vol. 11, pp 63-125.

(2) Y. Chen, Z. Guo and P. J. Sadler In *Cisplatin: Chemistry and Biochemistry of a Leading Anticancer Drug*; Lippert, B., Ed.; Wiley-VCH: Weinheim, Germany, 1999, pp 293-318.

(3) C. M. Riley, L. A. Sternson, A. J. Repta and S. A. Slyter (1983). Monitoring the reactions of cisplatin with nucleotides and methionine by reversed-phase high-performance liquid chromatography using cationic and anionic paring ions. *Anal. Biochem.*, **130**, 203-214.

(4) K. E. Sandman, P. Fuhrmann and S. J. Lippard (1998). A mechanism-based, solution-phase method for screening combinatorial mixtures of potential platinum anticancer drugs. *J. Biol. Inorg. Chem.*, **3**, 74-80.

(5) C. J. Ziegler, K. E. Sandman, C. H. Liang and S. J. Lippard (1999). Toxicity of platinum(II) amino acid (N,O) complexes parallels their binding to DNA as measured in a new solid phase assay involving a fluorescent HMG1 protein construct readout. *J. Biol. Inorg. Chem.*, **4**, 402-411.

(6) A. I. Ivanov, J. Christodoulou, J. A. Parkinson, K. J. Barnham, A. Tucker, J. Woodrow and P. J. Sadler (1998). Cisplatin binding sites on human albumin. *J. Biol. Chem.*, **273**, 14721-14730.

(7) I. Khalaila, C. S. Allardyce, C. S. Verma and P. J. Dyson (2005). A mass spectrometric and molecular modelling study of cisplatin binding to transferrin. *ChemBioChem*, **6**, 1788-1795.

(8) M. C. Cox, K. J. Barnham, T. A. Frenkiel, J. D. Hoeschele, A. B. Mason, Q.-Y. He, R. C. Woodworth and P. J. Sadler (1999). Identification of platination sites on human serum transferrin using 13C and 15N NMR spectroscopy. *J. Biol. Inorg. Chem.*, **4**, 621-631.

(9) C. R. Centerwall, J. Goodisman, D. J. Kerwood and J. C. Dabrowiak (2005). Cisplatin carbonato complexes. implications for uptake, antitumor properties, and toxicity. *J. Am. Chem. Soc.*, **127**, 12768-12769.

(10) C. R. Centerwall, K. A. Tacka, D. J. Kerwood, J. Goodisman, B. B. Toms, R. L. Dubowy and J. C. Dabrowiak (2006). Modification and uptake of a cisplatin carbonato complex by Jurkat cells. *Mol. Pharmacol.*, **70**, 348-355.

(11) A. J. Di Pasqua, J. Goodisman, D. J. Kerwood, B. B. Toms, R. L. Dubowy and J. C. Dabrowiak (2006). Activation of Carboplatin by Carbonate. *Chem. Res. Toxicol.*, **19**, 139-149.

(12) M. V. Keck and S. J. Lippard (1992). Unwinding of supercoiled DNA by platinum-ethidium and related complexes. *J. Am. Chem. Soc.*, **114**, 3386-3390.
(13) S. K. Mauldin, M. Plescia, F. A. Richard, S. D. Wyrick, R. D. Voyksner and S. G. Chaney (1988). Displacement of the bidentate malonate ligand from (d,l-trans-1,2-diaminocyclohexane)malonatoplatinum(II) by physiologically important compounds in vitro. *Biochem. Pharmacol.*, **37**, 3321-3333.
(14) A. M. J. Fichtinger-Schepman, J. L. Von der Veer, P. H. M. Lohman and J. Reedijk (1984). A simple method for the inactivation of monofunctionally DNA-bound cis-diamminedichloroplatinum(II). *J. Inorg. Biochem.*, **21**, 103-111.
(15) D. P. Bancroft, C. A. Lepre and S. J. Lippard (1990). Platinum-195 NMR kinetic and mechanistic studies of cis- and trans-diamminedichloroplatinum(II) binding to DNA. *J. Am. Chem. Soc.*, **112**, 6860-6871.
(16) A. M. J. Fichtinger-Schepman, R. A. Baan, A. Luiten-Schuite, M. Van Dijk and P. H. M. Lohman (1985). Immunochemical quantitation of adducts induced in DNA by cis-diamminedichloroplatinum(II) and analysis of adduct-related DNA-unwinding. *Chem. Biol. Interact.*, **55**, 275-288.
(17) A. M. Fichtinger-Schepman, A. T. van Oosterom, P. H. Lohman and F. Berends (1987). cis-Diamminedichloroplatinum(II)-induced DNA adducts in peripheral leukocytes from seven cancer patients: quantitative immunochemical detection of the adduct induction and removal after a single dose of cis-diamminedichloroplatinum(II). *Cancer Res.*, **47**, 3000-3004.
(18) R. P. Feazell and K. S. Lovejoy, Unpublished Results.
(19) K. A. Tacka, D. Szalda, A.-K. Souid, J. Goodisman and J. C. Dabrowiak (2004). Experimental and Theoretical Studies on the Pharmacodynamics of Cisplatin in Jurkat Cells. *Chem. Res. Toxicol.*, **17**, 1434-1444.
(20) K. J. Barnham, S. J. Berners-Price, T. A. Frenkiel, U. Frey and P. J. Sadler (1995). Platination pathways for reactions of cisplatin with GG single-stranded and double-stranded decanucleotides. *Angew. Chem., Int. Ed. Engl.*, **34**, 1874-1877.

Appendix B:

Cellular properties of a cell-permeable Zn^{2+}-sensitive MRI contrast agent and the Effect of Zinc Chelators on Cisplatin Cytotoxicity.

A portion of this material was published as part of Zhang, X-a., *et al.* "Water Soluble Porphyrins as a Dual-Function Molecular Imaging Platform for MRI and Fluorescence Zinc Sensing," **2006**, *Proc. Natl. Acad. Sci. USA.*

The Effect of Zn^{2+} Chelators on Cisplatin Cytotoxicity

Background and Methods

The cytotoxicity of cisplatin in combination with three compounds capable of coordinating Zn^{2+} was evaluated. The calcium salt of EDTA chelates many divalent metals, including zinc, and is cell membrane-impermeable. TPEN is a cell membrane-permeable Zn^{2+} chelator, and ZX1 is a cell membrane-impermeable Zn^{2+} chelator (Scheme B.1). We wished to test the hypothesis that chelating the zinc released upon induction of apoptosis would affect the cytotoxicity of the apoptosis-inducing agent cisplatin.

(A)

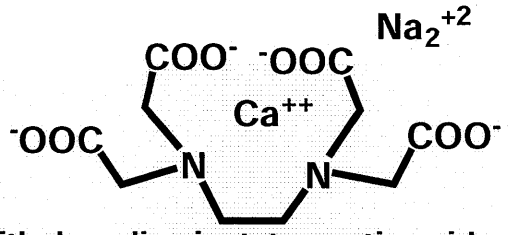

Ethylenediaminetetraacetic acid calcium disodium salt (Ca-EDTA)

(B)

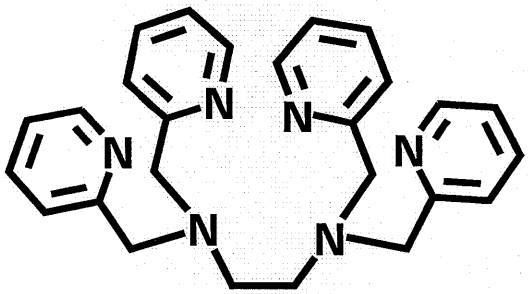

N,N,N',N'-tetrakis(2-pyridylmethyl)ethylenediamine (TPEN)

(C)

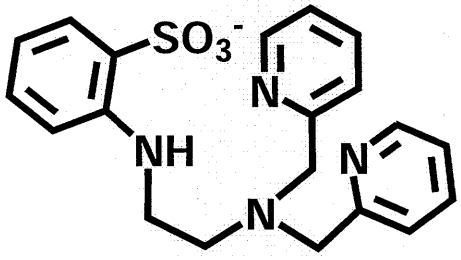

XAZ Cell Impermeable Chelator (ZX1)

Chart B.1. Zn^{2+} chelators used in an attempt to potentiate cisplatin cytotoxicity.

For the cytotoxicity experiments, HeLa ovarian cancer cells were incubated at 37°C in 5% CO_2 and grown in DMEM supplemented with 10% fetal bovine serum, 1% penicillin/streptomycin, and 1% 1 M Hepes buffer (pH 7.4). Cells were plated at 300 cells per well of a 96 well plate, reduced from the usual 500 cells per well to allow for possible acceleration of cell growth. After 24 h, cisplatin was added to concentrations of 0, 0.5, 1, 2, 5, 10, 15, 20, and 50 μM. The platinum-containing medium was removed after 7 h, Zn^{2+} chelators were added at concentrations of 1.5 μM (TPEN) or 150 μM (XAZ) and cells were incubated for four more days. For the assays done without cisplatin, Zn^{2+} chelators were directly added at various concentrations 24 h after cell plating. In all cases, cell survival was quantified by the MTT assay after a total of five days of growth.

Results and Conclusions

Plots of the cytotoxicity data are shown in Figure B.1. No statistically significant difference in cytotoxicity was observed in the experiments in which cisplatin and chelators were combined. The cytotoxicity data for the zinc chelators is shown in Figure B.2. TPEN is the most toxic of the Zn^{2+} chelators, with an IC_{50} of 3.8 μM and neither of the cell membrane-impermeable sensors showed measurable toxicity within the wide range of concentrations tested.

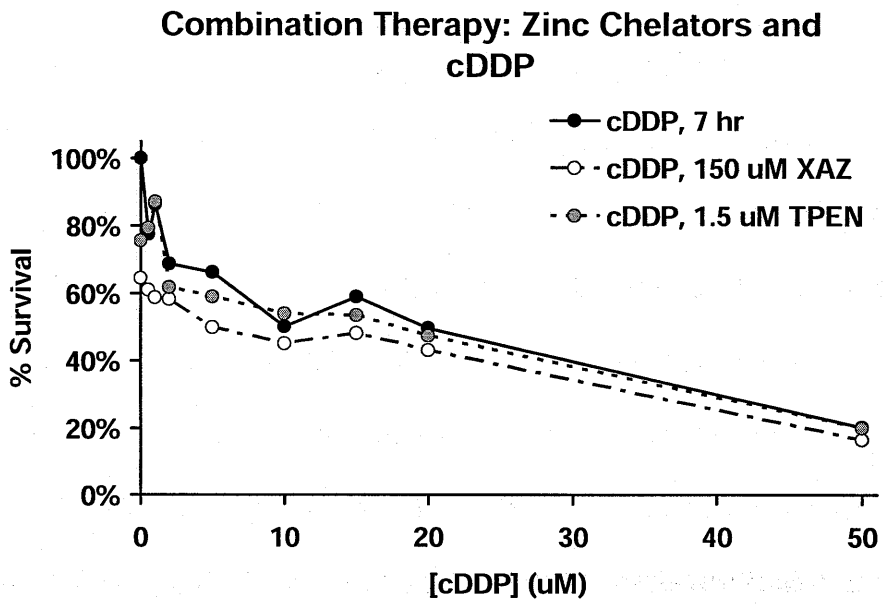

Figure B.1.Cytotoxicity assay showing the effect of Zn chelation on cisplatin cytotoxicity.

In conclusion, these experiments have shown that the two cell-impermeable chelators can be used in cells at high concentrations without worry of toxicity. Potentiation of cisplatin cytotoxicity due to chelation of extracellular zinc was not observed in this study.

If this investigation were continued, it is suggested that the amount of zinc in various batches of fetal bovine serum be quantified, because it may vary widely between batches. The amount of zinc released during apoptosis should be compared to the amount already in fetal bovine serum to determine if the difference in $[Zn^{2+}]$ after apoptosis is relevant. Finally, a fluorescent zinc detector should be employed to verify that Zn^{2+} release actually occurs in the chosen transformed cell line. In general, either neuronal or pancreatic cell lines may be better choices for the study than HeLa.

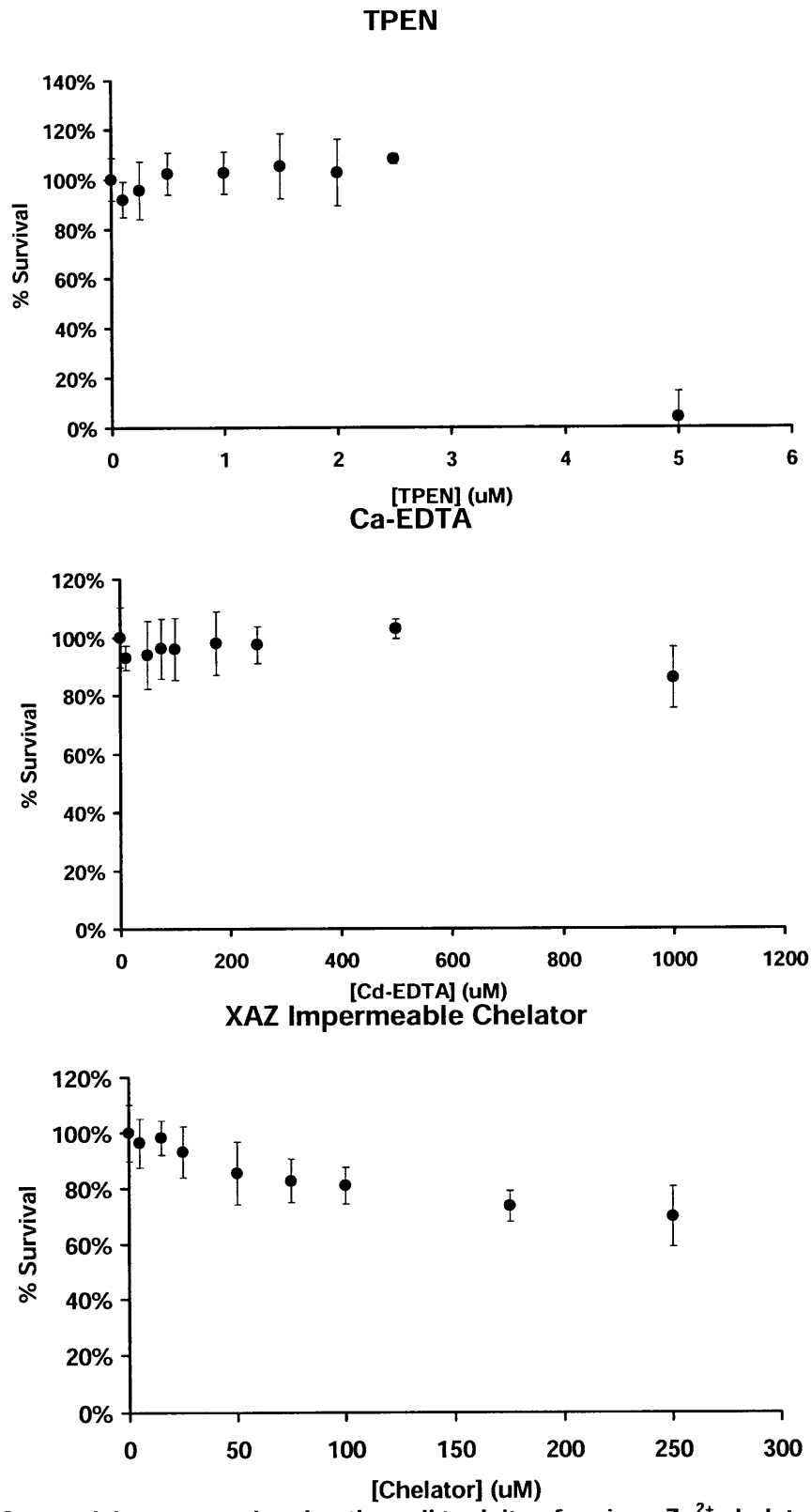

Figure B.2. Cytotoxicity assays showing the cell toxicity of various Zn^{2+} chelators.

Cellular properties of a cell-permeable Zn^{2+}-sensitive MRI contrast agent

Background

A molecular platform for dual-function fluorescence/MRI sensing of mobile zinc was synthesized by Xiao-an Zhang. Zinc-selective binding units were strategically attached to a water-soluble porphyrin template. The metal-free form, $(DPA\text{-}C_2)_2\text{-}TPPS_3$ (**1**), where DPA is dipicolylamine and $TPPS_3$ is 5-phenyl-10,15,20-tris(4-sulfonatophenyl)porphine, was found to be an excellent fluorescent sensor for zinc. The manganese derivative, $[(DPA\text{-}C_2)_2TPPS_3Mn(III)]$ (**2**), switches the function of the molecule to generate an MRI contrast agent (CA). Both metal-free and Mn(III)-inserted forms are efficiently taken up by live cells, and the intracellular zinc can be imaged by either fluorescence or MR, respectively.

Cell Culture

Suspension-adapted HEK-293 cells (Free-Style 293-F cell line; Invitrogen, Carlsbad, CA) were grown in 125 mL shaker flasks containing FreeStyle 293 Expression Medium (Invitrogen). Cultures were maintained at >90% viability by shaking at 125 rpm in a 37°C incubator with 8% CO_2 and subculturing at a 1:10 ratio upon reaching a density of 2×10^6 cells/mL. Cell density and viability were evaluated with a hemocytometer using 0.4% trypan blue staining. Cell pellets for MRI were prepared in 6 mL suspension cultures, to which either **2** or $Mn\text{-}TPPS_4$ was added to a final concentration of 100 μM, and incubated for 24 h. Where appropriate, zinc carried by the ionophore pyrithione was subsequently added to 200 μM, followed by incubation for an additional 10 min. Cell suspensions were thrice pelleted (10 min, 500 × g) and washed with phosphate-buffered saline (PBS), and the resulting loose pellet was inserted into

microtiter plates for imaging. Slides of cells growing in adherent monolayers were prepared by plating the suspension-adapted HEK-293 cells in 25 cm^2 flasks containing Dulbecco's Modified Eagle's Serum (DMEM; Invitrogen) with 10% fetal bovine serum (Hyclone, Logan, UT). After subculturing five times, cells were grown to 70% confluence on poly-D-lysine-coated glass cover slips and incubated with 5 μM of **1** for 24 h. Cells were then either incubated with 40 μM zinc carried by pyrithione for 10 min, fixed in 4% paraformaldehyde, washed with PBS and stained with Hoechst 33258 (0.4 μM, 10 min incubation in PBS), or directly fixed, stained with Hoechst dye, and imaged.

Fluorescence Microscopy

The cell fluorescence imaging experiments were performed with a Zeiss Axiovert 200M inverted epifluorescence microscope, equipped with a Hamamatsu EM-CCD digital camera C9100, and a MS200 XY Piezo Z stage (Applied Scientific Instruments, Inc.). An X-Cite® 120 metal-halide lamp (EXFO) was used as the light source. The fluorescence images were obtained by using a 63× oil immersion objective lenses and a customized optical filter (exciter: D425/50, emitter: E600lp, beamsplitter: 460dcxr, Chroma Technology Corp.). The microscope was operated with Volocity software (Improvision).

Manganese Atomic Absorption Spectroscopy

Cell monolayers were grown in 75 cm^2 plates to 70% confluence and treated with 100 μM of either **2** or Mn-$TPPS_4$, followed by incubation for 24 h. All fractionation steps were performed at 4°C. After twice pelleting by centrifugation (500 × g) and washing with PBS, cells were gently resuspended in five packed-cell volumes of ice-cold lysis buffer (10 mM Hepes, pH 7.9, 10 mM KCl, 1.5 mM $MgCl_2$, 1 mM dithiothreitol, 2 mM

phenylmethylsulfonyl fluoride) and incubated on ice for 15 min. After centrifugation (420 × g, 5 min) the pellet was resuspended in 2 packed-cell volumes of lysis buffer. Cell membranes were disrupted by drawing cells into a syringe with a 27-gauge syringe needle and ejecting ten times. After centrifugation (11,000 × g, 20 min), the supernatant was retained (cytosolic fraction) and the pellet was resuspended in 2/3 packed-cell volume of extraction buffer (20 mM Hepes, pH 7.9, 25% glycerol, 0.42 M NaCl, 1.5 mM $MgCl_2$ 1 mM dithiothreitol, 2 mM phenylmethylsulfonyl fluoride). The nuclei were disrupted with ten strokes using a fresh syringe and the suspension was shaken at 50 rpm for 30 min at 4°C and then centrifuged (20,000 × g, 5 min). The resulting pellet was retained as the membrane fraction and the supernatant as the nuclear fraction.

Manganese atomic absorption spectroscopic analyses of samples were performed on an Aanalyst 300 instrument equipped with an HGA-800 graphite furnace and using AAWinLab, version 3.0 (Perkin Elmer, Wellesley, MA). A hollow cathode manganese lamp with 279.5 nm emission was used with a slit width of 0.2 nm. Pyrolysis was performed at 1400 °C for 30 s and atomization at 2200 °C for 5 s.

Results: Intracellular Imaging

Because **1** (the metal free form, $(DPA\text{-}C_2)_2\text{-}TPPS_3$) is membrane-permeable in all cell lines tested to date, it can be employed in intracellular imaging of zinc by fluorescence microscopy. In order to use the same cell line for demonstration of both fluorescence and MR imaging, we selected HEK-293. Suspension cultures of HEK-293 enabled production of a sufficient number of cells for obtaining a cell pellet suitable for MRI and

could alternatively be plated as an adherent monolayer for fluorescence imaging studies. The latter, monolayer cultures were subcultured five times after the initial plating to allow the cells to adapt fully, after which they were grown to 70% confluence on glass cover slips and treated with **1** for fluorescence imaging. The cytotoxicity of **1** was evaluated in these adherent HEK-293 cells by incubating them with 5 μM **1** for 24 h.

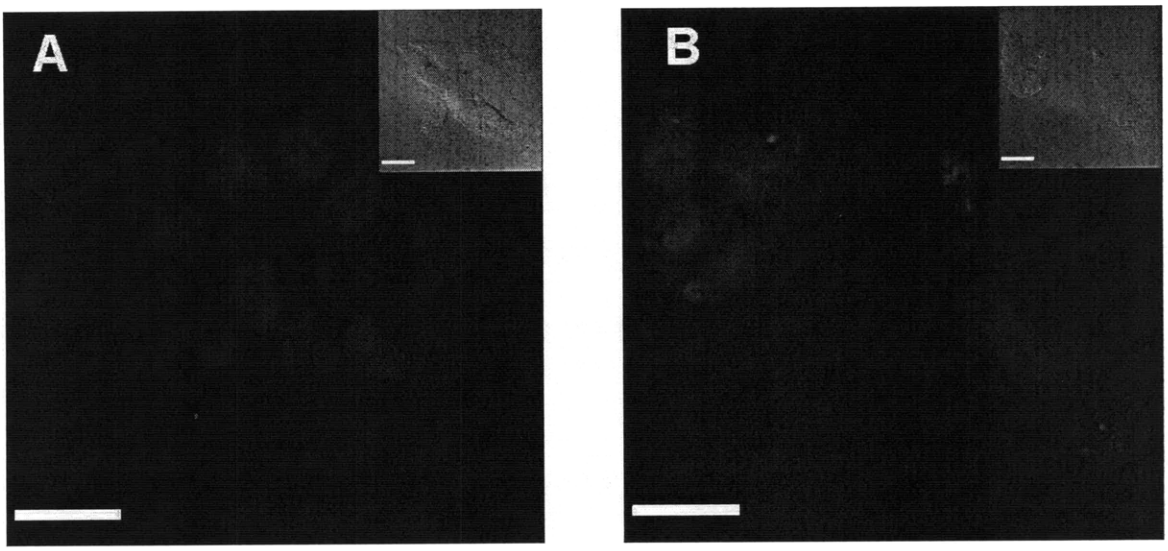

Fig. B.3.. Fluorescence imaging of intracellular zinc in fixed HEK-293 cells labeled with 1, shown in red, using a customized optical filter (exciter: D425/50, emitter: E600lp, beamsplitter: 460dcxr). The cell nucleus was stained with Hoechst 33258, shown in blue. The HEK-293 cells were incubated with 5 μM of 1 for 24 h prior to fixing. (A): Cells without addition of exogenous zinc; (B): Cells incubated with 40 μM Zn^{2+} carried by the ionophore pyrithione for 10 min before fixing. The inlet pictures are the corresponding bright field images. Bars are 25 μm.

These cells were healthy as compared to control, untreated cells according to analysis by cell counting and evaluation of viability using trypan blue and a hemocytometer. Fixed cells investigated by fluorescence imaging using a customized optical filter, which was especially designed to match the unusual excitation and emission profiles of **1**. The cell nuclei were co-stained with the blue fluorescent dye Hoechst 33258 (0.4 μM). The treated cells showed faint red fluorescence from **1**; a significant increase in the red fluorescence intensity occurred upon the addition of Zn^{2+} (40 μM) carried by the

ionophore pyrithione (2-mercaptopyridine-N-oxide), as shown in Fig. B.3 (B), indicating that **1** is taken up by the cell and the intracellular Zn^{2+} can be detected by fluorescence turn-on of **1**. Thus, $(DPA\text{-}C_2)_2\text{-}TPPS_3$ (**1**) is a valuable zinc fluorescence sensor and can be applied for intracellular zinc imaging.

Results: Cellular Uptake of (2)

As mentioned above, we chose to investigate a suspension-adapted HEK-293 cell line, which tolerates high-density growth and can produce a sufficiently large cell pellet for performing MRI in a multiwell plate. After a 24-h incubation with 100 μM **2**, the cell density was similar to that of untreated control cells, indicating that **2** has little cytoxicity. Centrifugation and washing with phosphate-buffered saline (PBS) yielded a dark-green cell pellet, a color typical of manganese porphyrins. This result indicates that **2** either accumulated intracellularly or became associated with the cell membrane. By comparison, the control cell pellet was pale white (Fig. B.4). To confirm the membrane permeability and further investigate the sub-cellular localization of **2**, the cells were lysed, and nuclear and cytosolic fractions were extracted and analyzed by flameless AAS (atomic absorption spectroscopy). The Mn absorption signal was calibrated by using a standard solution of known concentration. The results indicated that **2** is cell membrane-permeable and preferentially localizes in the nuclear fractions (5.62 mg Mn/L), rather than in the cytosol (0.78 mg Mn/L). By contrast, no Mn AAS signal was observed in the control cells under similar experimental conditions.

To investigate zinc-induced relaxivity changes in **2** inside cells, MR images were recorded and compared for cell pellets with and without exogenously introduced zinc. The HEK-293 cell suspension was divided equally into two flasks following a 24-h treatment with 100 μM **2**. A 200 μM portion of zinc pyrithione was then added to one of the samples and incubated for an additional 10 min. As in the solution studies, comparisons were made by using Mn-$TPPS_4$ as a reference compound. In addition, an untreated cell sample was prepared as a control. The cell suspensions were pelleted by centrifugation, washed and transferred into a multiwell plate for MRI analysis.

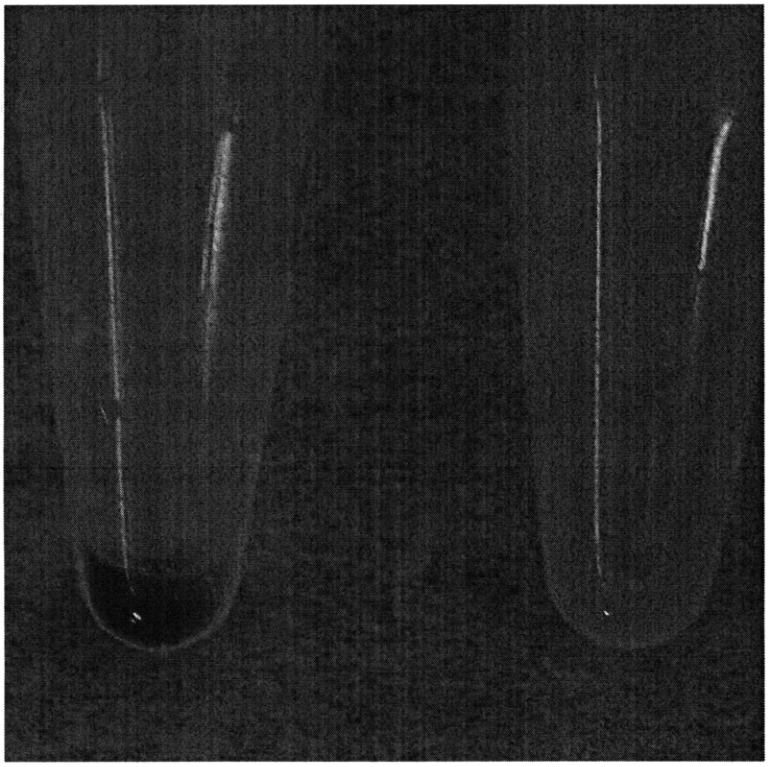

Figure B.4. Photographs of pellets of HeLa cells incubated with 100 μM (DPA-C_2)$_2$-$MnTPPS_3$ (2) for 24 h (left) and the blank control cells (right). The darker-colored pellet indicates cellular uptake of 2. Similar results were obtained for HEK 293 cells.

Biographical Sketch

The author was born in Flemington, NJ in 1981 and grew up in Vienna, VA. She graduated from Thomas Jefferson High School for Science and Technology in 1999. She graduated from Northwestern University in 2003 with dual degrees in Chemistry and from the Integrated Science Program. While at Northwestern, she conducted research in materials chemistry under the direction of Prof. Samuel Stupp and then completed photochemical research and an undergraduate honors thesis under the direction of Prof. Frederick Lewis. She received the Marple-Schweitzer award as the top graduating chemistry student at Northwestern in 2003. She spent the 2003-2004 academic year at the Max Planck Institute for Polymer Chemistry in Mainz, Germany on a Fulbright Scholarship in the lab of Prof. Wolfgang Knoll. She was supported by an NSF Graduate Research Fellowship and by ONCOETHIX/OTD during her thesis work.

Katherine Summer Lovejoy
lovejoy@mit.edu

MIT Department of Chemistry
77 Massachusetts Ave. 18-443
Cambridge, MA 02139
+1-617-253-1824

235 E. 27th St. #5B
New York, NY 10016
+1-917-561-0420

Education

Massachusetts Institute of Technology, (Cambridge, MA), Ph.D. candidate in bioinorganic chemistry; degree expected 12/08; GPA: 4.1/5.0.

Northwestern University, (Evanston, IL), B.A., June 2003, *cum laude,* Phi Beta Kappa, GPA: 3.69/4.0
Majors: 1) Chemistry and 2) Integrated Science (integrated physics, math, chemistry and biology).

Research

Massachusetts Institute of Technology, Prof. Stephen J. Lippard. Investigated biological mechanisms of action of platinum anticancer drugs; synthesized Pt(II) and Pt(IV) compounds; studied transcription and DNA repair *in vitro* and in cultured tissue; filed patent application on promising anti-tumor agent for treatment of colorectal cancer; supported by an NSF Graduate Fellowship. 12/04 to present.

Max Planck Institute for Polymer Chemistry, (Mainz, Germany), Prof. Wolfgang Knoll. Spectroscopically and electrochemically characterized cytochrome c oxidase in gold-tethered model biological membranes; discovered a robust model membrane system that led to a DARPA grant shared by the Knoll group and the University of Florida; supported by a Fulbright grant and NSF-REU. 8/03 to 8/04 and 6/01-8/01.

Northwestern University, Prof. Frederick Lewis. Investigated photochemical cyclization reactions of 2-ethynylbiphenyls; senior honors thesis. 9/02 to 6/03.

Northwestern University, Prof. Samuel Stupp. Devised formulation of amphiphilic block copolymers for drug delivery; grant awarded by Northwestern Committee for Undergraduate Research. 10/00 to 6/02.

IBM Almaden Research Center, Dr. Campbell Scott. Synthesized and characterized organic molecular wires on gold and palladium surfaces; NSF-REU project. 6/02 to 8/02.

Max Planck Institute for Polymer Chemistry, Prof. Wolfgang Knoll. Developed model membrane systems on gold surfaces; NSF-REU project. 6/01 to 8/01.

Fellowships

International Precious Metals Institute, Student Award, 4/07
Fulbright Grant, used for year of study at Max Planck Institute for Polymer Chemistry in Germany, 3/03
NSF Graduate Research Fellowship, 3/03
Deutscher Akademischer Austausch Dienst Graduate Award, 4/03
Goldwater Fellowship Nominee (1 of 4 from Northwestern University), 11/01
Undergraduate Research Grant, Northwestern Committee for Undergraduate Research, 12/01

Academic Honors and Service

Marple-Schweitzer Award, top graduating chemistry student, Northwestern University, 6/03
Basolo Oesper Award, for citizenship and service to chemistry department, Northwestern University, 6/03
Outstanding Presentation, Undergraduate Research Symposium, Northwestern University, 5/03
Student Advisory Board, Northwestern College of Arts and Science, chemistry rep., 5/01 to 6/03
Northwestern Curricular Policies Committee, student body representative, 9/02 to 6/03

Teaching Experience

Teaching Asistant, NSF "Chemistry Bonds" Workshop, for Prof. Stephen J. Lippard; "Principles of Bioinorganic Chemistry." Delivered 15 hours of lectures to 14 advanced graduate students, postdocs, and professors from the Middle East. Petra, Jordan, 3/07.

T.A., MIT 5.062, "Principles of Bioinorganic Chemistry," Prof. S.J. Lippard, 9/06 to 10/06.

T.A., MIT 5.112, "Principles of Chemical Science," Profs. S.T. Ceyer and C.C. Cummins, 9/04 to 12/04.

Leadership and Activities

President, American Chemical Society, Northwestern University undergraduate chapter, 5/02 to 5/03. Treasurer, 3/01 to 5/02. Initiated outreach partnership with Chicago Children's Museum.

Workshop Facilitator for Northwestern's General Chemistry course sequence, 6/02 to 6/03. Led weekly problem-solving section for seven undergraduates.

Associate Editor, Journal of Young Investigators, 9/05 to 5/03. Science Journalist 9/01 to 3/03, Reviewed submissions and wrote scientific features for the journal (supported by *Science* magazine). Wrote four published feature articles, available at www.jyi.org.

Editorial Assistant, National Academies of Science, Board on Physics and Astronomy (paid internship). Edited figures and acronyms for decadal survey: *Astronomy and Astrophysics in the New Millennium*, 6/00 to 8/00.

Publications

Lovejoy, K.S.; Todd, R.C.; Zhang, S.; McCormick, M.S.; D'Aquino, J.A.; Reardon, J.T.; Sancar, A.; Giacomini, K.M.; Lippard, S.J. "cis -Diammine(pyridine)chloroplatinum(II), a monofunctional platinum(II) antitumor agent: Uptake, structure, function, & prospects." *Proc. Natl. Acad. Sci. USA* **2008**, *105*, 26, 8902-8907.

Zhang, X.; **Lovejoy, K.S.**; Jasanoff, A.; Lippard, S.J. "Water-soluble porphyrins as dual-function molecular imaging platforms for MRI and fluorescence sensing." *Proc. Natl. Acad. Sci. USA* **2007**, *104*, 26, 10780-10785.

Todd, R.C.; **Lovejoy, K.S.**; Lippard, S.J. "Understanding the effect of carbonate ion on cisplatin binding to DNA." *J. Am. Chem. Soc.* **2007**, *129*, 20, 6370-6371.

Zhang, S.; **Lovejoy, K.S.**; Shima, J.E.; Lagpacan, L.L.; Shu, Y.; Lapuk, A.; Chen, Y.; Komori, T.; Gray, J.W.; Chen, X.; Lippard, S.J.; Giacomini, K.M. "Organic cation transporters are determinants of oxaliplatin cytotoxicity." *Cancer Res.* **2006**, *66*, 8847-8857.

Lewis, F.D.; Karagiannis, P.C.; Sajimon, M.C.; **Lovejoy, K.S.**; Zuo, X.; Rubin, M.; Gevorgyan, V. "Solvent dependent photocyclization and photophysics of some 2-ethynylbiphenyls." *Photochem. Photobiol. Sci.* **2006**, *5*, 4, 369-375.

Swanson, S.A.; McClain, R.; **Lovejoy, K.S.**; Alamdari, N.B.; Hamilton, J.S.; Scott, J.C. "Self-assembled diisocyanide monolayer films on gold and palladium." *Langmuir*. **2005**, *21,* 11, 5034-5039.

Schiller, SM.; Naumann, R.; **Lovejoy, K.**; Kunz, H.; Knoll, W. "Archaea analogue thiolipids for tethered bilayer lipid membranes on ultrasmooth gold surfaces." *Angewandte Chemie*. **2003**, *2*, 208.

Presentations

Lovejoy, K.S.; Zhang, S.; Giacomini, K.M.; Lippard, S.J. "Pt(II) substrates of organic cation transporters and cellular processing of related Pt-DNA adducts." *Abstracts of Papers of the American Chemical Society*. 2007, *234th Meeting*, INOR-181. Poster session.

Lovejoy, K.S.; Lippard, S.J. "Transport of oxaliplatin by organic cation transporters and rational design of platinum(II)-based transporter substrates." *11th Boston Regional Inorganic Chemistry Meeting*. October 2006. Invited speaker.

Lovejoy, K.S.; Storrie, H.H.; Stupp, S.I. "Novel cationic amphiphiles for gene therapy." *Abstracts of Papers of the American Chemical Society*. 2002, *223th Meeting*, CHED-671. Poster session.

Skills

Laboratory Management:

Tissue Culture Facility Manager, Lippard Lab: maintained cell lines and lab facility; trained new users.

Other well-developed skills in: grid confocal microscopy, surface plasmon resonance spectroscopy, radioisotopic labeling (^{32}P), dynamic light scattering, ellipsometry, FTIR, ^{195}Pt, Langmuir-Blodgett monolayer deposition, LC-MS, ion exchange chromatography, atomic absorption spectroscopy, nucleic acid manipulation, immunofluorescence labeling, and ELISA.

Languages and Citizenship:

English (native), German (fluent), US Citizen.

Other:

Competitive road cycling, classical viola.